Perturbative study of selected exclusive QCD processes at high and moderate energies

Renaud Boussarie

NNT : 2016SACLS280

THÈSE DE DOCTORAT
DE L'UNIVERSITÉ PARIS-SACLAY
PRÉPARÉE À L'UNIVERSITÉ PARIS SUD

LABORATOIRE DE PHYSIQUE THÉORIQUE
École doctorale n°564
Physique en Île de France
Spécialité de doctorat: Physique
par

M. RENAUD BOUSSARIE

Étude perturbative de différents processus exclusifs en QCD aux énergies hautes et modérées

Thèse présentée et soutenue au LPT Orsay, le 23 septembre 2016.

Composition du Jury :

M.	DAMIR BEČIREVIĆ	Directeur de Recherche *LPT Orsay*	(Président du jury)
M.	DMITRY IVANOV	Professeur associé *Sobolev Inst. of Mathematics*	(Rapporteur)
M.	JAMAL JALILIAN-MARIAN	Professeur *Baruch College*	(Rapporteur)
M.	FRANCK SABATIÉ	Chercheur CEA *IRFU*	(Examinateur)
M.	LECH SZYMANOWSKI	Professeur *NCBJ Varsovie*	(Directeur de thèse)
M.	SAMUEL WALLON	Maître de Conférences *LPT Orsay*	(Directeur de thèse)
M.	FRANÇOIS GELIS	Chercheur CEA *IPhT*	(Invité)
M.	STÉPHANE MUNIER	Chercheur CNRS *CPhT*	(Invité)

Acknowledgments

First I would like to thank my supervisors Lech Szymanowski and Samuel Wallon, whose impressive knowledge, support and dedication made these three years of PhD an incredibly enriching experience. I am also grateful to my close collaborators Andrey Grabovsky and Bernard Pire who provided me a staggering amount of additional information, respectively about small-x physics and about collinear physics.
I would like to thank the consecutive directors of LPT Henk Hilhorst and Sébastien Descotes-Genon, as well as the administrative team Mireille Calvet, Odile Heckenauer, Philippe Molle, Marie-Agnès Poulet and Jocelyne Raux for welcoming me and for their availability and their support, which made my work a pleasant experience and allowed me to attend many conferences, schools and workshop during my three years of PhD.
I am grateful to NCBJ Warsaw, Budker Institute of Nuclear Physics and the Novosibirsk State University for their hospitality.
I would also like to thank all the members of my jury for accepting to review my thesis and for their many relevant remarks and questions.
Finally, I would like to thank Ian Balitsky, Guillaume Beuf, Michel Fontannaz and Heribert Weigert for useful discussions, as well as Anselmino Mauro and Stefano Melis for providing us with the code we needed to evaluate the uncertainties in the last part of this thesis.

Abstract

At high enough energies, QCD processes can be factorized into a hard part, which can be computed by using the smallness of the strong coupling to apply the perturbative Feynman diagram method, and a non-perturbative part which has to be fitted to experimental data, modeled or computed using other tools like for example lattice QCD. However the smallness of the strong coupling in the perturbative part can be compensated by large logarithms which arise from the cancellation of soft or collinear divergences, or by the presence of multiple kinematic scales. Such logarithmically-enhanced contributions must be resummed, leading to the DGLAP evolution at moderate energies and to the BFKL or B-JIMWLK equation in the high energy limit. For the largest energies gluon recombination effects lead to saturation, which can be described in the color glass condensate (CGC) or shockwave formalism. In this thesis, we propose to study several exclusive perturbative QCD processes in order to get a better understanding of factorization, resummation and saturation effects.

In the first part we perform the first computation of an exclusive quantity at Next-to-Leading-Order (NLO) accuracy using the QCD shockwave formalism. We calculate the NLO amplitude for the diffractive production of an open quark-antiquark pair, then we manage to construct a finite cross section using this amplitude by studying the exclusive diffractive production of a dijet. Precise phenomenological and experimental analysis of this process should give a great insight on high energy resummation due to the exchange of a Pomeron in diffraction, which is naturally described by the resummation of logarithms emerging from the soft divergences of high energy QCD. Our result holds as the center of mass energy grows towards the saturation scale or for diffraction off a dense target so one could use it to study saturation effects.

In the second part we show how the experimental study of the photoproduction of a light meson and a photon at moderate energy should be a good probe for Generalized Parton Distributions (GPDs), one of the generalizations of the non-perturbative building blocks in collinear factorization. In principle such a study would give access to both helicity-conserving and helicity-flip GPDs. We give numerical predictions for this process at JLAB@12GeV.

Contents

List of publications

Impact factor for high-energy two and three jets diffractive production
R.Boussarie, A.V.Grabovsky, L.Szymanowski, S.Wallon
arXiv:1405.7676[hep-ph]
JHEP 1409 (2014) 026

Impact factor for high-energy two and three jets diffractive production
R.Boussarie, A.V.Grabovsky, L.Szymanowski, S.Wallon
arXiv:1503.01782[hep-ph]
AIP Conf.Proc. 1654 (2015) 030005

Transverse momentum dependent (TMD) parton distribution functions: status and prospects
R.Angeles-Martinez *et al.*
arXiv:1507.05267[hep-ph]
Acta Phys.Polon. B46 (2015) no.12, 2501-2534

Production of a forward J/Ψ and a backward jet at the LHC
R.Boussarie, B.Ducloué, L.Szymanowski, S.Wallon
arXiv:1511.02181[hep-ph]
To be published in J.Phys.Conf.Ser.

Diffractive production of jets at high-energy in the QCD shock-wave approach
R.Boussarie, A.V.Grabovsky, L.Szymanowski, S.Wallon
arXiv:1511.02785[hep-ph]
To be published in J.Phys.Conf.Ser.

On $\gamma N \to \gamma \rho N'$ at large $\gamma\rho$ invariant mass
R.Boussarie, B.Pire, L.Szymanowski, S.Wallon
arXiv:1511.04371[hep-ph]
To be published in J.Phys.Conf.Ser.

Photon dissociation into two and three jets : initial and final state corrections
R.Boussarie, A.V.Grabovsky, L.Szymanowski, S.Wallon
arXiv:1512.00774[hep-ph]
Acta Phys.Polon.Supp. 8 (2015) 897

Revealing transversity GPDs through the photoproduction of a photon and a ρ
R.Boussarie, B.Pire, L.Szymanowski, S.Wallon
arXiv:1602.01774[hep-ph]
EPJ Web Conf. 112 (2016) 01006

On the one loop $\gamma^{(*)} \to q\bar{q}$ impact factor and the exclusive diffractive cross section for the production of two or three jets
R.Boussarie, A.V.Grabovsky, L.Szymanowski, S.Wallon
arXiv:1606.00419[hep-ph]
To be published in JHEP

Exclusive photoproduction of a $\gamma\rho$ pair with a large invariant mass
R.Boussarie, B.Pire, L.Szymanowski, S.Wallon
arXiv:1609.03830[hep-ph]
Submitted to JHEP

Photoproduction of a large invariant mass $\gamma\rho$ pair at small momentum transfer
R.Boussarie, B.Pire, L.Szymanowski, S.Wallon
arXiv:1609.05144[hep-ph]

Chapter 1

Résumé français

La thèse présentée ici traite de différents processus exclusifs en Chromodynamique quantique (QCD), décrits à l'aide des outils de QCD perturbative, utilisables aux énergies hautes et modérément hautes. Ces outils reposent sur la factorisation des processus hadroniques en une partie dite *dure*, calculable à l'aide des méthodes habituelles des diagrammes de Feynman grâce à la petitesse de la constante de couplage de QCD α_s permettant l'expansion perturbative en puissances α_s^n, et une partie *non perturbative* qui requiert des méthodes différentes comme par exemple la QCD sur réseau, ou doit être contrainte par les données expérimentales.

L'introduction de ce manuscrit présente une description des différentes factorisations en QCD perturbative, qui seront mises en œuvre dans la thèse. Considérant un processus hadronique avec une énergie au centre de masse s et impliquant une échelle dure Q^2, deux régimes cinématiques principaux peuvent être distingués: le régime *colinéaire* aux énergies modérées $s \sim Q^2$ et le régime de *Regge-Gribov* aux plus hautes énergies $s \gg Q^2$. La factorisation colinéaire s'appliquant dans le premier cas met en jeu des partons d'impulsion colinéaire au hadron, et la factorisation dite k_t s'appliquant dans le deuxième cas implique l'échangées de gluons de basse énergie (par rapport au hadron) avec un moment transverse non nul. La factorisation en QCD est liée à la présence de grands logarithmes après compensation de divergences infrarouges dans les observables physiques. En factorisation colinéaire les termes en $\alpha_s \ln(Q^2)$ sont resommés par l'équation de Dokshitzer, Gribov, Lipatov, Altarelli, Parisi (DGLAP) et en factorisation k_t par les termes en $\alpha_s \ln(s)$ sont resommés par l'équation de Balitsky, Fadin, Kuraev, Lipatov (BFKL) et par ses extensions non-linéaires Balitsky, Kovchegov (BK) et Jalilian-Marian, Iancu, McLerran, Weigert, Leonidov, Kovner (JIMWLK) comprenant les effets de saturation gluonique aux énergies asymptotiques.

Dans la première partie de cette thèse, le formalisme dit des *ondes de choc de QCD*, l'extension non-linéaire de la factorisation k_t, est dérivé en détail. Aux énergies asymptotiques, un nucléon se comporte comme un système très dense de gluons faiblement couplés. Dans le référentiel d'un projectile qui rencontre ce nucléon, ce projectile voit le champ de couleur effectif du nucléon qui possède alors une structure spatio-temporelle similaire à une onde de choc. Le formalisme en question étudie l'évolution de ce champ effectif avec effets de recombinaison des gluons (responsables des effets de saturation), et son couplage au projectile.
Plus précisément le bloc non perturbatif de ce formalisme est constitué d'éléments de matrices du type $\langle P'|\mathbf{W}|P\rangle$, où P' (resp. P) est l'état sortant (resp. entrant) de la cible hadronique et $\mathbf{W}$ est construit à partir de lignes de Wilson

$$U_z \equiv \mathcal{T} e^{ig \int dz^+ b^-(z)}, \tag{1.1}$$

constituées de gluons lents du champ b^μ de la cible. Du point de vue du projectile, le couplage à ce champ est instantané et *eikonal* : $b^\mu(z) = \delta(z^+) b^-(\vec{z}) n_2^\mu$. Ce champ est le champ *d'onde de choc*, et il est possible de dériver de manière effective les règles de Feynman nécessaires pour le calcul du facteur d'impact d'un projectile en présence de ce champ.

Dans ce manuscrit les règles de Feynman effectives en présence du champ d'onde de choc sont explicitées, et l'équation d'évolution BK-JIMWLK pour l'opérateur dipolaire $\mathcal{U}_{z_i z_j} \equiv 1 - \frac{1}{N_c}\mathrm{Tr}(U_{z_i} U^\dagger_{z_j})$ apparaissant dans un tel formalisme est redérivée en dimension quelconque, puis il est montré que la limite

quadridimensionnelle du résultat correspond bien à l'équation telle qu'elle est présentée dans la littérature

$$\frac{\partial \mathcal{U}_{z_i z_j}}{\partial \eta} = \frac{\alpha_s N_c}{2\pi^2} \int d^2\vec{z}_k \frac{(\vec{z}_i - \vec{z}_j)^2}{(\vec{z}_i - \vec{z}_k)^2 (\vec{z}_k - \vec{z}_j)^2} [\mathcal{U}_{z_i z_k} + \mathcal{U}_{z_k z_j} - \mathcal{U}_{z_i z_j} - \mathcal{U}_{z_i z_k} \mathcal{U}_{z_k z_j}], \tag{1.2}$$

où η est la séparation de rapidité, un paramètre qui contrôle la séparation entre les gluons du facteur d'impact du projectile et les gluons de voie t provenant de la cible. Dans la limite linéaire où le terme en $\mathcal{U}_{z_i z_k} \mathcal{U}_{z_k z_j}$ est négligé, cette équation est équivalente à la formulation en espace des coordonnées de l'équation BFKL.

Une fois les règles de Feynman et l'équation d'évolution définies, le calcul au premier ordre de précision sous-dominant du *facteur d'impact* (partie dure en factorisation k_t) d'un processus diffractif exclusif est fait en détail.

La diffraction en QCD est l'une des découvertes majeures du collisionneur HERA : il a été observé qu'environ 10% des événements $\gamma^* p \to X$ révélaient un intervalle de rapidité entre les particules produites dans la zone de fragmentation du proton et les particules produites dans celle du photon virtuel. La présence de cet intervalle de rapidité nécessite de décrire la diffraction par l'échange d'une particule effective ayant les nombres quantiques du vide, le *Pomeron*. Deux modèles principaux ont été développés pour cet échange de Pomeron, l'un dans le cadre de la factorisation colinéaire et l'autre dans le cadre de la factorisation k_t. Des analyses expérimentales récentes semblant favoriser le deuxième modèle dans le régime de faible masse diffractive, le but du calcul présenté dans ce manuscrit est d'améliorer les résultats théoriques disponibles pour la description de la production diffractive exclusive d'une paire de jets vers l'avant.

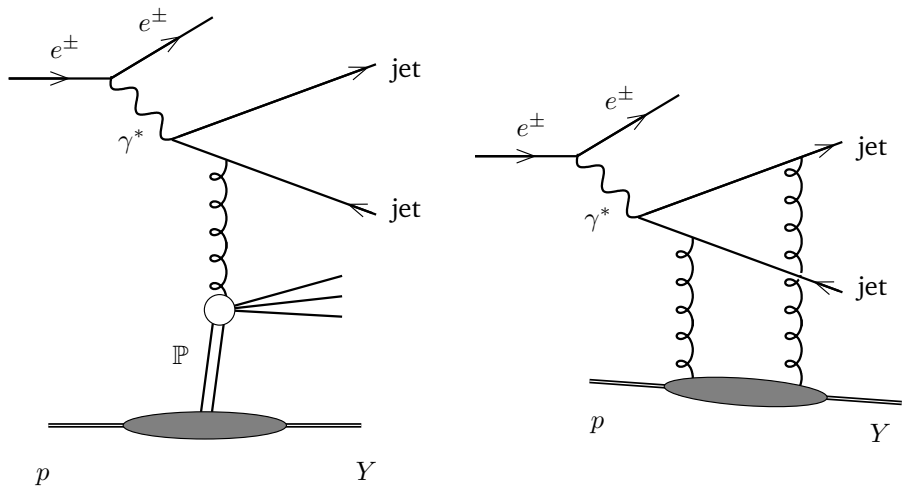

Figure 1.1: Modèles pour la production diffractive d'un double jet vers l'avant : *resolved Pomeron* (gauche) et *direct Pomeron* (droite)

Pour ceci, l'amplitude complète à l'ordre sous-dominant est obtenue, l'échange d'un Pomeron en voie t étant décrit par l'action d'opérateurs dipolaire et double-dipolaire sur les états entrant et sortant de la cible hadronique, afin de pouvoir inclure les effets de saturation dans les prédictions numériques futures basées sur le résultat présenté ici.

Dans un premier temps les règles de Feynman effectives sont utilisées afin de construire le facteur d'impact pour la production diffractive vers l'avant d'une paire quark-antiquark ($q\bar{q}$) au premier ordre sous-dominant. Pour cela il est nécessaire de calculer le diagramme présenté ci-dessous et toutes les corrections virtuelles à ce diagramme.

Ensuite celui pour la production diffractive vers l'avant d'un quark, un antiquark et un gluon ($q\bar{q}g$) est calculé à l'ordre dominant, à partir des diagrammes ci-dessous et de leurs symétriques par l'échange quark-antiquark :

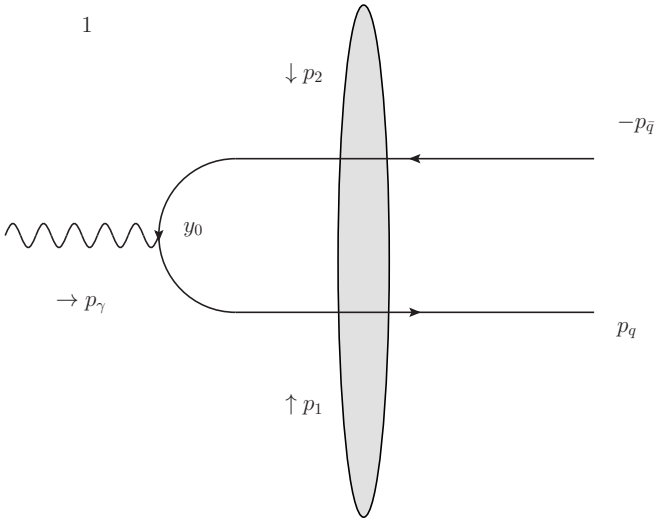

Figure 1.2: Facteur d'impact d'ordre dominant. Le bloc gris indique l'interaction avec le champ d'onde de choc, avec transfert d'impulsions effectives p_1 et p_2.

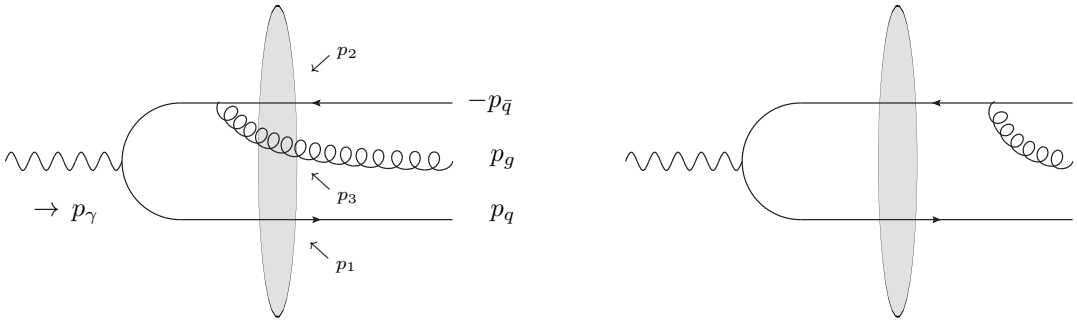

Figure 1.3: Diagrammes dominants pour l'amplitude $\gamma^* \rightarrow q\bar{q}g$ amplitude, avec échange effectif d'impulsions p_1, p_2 and p_3.

Les deux facteurs d'impact obtenus sont combinés afin d'obtenir la description à l'ordre sous-dominant de la production diffractive exclusive d'une paire de jets vers l'avant avec la cinématique la plus générale. Tous les mécanismes d'annulation de l'ensemble des divergences sont présentés. Nous montrons comment l'équation d'évolution dipolaire permet d'annuler la divergence de rapidité et nous décrivons les effets de la renormalisation sur les divergences ultraviolettes. La divergence *molle et colinéaire* est annulée par la redéfinition des observables physiques *via* un algorithme de jet. Les divergences *molle* et *colinéaire* de la contribution $q\bar{q}g$ sont isolées et réécrites de manière à faire apparaître leur forme habituelle où le terme dominant est un facteur global, et enfin annulées par les divergences restantes de la contribution $q\bar{q}$.

Nous obtenons ainsi une expression finie pour la section efficace d'un processus exclusif à l'ordre sous-dominant aux énergies asymptotiques avec effets de saturation gluonique. De très nombreuses autres observables peuvent être obtenues à partir des deux facteurs d'impact avec production ouverte de $q\bar{q}$ ou $q\bar{q}g$ ici obtenus, et plus généralement des techniques qui ont été développées dans ce but durant ce travail de thèse. Certaines de ces observables sont présentées pour leur intérêt théorique ou expérimental: section efficace totale $\gamma^* p \rightarrow \gamma^* p$, qui permettrait de vérifier par le calcul direct des résultats précédents obtenus indirectement et d'avoir accès à la trajectoire du Pomeron perturbatif à la précision sous-dominante ; facteur d'impact pour des processus diffractifs exclusifs tels que la production d'un méson ρ^0 à l'ordre sous-dominant, ou encore, sur le plan formel, clarification du lien entre le formalisme des ondes de choc et le formalisme historique plus classique BFKL, non-trivialement équivalent dans la limite où les effets

de saturation gluonique sont négligeables. Sur le plan phénoménologique, l'intérêt principal du calcul présenté ici est la très grande variété des prédictions possibles dont il pourrait servir de base. En effet la généralité de la cinématique, l'utilisation du formalisme des ondes de choc valable jusqu'aux échelles de saturation, et le fait que, les divergences étant annulées, la factorisation est prouvée à l'ordre considéré, permettent de décrire le processus dans n'importe quel type de collisions : électron-proton, électron-ion, et collisions ultrapériphériques proton-proton et proton-ion, où le photon initial est émis par un hadron ou un ion. En conséquence, ce résultat est utilisable aussi bien pour décrire des données existantes (par exemple les analyses récentes des données de HERA), pour obtenir des prédictions pour des expériences en cours d'analyse ou prévues (par exemple au LHC ou à RHIC) ou pour des expériences futures (par exemple pour les projets futurs EIC ou LHeC). La grande précision des résultats de cette thèse devrait permettre une meilleure description des mécanismes de resommation molle, et grâce à leur applicabilité aux collisions impliquant aussi bien des hadrons que des ions lourds, une meilleure compréhension des effets de saturation gluonique devrait en découler.

La deuxième partie de ce manuscrit traite de la question de la structure interne du proton *via* un processus exclusif aux énergies plus modérées. Nous y présentons une étude de faisabilité détaillée pour la photoproduction d'un méson ρ^0 et d'un photon avec une grande masse invariante $M_{\gamma\rho}$ constituant une échelle dure pour permettre l'application de la factorisation colinéaire. Il a été prouvé pour certains processus que la factorisation colinéaire était applicable quel que soit l'ordre de précision du calcul du sous-processus partonique en puissance de α_s. En rapprochant le processus proposé dans cette deuxième partie de deux d'entre eux, nous nous convaicons tout d'abord que la factorisation colinéaire devrait s'appliquer dans notre cas. Nous procédons ainsi à la factorisation proprement dite, en une partie dure et deux éléments de matrice non-perturbatifs : une Amplitude de Distribution (DA) pour le méson et des Distributions de Partons Généralisées (GPD) pour le nucléon cible.

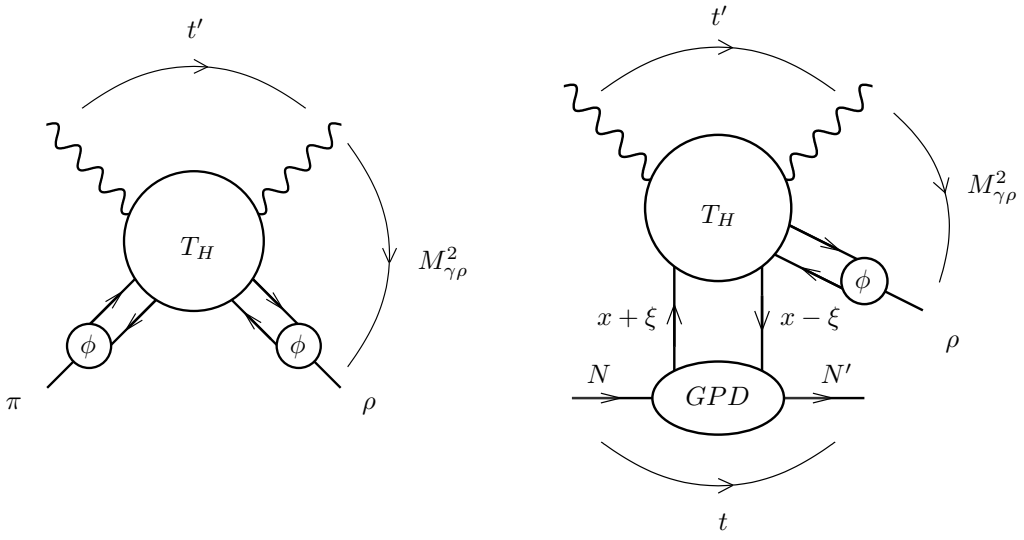

Figure 1.4: Similarité de la factorisation du processus étudié avec la Diffusion à Grand Angle $\gamma\pi \to \gamma\rho$, en partie dure T_H, DA ϕ et GPD.

Au *twist* dominant (ici terme dominant dans l'expansion en puissances de $M_{\gamma\rho}$), la DA du méson est paire (resp. impaire) en termes de chiralité si sa polarisation est longitudinale (resp. transverse). Il existe en tout 8 GPDs possibles, dont 4 de chiralité paire et 4 de chiralité impaire. Par conservation de la chiralité, le processus permet donc théoriquement de mesurer les GPDs paires tout comme les impaires, selon la polarisation du méson. Nous nous plaçons pour notre étude à dans la limite quasi-diagonale, où l'impulsion échangée en voie t est négligeable. Dans cette limite, seulement 2 GPD paires et une GPD impaire contribuent. Les diagrammes de Feynman avec les projections de Fierz correspondantes qui constitutent la partie dure associée à chacun des cas sont calculés analytiquement.
Dans le cadre de la factorisation colinéaire, le processus total s'écrit comme la convolution de la partie dure avec une DA et une GPD. La DA est une fonction de deux variables : la fraction z d'impulsion du

quark de la paire quark-antiquark constituant le ρ^0 à l'ordre de précision considéré et une échelle de factorisation μ_F. Dans la limite où μ_F tend vers l'infini la DA a une forme analytique simple, que nous utilisons pour notre étude de faisabilité afin de faire la convolution de la partie dure avec la DA analytiquement. Pour ce qui est de la GPD, nous nous basons sur l'*ansatz* de Radyushkin, qui permet de modéliser l'élément de matrice non-diagonal comme la convolution d'une Distribution de Parton (PDF) avec une fonction de profil. À partir de cette *ansatz* et de valeurs extraites expérimentalement pour les PDF, nous construisons des valeurs numériques pour les GPD, et nous faisons enfin la convolution restante avec la partie dure.

À partir de ces résultats, nous concluons notre étude de faisabilité dans le cas particulier d'une expérience à JLab@12GeV en proposant les sections efficaces différentielle et totale, ainsi qu'un taux de comptage prenant en compte les contraintes expérimentales de luminosité. Nous étudions également les effets d'une coupure angulaire sur ces nombres, afin de vérifier que les caractéristiques du détecteur ne soient pas trop contraignantes.
Les statistiques très prometteuses obtenues montrent que le processus considéré constitue une excellente façon d'extraire expérimentalement de l'information sur les GPD, avec ou sans renversement de l'hélicité des quarks (suivant la polarisation du ρ^0 produit. Cependant la différence de magnitude entre les contribution paire et impaire de chiralité implique qu'afin de mettre en évidence les GPD impaires (GPD de transversité, jusqu'ici expérimentalement inaccessibles), une étude théorique plus approfondie est nécessaire. L'étude serait aisément reproductible pour d'autres expériences (par exemple à COMPASS, au LHC, ou dans des futurs collisionneurs comme EIC ou LHeC). L'intérêt de la classe de processus ici étudiée est de permettre de tester phénoménologiquement l'universalité des GPD, qui sont jusqu'à présent essentiellement étudiées dans le cadre de la diffusion Compton profondément virtuelle ou de la production virtuelle exclusive de mésons.

Le manuscrit présenté ici montre ainsi en quoi l'étude de quelques processus exclusifs peut permettre d'adresser plusieurs questions fondamentale de la QCD : les effets de resommation à haute énergie, les effets de saturation, et la physique non-perturbative liée à la structure interne du proton. Plusieurs outils théoriques ont été développés en vue de prédictions numériques précises dans un futur proche, et une étude complète de faisabilité aux prédictions prometteuses est présentée, reproductible pour de nombreuses expériences.

Part I

Introduction

Quantum Chromodynamics (QCD) is the quantum field theory of strong interactions. It is based on the non-abelian gauge group $SU(N_c)$, where $N_c = 3$ is the number of quark colors. It contains by itself a natural extension of the so-called naive parton model which was proposed by Feynman and Bjorken [1, 2] as an explanation for the Bjorken scaling observed in inclusive Deep Inelastic Scattering (DIS) events at SLAC in the sixties. QCD successfully describes even the strangest properties of the strong interaction. Indeed as shown by Wilczek, Politzer and Gross [3–5], QCD is an asymptotically free theory due to its non-abelian character given the number of quark degrees of freedom we know. This explains why partons in a strongly bound hadronic state behave like free particles. The major difficulty for the theoretical description of QCD processes is due to *confinement* : the direct observation of partons as isolated free particles is impossible, one can only observe colorless bound states formed by several partons. The mere existence of gluons was only proven in 1979 at PETRA. There are several ways of circumventing confinement to describe strong interaction processes, among which perturbative QCD.

When describing a QCD process using perturbation theory, at least two scales (which might be of the same order) are involved : the center-of-mass energy s of the whole process and a hard scale $Q^2 > \Lambda^2_{QCD}$. Typically Q^2 will be a photon virtuality, a squared transverse momentum, the squared mass of a heavy quark or the invariant mass of a subprocess. Perturbative QCD relies on the factorization of the total process into a *hard part* and a *non-perturbative part*. The latter contains the long distance dynamics of the parton inside hadrons and it cannot be computed with the usual methods. One has to either fit it to the experimental data, build a phenomenological model or use methods like lattice QCD to obtain a description of non-perturbative quantities. Factorization implies that these quantities must be *universal*, so experiments actually allow one to extract consistent information on the non-perturbative dynamics. The computation of the hard part relies on the smallness of the strong coupling constant $\alpha_s(Q^2)$ at hard enough scales, so that one can use the usual perturbative methods of Feynman diagrams. However due to the presence of infrared divergences, or in some cases to the presence of additional scales, large logarithms tend to appear when computing hard parts. Indeed for example in dimensional regularization, quantities like

$$\frac{1}{\epsilon}\left(Q^2\right)^{\epsilon} = \frac{1}{\epsilon} + \ln\left(Q^2\right) + O(\epsilon) \tag{1.3}$$

will appear when considering collinear gluon dynamics in the massless quark limit. In an infrared and collinearly safe observable, the $\frac{1}{\epsilon}$ pole cancels, but the logarithms remain. Thus $\alpha_s \ln\left(Q^2\right)$ terms arise. Large logarithms can compensate the smallness of the coupling constant, in which case these terms are of order 1. This means that the α_s-expansion is not a completely valid one and one has to extract terms of type

$$\alpha_s^n \ln^p\left(Q^2\right) \tag{1.4}$$

at all orders of this expansion. There are two main kinematic regimes of perturbative QCD, leading to two different formalisms : *collinear factorization* and k_t*-factorization*. The first regime is the so-called *Bjorken limit* $Q^2 \to \infty$ at moderate s or equivalently at moderately small *Bjorken x*, given by $x = \frac{Q^2}{s}$, and the second one is the so-called *Regge-Gribov* or *semihard* limit $s \gg Q^2$ or equivalently $x \to 0$.

The Bjorken limit of QCD is dominated by collinear dynamics : large logarithms of Q^2 arise from the cancellation of collinear divergences. The resummation of such logarithms leads to the Dokshitzer-Gribov-Lipatov-Altarelli-Parisi (DGLAP) evolution equation [6–9] for the Parton Distribution Functions (PDFs) and to the Efremov-Radyushkin-Brodsky-Lepage evolution equation [10–12] for the Distribution Amplitudes (DAs). PDFs and DAs are the basic non-perturbative building blocks in the collinear factorization framework which is to be used in such kinematics. Factorization in the Bjorken limit at leading twist (*i.e.* for the dominant term in the $\frac{1}{Q}$ expansion) has been proven at all orders in α_s in the hard part for several processes, such as Deeply Virtual Compton Scattering (DVCS) [13, 14], i.e. $\gamma^* p \to \gamma p$, and Deeply Virtual Meson Production (DVMP) [15], i.e. $\gamma^* p \to V p$, where V is a light meson. Both processes are described in Fig. 1.5.

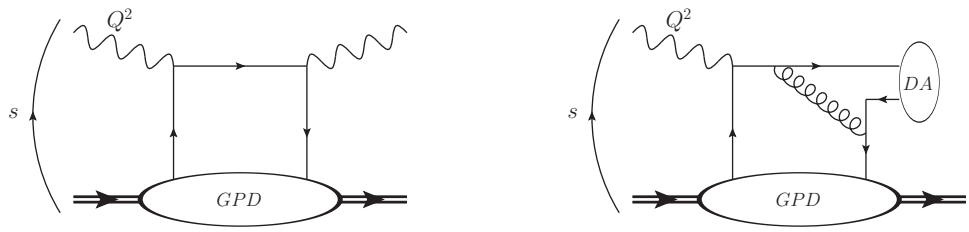

Figure 1.5: Collinear factorization for DVCS (left) and DVMP (right). Generalized Parton Distributions (GPDs) are the non-forward extensions of PDFs

The behaviour of the PDFs as a function of x, measured at HERA, are shown in Fig.1.6. Such results show that as the center-of-mass energy of the process grows, or equivalently as x decreases, the contribution from exchanged gluons start dominating the process more and more.

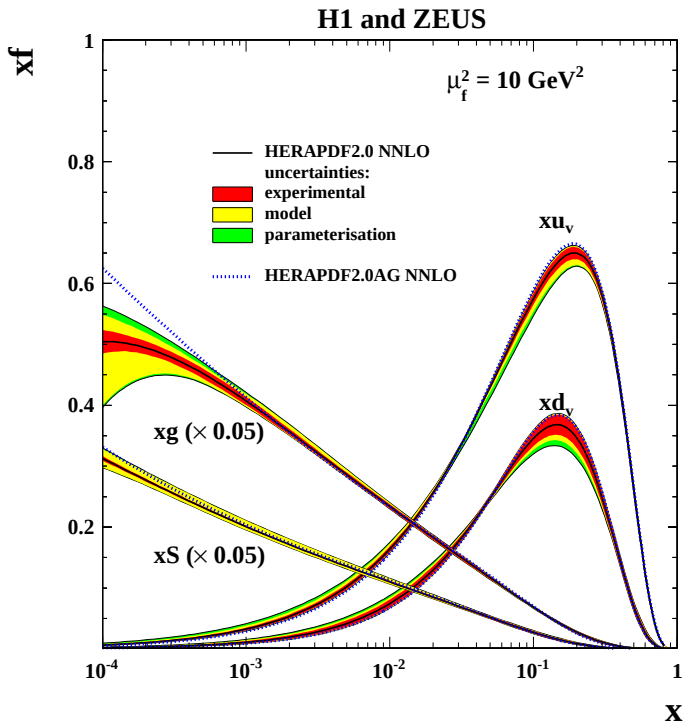

Figure 1.6: Parton distribution functions [H1 and ZEUS collaborations, 2015]

This is actually natural in the second main QCD factorization formalism. QCD in the Regge limit is dominated by soft gluon dynamics : large logarithms of x arise from the cancellation of soft divergences. Such $\alpha_s \ln(x)$ terms are resummed by the Balitsky-Fadin-Kuraev-Lipatov (BFKL) equation [16–19]. One of the most successful features of the BFKL approach is that it is consistent with pre-QCD results from Regge theory. In Regge theory, which describes the strong interaction at small values of x, one can show that processes are dominated by the exchange of an effective particle which carries the quantum numbers of the vacuum, called the Pomeron. In the BFKL framework, a Pomeron is naturally described as an effective ladder of t-channel gluons as shown in Fig. 1.7.

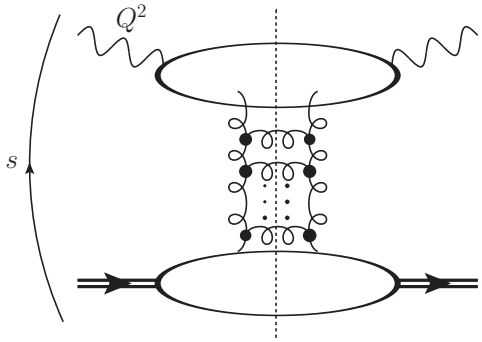

Figure 1.7: BFKL description of the $\gamma^* p \to \gamma^* p$ cross section. Black dots stand for Lipatov's effective vertex

Fig. 1.8 sums up what was adressed : for large Q^2 and moderate s, collinear factorization applies and one seems to probe point-like quarks (the transverse resolution is of order Q^{-1}). As s grows, the target appears to become a denser and denser gluon medium, until at some point it becomes infinitely dense. This infinite density is of course a physically incomplete picture. In the BFKL formalism, it appears mathematically via the violation of the Froissard bound. Indeed at large s, cross sections behave like a power of s

$$\sigma \propto s^{\alpha_P(t)-1}, \tag{1.5}$$

where $\alpha_{\mathbb{P}}$ is the *Pomeron intercept*. This is compatible with the BFKL result

$$\alpha_{\mathbb{P}}(0) \quad = \quad 1 + \frac{\alpha_s 4N_c}{\pi} \ln(2) > 1. \tag{1.6}$$

However it was shown by Froissart that the conservation of probability, as encoded through the unitarity of the S-matrix, requires the cross section to grow slower than $\ln^2(s)$ [20]. Thus at very large center-of-mass energies, the BFKL picture is incomplete : one needs some kind of saturation effects to occur in order to slow down the growth of the cross section with s.

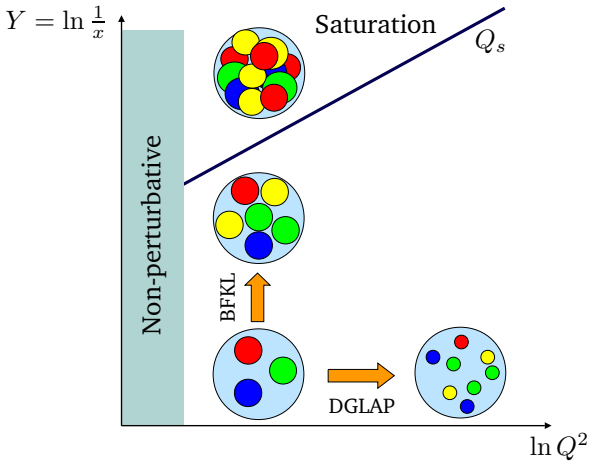

Figure 1.8: From collinear factorization to saturation

The idea to incorporate recombination terms through triple-Pomeron vertices (see Fig. 1.9) to obtain non-linear terms in the evolution equation was first introduced by Gribov, Levin and Ryskin [21]. Such an approach relies on the resummation of double logarithms $\alpha_s \ln(s) \ln(Q^2)$ and constitutes a first step towards saturation.

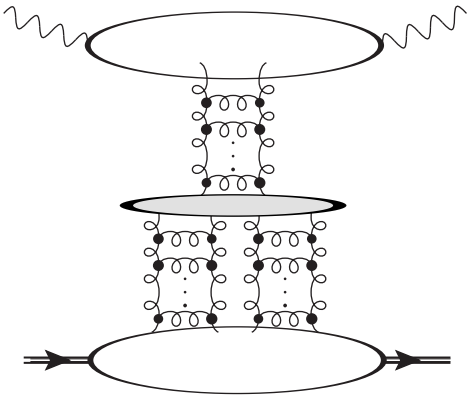

Figure 1.9: “Fan” diagram involving a triple pomeron vertex

A more involved evolution equation was later derived by Balitsky in the so-called *shockwave* approach [22–25] and by Jalilian-Marian, Iancu, McLerran, Weigert, Leonidov and Kovner (JIMWLK) in the so-called *Color Glass Condensate* (CGC) approach [26–34]. This Balitsky-JIMWLK (B-JIMWLK) equation (actually a hierarchy of equations, see part 2 of this thesis for further details) reduces, in the dipole operator case and in the double logarithmic limit, to the GLR equation. Its large-N_c truncation was recovered by Kovchegov using Mueller's dipole formalism [35, 36]. It is estimated that the CGC formalism (or equivalently Balitsky's shockwave formalism) must be applied instead of the BFKL formalism for values of Q^2 outside the

$$Q_s^2(x) < Q^2 < \frac{Q_s^4(x)}{\Lambda_{QCD}^2} \tag{1.7}$$

range, where $Q_s^2(x) \equiv \left(Ax^{-1}\right)^{\frac{1}{3}} \Lambda_{QCD}^2$ is the *saturation scale* and A is the mass number of the target [37]. The upper bound is linked to the fact that for too large values of Q^2, k_t-factorization is no longer the right formalism to use.

In the first chapter of this thesis, we will study diffraction in the shockwave formalism. We will start by giving an introduction to Balitsky's shockwave approach for CGC computations. We first derive the tools which are needed to compute impact factors in such a frame : the Feynman rules in the presence of an external field built from slow gluons and the B-JIMWLK evolution equation for dipole operators in D dimension, both in coordinate and in momentum space. Then we will detail the computation of the impact factor for the diffractive open production of a quark-antiquark pair at NLO accuracy and the impact factor for the diffractive open production of a quark, and antiquark and a gluon. From these impact factors, we will finally build the impact factor for the exclusive production of a dijet in diffractive DIS with an emphasis on the mechanisms which are involved to cancel the divergences. We conclude by giving a list of several possible phenomenological applications and theoretical extensions or adaptations of our results.

In the second chapter, we will show how exclusive processes allow one to extract non-perturbative quantities experimentally. We will calculate the cross section for the photoproduction of a ρ meson and a photon at leading twist and at leading order in α_s and we make a full feasibility study for this process at JLAB@12GeV. We will detail the computation steps and the numerical methods which are used to obtain our estimates.

Part II

Diffraction in the shockwave approach

Chapter 2

An introduction to the shockwave formalism

The shockwave formalism, or equivalently its CGC formulation, applies when one considers the scattering of a dilute projectile on a dense target with high center-of-mass energy. The most straightforward example of such a CGC process would be DIS off a heavy ion, but DIS off a proton can also be described in the shockwave formalism if the center of mass energy of the collision is large enough. Note that the CGC formalism can also be used in nucleus-nucleus collisions [38]. Let us consider such a process with semihard kinematics $s \gg Q^2 \gg \Lambda^2_{QCD}$, where Q^2 is the hard scale of the process, so that k_t-factorization applies. We will focus on diffractive DIS : our probe will be a photon with a large momentum along the $p^3 > 0$ direction and the target will be a nucleon with a large momentum along the $p^3 < 0$ direction. We introduce two lightcone vectors n_1 and n_2 as such :

$$n_1 \equiv \frac{1}{\sqrt{2}}\left(1, 0_\perp, 1\right), \quad n_2 \equiv \frac{1}{\sqrt{2}}\left(1, 0_\perp, -1\right), \quad n_1^+ = n_2^- = (n_1 \cdot n_2) = 1. \tag{2.1}$$

For any vector p we denote

$$p^+ = p_- \equiv (p \cdot n_2) = \frac{1}{\sqrt{2}}\left(p^0 + p^3\right), \qquad p_+ = p^- \equiv (p \cdot n_1) = \frac{1}{\sqrt{2}}\left(p^0 - p^3\right), \tag{2.2}$$

$$p = p^+ n_1 + p^- n_2 + p_\perp, \tag{2.3}$$

so that

$$(p \cdot k) = p^\mu k_\mu = p^+ k^- + p^- k^+ + (p_\perp \cdot k_\perp) \equiv p_+ k_- + p_- k_+ - (\vec{p} \cdot \vec{k}). \tag{2.4}$$

In this chapter and in the next one, we will work in dimension $D \equiv 2 + d \equiv 4 + 2\epsilon$, so the transverse momentum components will lay in a d-dimensional space. We will introduce a regularization scale μ with the dimension of a mass, since in dimensional regularization the coupling constant is a dimensional quantity :

$$g_0 = g\,\mu^{-\epsilon}, \quad \alpha_{s0} = \alpha_s\,\mu^{-2\epsilon}. \tag{2.5}$$

With these lightcone notations and in the Regge limit the projectile momentum p_p and the target momentum p_t will have large components respectively along n_1 and along n_2, so that :

$$p_p^+,\, p_t^- \sim \sqrt{\frac{s}{2}}. \tag{2.6}$$

The B-JIMWLK picture is a k_t-factorization formalism : the cross section is factorized into a projectile impact factor and a target impact factor with the exchange of eikonal gluons with *non-sense polarizations* in t-channel. The shockwave approach relies on the separation of the gluonic field depending on its rapidity (see Fig. 2), in the spirit of the renormalization group : one integrates over the fast modes in the impact factor, and the integration over the slow modes will lead to a renormalization equation for the effective Wilson lines exchanged in t-channel.

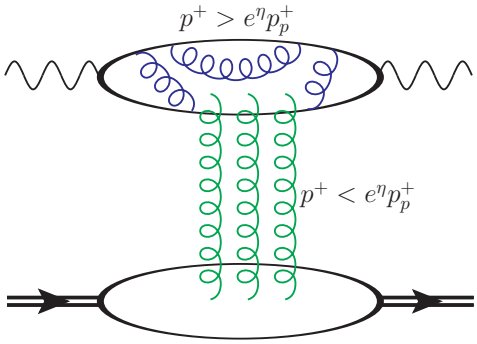

Figure 2.1: Rapidity separation

When considering the projectile, gluons with positive $+$-momentum above a certain cutoff $e^\eta p_p^+$ ($\eta < 0$) will contribute to the quantum corrections to the impact factor while the gluons with $+$-momentum lower than this cutoff will act as an external field and will be treated as Wilson line operators. The quantum corrections to the Wilson lines will lead to the resummation of logarithms, which contribute to the B-JIMWLK evolution equation for the Wilson lines. This evolution equation then allows one to get rid of the non-physical cutoff $e^\eta p_p^+$ and is the non-linear extension of the BFKL equation in the shockwave picture.

The B-JIMWLK equation was derived at LL accuracy in [22–34]. Its large N_c limit (or equivalently its mean field approximation) was derived in Mueller's dipole picture in [35, 36]. Progress has been made towards a general NLL description of the evolution equation in Balitsky's picture in [39], and the JIMWLK Hamiltonian is known at NLL accuracy [40]. B-JIMWLK evolution is now known explicitly at LL and NLL accuracy for the dipole operator [41–44], for the 3-point operator [45,46] and for 4-point operators [47–51]. Some progress has been made towards moderate-x extensions of B-JIMWLK in [52, 53]. In the CGC picture for a dense target, "next-to-eikonal" and "next-to-next-to-eikonal" $A^{-1}-$corrections have been computed in [54, 55].

Throughout this chapter, we will develop some techniques to compute projectile impact factors. We will write the complete set of Feynman rules for such a computation, then we will derive the B-JIMWLK evolution equation in D dimensions in coordinate space and in momentum space.

2.1 The boosted gluonic field

Let us consider a gluon field $b_0^\mu(z)$ in the target rest frame. We go to the projectile rest frame by a Lorentz transformation with velocity β along the z^+ axis. We introduce the new coordinates as :

$$\left(x^+, x^-, \vec{x}\right) \equiv \left(\frac{z^+}{\Lambda}, \Lambda z^-, \vec{z}\right), \tag{2.7}$$

$$\Lambda \equiv \sqrt{\frac{1+\beta}{1-\beta}}. \tag{2.8}$$

Then the gluonic field in the new frame b^μ reads :

$$\begin{aligned} b^+\left(x^+, x^-, \vec{x}\right) &= \frac{1}{\Lambda} b_0^+(\Lambda x^+, \frac{x^-}{\Lambda}, \vec{x}), \\ b^-\left(x^+, x^-, \vec{x}\right) &= \Lambda b_0^-(\Lambda x^+, \frac{x^-}{\Lambda}, \vec{x}), \\ b^i\left(x^+, x^-, \vec{x}\right) &= b_0^i(\Lambda x^+, \frac{x^-}{\Lambda}, \vec{x}). \end{aligned} \tag{2.9}$$

We will assume that the field vanishes at infinity. Then for a very large boost, the right-hand side of Eq. (2.9) involves the field at close to infinite lightcone time x^+, which then vanishes for both the $+$ and

i components of the field. Thus up to a Λ^{-1} correction, one can write :

$$\begin{aligned} b^+\left(x^+,\, x^-,\, \vec{x}\right) &= 0\,, \\ b^-\left(x^+,\, x^-,\, \vec{x}\right) &= \Lambda b_0^+(\Lambda x^+,\, \frac{x^-}{\Lambda},\, \vec{x}\,)\,, \\ b^i\left(x^+,\, x^-,\, \vec{x}\right) &= 0\,. \end{aligned} \tag{2.10}$$

The $-$ component of the field loses any dependence on x^- since for large Λ it will always be evaluated at $x^- = 0$. One can trivially check via the action on a test function that for any integrable function F,

$$\lim_{\Lambda\to\infty} \Lambda F\left(\Lambda x\right) \quad \propto \quad \delta\left(x\right)\,. \tag{2.11}$$

Thus we can finally write

$$b^\mu\left(x^+,\, x^-,\, \vec{x}\right) \quad = \quad b^-\left(x^+,\, \vec{x}\right) n_2^\mu \quad \equiv \quad \delta\left(x^+\right) \mathbf{B}\left(\vec{x}\right) n_2^\mu\,. \tag{2.12}$$

Let us now consider the collision of our projectile with a large momentum p_p along p^+ on a target with a large momentum p_t along p^- and with mass m_t. Then the energy of the target in the projectile's frame is

$$E \,=\, \frac{m_t}{\sqrt{1-\beta^2}} \,=\, \frac{p_t^+ + p_t^-}{\sqrt{2}} \,\sim\, \frac{p_t^-}{\sqrt{2}}\,. \tag{2.13}$$

Hence the boost to go from the target frame to the projectile frame is of order

$$\beta \quad \sim \quad 1 - \frac{m_t^2}{(p_t^-)^2}. \tag{2.14}$$

Thus

$$\Lambda \quad \sim \quad \sqrt{2}\frac{p_t^-}{m}. \tag{2.15}$$

Hence basically

$$\Lambda \quad \sim \quad \sqrt{\frac{s}{m_t}} \tag{2.16}$$

when $p_p^+ \sim p_t^- \sim \sqrt{\frac{s}{2}}$. This is the reason why we will always consider Λ^{-1} corrections to be of order $\frac{1}{\sqrt{s}}$ hence negligible. When computing a projectile impact factor, the field from the target will thus be described as an external field with the form of Eq. (2.12). This is the picture we will use from now on.

2.2 Feynman rules in the shockwave field

2.2.1 Lagrangian

The QCD Lagrangian $\mathcal{L}$ reads :

$$\mathcal{L} \quad = \quad -\frac{1}{4}\mathcal{F}_{a\mu\nu}\mathcal{F}^{a\mu\nu} + i\bar{\psi}\hat{D}\psi \tag{2.17}$$

$$\begin{aligned} &= \mathcal{L}_{free} - g f_{abc}\left(\partial_\mu \mathcal{A}_\nu^a\right)\left(\mathcal{A}^{\mu b}\mathcal{A}^{\nu c}\right) - \frac{1}{4}g^2 f_{abc}f_{ade}\left(\mathcal{A}_\mu^a \mathcal{A}_\nu^b \mathcal{A}^{\mu d}\mathcal{A}^{\nu e}\right) \\ &\quad + i\bar{\psi}\left(-igt^a\hat{\mathcal{A}}^a\right)\psi, \end{aligned} \tag{2.18}$$

where we separated the interacting part and the non-interacting part $\mathcal{L}_{free}$. Throughout this thesis, we will use the notation $\hat{k} \equiv \gamma^\mu k_\mu$. Let us split the gluonic field into the internal field A_μ and the external field b_μ :

$$\mathcal{A}_\mu^a \quad = \quad A_\mu^a + b_\mu^a\,. \tag{2.19}$$

Using the fact that $b^\mu b_\mu \propto n_2^2 = 0$, one gets :

$$\begin{aligned}\mathcal{L} &= -gf_{abc}\left[\left(\left(A^b\cdot\partial\right)A^a+\left(b^b\cdot\partial\right)A^a\right)\cdot\left(A^c+b^c\right)+\left(\left(A^b\cdot\partial\right)b^a+\left(b^b\cdot\partial\right)b^a\right)\cdot A^c\right]\\ &\quad -\frac{1}{4}g^2f_{abc}f_{ade}\left[\left(\left(A^a\cdot A^d\right)+\left(b^d\cdot A^a\right)\right)\left(\left(A^b\cdot A^e\right)+\left(b^e\cdot A^b\right)+\left(b^b\cdot A^e\right)\right)\right.\\ &\quad \left.+\left(b^a\cdot A^d\right)\left(\left(A^b\cdot A^e\right)+\left(b^e\cdot A^b\right)+\left(b^b\cdot A^e\right)\right)\right]\\ &\quad +i\bar\psi\left[-igt^a\left(\hat A^a+\hat b^a\right)\right]\psi\,. \end{aligned} \tag{2.20}$$

Using the lightcone gauge $(n_2\cdot A)=0$ simplifies this Lagrangian a great deal since in that case $(b\cdot A)=0$. It becomes :

$$\begin{aligned}\mathcal{L} &= -gf_{abc}\left(A^b\cdot\partial\right)\left(A^a\cdot A^c\right)-\frac{1}{4}g^2f_{abc}f_{ade}\left[\left(A^a\cdot A^d\right)\left(A^b\cdot A^e\right)\right]\\ &\quad +i\bar\psi\left[-igt^a\hat A^a\right]\psi\\ &\quad -gf_{abc}\left(b^b\cdot\partial\right)\left(A^a\cdot A^c\right)+gt^a\left(\bar\psi\hat b^a\psi\right)\,. \end{aligned} \tag{2.21}$$

The part where the internal field interacts with the shockwave field thus reads :

$$\mathcal{L}_{int} = -gf_{acb}b^{-c}g_{\alpha\beta}\left[A^a_\alpha\frac{\partial A^b_\beta}{\partial x^-}\right]+g\left(\bar\psi t^a\hat b^a\psi\right). \tag{2.22}$$

2.2.2 Quark propagator through the shockwave field

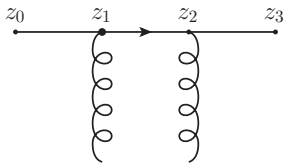

Figure 2.2: Quark propagator with 2 interactions with the external field

Using the Lagrangian in Eq. (2.22) one can write the propagator for a quark interacting twice with the external field while propagating from point z_0 at negative lightcone time to point z_3 at positive lightcone time (Fig. 2.2) :

$$\begin{aligned}G\left(z_3,\,z_0\right)|_{z_3^+>0>z_0^+} &= \int d^Dz_2d^Dz_1G_0\left(z_{32}\right)\left[igb^-\left(z_2\right)\gamma^+\right]G_0\left(z_{21}\right)\left[igb^-\left(z_1\right)\gamma^+\right]G_0\left(z_{10}\right)\\ &= \int d^Dz_2d^Dz_1\left[igb^-\left(z_2\right)igb^-\left(z_1\right)\right]\int\frac{d^Dp_3}{\left(2\pi\right)^D}\frac{d^Dp_2}{\left(2\pi\right)^D}\frac{d^Dp_1}{\left(2\pi\right)^D}\\ &\quad \times G_0\left(p_3\right)\gamma^+G_0\left(p_2\right)\gamma^+G_0\left(p_1\right)\\ &\quad \times\exp\left[-i\left(p_3\cdot z_3\right)+i\left(p_3-p_2\right)\cdot z_2+i\left(p_2-p_1\right)\cdot z_1+i\left(p_1\cdot z_0\right)\right]. \end{aligned} \tag{2.23}$$

Here, G_0 is the free quark propagator. $b^-\left(z\right)$ does not depend on z^- so one can integrate w.r.t. z_2^- and z_1^- to get the explicit conservation of the + component of the momentum $\delta\left(p_3^+-p_2^+\right)\delta\left(p_2^+-p_1^+\right)$. Then :

$$\begin{aligned}G\left(z_3,\,z_0\right)|_{z_3^+>0>z_0^+} &= \left(2\pi\right)^2\int dz_2^+dz_1^+d^d\vec z_2d^d\vec z_1\left[igb^-\left(z_2^+,\,\vec z_2\right)igb^-\left(z_1^+,\,\vec z_1\right)\right]\\ &\quad \times\int dp^+\int\frac{d^d\vec p_3}{\left(2\pi\right)^D}\frac{d^d\vec p_2}{\left(2\pi\right)^D}\frac{d^d\vec p_1}{\left(2\pi\right)^D}\exp\left[i\left(\vec p_3\cdot\vec z_{32}\right)+i\left(\vec p_2\cdot\vec z_{21}\right)+i\left(\vec p_1\cdot\vec z_{10}\right)-ip^+z_{30}^-\right]\\ &\quad \times\int dp_3^-\frac{i\left(p^+\gamma^-+\hat p_{3\perp}\right)}{2p^+\left(p_3^--\frac{\vec p_3^{\,2}-i0}{2p^+}\right)}\exp\left[-ip_3^-z_{32}^+\right] \end{aligned} \tag{2.24}$$

$$\times \int dp_2^- \gamma^+ \frac{i\left(p^+\gamma^- + \hat{p}_{2\perp}\right)}{2p^+\left(p_2^- - \frac{\vec{p}_2^{\,2}-i0}{2p^+}\right)}\gamma^+ \exp\left[-ip_2^- z_{21}^+\right]$$
$$\times \int dp_1^- \frac{i\left(p^+\gamma^- + \hat{p}_{1\perp}\right)}{2p^+\left(p_1^- - \frac{\vec{p}_1^{\,2}-i0}{2p^+}\right)} \exp\left[-ip_1^- z_{10}^+\right].$$

Note that throughout this thesis, every integral written without bound is taken from $-\infty$ to $+\infty$. A straightforward pole integration gives :

$$\begin{aligned} G\left(z_3,\, z_0\right)|_{z_3^+>0>z_0^+} &= (2\pi)^5 \int dz_2^+ dz_1^+ d^d\vec{z}_2 d^d\vec{z}_1 \left[igb^-\left(z_2^+,\,\vec{z}_2\right) igb^-\left(z_1^+,\,\vec{z}_1\right)\right] \\ &\times \int dp^+ \theta\left(p^+\right)\theta\left(z_{32}^+\right)\theta\left(z_{21}^+\right)\theta\left(z_{10}^+\right)\exp\left[-ip^+ z_{30}^-\right] \\ &\times \int \frac{d^d\vec{p}_3}{(2\pi)^D}\frac{\left(p^+\gamma^- + \hat{p}_{3\perp}\right)}{2p^+}\exp\left[-i\frac{z_{32}^+}{2p^+}\left\{\left(\vec{p}_3 - \frac{p^+}{z_{32}^+}\vec{z}_{32}\right)^2 - \left(\frac{p^+}{z_{32}^+}\right)^2 \vec{z}_{32}^{\,2} - i0\right\}\right] \\ &\times \int \frac{d^d\vec{p}_2}{(2\pi)^D}\gamma^+ \exp\left[-i\frac{z_{21}^+}{2p^+}\left(\vec{p}_2^{\,2} - i0\right) + i\left(\vec{p}_2\cdot\vec{z}_{21}\right)\right] \\ &\times \int \frac{d^d\vec{p}_1}{(2\pi)^D}\frac{\left(p^+\gamma^- + \hat{p}_{1\perp}\right)}{2p^+}\exp\left[-i\frac{z_{10}^+}{2p^+}\left\{\left(\vec{p}_1 - \frac{p^+}{z_{10}^+}\vec{z}_{10}\right)^2 - \left(\frac{p^+}{z_{10}^+}\right)^2 \vec{z}_{10}^{\,2} - i0\right\}\right]. \end{aligned} \tag{2.25}$$

We saw previously that up to a $\frac{1}{\sqrt{s}}$ correction, $b^-\left(z^+,\,\vec{z}\right) \propto \delta\left(z^+\right)$. Thus the $\vec{p}_2$ gaussian integral shrinks into a δ function up to $\frac{1}{\sqrt{s}}$, which allows one to show explicitely that the interaction with the shockwave field occurs at a single transverse coordinate. To make the $\vec{p}_3$ and $\vec{p}_1$ gaussian integrals converge, let us note that $\frac{z_{32}^+}{p^+} > 0$. One can replace $i0$ by $i0C$ for any positive C. This way one can manipulate the $i0$ factors :

$$\begin{aligned} & -i\frac{z_{32}^+}{2p^+}\left[\left(\vec{p}_3 - \frac{p^+}{z_{32}^+}\vec{z}_{32}\right)^2 - \left(\frac{p^+}{z_{32}^+}\right)^2 \vec{z}_{31}^{\,2} - i0\right] \\ = & -i\frac{z_{32}^+}{2p^+}\left[\left\{\left(\vec{p}_3 - \frac{p^+}{z_{32}^+}\vec{z}_{32}\right)^2 - i0\right\} - \left(\frac{p^+}{z_{32}^+}\right)^2\left(\vec{z}_{31}^{\,2} + i0\right)\right] \\ = & -i\frac{z_{32}^+}{2p^+}\left(1 - i0\right)\left(\vec{p}_3 - \frac{p^+}{z_{32}^+}\vec{z}_{32}\right)^2 + i\frac{p^+}{2z_{32}^+}\left(\vec{z}_{31}^{\,2} + i0\right). \end{aligned} \tag{2.26}$$

A similar trick can be used for $\vec{p}_1$. Thus one finally ends up with three convergent transverse integrations. Performing them gives :

$$\begin{aligned} G\left(z_3,\, z_0\right)|_{z_3^+>0>z_0^+} &= \int dz_2^+ dz_1^+ d^d\vec{z}_2 d^d\vec{z}_1 \left[igb^-\left(z_2^+,\,\vec{z}_2\right) igb^-\left(z_1^+,\,\vec{z}_1\right)\right] \frac{\delta\left(\vec{z}_{21}\right)}{4\left(2\pi\right)^{2D-3}} \\ &\times \left(\gamma^- + \frac{\hat{z}_{31\perp}}{z_{32}^+}\right)\gamma^+\left(\gamma^- + \frac{\hat{z}_{10\perp}}{z_{10}^+}\right)\int dp^+\left(\frac{-2i\pi p^+}{z_{32}^+}\right)^{\frac{d}{2}}\left(\frac{-2i\pi p^+}{z_{10}^+}\right)^{\frac{d}{2}} \\ &\times\theta\left(p^+\right)\theta\left(z_{32}^+\right)\theta\left(z_{21}^+\right)\theta\left(z_{10}^+\right) \\ &\times \exp\left[-ip^+ z_{30}^- + i\frac{p^+}{2z_{32}^+}\left(\vec{z}_{31}^{\,2} + i0\right) + i\frac{p^+}{2z_{10}^+}\left(\vec{z}_{10}^{\,2} + i0\right)\right] \end{aligned} \tag{2.27}$$

$$\begin{aligned} &= i\frac{\Gamma\left(D-1\right)}{4\left(2\pi\right)^{D-1}}\int dz_2^+ dz_1^+ d^d\vec{z}_1 \left[igb^-\left(z_2^+,\,\vec{z}_1\right) igb^-\left(z_1^+,\,\vec{z}_1\right)\right] \\ &\times \frac{\left(z_3^+\gamma^- + \hat{z}_{31\perp}\right)\gamma^+\left(-z_0^+\gamma^- + \hat{z}_{10\perp}\right)}{\left(-z_3^+ z_0^+\right)^{\frac{D}{2}}}\frac{\theta\left(z_{32}^+\right)\theta\left(z_{21}^+\right)\theta\left(z_{10}^+\right)}{\left(-z_{30}^- + \frac{\vec{z}_{31}^{\,2}+i0}{2z_3^+} - \frac{\vec{z}_{10}^{\,2}+i0}{2z_0^+}\right)^{D-1}}. \end{aligned} \tag{2.28}$$

Let us define

$$U_{\vec{z}}^{(2)} = (ig)^2 \int dz_2^+ dz_1^+ \theta\left(z_{32}^+\right)\theta\left(z_{21}^+\right)\theta\left(z_{10}^+\right) b^-\left(z_2^+,\,\vec{z}\right) b^-\left(z_1^+,\,\vec{z}\right). \tag{2.29}$$

Then

$$G\left(z_3,\,z_0\right)|_{z_3^+>0>z_0^+} \;=\; i\frac{\Gamma\left(D-1\right)}{4\left(2\pi\right)^{D-1}}\int d^d\vec{z}_1 U^{(2)}_{\vec{z}_1}\frac{\left(z_3^+\gamma^- + \hat{z}_{31\perp}\right)\gamma^+\left(-z_0^+\gamma^- + \hat{z}_{10\perp}\right)}{\left(-z_3^+ z_0^+\right)^{\frac{D}{2}}\left(-z_{30}^- + \frac{\vec{z}_{31}^{\,2}}{2z_3^+} - \frac{\vec{z}_{10}^{\,2}}{2z_0^+} + i0\right)^{D-1}}\,. \quad (2.30)$$

The physical interpretation of this expression is not obvious, although it was now proven that the quark field interacts instantly and at a single transverse point with the external gluonic field. The following computation will give a more meaningful, although less complete, expression. Let us define

$$\tilde{G}\left(z_3,\,z_0\right)|_{z_3^+>0>z_0^+} \;\equiv\; -\int d^D z_1 \delta\left(z_1^+\right) G_0\left(z_{31}\right)\gamma^+ G_0\left(z_{10}\right)\theta\left(z_3^+\right)\theta\left(-z_0^+\right) U^{(2)}_{\vec{z}_1}\,, \quad (2.31)$$

and compare it to our result for $G\left(z_3,\,z_0\right)$. One has :

$$\tilde{G}\left(z_3,\,z_0\right)|_{z_3^+>0>z_0^+} \;=\; \left[\frac{\Gamma\left(\frac{D}{2}\right)}{2\pi^{\frac{D}{2}}}\right]^2\int dz_1^- d^d\vec{z}_1 U^{(2)}_{\vec{z}_1}\frac{\left(z_3^+\gamma^- + \hat{z}_{31\perp}\right)\gamma^+\left(-z_0^+\gamma^- + \hat{z}_{10\perp}\right)}{\left(-2z_3^+ z_{31}^- + \vec{z}_{31}^{\,2} + i0\right)^{\frac{D}{2}}\left(2z_0^+ z_{10}^- + \vec{z}_{10}^{\,2} + i0\right)^{\frac{D}{2}}}\,. \quad (2.32)$$

One now has to use the Schwinger representation for the denominators :

$$\frac{1}{\left(A\pm i0\right)^n} = \frac{\left(\mp i\right)^n}{\Gamma(n)}\int_0^{+\infty} d\alpha(\alpha^{n-1}) e^{\pm i\alpha\left(A\pm i0\right)}. \quad (2.33)$$

Integrating straightforwardly w.r.t. z_1^- then w.r.t. one of the Schwinger parameters, one gets :

$$\begin{aligned}\tilde{G}\left(z_3,\,z_0\right)|_{z_3^+>0>z_0^+} \;&=\; -\frac{\left(-i\right)^D}{4\pi^{D-1}}\int d^d\vec{z}_1\left(-\frac{z_3^+}{z_0^+}\right)^{\frac{d}{2}}\frac{\left(z_3^+\gamma^- + \hat{z}_{31\perp}\right)\gamma^+\left(-z_0^+\gamma^- + \hat{z}_{10\perp}\right)}{z_0^+}\\ &\times U^{(2)}_{\vec{z}_1}\int_0^{+\infty} d\alpha_1\left(\alpha_1\right)^d \exp\left[i\alpha_1\left(-2z_3^+ z_{30}^- + \vec{z}_{31}^{\,2} - \frac{z_3^+}{z_0^+}\vec{z}_{10}^{\,2} + i0\right)\right]\,. \quad (2.34)\end{aligned}$$

Integrating w.r.t. the Schwinger parameter now gives :

$$\begin{aligned}\tilde{G}\left(z_3,\,z_0\right)|_{z_3^+>0>z_0^+} \;&=\; \frac{i\Gamma\left(D-1\right)}{4\left(2\pi\right)^{D-1}}\int d^d\vec{z}_1\frac{\left(z_3^+\gamma^- + \hat{z}_{31\perp}\right)\gamma^+\left(-z_0^+\gamma^- + \hat{z}_{10\perp}\right)}{\left(-z_3^+ z_0^+\right)^{\frac{D}{2}}}\\ &\times\frac{\theta\left(z_3^+\right)\theta\left(-z_0^+\right)U^{(2)}_{\vec{z}_1}}{\left(-z_{30}^- + \frac{\vec{z}_{31}^{\,2}}{2z_3^+} - \frac{\vec{z}_{10}^{\,2}}{2z_0^+} + i0\right)^{D-1}}\,. \quad (2.35)\end{aligned}$$

The comparison with Eq. (2.30) allows us to conclude :

$$G\left(z_3,\,z_0\right)|_{z_3^+>0>z_0^+} \;=\; \tilde{G}\left(z_3,\,z_0\right)|_{z_3^+>0>z_0^+}\,. \quad (2.36)$$

We thus found a second expression for $G\left(z_3,\,z_0\right)$. The physical interpretation of Eq. (2.31) is very clear. The quark propagator can be decomposed in three parts : first the quark propagates from z_0 to z_1, then it interacts instantly at $z_1^+ = 0$ with the external field, then it propagates again from z_1 to z_3. Let us note that $U^{(2)}_{\vec{z}}$ is actually the $\left(ig\right)^2$ term in the (ig)-expansion of the Wilson line

$$\left[z_3^+,\,z_0^+\right]_{\vec{z}} \;=\; \mathcal{P}\exp\left[ig\int_{z_0^+}^{z_3^+} dz^+ b^-\left(z^+,\,\vec{z}\right)\right]\,, \quad (2.37)$$

where $\mathcal{P}$ is the time-ordered product. It is then easy to generalize $G\left(z_3,\,z_0\right)$ as follows :

$$G\left(z_3,\,z_0\right)|_{z_3^+>0>z_0^+} \;=\; \int d^D z_1\delta\left(z_1^+\right) G_0\left(z_{31}\right)\gamma^+ G_0\left(z_{10}\right)\left[z_3^+,\,z_0^+\right]_{\vec{z}_1}\,. \quad (2.38)$$

The recursion goes as follows : let us define $G^{(n)}(z_3,\,z_0)$ the propagator with n interactions with the external field and $\left[z_3^+,\,z_0^+\right]_{\vec{z}_1}^{(n)}$ the $(ig)^n$ term in the expansion of $\left[z_3^+,\,z_0^+\right]_{\vec{z}_1}$ and suppose we proved

$$G^{(n)}(z_3,\,z_0)\,|_{z_3^+>0>z_0^+} \;=\; \int d^D z_1 \delta\left(z_1^+\right) G_0\left(z_{31}\right)\gamma^+ G_0\left(z_{10}\right)\left[z_3^+,\,z_0^+\right]_{\vec{z}_1}^{(n)}\,. \tag{2.39}$$

Then

$$G^{(n+1)}(z_3,\,z_0)\,|_{z_3^+>0>z_0^+} \;=\; \int d^D z_2 G_0\left(z_{32}\right)\left[ig\gamma^+ b^-\left(z_2\right)\right] G^{(n)}\left(z_2,\,z_0\right) \tag{2.40}$$

$$\begin{aligned} &= (ig)\int d^D z_2 d^D z_1 b^-\left(z_2\right)\delta\left(z_1^+\right)\left[G_0\left(z_{32}\right)\gamma^+ G_0\left(z_{21}\right)\gamma^+ G_0\left(z_{10}\right)\right] \\ &\quad\times\theta\left(z_2^+\right)\left[z_2^+,\,z_0^+\right]_{\vec{z}_1}^{(n)}\,. \end{aligned} \tag{2.41}$$

The integration is exactly the same as before :

$$\begin{aligned} G^{(n+1)}(z_3,\,z_0)\,|_{z_3^+>0>z_0^+} &= \int d^D z_1\delta\left(z_1^+\right)\left[G_0\left(z_{31}\right)\gamma^+ G_0\left(z_{10}\right)\right] \\ &\quad\times(ig)\int dz_2^+\theta\left(z_{32}^+\right)\theta\left(z_2^+\right)\theta\left(-z_0^+\right) b^-\left(z_2^+,\,\vec{z}_1\right)\left[z_2^+,\,z_0^+\right]_{\vec{z}_1}^{(n)}\,. \end{aligned} \tag{2.42}$$

Given the definition (2.37) of the Wilson lines, it is now straightforward that

$$G^{(n+1)}(z_3,\,z_0)\,|_{z_3^+>0>z_0^+} = \int d^D z_1\delta\left(z_1^+\right)\left[G_0\left(z_{31}\right)\gamma^+ G_0\left(z_{10}\right)\right]\theta\left(z_3^+\right)\theta\left(-z_0^+\right)\left[z_3^+,\,z_0^+\right]_{\vec{z}_1}^{(n+1)}\,. \tag{2.43}$$

This ends the proof of recursivity of this property.
We proved the $n=2$ step already, and the $n=1$ step is trivial. Let us prove the $n=0$ step by setting the Wilson lines to identity in Eq. (2.34) :

$$\begin{aligned} G^{(0)}(z_3,\,z_0)\,|_{z_3^+>0>z_0^+} &= -\frac{(-i)^D}{4\pi^{D-1}}\int d^d\vec{z}_1\left(-\frac{z_3^+}{z_0^+}\right)^{\frac{d}{2}}\frac{\left(z_3^+\gamma^- + \hat{z}_{31\perp}\right)\gamma^+\left(-z_0^+\gamma^- + \hat{z}_{10\perp}\right)}{z_0^+} \\ &\quad\times\int_0^{+\infty} d\alpha_1\left(\alpha_1\right)^d\exp\left[i\alpha_1\left(-2z_3^+ z_{30}^- + \vec{z}_{31}^{\,2} - \frac{z_3^+}{z_0^+}\vec{z}_{10}^{\,2} + i0\right)\right]\,. \end{aligned} \tag{2.44}$$

By shifting $\vec{z}_1$ to get a gaussian and integrating, this becomes :

$$\begin{aligned} G^{(0)}(z_3,\,z_0)\,|_{z_3^+>0>z_0^+} &= -\frac{(-i)^D}{4\pi^{D-1}z_0^+}\left(-\frac{z_3^+}{z_0^+}\right)^{\frac{d}{2}}\int_0^{+\infty} d\alpha_1\left(\alpha_1\right)^{\frac{d}{2}} \\ &\quad\left[-2z_3^+ z_0^+\left(\gamma^-\right) - 2\frac{z_3^+ z_0^+}{z_{30}^+}\left(\hat{z}_{30\perp}\right) - \frac{z_3^+ z_0^+\vec{z}_{30}^{\,2}}{\left(z_{30}^+\right)^2}\left(\gamma^+\right) + i\frac{d}{2}\frac{z_0^+}{\alpha_1 z_{30}^+}\left(\gamma^+\right)\right] \\ &\quad\times\exp\left[i\alpha_1\left(-2z_3^+ z_{30}^- + \frac{z_3^+}{z_{30}^+}\vec{z}_{30}^{\,2} + i0\right)\right]\left(\frac{-i\pi z_0^+}{z_{30}^+}\right)^{\frac{d}{2}}\,. \end{aligned} \tag{2.45}$$

The last integration finally gives :

$$\begin{aligned} G^{(0)}(z_3,\,z_0)\,|_{z_3^+>0>z_0^+} &= \frac{i\Gamma\left(\frac{D}{2}\right)}{2\pi^{\frac{D}{2}}}\frac{\hat{z}_{30}}{\left(-z_{30}^2+i0\right)^{\frac{D}{2}}} \\ &= G_0\left(z_3,\,z_0\right)\,. \end{aligned} \tag{2.46}$$

This ends our proof. Let us finally define

$$\begin{aligned} U_{\vec{z}} &\equiv \left[-\infty,\,+\infty\right]_{\vec{z}} \\ &= \mathcal{P}\exp\left[ig\int_{-\infty}^{+\infty} dz^+ b^-\left(z^+,\,\vec{z}\right)\right]\,, \end{aligned} \tag{2.47}$$

and its Fourier transform

$$U(p_\perp) \equiv \int d^d z_\perp e^{i(p_\perp \cdot z_\perp)} U_{\vec{z}} \tag{2.48}$$

Let us note that for $z_1^+ z_0^+ > 0$, $\left[z_1^+,\, z_0^+\right]_{\vec{z}} = 1$ and for $z_1^+ z_0^+ < 0$, $\left[z_1^+,\, z_0^+\right]_{\vec{z}} = U_{\vec{z}}$.
Indeed $b^-(z) \propto \delta(z^+)$ so if the z^+ integration does not cross the $z^+ = 0$ line it is null and if it does one can add the integrations from $-\infty$ to z_0^+ and from z_1^+ to $+\infty$ for free. For this reason, we will work with $U_{\vec{z}}$ rather than $\left[z_0^+,\, z_1^+\right]_{\vec{z}}$ throughout most of this thesis. The complete set of Feynman rules in the presence of the shockwave field can be derived using the same steps as used in the previous derivation. They are all presented in the following section.

2.2.3 Feynman rules with a shockwave field

In this section, we will present the whole set of Feynman rules for computations in the shockwave formalism. We will not give details on their derivation, which is very similar to the previous computation. We will always distinguish two cases : for the propagators, we will write the *free propagators* when the parton propagates between two points with the same lightcone time sign so that it does not cross the shockwave, and the propagator through the shockwave field in the other cases ; for the external lines we will write the *free external lines* when the particle is emitted at a point with positive lightcone time so that it does not cross the shockwave field, and the external line through the shockwave field when it is emitted at negative lightcone time. The color indices are not explicitly written. In the free quantities they are the usual ones and in the presence of the shockwave field they are carried by the Wilson lines, which are in the fundamental representation for quarks and antiquarks and in the adjoint representation for gluons.

Free propagators

Note that there is no unambiguous definition for the free gluon propagator in the coordinate space due to the $\frac{1}{p^+}$ gauge pole.

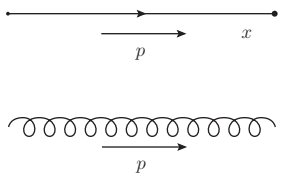

$$\hat{G}_0(p) = \frac{i\hat{p}}{p^2 + i0} \tag{2.49}$$

$$\hat{G}_0(x) = \frac{\Gamma\left(\frac{D}{2}\right)}{2\pi^{\frac{D}{2}}} \frac{i\hat{x}}{(-x^2 + i0)^{\frac{D}{2}}} \tag{2.50}$$

$$G_0^{\mu\nu}(p) = \frac{-i}{p^2 + i0}\left[g^{\mu\nu} - \frac{p^\mu n_2^\nu + p^\nu n_2^\mu}{p^+}\right] \tag{2.51}$$

Figure 2.3: Free propagators

We will sometimes use the following notation for the gluonic propagator :

$$d^{\mu\nu}(p) \equiv d_0^{\mu\nu}(p) - \frac{n_2^\mu n_2^\nu}{(p^+)^2} p^2, \tag{2.52}$$

$$d_0^{\mu\nu}(p) \equiv g_\perp^{\mu\nu} - \frac{p_\perp^\mu n_2^\nu + p_\perp^\nu n_2^\mu}{p^+} - \frac{n_2^\mu n_2^\nu}{(p^+)^2} \vec{p}^2. \tag{2.53}$$

Propagators through the shockwave field

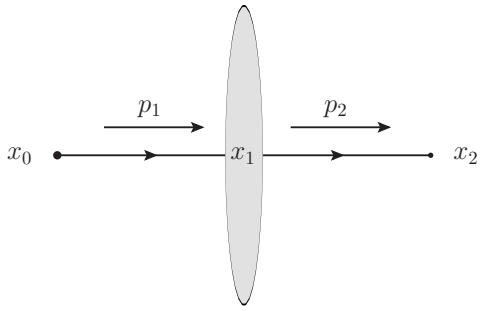

Figure 2.4: Quark propagator through the shockwave field

$$\hat{G}\left(x_2,\, x_0\right)|_{x_2^+>0>x_0^+} = -\int d^D x_1 \delta(x_1^+) U_{\vec{x}_1} \hat{G}_0(x_{21}) \gamma^+ \hat{G}_0(x_{10}) \tag{2.54}$$

$$= \frac{i\Gamma\left(d+1\right)}{4\left(2\pi\right)^{d+1}} \int d^d\vec{x}_1 \frac{U_{\vec{x}_1} \hat{x}_{21} \gamma^+ \hat{x}_{10}}{\left(-x_0^+ x_2^+\right)^{\frac{D}{2}} \left(-x_{20}^- - \frac{\vec{x}_{10}^{\,2}}{2x_0^+} + \frac{\vec{x}_{21}^{\,2}}{2x_2^+} + i0\right)^{d+1}} \tag{2.55}$$

$$= \int \frac{dp_1^+ d^d p_{1\perp}}{(2\pi)^{d+1}} \int \frac{dp_2^+ d^d p_{2\perp}}{(2\pi)^{d+1}} e^{-ix_2^- p_2^+ - i(p_{2\perp}\cdot x_{2\perp})} e^{ix_0^- p_1^+ + i(p_{1\perp}\cdot x_{0\perp})} 2\pi\delta(p_{12}^+)\theta(p_2^+)$$
$$\times e^{ix_2^+ \frac{p_{2\perp}^2 + i0}{2p_2^+}} e^{-ix_0^+ \frac{p_{1\perp}^2 + i0}{2p_1^+}} \frac{\gamma^- p_2^+ + \hat{p}_{2\perp}}{2p_2^+} \gamma^+ U(p_{21\perp}) \frac{\gamma^- p_1^+ + \hat{p}_{1\perp}}{2p_1^+}, \tag{2.56}$$

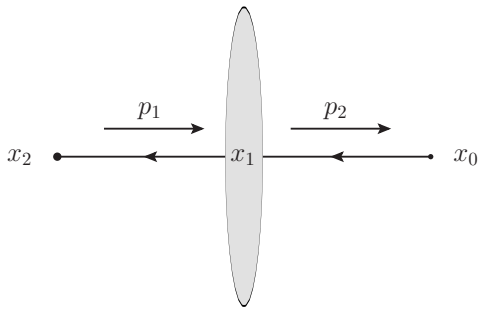

Figure 2.5: Antiquark propagator through the shockwave field

$$\hat{G}\left(x_2,\, x_0\right)|_{x_0^+>0>x_2^+} = -\int d^D x_1 \delta(x_1^+) U_{\vec{x}_1}^\dagger \hat{G}_0(x_{21}) \gamma^+ \hat{G}_0(x_{10}) \tag{2.57}$$

$$= -\frac{i\Gamma\left(d+1\right)}{4\left(2\pi\right)^{d+1}} \int d^d\vec{x}_1 \frac{U_{\vec{x}_1}^\dagger \hat{x}_{21} \gamma^+ \hat{x}_{10}}{\left(-x_0^+ x_2^+\right)^{\frac{D}{2}} \left(x_{20}^- + \frac{\vec{x}_{10}^{\,2}}{2x_0^+} - \frac{\vec{x}_{21}^{\,2}}{2x_2^+} + i0\right)^{d+1}} \tag{2.58}$$

$$= -\int \frac{dp_1^+ d^d p_{1\perp}}{(2\pi)^{d+1}} \int \frac{dp_2^+ d^d p_{2\perp}}{(2\pi)^{d+1}} e^{-ix_0^- p_2^+ - i(p_{2\perp}\cdot x_{0\perp})} e^{ix_2^- p_1^+ + i(p_{1\perp}\cdot x_{2\perp})} 2\pi\delta(p_{12}^+)\theta(p_2^+)$$
$$\times e^{ix_0^+ \frac{p_{2\perp}^2 + i0}{2p_2^+}} e^{-ix_2^+ \frac{p_{1\perp}^2 + i0}{2p_1^+}} \frac{\gamma^- p_1^+ + \hat{p}_{1\perp}}{2p_1^+} \gamma^+ U^\dagger(p_{12\perp}) \frac{\gamma^- p_2^+ + \hat{p}_{2\perp}}{2p_2^+}\,. \tag{2.59}$$

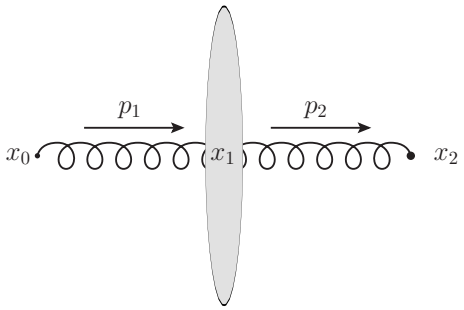

Figure 2.6: Gluon propagator through the shockwave field

$$G_{\mu\nu}\left(x_2,\,x_0\right)\big|_{x_2^+>0>x_0^+} = -\frac{\Gamma\left(d\right)}{2\left(2\pi\right)^{d+1}}\int d^d\vec{x}_1\frac{\left[x_2^+ g_{\perp\mu}^{\alpha}-x_{21\perp}^{\alpha}n_{2\mu}\right]U_{\vec{x}_1}\left[-x_0^+ g_{\perp\alpha\nu}-x_{10\perp\alpha}n_{2\nu}\right]}{\left(-x_0^+x_2^+\right)^{\frac{d}{2}+1}\left(-x_{20}^- + \frac{\vec{x}_{21}^{\,2}}{2x_2^+}-\frac{\vec{x}_{10}^{\,2}}{2x_0^+}+i0\right)^d} \tag{2.60}$$

$$= -\int\frac{dp_1^+d^dp_{1\perp}}{(2\pi)^{d+1}}\int\frac{dp_2^+d^dp_{2\perp}}{(2\pi)^{d+1}}e^{-ip_2^+x_2^- + ip_1^+x_0^-}e^{-i(p_{2\perp}\cdot x_{2\perp})+i(p_{1\perp}\cdot x_{0\perp})} \tag{2.61}$$
$$\times\pi\frac{\delta(p_{12}^+)\theta(p_2^+)}{p_1^+}e^{i\frac{p_{2\perp}^2+i0}{2p_2^+}x_2^+ - i\frac{p_{1\perp}^2+i0}{2p_1^+}x_0^+}d_{0\mu\alpha}(p_2^+,p_{2\perp})U(p_{21\perp})g_{\perp}^{\alpha\delta}d_{0\delta\nu}(p_1^+,p_{1\perp})\,,$$

Free external lines

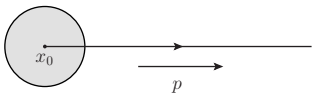

$$\bar{u}\left(p,\,x_0\right)\big|_{x_0^+>0} = \theta\left(p^+\right)\frac{\bar{u}_p}{\sqrt{2p^+}}e^{i(p\cdot x_0)} \tag{2.62}$$

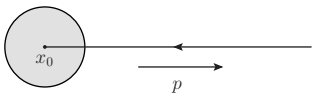

$$v\left(p,\,x_0\right)\big|_{x_0^+>0} = \theta\left(p^+\right)\frac{v_p}{\sqrt{2p^+}}e^{i(p\cdot x_0)} \tag{2.63}$$

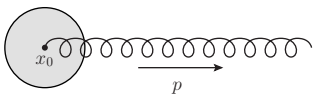

$$\epsilon_{\mu}^{*}\left(p,\,x_0\right)\big|_{x_0^+>0} = \theta\left(p^+\right)\frac{\epsilon_{\mu}^{*}}{\sqrt{2p^+}}e^{i(p\cdot x_0)} \tag{2.64}$$

Figure 2.7: Free external lines

External lines through the shockwave field

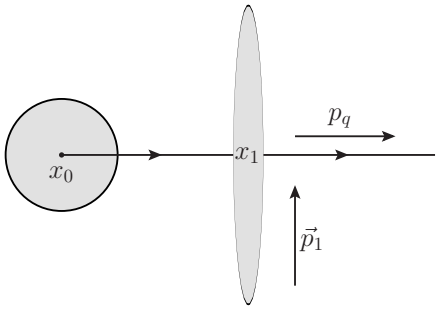

Figure 2.8: Quark line through the shockwave field

$$
\begin{aligned}
\left[\bar{u}\left(p_q,\, x_0\right)\right]^a_{0>x_0^+} &= \frac{(-i)^{\frac{d}{2}}}{2\left(2\pi\right)^{\frac{d}{2}}}\left(\frac{p_q^+}{-x_0^+}\right)^{\frac{d}{2}}\theta\left(p_q^+\right)\theta\left(-x_0^+\right)\int d^d\vec{x}_1\left(U^a_{\vec{x}_1}\right) \qquad (2.65)\\
&\quad \frac{\bar{u}_{p_q}}{\sqrt{2p_q^+}}\gamma^+\frac{-x_0^+\gamma^- + \hat{x}_{10\perp}}{-x_0^+}\exp\left[ip_q^+\left(x_0^- - \frac{\vec{x}_{10}^{\,2}}{2x_0^+} + i0\right) - i\left(\vec{p}_q\cdot\vec{x}_1\right)\right]\\
&= \frac{\theta\left(p_q^+\right)\theta\left(-x_0^+\right)}{\sqrt{2p_q^+}}\int\frac{d^d\vec{p}_1}{\left(2\pi\right)^d}\exp\left[ip_q^+x_0^- + ix_0^+\left(\frac{\vec{p}_{q1}^{\,2} - i0}{2p_q^+}\right) - i\left(\vec{p}_{q1}\cdot\vec{x}_0\right)\right] \qquad (2.66)\\
&\quad \left[U^a\left(\vec{p}_1\right)\right]\bar{u}_{p_q}\frac{\gamma^+\left(p_q^+\gamma^- + \hat{p}_{q1\perp}\right)}{2p_q^+}
\end{aligned}
$$

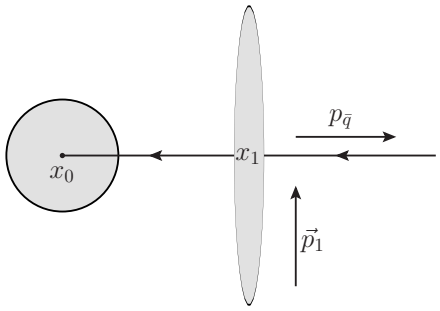

Figure 2.9: Antiquark line through the shockwave field

$$
\begin{aligned}
\left[v\left(p_{\bar{q}},\, x_0\right)\right]^a_{0>x_0^+} &= -\frac{(-i)^{\frac{d}{2}}}{2\left(2\pi\right)^{\frac{d}{2}}}\left(\frac{p_{\bar{q}}^+}{-x_0^+}\right)^{\frac{d}{2}}\theta\left(p_{\bar{q}}^+\right)\theta\left(-x_0^+\right)\int d^d\vec{x}_1\left(U^{a\dagger}_{\vec{x}_1}\right) \qquad (2.67)\\
&\quad \exp\left[ip_{\bar{q}}^+\left(x_0^- - \frac{\vec{x}_{10}^{\,2}}{2x_0^+} + i0\right) - i\left(\vec{p}_{\bar{q}}\cdot\vec{x}_1\right)\right]\frac{-x_0^+\gamma^- + \hat{x}_{10\perp}}{-x_0^+}\gamma^+\frac{v_{p_{\bar{q}}}}{\sqrt{2p_{\bar{q}}^+}}\\
&= -\theta\left(p_{\bar{q}}^+\right)\theta\left(-x_0^+\right)\int\frac{d^d\vec{p}_1}{\left(2\pi\right)^d}\left[U^{a\dagger}\left(-\vec{p}_1\right)\right] \qquad (2.68)\\
&\quad \exp\left[ip_{\bar{q}}^+x_0^- + ix_0^+\left(\frac{\vec{p}_{\bar{q}1}^{\,2} - i0}{2p_{\bar{q}}^+}\right) - i\left(\vec{p}_{\bar{q}1}\cdot\vec{x}_0\right)\right]\frac{\left(p_{\bar{q}}^+\gamma^- + \hat{p}_{\bar{q}1\perp}\right)}{2p_{\bar{q}}^+}\gamma^+\frac{v_{p_{\bar{q}}}}{\sqrt{2p_{\bar{q}}^+}}
\end{aligned}
$$

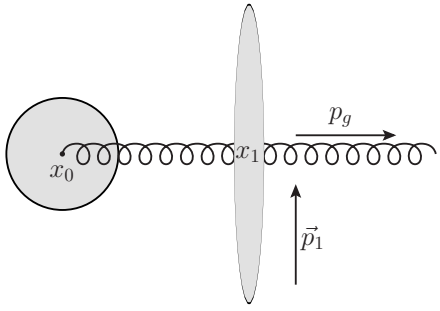

Figure 2.10: Gluon line through the shockwave field

$$
\begin{aligned}
\left[\epsilon^*_\nu\left(p_g,\,x_0\right)\right]^{ab}_{0>x_0^+} &= \frac{(-i)^{\frac{d}{2}}}{(2\pi)^{\frac{d}{2}}}\left(\frac{p_g^+}{-x_0^+}\right)^{\frac{d}{2}}\theta\left(p_g^+\right)\theta\left(-x_0^+\right)\frac{\epsilon^*_{p_g\sigma}}{\sqrt{2p_g^+}} \qquad (2.69)\\
&\int d^d\vec{x}_1\left(U^{ab}_{\vec{x}_1}\right)\left[\frac{-x_0^+ g^\sigma_{\perp\nu}-x^\sigma_{10\perp}n_{2\nu}}{-x_0^+}\right]\exp\left[ip_g^+\left(x_0^- - \frac{\vec{x}_{10}^{\,2}}{2x_0^+}+i0\right)-i\left(\vec{p}_g\cdot\vec{x}_1\right)\right]\\
&= \theta\left(p_g^+\right)\theta\left(-x_0^+\right)\frac{\epsilon^*_{p_g\sigma}}{\sqrt{2p_g^+}}\int\frac{d^d\vec{p}_1}{(2\pi)^d}\exp\left[ip_g^+\left(x_0^-+i0\right)+i\frac{x_0^+}{2p_g^+}\vec{p}_{g1}^{\,2}-i\left(\vec{p}_{g1}\cdot\vec{x}_0\right)\right]\\
&\left[U^{ab}\left(\vec{p}_1\right)\right]\left(g^\sigma_{\perp\nu}-\frac{p^\sigma_{g1\perp}}{p_g^+}n_{2\nu}\right). \qquad (2.70)
\end{aligned}
$$

2.3 B-JIMWLK equation for the dipole operator in D dimensions

2.3.1 B-JIMWLK equation for the dipole operator in D dimensions in the coordinate space

Let us decompose the external field at rapidity $\eta_1=\eta+\Delta\eta$ as follows :

$$
b^-_{\eta+\Delta\eta}\left(z\right) = b^-_\eta\left(z\right)+b^-_{\Delta\eta}\left(z\right), \qquad (2.71)
$$

where

$$
\begin{aligned}
b^-_{\Delta\eta}\left(z\right) &\equiv \int\frac{d^Dp}{(2\pi)^D}e^{-i(p\cdot z)}b^-\left(p\right)\theta\left(e^{\eta+\Delta\eta}p_p^+-p^+\right)\theta\left(p^+-e^\eta p_p^+\right) \qquad (2.72)\\
&= O\left(\Delta\eta\right)
\end{aligned}
$$

contains the gluons with $+$-momenta between $e^\eta p_p^+$ and $e^{\eta+\Delta\eta}p_p^+$. Let us rewrite the definition of the Wilson lines (2.37) :

$$
\left[x^+,\,y^+\right]^{\eta_1}_{\vec{z}} = \sum_N\int_{x^+}^{y^+}dz_1^+\left(ig\right)b^-_{\eta_1}\left(z_1^+,\,\vec{z}\right)\int_{x^+}^{z_1^+}dz_2^+\left(ig\right)b^-_{\eta_1}\left(z_2^+,\,\vec{z}\right)...\int_{x^+}^{z_{N-1}}dz_N^+\left(ig\right)b^-_{\eta_1}\left(z_N^+,\,\vec{z}\right) \qquad (2.73)
$$

Expanding this equation in the second order in $igb_{\Delta\eta}$ and using the fact that $\left[z_i^+,\,z_j^+\right]^\eta_{\vec{z}}=1$ if $z_i^+z_j^+>0$, one can get :

$$
\begin{aligned}
\left[x^+,\,y^+\right]^{\eta+\Delta\eta}_{\vec{z}} &= \left[x^+,\,y^+\right]^\eta_{\vec{z}}+\left(ig\right)\int_{x^+}^{y^+}dz_1^+\left[x^+,\,z_1^+\right]^\eta_{\vec{z}}b^-_{\Delta\eta}\left(z_1^+,\,\vec{z}\right)\left[z_1^+,\,y^+\right]^\eta_{\vec{z}} \qquad (2.74)\\
&+\left(ig\right)^2\int_{x^+}^{y^+}dz_1^+dz_2^+\left[x^+,\,z_1^+\right]^\eta_{\vec{z}}b_{\Delta\eta}\left(z_1^+,\,\vec{z}\right)\left[z_1^+,\,z_2^+\right]^\eta_{\vec{z}}b_{\Delta\eta}\left(z_2^+,\,\vec{z}\right)\left[z_2^+,\,y^+\right]^\eta_{\vec{z}}\theta\left(z_{21}^+\right).
\end{aligned}
$$

Let us consider the matrix element for two eikonal lines moving through the shockwave field at rapidity $\eta_1=\eta+\Delta\eta$ and with a color singlet interaction with the external field. When computing such a matrix element $\langle 0|...\left[x^+,\,y^+\right]^{\eta+\Delta\eta}_{\vec{z}}...|0\rangle$ at small $\Delta\eta$, the b_η fields will be considered as classical, and the $b_{\Delta\eta}$ fields will contribute to the quantum fluctuations leading to the evolution equation. In our case one line will involve $\left[-\infty,\,+\infty\right]^{\eta+\Delta\eta}_{\vec{z}_1}$ and the other one will involve $\left(\left[-\infty,\,+\infty\right]^{\eta+\Delta\eta}_{\vec{z}_2}\right)^\dagger$. The quantum corrections involving $b_{\Delta\eta}$ fields will lead to 10 Feynman diagrams to be computed. Among these 10 Feynman diagrams, 4 involve contributions where the $b_{\Delta\eta}$ gluon is emitted before the $z^+=0$ lightcone time and reabsorbed after this line, thus involving an additional adjoint Wilson line $\left(U^\eta_{\vec{z}_3}\right)^{ab}$ when the gluon crosses the shockwave field as shown in Fig. 2.11

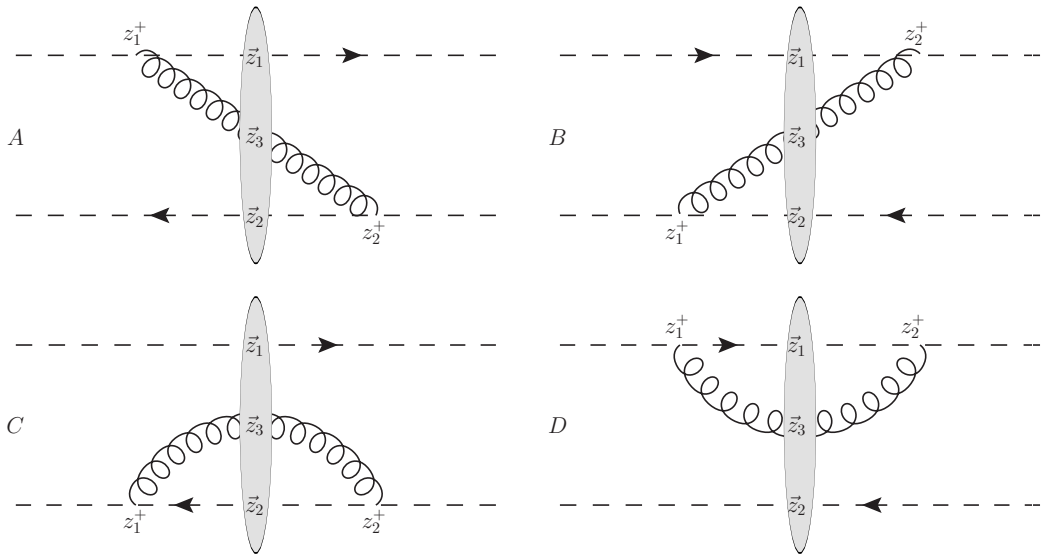

Figure 2.11: Double dipole contribution to the B-JIMWLK evolution of the dipole operator

The propagator built from $b_{\Delta\eta}$ fields reads :

$$\begin{aligned}\left(G^{\mu\nu}_{\Delta\eta}\right)^{ab} &= (-i)^d \int \frac{d^d\vec{z}_3}{(2\pi)^{d+1}} \left(U_{\vec{z}_3}\right)^{ab} \int_{e^\eta}^{e^{\eta+\Delta\eta}} dp^+ \frac{\left(p^+\right)^{d-1}}{2\left(-z_2^+ z_1^+\right)^{\frac{d}{2}+1}} \\ &\quad \times \exp\left[-ip^+\left\{z_{21}^- - \frac{\vec{z}_{21}^{\,2}}{2z_2^+} + \frac{\vec{z}_{31}^{\,2}}{2z_1^+} - i0\right\}\right] \left(\vec{z}_{23}\cdot\vec{z}_{31}\right)\left(n_2^\mu n_2^\nu\right) .\end{aligned} \tag{2.75}$$

The contribution from diagram A then reads

$$\begin{aligned} I_A &= (ig)(-ig)\mu^{-2\epsilon}\int_{-\infty}^0 dz_1^+ \int_0^{+\infty} dz_2^+ \\ &\quad \times \mathrm{Tr}\left(\left[+\infty, z_1^+\right]^\eta_{\vec{z}_1} t^b \left[z_1^+, -\infty\right]^\eta_{\vec{z}_1} \left[-\infty, z_2^+\right]^\eta_{\vec{z}_2} t^a \left[z_2^+, +\infty\right]^\eta_{\vec{z}_2}\right)\left(G_{\Delta\eta}\right)^{ab} \end{aligned} \tag{2.76}$$

$$\begin{aligned} &= \frac{(-i)^d g^2\mu^{-2\epsilon}}{2(2\pi)^{d+1}} \mathrm{Tr}\left(U^\eta_{\vec{z}_1} t^b U^{\eta\dagger}_{\vec{z}_2} t^a\right) \int d^d\vec{z}_3 \left(U^\eta_{\vec{z}_3}\right)^{ab} \int_{e^\eta}^{e^{\eta+\Delta\eta}} dp^+ \left(p^+\right)^{d-1} \\ &\quad \times \int_{-\infty}^0 \frac{dz_1^+}{\left(-z_1^+\right)^{\frac{d}{2}+1}} \int_0^{+\infty} \frac{dz_2^+}{\left(z_2^+\right)^{\frac{d}{2}+1}} \exp\left[-ip^+\left\{z_{21}^- - \frac{\vec{z}_{23}^{\,2}}{2z_2^+} + \frac{\vec{z}_{31}^{\,2}}{2z_1^+} - i0\right\}\right]\left(\vec{z}_{23}\cdot\vec{z}_{31}\right) \end{aligned} \tag{2.77}$$

$$= \frac{g^2\mu^{-2\epsilon}2^d\left[\Gamma\left(\frac{d}{2}\right)\right]^2}{2(2\pi)^{d+1}} \int d^d\vec{z}_3 \frac{\left(\vec{z}_{23}\cdot\vec{z}_{31}\right)}{\left(\vec{z}_{23}^{\,2}\right)^{\frac{d}{2}}\left(\vec{z}_{31}^{\,2}\right)^{\frac{d}{2}}} \left[\mathrm{Tr}\left(U^\eta_{\vec{z}_1} t^b U^{\eta\dagger}_{\vec{z}_2} t^a\right)\left(U^\eta_{\vec{z}_3}\right)^{ab}\right] \int_{e^\eta}^{e^{\eta+\Delta\eta}} \frac{dp^+}{p^+} e^{-ip^+\left(z_{21}^- - i0\right)}.$$

Thus

$$I_A \sim \frac{g^2\mu^{-2\epsilon}2^d\left[\Gamma\left(\frac{d}{2}\right)\right]^2}{2(2\pi)^{d+1}} \int d^d\vec{z}_3 \frac{\left(\vec{z}_{23}\cdot\vec{z}_{31}\right)}{\left(\vec{z}_{23}^{\,2}\right)^{\frac{d}{2}}\left(\vec{z}_{31}^{\,2}\right)^{\frac{d}{2}}} \left[\mathrm{Tr}\left(U^\eta_{\vec{z}_1} t^b U^{\eta\dagger}_{\vec{z}_2} t^a\right)\left(U^\eta_{\vec{z}_3}\right)^{ab}\right](\Delta\eta) . \tag{2.78}$$

The contribution from diagram B can be obtained from diagram A by performing $(ig) \leftrightarrow (-ig)$ and $\vec{z}_2 \leftrightarrow \vec{z}_1$. Then one can easily show that $I_B = I_A$. Diagram C reads

$$\begin{aligned} I_C &= (-ig)^2\mu^{-2\epsilon}\int_{-\infty}^0 dz_1^+ \int_0^{+\infty} dz_2^+ \mathrm{Tr}\left(\left[-\infty, z_2^+\right]^\eta_{\vec{z}_2} t^a \left[z_2^+, z_1^+\right]^\eta_{\vec{z}_2} t^b \left[z_1^+, +\infty\right]^\eta_{\vec{z}_2} \left[+\infty, -\infty\right]^\eta_{\vec{z}_2}\right)\left(G_{\Delta\eta}\right)^{ba} \\ &= (-ig)^2\mu^{-2\epsilon}\int_{-\infty}^0 dz_1^+ \int_0^{+\infty} dz_2^+ \mathrm{Tr}\left(t^a U^{\eta\dagger}_{\vec{z}_2} t^b U^\eta_{\vec{z}_1}\right)(-i)^d \int \frac{d^d\vec{z}_3}{(2\pi)^{d+1}}\left(U^\eta_{\vec{z}_3}\right)^{ba} \end{aligned} \tag{2.79}$$

$$\times \int_{e^\eta}^{e^{\eta+\Delta\eta}} dp^+ \frac{(p^+)^{d-1}}{2\left(-z_2^+ z_1^+\right)^{\frac{d}{2}+1}} \exp\left[-ip^+\left\{z_{21}^- - \frac{\vec{z}_{32}^{\,2}}{2z_2^+} + \frac{\vec{z}_{32}^{\,2}}{2z_1^+} - i0\right\}\right](\vec{z}_{23}\cdot\vec{z}_{32})$$

$$\sim \frac{g^2\mu^{-2\epsilon}\left[\Gamma\left(\frac{d}{2}\right)\right]^2 2^d}{2\left(2\pi\right)^{d+1}} \int d^d\vec{z}_3 \mathrm{Tr}\left(t^a U^{\eta\dagger}_{\vec{z}_2} t^b U^{\eta}_{\vec{z}_1}\right)\left(U^{\eta}_{\vec{z}_3}\right)^{ba} \frac{1}{\left(\vec{z}_{32}^{\,2}+i0\right)^{d-1}}(\Delta\eta)\,. \tag{2.80}$$

Diagram D is then obtained from diagram C by performing $(ig)\leftrightarrow(-ig)$ and $\vec{z}_2\leftrightarrow\vec{z}_1$. It reads

$$I_D = \frac{g^2\mu^{-2\epsilon}\left[\Gamma\left(\frac{d}{2}\right)\right]^2 2^d}{2\left(2\pi\right)^{d+1}} \int d^d\vec{z}_3 \mathrm{Tr}\left(t^a U^{\eta\dagger}_{\vec{z}_2} t^b U^{\eta}_{\vec{z}_1}\right)\left(U^{\eta}_{\vec{z}_3}\right)^{ba} \frac{1}{\left(\vec{z}_{31}^{\,2}\right)^{d-1}}(\Delta\eta)\,. \tag{2.81}$$

Finally the total contribution with the gluon crossing the shockwave reads :

$$I_R \equiv (I_A + I_B + I_C + I_D) \tag{2.82}$$

$$= \frac{\alpha_s\mu^{-2\epsilon}\Delta\eta\left[\Gamma\left(\frac{d}{2}\right)\right]^2}{\pi^d} \int d^d\vec{z}_3 \mathrm{Tr}\left(t^a U^{\eta}_{\vec{z}_1} t^b U^{\eta\dagger}_{\vec{z}_2}\right)\left(U^{\eta}_{\vec{z}_3}\right)^{ab} \tag{2.83}$$

$$\times\left[\frac{2\left(\vec{z}_{23}\cdot\vec{z}_{31}\right)}{\left(\vec{z}_{23}^{\,2}\right)^{\frac{d}{2}}\left(\vec{z}_{31}^{\,2}\right)^{\frac{d}{2}}} + \frac{1}{\left(\vec{z}_{23}^{\,2}\right)^{d-1}} + \frac{1}{\left(\vec{z}_{31}^{\,2}\right)^{d-1}}\right].$$

Let us consider the total dipole contribution. To get it explicitely, one should compute the following diagrams :

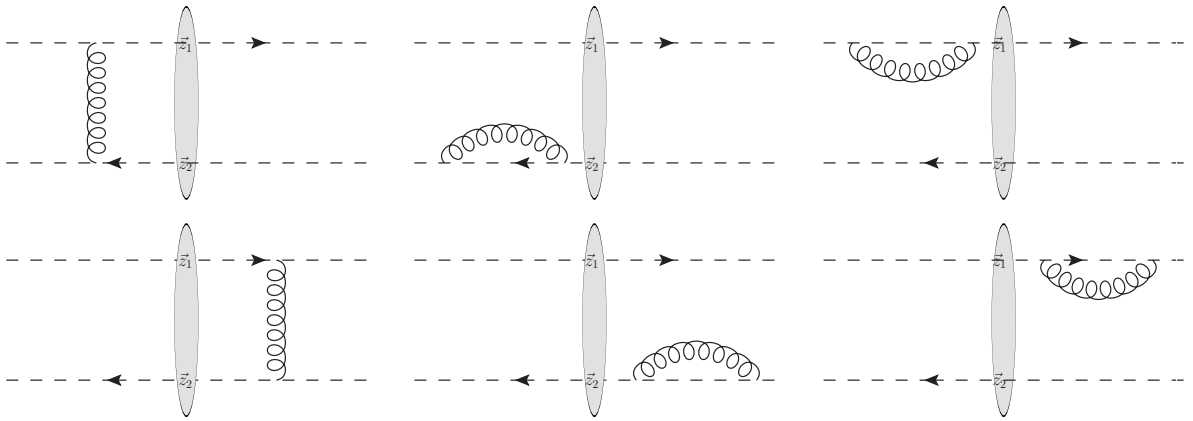

Figure 2.12: Dipole contribution to the B-JIMWLK evolution of the dipole operator

However it can be obtained without any computation. It must have the form :

$$I_V \equiv C_V \,\mathrm{Tr}\left(U^{\eta}_{\vec{z}_1} U^{\eta\dagger}_{\vec{z}_2}\right). \tag{2.84}$$

Let us develop the Wilson lines at the lowest order in I_R by setting $U^{\eta}_{\vec{z}_{1,2,3}} = 1$:

$$I_R \to \frac{\alpha_s\mu^{-2\epsilon}\Delta\eta\left[\Gamma\left(\frac{d}{2}\right)\right]^2}{\pi^d}\frac{N_c^2-1}{2}\int d^d\vec{z}_3\left[\frac{2\left(\vec{z}_{23}\cdot\vec{z}_{31}\right)}{\left(\vec{z}_{23}^{\,2}\right)^{\frac{d}{2}}\left(\vec{z}_{31}^{\,2}\right)^{\frac{d}{2}}} + \frac{1}{\left(\vec{z}_{23}^{\,2}\right)^{d-1}} + \frac{1}{\left(\vec{z}_{31}^{\,2}\right)^{d-1}}\right]. \tag{2.85}$$

Now let us notice that if all the Wilson lines are set to 1 in the total contribution must vanish :

$$\left(I_R + I_V\right)|_{U^{\eta}_{\vec{z}_{1,2,3}}\to 1} = 0\,. \tag{2.86}$$

Indeed we are computing the linear term in the $\Delta\eta$ expansion of the dipole operator. When every Wilson line is set to 1, any dependence on η disappears so this term in the expansion in exactly 0. Thus :

$$C_V = -\frac{\alpha_s\mu^{-2\epsilon}\Delta\eta\left[\Gamma\left(\frac{d}{2}\right)\right]^2}{\pi^d}\frac{N_c^2-1}{2N_c}\int d^d\vec{z}_3\left[\frac{2\left(\vec{z}_{23}\cdot\vec{z}_{31}\right)}{\left(\vec{z}_{23}^{\,2}\right)^{\frac{d}{2}}\left(\vec{z}_{31}^{\,2}\right)^{\frac{d}{2}}} + \frac{1}{\left(\vec{z}_{23}^{\,2}\right)^{d-1}} + \frac{1}{\left(\vec{z}_{31}^{\,2}\right)^{d-1}}\right]. \tag{2.87}$$

Hence the dipole contribution reads :

$$I_V = -\frac{\alpha_s \mu^{-2\epsilon} \Delta\eta \left[\Gamma\left(\frac{d}{2}\right)\right]^2}{\pi^d} \frac{N_c^2-1}{2N_c} \int d^d\vec{z}_3 \left[\frac{2\left(\vec{z}_{23}\cdot\vec{z}_{31}\right)}{\left(\vec{z}_{23}^{\,2}\right)^{\frac{d}{2}}\left(\vec{z}_{31}^{\,2}\right)^{\frac{d}{2}}} + \frac{1}{\left(\vec{z}_{23}^{\,2}\right)^{d-1}} + \frac{1}{\left(\vec{z}_{31}^{\,2}\right)^{d-1}}\right] \mathrm{Tr}\left(U^{\eta}_{\vec{z}_1} U^{\eta\dagger}_{\vec{z}_2}\right) . \quad (2.88)$$

One concludes by taking the $\Delta\eta \to 0$ limit :

$$\begin{aligned}\frac{\partial \mathrm{Tr}\left(U^{\eta}_{\vec{z}_1} U^{\eta\dagger}_{\vec{z}_2}\right)}{\partial\eta} &= \frac{\alpha_s \mu^{-2\epsilon}\left[\Gamma\left(\frac{d}{2}\right)\right]^2}{\pi^d} \int d^d\vec{z}_3 \left[\mathrm{Tr}\left(U^{\eta}_{\vec{z}_1} t^b U^{\eta\dagger}_{\vec{z}_2} t^a\right)\left(U_{\vec{z}_3}\right)^{ab} - \frac{N_c^2-1}{2N_c}\mathrm{Tr}\left(U^{\eta}_{\vec{z}_1} U^{\eta\dagger}_{\vec{z}_2}\right)\right] \\ &\times \left[\frac{2\left(\vec{z}_{23}\cdot\vec{z}_{31}\right)}{\left(\vec{z}_{23}^{\,2}\right)^{\frac{d}{2}}\left(\vec{z}_{31}^{\,2}\right)^{\frac{d}{2}}} + \frac{1}{\left(\vec{z}_{23}^{\,2}\right)^{d-1}} + \frac{1}{\left(\vec{z}_{31}^{\,2}\right)^{d-1}}\right] . \quad (2.89)\end{aligned}$$

Let us introduce the dipole operators

$$\mathcal{U}^{\eta}_{ij} = 1 - \frac{1}{N_c}\mathrm{Tr}\left(U^{\eta}_{\vec{z}_i} U^{\eta\dagger}_{\vec{z}_j}\right) . \quad (2.90)$$

First let us note that

$$\left(U^{\eta}_{\vec{z}_3}\right)^{ab} = 2\mathrm{Tr}\left(t^a U^{\eta}_{\vec{z}_3} t^b U^{\eta\dagger}_{\vec{z}_3}\right) , \quad (2.91)$$

which can be shown easily by using the definition of the action of the operator in the adjoint representation on an element of the group :

$$\left(U^{\eta}_{\vec{z}_3}\right)^{ab} t^b = U^{\eta}_{\vec{z}_3} t^a U^{\eta\dagger}_{\vec{z}_3} , \quad (2.92)$$

where the operators on the right hand side are in the fundamental representation. By multiplying this on the right by a fundamental matrix t^c and by taking the trace, one obtains Eq. (2.91). Using Eq. (2.91) and the Fierz identity

$$\left(t^a_{ij}\right)\left(t^a_{kl}\right) = \frac{1}{2}\delta_{il}\delta_{jk} - \frac{1}{2N_c}\delta_{ij}\delta_{kl} , \quad (2.93)$$

we can show that

$$\begin{aligned}&\mathrm{Tr}\left(U^{\eta}_{\vec{z}_1} t^b U^{\eta\dagger}_{\vec{z}_2} t^a\right)\left(U^{\eta}_{\vec{z}_3}\right)^{ab} - \frac{N_c^2-1}{2N_c}\mathrm{Tr}\left(U^{\eta}_{\vec{z}_1} U^{\eta\dagger}_{\vec{z}_2}\right) \\ &= 2\mathrm{Tr}\left(t^a U^{\eta}_{\vec{z}_3} t^b U^{\eta\dagger}_{\vec{z}_3}\right)\mathrm{Tr}\left(t^a U^{\eta}_{\vec{z}_1} t^b U^{\eta\dagger}_{\vec{z}_2}\right) - \frac{N_c^2-1}{2N_c}\mathrm{Tr}\left(U^{\eta}_{\vec{z}_1} U^{\eta\dagger}_{\vec{z}_2}\right) \quad (2.94) \\ &= 2\left[\frac{1}{2}\delta_{in}\delta_{jm} - \frac{1}{2N_c}\delta_{ij}\delta_{mn}\right]\left[\frac{1}{2}\delta_{kq}\delta_{pl} - \frac{1}{2N_c}\delta_{kl}\delta_{pq}\right] \\ &\quad \times \left(U^{\eta}_{\vec{z}_3}\right)_{jk}\left(U^{\eta\dagger}_{\vec{z}_3}\right)_{li}\left(U^{\eta}_{\vec{z}_1}\right)_{np}\left(U^{\eta\dagger}_{\vec{z}_2}\right)_{qm} - \frac{N_c^2-1}{2N_c}\mathrm{Tr}\left(U^{\eta}_{\vec{z}_1} U^{\eta\dagger}_{\vec{z}_2}\right) \quad (2.95) \\ &= \frac{1}{2}\left[\mathrm{Tr}\left(U^{\eta}_{\vec{z}_1} U^{\eta\dagger}_{\vec{z}_3}\right)\mathrm{Tr}\left(U^{\eta}_{\vec{z}_3} U^{\eta\dagger}_{\vec{z}_2}\right) - N_c\mathrm{Tr}\left(U^{\eta}_{\vec{z}_1} U^{\eta\dagger}_{\vec{z}_2}\right)\right] \quad (2.96) \\ &= \frac{N_c^2}{2}\left[\mathcal{U}^{\eta}_{12} - \mathcal{U}^{\eta}_{13} - \mathcal{U}^{\eta}_{32} + \mathcal{U}^{\eta}_{13}\mathcal{U}^{\eta}_{32}\right] . \quad (2.97)\end{aligned}$$

The evolution equation finally reads :

$$\begin{aligned}&\frac{\partial \mathcal{U}^{\eta}_{12}}{\partial\eta} = \frac{\alpha_s N_c \left[\Gamma\left(\frac{d}{2}\right)\right]^2 \left(\mu^2\right)^{1-\frac{d}{2}}}{2\pi^d} \quad (2.98) \\ &\times \int d^d\vec{z}_3 \left[\mathcal{U}^{\eta}_{13} + \mathcal{U}^{\eta}_{32} - \mathcal{U}^{\eta}_{12} - \mathcal{U}^{\eta}_{13}\mathcal{U}^{\eta}_{32}\right]\left[\frac{2\left(\vec{z}_{23}\cdot\vec{z}_{31}\right)}{\left(\vec{z}_{23}^{\,2}\right)^{\frac{d}{2}}\left(\vec{z}_{31}^{\,2}\right)^{\frac{d}{2}}} + \frac{1}{\left(\vec{z}_{23}^{\,2}\right)^{d-1}} + \frac{1}{\left(\vec{z}_{31}^{\,2}\right)^{d-1}}\right] .\end{aligned}$$

For $D = 4$ one recovers the usual B-JIMWLK equation for the dipole operator

$$\frac{\partial \mathcal{U}_{12}^{\eta}}{\partial \eta} = \frac{\alpha_s N_c}{2\pi^2} \int d^2\vec{z}_3 \left(\frac{\vec{z}_{12}^{\,2}}{\vec{z}_{23}^{\,2}\vec{z}_{31}^{\,2}} \right) \left[\mathcal{U}_{13}^{\eta} + \mathcal{U}_{32}^{\eta} - \mathcal{U}_{12}^{\eta} - \mathcal{U}_{13}^{\eta}\mathcal{U}_{32}^{\eta} \right] . \tag{2.99}$$

This equation involves a double dipole operator $\mathcal{U}_{13}\mathcal{U}_{32}$, which can only be described as the product of two dipole operators in the mean-field (or large N_c) approximation. In general, one should also use the evolution equation for this new operator, which will involve another operator and so on and so forth. Thus Eq. (2.98) is not a closed equation. One should actually solve an infinity of equations, know as Balitsky's hierarchy of equations. The JIMWLK equation in its hamiltonian form allows for a more compact definition of this hierarchy. In the large N_c limit, Eq. (2.99) reduces to the closed Balitsky-Kovchegov equation.

2.3.2 B-JIMWLK equation for the dipole operator in D dimensions in the momentum space

Let us introduce the Fourier transform of the dipole and double dipole operators :

$$\tilde{\mathcal{U}}_{ij}^{\eta}(\vec{p}_1, \vec{p}_2) \equiv \int d^d\vec{z}_1 d^d\vec{z}_2 e^{-i(\vec{p}_1\cdot\vec{z}_1)-i(\vec{p}_2\cdot\vec{z}_2)} \mathcal{U}_{12}^{\eta} , \tag{2.100}$$

and

$$\begin{aligned} &\widetilde{\mathcal{U}_{13}^{\eta}\mathcal{U}_{32}^{\eta}}(\vec{p}_1, \vec{p}_2, \vec{p}_3) \\ &\equiv \int d^d\vec{z}_1 d^d\vec{z}_2 d^d\vec{z}_3 \mathcal{U}_{13}^{\eta}\mathcal{U}_{32}^{\eta} e^{-i(\vec{p}_1\cdot\vec{z}_1)-i(\vec{p}_2\cdot\vec{z}_2)-i(\vec{p}_3\cdot\vec{z}_3)} . \end{aligned} \tag{2.101}$$

Then the B-JIMWLK equation for the dipole operator can be rewritten as

$$\begin{aligned} \frac{\partial \tilde{\mathcal{U}}_{12}^{\eta}}{\partial \eta} &= \frac{\alpha_s N_c \left[\Gamma\left(\frac{d}{2}\right)\right]^2}{2\pi^d \left(\mu^2\right)^{\frac{d-2}{2}}} \int d^d\vec{z}_1 d^d\vec{z}_2 d^d\vec{z}_3 \left[\mathcal{U}_{13}^{\eta} + \mathcal{U}_{32}^{\eta} - \mathcal{U}_{12}^{\eta} - \mathcal{U}_{13}^{\eta}\mathcal{U}_{32}^{\eta} \right] \\ &\quad \times \left[\frac{2\left(\vec{z}_{23}\cdot\vec{z}_{31}\right)}{\left(\vec{z}_{23}^{\,2}\right)^{\frac{d}{2}}\left(\vec{z}_{31}^{\,2}\right)^{\frac{d}{2}}} + \frac{1}{\left(\vec{z}_{23}^{\,2}\right)^{d-1}} + \frac{1}{\left(\vec{z}_{31}^{\,2}\right)^{d-1}} \right] e^{-i(\vec{p}_1\cdot\vec{z}_1)-i(\vec{p}_2\cdot\vec{z}_2)} \\ &= \frac{\alpha_s N_c \left[\Gamma\left(\frac{d}{2}\right)\right]^2}{2\pi^d \left(\mu^2\right)^{\frac{d-2}{2}}} \int d^d\vec{z}_1 d^d\vec{z}_2 d^d\vec{z}_3 \int \frac{d^d\vec{q}_1 d^d\vec{q}_2 d^d\vec{q}_3}{(2\pi)^{3d}} \left[\tilde{\mathcal{U}}_{13}^{\eta} + \tilde{\mathcal{U}}_{32}^{\eta} - \tilde{\mathcal{U}}_{12}^{\eta} - \widetilde{\mathcal{U}_{13}^{\eta}\mathcal{U}_{32}^{\eta}} \right] (\vec{q}_1, \vec{q}_2, \vec{q}_3) \\ &\quad \times \left[\frac{2\left(\vec{z}_{23}\cdot\vec{z}_{31}\right)}{\left(\vec{z}_{23}^{\,2}\right)^{\frac{d}{2}}\left(\vec{z}_{31}^{\,2}\right)^{\frac{d}{2}}} + \frac{1}{\left(\vec{z}_{23}^{\,2}\right)^{d-1}} + \frac{1}{\left(\vec{z}_{31}^{\,2}\right)^{d-1}} \right] e^{-i(\vec{p}_1\cdot\vec{z}_1)-i(\vec{p}_2\cdot\vec{z}_2)+i(\vec{q}_1\cdot\vec{z}_1)+i(\vec{q}_2\cdot\vec{z}_2)+i(\vec{q}_3\cdot\vec{z}_3)} \end{aligned} \tag{2.102}$$

We will need the expressions for the following integrals :

$$\begin{aligned} \int \frac{d^d\vec{z}}{\left(\vec{z}^{\,2}\right)^n} e^{i(\vec{p}\cdot\vec{z})} &= \frac{(-i)^n}{\Gamma(n)} \int_0^{+\infty} d\alpha \left(\alpha^{n-1}\right) \int d^d\vec{z} \exp\left[i\alpha\left(\vec{z}^{\,2} + i0\right) + i\left(\vec{p}\cdot\vec{z}\right) \right] \\ &= \frac{(-i)^n (i\pi)^{\frac{d}{2}}}{\Gamma(n)} \int_0^{+\infty} d\alpha \left(\alpha^{n-1-\frac{d}{2}} \right) \exp\left[-i\frac{\vec{p}^{\,2}}{4\alpha}(1 - i0) \right] \\ &= \frac{(-i)^n (i\pi)^{\frac{d}{2}}}{\Gamma(n)} \int_0^{+\infty} d\beta \left(\beta^{-1+\frac{d}{2}-n} \right) \exp\left[-i\frac{\vec{p}^{\,2}}{4}\beta(1 - i0) \right] \\ &= \frac{\pi^{\frac{d}{2}}\Gamma\left(\frac{d}{2} - n\right)}{\Gamma(n)} \left(\frac{4}{\vec{p}^{\,2}} \right)^{\frac{d}{2}-n} , \end{aligned} \tag{2.103}$$

and

$$\begin{aligned}
\int \frac{d^d\vec{z}}{\left(\vec{z}^{\,2}\right)^n} e^{i(\vec{p}\cdot\vec{z})}\vec{z} &= \frac{(-i)^n}{\Gamma(n)}\int_0^{+\infty} d\alpha\left(\alpha^{n-1}\right)\int d^d\vec{z}\exp\left[i\alpha\left(\vec{z}^{\,2}+i0\right)+i\left(\vec{p}\cdot\vec{z}\right)\right]\vec{z} \\
&= \frac{(-i)^n(i\pi)^{\frac{d}{2}}}{\Gamma(n)}\int_0^{+\infty} d\alpha\left(\alpha^{n-1-\frac{d}{2}}\right)\exp\left[-i\frac{\vec{p}^{\,2}}{4\alpha}(1-i0)\right]\left(-\frac{\vec{p}}{2\alpha}\right) \\
&= \frac{(-i)^n(i\pi)^{\frac{d}{2}}}{\Gamma(n)}\int_0^{+\infty} d\beta\left(\beta^{\frac{d}{2}-n}\right)\exp\left[-i\frac{\vec{p}^{\,2}}{4}\beta(1-i0)\right]\left(-\frac{\vec{p}}{2}\right) \\
&= \frac{i\pi^{\frac{d}{2}}\Gamma\left(\frac{d}{2}-n+1\right)}{\Gamma(n)}\left(\frac{\vec{p}}{2}\right)\left(\frac{4}{\vec{p}^{\,2}}\right)^{\frac{d}{2}-n+1}. \qquad (2.104)
\end{aligned}$$

Then one gets :

$$\begin{aligned}
\frac{\partial\tilde{\mathcal{U}}^{\eta}_{12}}{\partial\eta}(\vec{p}_1,\vec{p}_2) &= \frac{\alpha_s N_c\left[\Gamma\left(\frac{d}{2}\right)\right]^2}{2\pi^d\left(\mu^2\right)^{\frac{d-2}{2}}}\int\frac{d^d\vec{q}_1 d^d\vec{q}_2 d^d\vec{q}_3}{(2\pi)^{2d}}\left[\tilde{\mathcal{U}}^{\eta}_{13}+\tilde{\mathcal{U}}^{\eta}_{32}-\tilde{\mathcal{U}}^{\eta}_{12}-\widetilde{\mathcal{U}^{\eta}_{13}\mathcal{U}^{\eta}_{32}}\right](\vec{q}_1,\vec{q}_2,\vec{q}_3) \qquad (2.105) \\
&\times\left[-2\int d^d\vec{z}_{13}d^d\vec{z}_{23}\frac{(\vec{z}_{23}\cdot\vec{z}_{13})}{\left(\vec{z}^{\,2}_{23}\right)^{\frac{d}{2}}\left(\vec{z}^{\,2}_{31}\right)^{\frac{d}{2}}}e^{-i(\vec{p}_1-\vec{q}_1)\cdot\vec{z}_{13}-i(\vec{p}_2-\vec{q}_2)\cdot\vec{z}_{23}}\delta\left(\vec{p}_1+\vec{p}_2-\vec{q}_1-\vec{q}_2-\vec{q}_3\right)\right. \\
&+\int d^d\vec{z}_{23}\frac{1}{\left(\vec{z}^{\,2}_{23}\right)^{d-1}}\exp\left[-i\left(\vec{p}_2-\vec{q}_2\right)\cdot\vec{z}_{23}\right](2\pi)^d\delta\left(\vec{p}_1-\vec{q}_1\right)\delta\left(\vec{p}_2-\vec{q}_2-\vec{q}_3\right) \\
&\left.+\int d^d\vec{z}_{31}\frac{1}{\left(\vec{z}^{\,2}_{31}\right)^{d-1}}\exp\left[-i\left(\vec{q}_3\cdot\vec{z}_{31}\right)\right](2\pi)^d\delta\left(\vec{p}_1-\vec{q}_1-\vec{q}_3\right)\delta\left(\vec{p}_2-\vec{q}_2\right)\right]
\end{aligned}$$

One finally gets the D-dimensional momentum space expression for the B-JIMWLK dipole evolution equation :

$$\begin{aligned}
&\frac{\partial\tilde{\mathcal{U}}^{\eta}_{12}}{\partial\eta}(\vec{p}_1,\vec{p}_2) = 2\alpha_s N_c\left(\mu^2\right)^{1-\frac{d}{2}}\int\frac{d^d\vec{q}_1 d^d\vec{q}_2 d^d\vec{q}_3}{(2\pi)^{2d}}\delta\left(\vec{p}_1+\vec{p}_2-\vec{q}_1-\vec{q}_2-\vec{q}_3\right) \\
&\times\left[\tilde{\mathcal{U}}^{\eta}_{13}+\tilde{\mathcal{U}}^{\eta}_{32}-\tilde{\mathcal{U}}^{\eta}_{12}-\widetilde{\mathcal{U}^{\eta}_{13}\mathcal{U}^{\eta}_{32}}\right](\vec{q}_1,\vec{q}_2,\vec{q}_3) \qquad (2.106) \\
&\times\left[2\frac{(\vec{p}_1-\vec{q}_1)\cdot(\vec{p}_2-\vec{q}_2)}{\left(\vec{p}_1-\vec{q}_1\right)^2\left(\vec{p}_2-\vec{q}_2\right)^2}+\frac{\pi^{\frac{d}{2}}\Gamma\left(1-\frac{d}{2}\right)\left[\Gamma\left(\frac{d}{2}\right)\right]^2}{\Gamma(d-1)}\left(\frac{\delta\left(\vec{p}_1-\vec{q}_1\right)}{\left[\left(\vec{p}_2-\vec{q}_2\right)^2\right]^{1-\frac{d}{2}}}+\frac{\delta\left(\vec{p}_2-\vec{q}_2\right)}{\left[\left(\vec{p}_1-\vec{q}_1\right)^2\right]^{1-\frac{d}{2}}}\right)\right].
\end{aligned}$$

Chapter 3

Diffractive exclusive production of a foward dijet in the shockwave approach

3.1 Introduction

For several decades diffraction has been one of the most intriguing phenomena of strong interaction. The HERA research program has shown for the first time that diffractive processes in the semi-hard regime can be measured and studied based on QCD, giving one of the main tools to access the internal dynamics of the nucleon in a regime of very high gluon densities[1]. One of the most important discoveries of HERA is the fact that about 10 % of the $\gamma^* p \to X$ deep inelastic scattering (DIS) events reveal a rapidity gap between the proton remnants and the hadrons coming from the fragmentation region of the initial virtual photon, as shown in Fig. 3.1 : the extra data compared to predictions consist of such events.

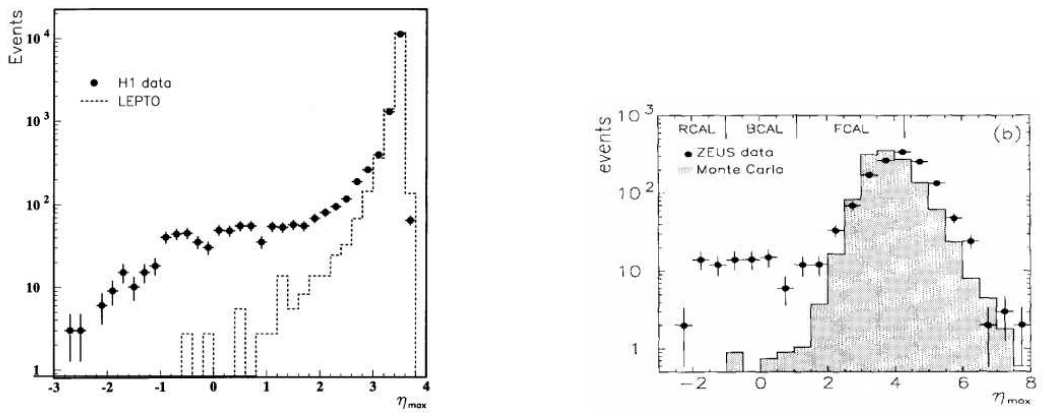

Figure 3.1: H1 and ZEUS results for DIS

This subset of events, called diffractive deep inelastic scattering (DDIS), are of type $\gamma^* p \to X\,Y$ [58–65], where Y is the outgoing proton or one of its low-mass excited states, and X is the diffractive final state. Apart from the inclusive DDIS data, one can further focus on more exclusive observables, like diffractive jet(s) or meson production.

Due to the existence of a rapidity gap between X and Y, it is natural to describe diffraction through a Pomeron exchange in the $t-$channel between these X and Y states. This is a common concept underlying the approaches to describe diffraction within perturbative QCD.

In the collinear factorization framework, justified by the existence of a hard scale (the photon virtuality Q^2 in DIS), a QCD factorization theorem for diffraction was derived [66]. Similarly to DIS off a proton,

[1] For reviews, see Refs. [56, 57].

one has to introduce diffractive structure functions, which are convolutions of coefficient functions with diffractive parton distributions. In this *resolved* Pomeron model, such distributions describe the partonic content of the Pomeron, similarly to the usual parton distribution functions for proton in DIS.

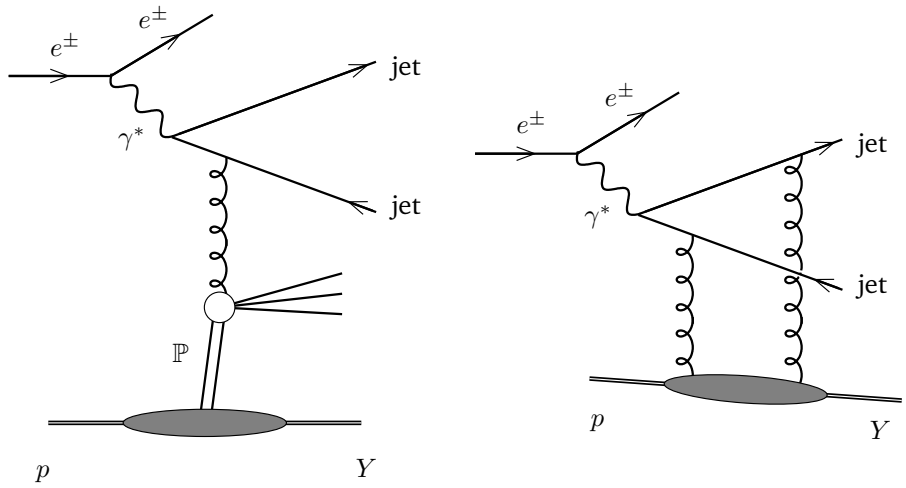

Figure 3.2: Resolved (left panel) and direct Pomeron (right panel) contributions to dijet production.

At higher energies, it is natural to model the diffractive events by a direct Pomeron contribution involving the coupling of a Pomeron with the diffractive state X of invariant mass M. For low values of M^2, X can be modeled by a $q\bar{q}$ pair, while for larger values of M^2, the cross section with an additional produced gluon, i.e. $X = q\bar{q}g$, is enhanced. Based on such a model, with a simplified two-gluon exchange picture for the Pomeron, a good description of HERA data for diffraction was achieved [67]. Interestingly, the $q\bar{q}$ component with a longitudinally polarized photon plays a crucial role in the region of small diffractive mass M, although it is a twist-4 contribution. It is a typical signature of such models.

In this direct Pomeron contribution, the $q\bar{q}g$ diffractive state has been studied in two particular limits. First, at large Q^2, a collinear approximation can be used, based on the fact that the transverse momentum of the gluon is much smaller than the transverse momentum of the emitter [68–70]. Second, for very large M^2, contributions with a strong ordering of longitudinal momenta are enhanced [71, 72]. These two limiting results were combined in a single model, and applied to HERA data for DDIS in [73].

This chapter is based on our work in [74,75] towards a complete next-to-leading order (NLO) description of the direct coupling of the Pomeron to the diffractive X state. To be more specific, the Pomeron should be understood here as a color singlet QCD shockwave, in the spirit of Balitsky's high energy operator expansion [22–25] or in its color glass condensate formulation [26–34].

In our first publication on this subject [74], we computed the $\gamma^{(*)} \to q\bar{q}g$ impact factor and rederived the $\gamma^{(*)} \to q\bar{q}$ impact factor, both at tree level[2]. In this chapter, we will detail the complete computation of the virtual contributions which can be found in [75] [3], and we will compute the one-loop $\gamma^{(*)} \to q\bar{q}$ impact factor. We emphasize that in these results, the impact factors are computed without any soft or collinear approximation for the emitted gluon, in contrast with the results reported until now in the literature. This presents an important step towards a consistent description of inclusive DDIS, or exclusive diffractive dijet production, in the fragmentation region of the scattered photon, i.e. in the forward rapidity region, with NLO precision. Since the results we derive are obtained in the QCD shockwave approach, and depend on the total available center-of-mass energy, the present framework is rather general and can have many applications. Indeed, below the saturation regime, one might describe the $t-$channel exchanged state in the linear BFKL regime [16–19], here with NLL precision [78–81]. At higher energies beyond the saturation limit, the Wilson-line operators evolve with respect to rapidity according to the B-JIMWLK hierarchy as described in the previous chapter.

We calculate the matrix element for the $\gamma^{(*)} \to q\bar{q}$ transition in the shockwave background of the target. It depends on the target via the matrix elements of the two Wilson line operators $\mathcal{U}_{ij}$ and $\mathcal{U}_{ik}\mathcal{U}_{kj}$

[2]Here the photon can be either on-shell or off-shell, hence the notation $\gamma^{(*)}$.
[3]Partial results of the present study were also presented in Refs. [76, 77].

defined in Eq. 2.90 between the in and out target states. For hadronic targets these matrix elements are to be described by some models. For example for the dipole operator there are several saturation models, inspired by the Golec-Biernat and Wüsthoff model [82, 83], while for the quadrupole operator we are not aware about any such model at the moment. These Wilson line operators can also be calculated as solutions of their NLO B-JIMWLK evolution equations with the initial conditions at the rapidity of the target. In the linear limit (BFKL) for forward scattering these solutions are known analytically with a running coupling [84, 85]. In addition, in the low density regime one can always linearize the second Wilson line operator and write the cross section in terms of matrix elements of color dipoles only.

Here we will focus on the details of the coupling of these Wilson-line operators to the diffractive state with general semihard kinematics. The various possible regimes for phenomenological applications will be the subject of future studies.

Next, motivated by the phenomenological importance of our results, we study in detail the cross section for exclusive dijet production in diffraction, as was recently reported by ZEUS [86], and we show explicitely how these cancellations occur in a detailed way. For this purpose, we derive the differential cross section for the $\gamma^* P \to q\bar{q}P'$ transition. Taking the corresponding matrix element from Ref. [74] we also calculate the $\gamma^* P \to q\bar{q}gP'$ cross section. Combining them, we will write the $\gamma^* P \to 2jets\, P'$ exclusive cross section in the small cone approximation.

This chapter is organized as follows. The next section contains the definitions and the kinematics. Then we briefly introduce the basic notations and reproduce the LO $\gamma^{(*)} \to q\bar{q}$ impact factor. Section 3.4 gives the general expression for the $\gamma^{(*)} \to q\bar{q}$ impact factor at one-loop accuracy. Section 3.5 gives the $\gamma^{(*)} \to q\bar{q}g$ impact factor at Born order in arbitrary dimensions. Section 3.6 gives the $\gamma^{(*)} P \to q\bar{q}P'$ cross section at leading and next-to-leading order. Section 3.7 gives the $\gamma^{(*)} P \to q\bar{q}gP'$ cross section at leading order. Section 3.8 gives the final result for exclusive $\gamma^* P \to dijet P'$ transition, showing explicitly the cancellation of divergencies, based on the two previous sections. Some possible phenomenological applications and theoretical extensions or adaptations will be described in the next chapter.

3.2 Definitions

For a moment, we will consider the open production of partons, the conversion into jets will be discussed later in this chapter. We denote the initial photon vector as p_γ, and the outgoing quark and antiquark vectors as p_q, and $p_{\bar{q}}$. In the real correction, an additional external gluon is emitted. Its momentum will be denoted as p_g. We will focus on diffraction off a proton P which remains intact after the interaction[4]. We denote the initial and final proton momenta as p_0 and p_0'. We consider semihard kinematics with the hard scale

$$s = (p_\gamma + p_0)^2 \gg |p_\gamma^2|,\ M_P^2,\ |p_{00'}^2|. \tag{3.1}$$

M_P is the proton mass. The semihard scale comes from either the photon virtuality $|p_\gamma^2|$, the momentum transfer $|p_{00'}^2|$, or the invariant mass of the produced jets. In such kinematics one can write

$$s \simeq 2p_\gamma^+ p_0^-, \tag{3.2}$$

and choose the reference frame where

$$p_\gamma^+, p_0^- \sim \sqrt{s}. \tag{3.3}$$

In the case of our process, we write

$$p_\gamma^+ \sim p_q^+ \sim p_{\bar{q}}^+ \gg p_0^+, p_0'^+, \quad p_0^- \gg p_\gamma^-, p_{\bar{q}}^-, p_q^-. \tag{3.4}$$

The longitudinal momentum fractions of the $q\bar{q}$ pair are defined by

$$\frac{p_q^+}{p_\gamma^+} \equiv x_q, \quad \frac{p_{\bar{q}}^+}{p_\gamma^+} \equiv x_{\bar{q}}. \tag{3.5}$$

For simplicity we consider a forward photon with virtuality Q and no transverse momentum :

$$\vec{p}_\gamma = 0, \quad p_\gamma^\mu = p_\gamma^+ n_1^\mu - \frac{Q^2}{2p_\gamma^+} n_2^\mu, \quad Q^2 \equiv -p_\gamma^2 > 0. \tag{3.6}$$

[4] Our calculation can be used for other processes later on with minor modifications

We will denote its transverse polarization as ε_T. Its longitudinal polarization vector reads

$$\varepsilon_L^\alpha = \frac{p_\gamma^+}{Q} n_1^\alpha + \frac{Q}{2p_\gamma^+} n_2^\alpha. \tag{3.7}$$

We work in the shockwave formalism in the light-cone gauge $\mathcal{A} \cdot n_2 = 0$ and in dimension $D \equiv 2 + d \equiv 4 + 2\epsilon$. The Feynman rules for this formalism can be read in Section 2.2.3. To construct the cross section after calculating the impact factor one has to integrate w.r.t. the field b generated by the proton. Technically it means that one has to treat the field b as an operator and use the matrix element of the total Wilson operator between the proton states

$$U_i \cdots \to \langle P'_{p'_0} | T(U_i \dots) | P_{p_0} \rangle. \tag{3.8}$$

For simplicity of the notations we will still use the operator U instead of its matrix element during the calculation of the impact factor, and return to the matrix element later on. In our computation we do not need the $\beta-$function correction since renormalization effects start at the next-to-next-to leading order in the impact factor. We also introduce a regularization cutoff α for the spurious light cone singularity $p_g^+ \to 0$. Evolving the operators U_r^ρ from rapidities $\rho = \alpha$ to $\rho = e^\eta$ with the help of the BK equation will allow us to cancel rapidity singularities, as shown in Section 3.4.9.

3.3 Leading order amplitude

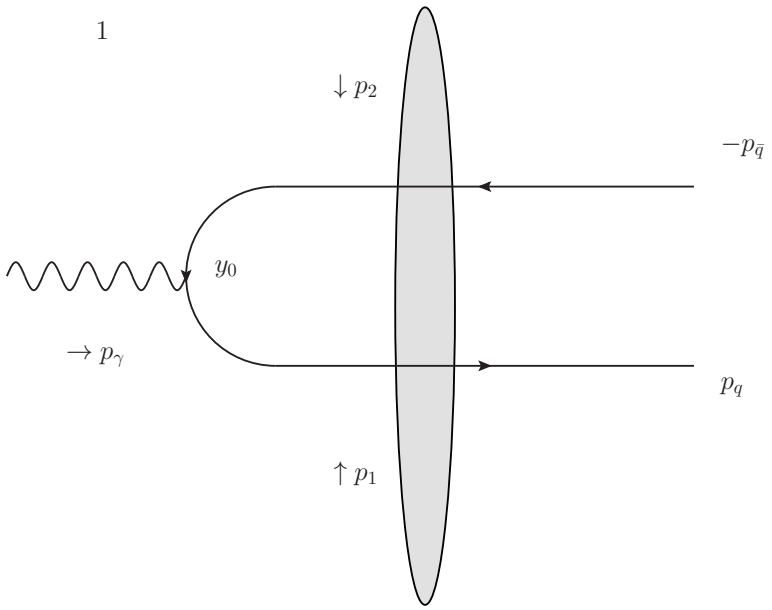

Figure 3.3: LO impact factor. The momenta p_1 and p_2 go from the shockwave to the quark and antiquark.

The matrix element for the EM current in the shockwave background reads

$$\tilde{M}^\alpha = -ie_q \int d^D y_0 \frac{e^{-i(p_\gamma \cdot y_0)}}{\sqrt{2p_\gamma^+}} \frac{\delta_l^n}{\sqrt{N_c}} \langle 0 | T(b^l_{p_{\bar{q}}}(a_{p_q})_n \overline{\psi}(y_0) \gamma^\alpha \psi(y_0) e^{i \int \mathcal{L}_i(z) dz}) | 0 \rangle_{sw}. \tag{3.9}$$

Here a and b are the quark and antiquark annihilation operators, e_q is the quark electric charge, and $\frac{\delta_l^n}{\sqrt{N_c}}$ is the projector on the color singlet. To shorten the notation we will work throughout this thesis with the reduced matrix element $\tilde{T}^\alpha$defined by :

$$\tilde{M}^\alpha \equiv \frac{-ie_q}{\sqrt{2p_\gamma^+}\sqrt{N_c}(2\pi)^{D-3}} \frac{-i\delta(p_q^+ + p_{\bar{q}}^+ - p_\gamma^+)}{\sqrt{2p_{\bar{q}}^+}\sqrt{2p_q^+}} \tilde{T}^\alpha. \tag{3.10}$$

Its expression at LO is obtained using the Feynman rules in the shockwave background as found in Section 2.2.3. The result can be written as

$$\tilde{T}_0^\alpha = \int d^d p_{1\perp} d^d p_{2\perp} \delta(p_{q1\perp} + p_{\bar{q}2\perp} - p_{\gamma\perp}) \,\mathrm{Tr}[U(p_{1\perp})U^\dagger(-p_{2\perp})]\Phi_0^\alpha(p_{1\perp}, p_{2\perp})\,. \tag{3.11}$$

After subtraction of the noninteracting part one gets

$$T_0^\alpha \equiv \tilde{T}_0^\alpha - \tilde{T}_0^\alpha|_{U_1,U_2\to 1} \tag{3.12}$$

$$= -N_c \int d^d p_{1\perp} d^d p_{2\perp} \delta(p_{q1\perp} + p_{\bar{q}2\perp} - p_{\gamma\perp}) \tilde{\mathcal{U}}_{12} \Phi_0^\alpha(p_{1\perp}, p_{2\perp})\,, \tag{3.13}$$

where $\tilde{\mathcal{U}}_{12}$ is the dipole operator as defined in Eq. (2.90). When computing a cross section rather than an impact factor, one must act on the target with this operator as in Eq. (3.8). The function

$$\Phi_0^\alpha \equiv \Phi_0^\alpha(p_{1\perp}, p_{2\perp}) \tag{3.14}$$

is the LO impact factor and we will often suppress its dependence on variables for brevity. Its components have the following form, with $x \equiv x_q$ and $\bar{x} = 1 - x = x_{\bar{q}}$:

$$\Phi_0^+ = -\frac{p_\gamma^+}{p_\gamma^-}\Phi_0^- = \frac{2x\bar{x}p_\gamma^+}{\vec{p}_{q1}^{\,2} + x\bar{x}Q^2}(\overline{u}_{p_q}\gamma^+ v_{p_{\bar{q}}}), \tag{3.15}$$

$$\Phi_0^i = \frac{\overline{u}_{p_q}((1-2x)p_{q1\perp}^i + \frac{1}{2}[\hat{p}_{q1\perp}, \gamma^i])\gamma^+ v_{p_{\bar{q}}}}{\vec{p}_{q1}^{\,2} + x\bar{x}Q^2}\,. \tag{3.16}$$

This can be shown straightforwardly by writing using the expressions for the quark and antiquark lines in the shockwave field. The first equality in Eq. (3.15) holds thanks to the electromagnetic gauge invariance, which will allow us to deduce the $-$ component of the impact factor from its $+$ component.

3.4 Next-to-Leading order amplitude

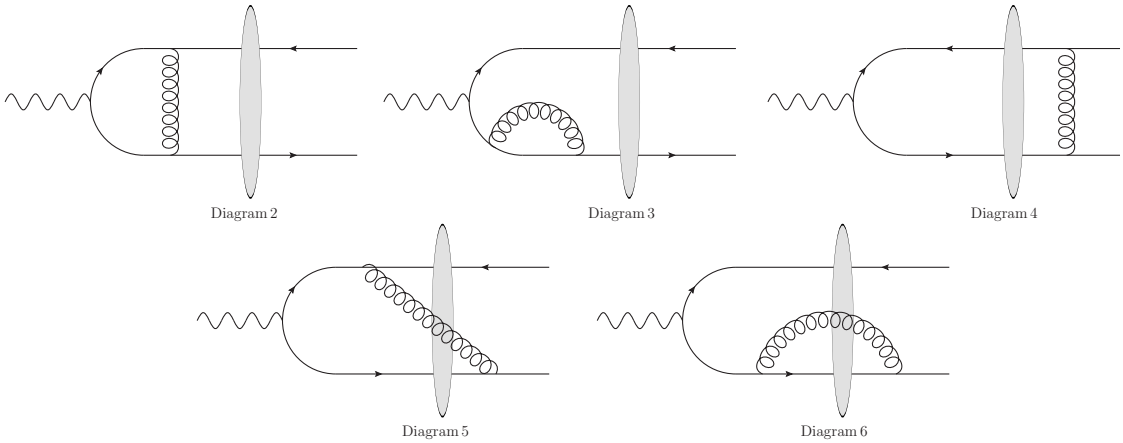

Figure 3.4: NLO diagrams

There are 8 one-loop diagrams contributing to the matrix element T_1. Five of them are presented in Fig. 3.4. The remaining ones can be obtained from diagrams 3, 5 and 6 via the substitution $p_q \leftrightarrow p_{\bar{q}}$, $\bar{u}_q \leftrightarrow v_{\bar{q}}$, $p_1 \leftrightarrow p_2$, which we will denote $(q \leftrightarrow \bar{q})$.

3.4.1 Color factors and Wilson line operators

For virtual diagrams, the projector on the color singlet is $\frac{\delta_{im}}{\sqrt{N_c}}$, where i and m are the respective colors of the quark and the antiquark. There are two kinds of virtual diagrams. The diagrams of each kind will

all involve the same Wilson line operator. For diagrams without the gluon crossing the shockwave after projecting on the color singlet state the Wilson line operator will be :

$$C_1 = \left[U\left(\vec{p}_1\right)\right]_{ij}\left(t^a\right)_{jk}\left(t^a\right)_{kl}\left[U^\dagger\left(-\vec{p}_2\right)\right]_{lm}\frac{\delta_{im}}{\sqrt{N_c}} \tag{3.17}$$

$$= \frac{1}{\sqrt{N_c}}\left(\frac{N_c^2-1}{2N_c}\right)\mathrm{Tr}\left[U\left(\vec{p}_1\right)U^\dagger\left(-\vec{p}_2\right)\right]. \tag{3.18}$$

For diagrams with the gluon crossing the shockwave one has to use Eq. (2.91) and the Fierz identity. The Wilson line operator will read

$$C_2 = \frac{1}{\sqrt{N_c}}\left(t^a\right)_{ij}\left[U\left(\vec{p}_1\right)\right]_{jk}\left(t^b\right)_{kl}\left[U^\dagger\left(-\vec{p}_2\right)\right]_{li}\left[U^{ab}\left(\vec{p}_3\right)\right] \tag{3.19}$$

$$= \frac{2}{\sqrt{N_c}}\left(t^a\right)_{ij}\left(t^a\right)_{mn}\left(t^b\right)_{kl}\left(t^b\right)_{pq}\left[U\left(\vec{p}_1\right)\right]_{jk}\left[U^\dagger\left(-\vec{p}_2\right)\right]_{li}\left[U\left(\vec{p}_3\right)\right]_{np}\left[U^\dagger\left(\vec{p}_3\right)\right]_{qm} \tag{3.20}$$

$$= \frac{1}{2\sqrt{N_c}}\left[\delta_{in}\delta_{jm}-\frac{1}{N_c}\delta_{ij}\delta_{mn}\right]\left[\delta_{kq}\delta_{lp}-\frac{1}{N_c}\delta_{kl}\delta_{pq}\right]\left[U\left(\vec{p}_1\right)\right]_{jk}\left[U^\dagger\left(-\vec{p}_2\right)\right]_{li}\left[U\left(\vec{p}_3\right)\right]_{np}\left[U^\dagger\left(\vec{p}_3\right)\right]_{qm}$$

$$= \frac{1}{2\sqrt{N_c}}\left(\mathrm{Tr}\left[U\left(\vec{p}_1\right)U^\dagger\left(\vec{p}_3\right)\right]\mathrm{Tr}\left[U\left(\vec{p}_3\right)U^\dagger\left(-\vec{p}_2\right)\right]-\frac{1}{N_c}\mathrm{Tr}\left[U\left(\vec{p}_1\right)U^\dagger\left(-\vec{p}_2\right)\right]\right)$$

$$= \frac{1}{2\sqrt{N_c}}\left(\mathrm{Tr}\left[U\left(\vec{p}_1\right)U^\dagger\left(\vec{p}_3\right)\right]\mathrm{Tr}\left[U\left(\vec{p}_3\right)U^\dagger\left(-\vec{p}_2\right)\right]-N_c\mathrm{Tr}\left[U\left(\vec{p}_1\right)U^\dagger\left(-\vec{p}_2\right)\right]\right)$$
$$+\frac{1}{\sqrt{N_c}}\left(\frac{N_c^2-1}{2N_c}\right)\mathrm{Tr}\left[U\left(\vec{p}_1\right)U^\dagger\left(-\vec{p}_2\right)\right] \tag{3.21}$$

By subtracting the non-interacting part where all Wilson lines are identity and using the dipole and double dipole operators as defined in Eq. (2.100) and Eq. (2.101), one can write the two color structures as :

$$C_1' \equiv C_1 - C_1|_{U\to 1} \tag{3.22}$$

$$= -\sqrt{N_c}\left(\frac{N_c^2-1}{2N_c}\right)\tilde{\mathcal{U}}_{12}\,, \tag{3.23}$$

$$C_2' \equiv C_2 - C_2|_{U\to 1} \tag{3.24}$$

$$= -\sqrt{N_c}\frac{N_c}{2}\left[\tilde{\mathcal{U}}_{13}+\tilde{\mathcal{U}}_{32}-\tilde{\mathcal{U}}_{12}-\widetilde{\mathcal{U}_{13}\mathcal{U}_{32}}\right] \tag{3.25}$$
$$-\sqrt{N_c}\left(\frac{N_c^2-1}{2N_c}\right)\tilde{\mathcal{U}}_{12}\,.$$

Similarly to the LO impact factor, we will thus write :

$$T_1^\alpha = -\alpha_s\frac{N_c\Gamma(1-\epsilon)}{(4\pi)^{1+\epsilon}}\int d^dp_{1\perp}d^dp_{2\perp}\left\{\delta(p_{q1\perp}+p_{\bar{q}2\perp}-p_{\gamma\perp})\left(\frac{N_c^2-1}{N_c}\right)\left[\tilde{\mathcal{U}}_{12}\right]\Phi_1^\alpha\right.$$
$$\left.+N_c\int\frac{d^dp_{3\perp}}{(2\pi)^d}\delta(p_{q1}+p_{\bar{q}2}-p_{\gamma\perp}-p_{3\perp})\left[\tilde{\mathcal{U}}_{13}+\tilde{\mathcal{U}}_{32}-\tilde{\mathcal{U}}_{12}-\widetilde{\mathcal{U}_{13}\mathcal{U}_{32}}\right]\Phi_2^\alpha\right\}. \tag{3.26}$$

From Eq. (3.24) one can see that the diagrams in which the gluon crossed the $z^+=0$ line will contribute to both Φ_1^α and Φ_2^α, while the other ones will contribute only to Φ_1^α.

3.4.2 Computation steps

Assuming the gauge invariance of the impact factor, we will restrict ourselves to computing Φ_D^+ and $\Phi_{D\perp}^i$ for some diagrams. The contribution Φ_D^- from a gauge invariant set of diagrams D is then deduced

using the gauge invariance relation

$$p_\gamma^+ \Phi_D^- - \frac{Q^2}{2p_\gamma^+}\Phi_D^+ \quad = \quad 0\,. \tag{3.27}$$

We will first verify this relation for a gauge invariant set of diagrams, then we will assume it holds for the other sets. The steps which are involved to compute all the virtual diagrams are the same.

- First we write the diagram as the integral over the coordinate of every vertex, with the building blocks in Section 2.2.
- The building blocks, including those for partons which do not cross the shockwave, will be written in their mixed space representation, as a function of a lightcone time x^+ and a momentum. For example the propagator for a quark which is emitted and reabsorbed at lightcone times of the same sign will be written as

$$\begin{aligned} G\left(x\right) \quad = \quad & \int \frac{dp^+ d^d\vec{p}}{2p^+\left(2\pi\right)^{d+1}} \exp\left[-ix^+\frac{\vec{p}^{\,2}-i0}{2p^+} - ip^+x^- + i\left(\vec{p}\cdot\vec{x}\right)\right] \\ & \times\left[\left(p^+\gamma^- + \frac{\vec{p}^{\,2}}{2p^+}\gamma^+ + \hat{p}_\perp\right)\left(\theta(p^+)\theta(x^+) - \theta(-p^+)\theta(-x^+)\right) + i\delta\left(x^+\right)\gamma^+\right]. \end{aligned} \tag{3.28}$$

- Integrating w.r.t. the $-$ component and the transverse components of the vertex coordinates will give the explicit conservation of $+$ and transverse momentum (taking into account the t-channel momentum from the shockwaves)
- Then all the momenta except one can be integrated trivially. We will always keep the momentum l of the loop gluon as the last integration parameter.
- Integrating w.r.t. the $+$ component of the coordinates will finally allow one to write the diagrams as an integral with only $l_\perp$ and l^+ for variables. The $l_\perp$ integration can be performed using the usual methods (Feynman's or Schwinger's trick, etc.). It will be regulated by the dimensional regulator $D = 4 + 2\epsilon$, while the l^+ integration will be regulated using the lower rapidity cutoff αp_γ^+.

Our method is actually equivalent to the use of lightcone perturbation theory. Indeed :

- once only l^+ and $l_\perp$ remain, the numerator of the propagator of every intermediate particle will contain two terms. One will correspond to the instantaneous exchange of the particle, for example the $\delta\left(x^+\right)$ term in Eq. (3.28), while the other one will correspond to the numerator of an on-shell particle, for example the first term in the brackets of Eq. (3.28).
- In Eq. (3.28), the non-instantaneous term contains two terms, with two different orientations in time. With the exception of the loop gluon, the intermediate particle will always have only one time orientation, the other one would correspond to a parton moving back in time.
- At each vertex, the $+$ and transverse components of the momentum are conserved, however the $-$ component is not.
- The denominators which will remain will correspond to the so-called *energy denominators* in light-cone perturbation theory.

We will make this comparison with greater details on an example.
The finite contribution of some of the NLO diagrams cannot be written in a compact enough way to fit in this thesis. Their finite contribution to the cross section as $\sum_{\lambda_q,\,\lambda_{\bar{q}}}\left[\left(\Phi_D^\alpha\Phi_0^{\beta *}\right) + \left(\Phi_0^\alpha\Phi_D^{\beta *}\right)\right]$ will be written in Appendix A.1. The divergent part of those diagrams will be displayed here. To extract this divergent part, we will write :

$$\begin{aligned} \int_\alpha^{z_0} dz\,\Phi_D(z) \quad &\simeq \quad \int_\alpha^{z_0} dz\,\Phi_D^{(0)}(z) + \int_0^{z_0} dz\,\left[\Phi_D(z) - \Phi_D^{(0)}(z)\right] \\ &\equiv \quad \int_\alpha^{z_0} dz\,\Phi_D^{(0)}(z) + \int_0^{z_0} dz\,\left[\Phi_D(z)\right]_+\,, \end{aligned} \tag{3.29}$$

where we explicitly extract the non-integrable part $\Phi_D^{(0)}$ of Φ_D, writing $\Phi_D(z) = \Phi_D^{(0)}(z) + O(\ln z)$ for $z \to 0$, z being the $+$ momentum fraction of the gluon : $z \equiv \frac{l^+}{p_\gamma^+}$ with l the gluon momentum. What we call the divergent part of Φ_D will be made of the first term in the right-hand side of Eq. (3.29) and the $\frac{1}{\epsilon}$ dimensional pole in the second term.

3.4.3 Diagram 2 : vertex correction

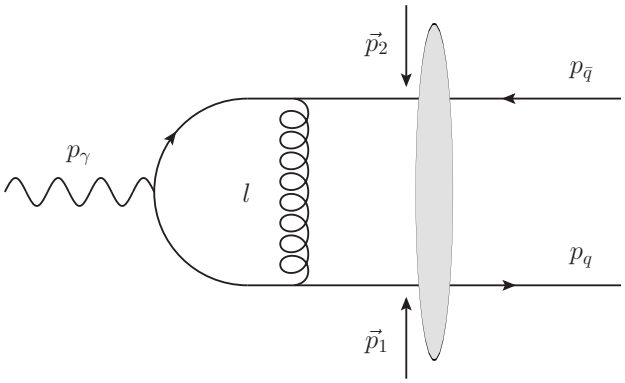

Figure 3.5: Vertex correction

Using the mixed space representation for the propagators and external lines, one can write :

$$
\begin{aligned}
M_2^\alpha &= \frac{-ie_q}{\sqrt{2p_\gamma^+}}(ig)^2 \int d^D y_0 d^D y_1 d^D y_2 \theta\left(-y_0^+\right)\theta\left(-y_1^+\right)\theta\left(-y_2^+\right)\bar{u}_i\left(p_q,\, y_2\right)\gamma^\mu t^a G\left(y_{20}\right)\gamma^\alpha G\left(y_{01}\right)\gamma^\nu \qquad (3.30)\\
&\quad \times t^a v_m\left(p_{\bar{q}},\, y_1\right) G_{\mu\nu}\left(y_{21}\right)\exp\left[-i\left(p_\gamma \cdot y_0\right)\right]\frac{\delta_{mi}}{\sqrt{N_c}}\\
&= \frac{-ie_q}{\sqrt{2p_\gamma^+}}(ig)^2 \int d^D y_0 d^D y_1 d^D y_2 \theta\left(-y_0^+\right)\theta\left(-y_1^+\right)\theta\left(-y_2^+\right)\left(\frac{N_c^2-1}{2N_c\sqrt{N_c}}\right)\frac{\theta\left(p_q^+\right)\theta\left(p_{\bar{q}}^+\right)}{\sqrt{2p_q^+ 2p_{\bar{q}}^+}} \qquad (3.31)\\
&\quad \times \int \frac{d^d\vec{p}_1}{(2\pi)^d}\frac{d^d\vec{p}_2}{(2\pi)^d}\left(-N_c\tilde{\mathcal{U}}_{12}\right)\int \frac{dp^+ d^d\vec{p}}{2p^+(2\pi)^{d+1}}\frac{dk^+ d^d\vec{k}}{2k^+(2\pi)^{d+1}}\frac{dl^+ d^d\vec{l}}{2l^+(2\pi)^{d+1}}\\
&\quad \times \exp\left[i\left(p_q^+ - p^+ - l^+\right)y_2^- + i\left(p_{\bar{q}}^+ + l^+ + k^+\right)y_1^- + i\left(p^+ - p_\gamma^+ - k^+\right)y_0^- - ip_\gamma^- y_0^+\right]\\
&\quad \times \exp\left[i\left(\vec{p}+\vec{l}-\vec{p}_{q1}\right)\cdot\vec{y}_2 - i\left(\vec{k}+\vec{l}+\vec{p}_{\bar{q}2}\right)\cdot\vec{y}_1 - i\left(\vec{p}-\vec{k}\right)\cdot\vec{y}_0\right]\\
&\quad \times \exp\left[iy_1^+\left(\frac{\vec{p}_{\bar{q}2}^{\,2}-i0}{2p_{\bar{q}}^+}\right) - iy_{01}^+\left(\frac{\vec{k}^{\,2}-i0}{2k^+}\right) - iy_{20}^+\left(\frac{\vec{p}^{\,2}-i0}{2p^+}\right) + iy_2^+\left(\frac{\vec{p}_{q1}^{\,2}-i0}{2p_q^+}\right) - iy_{21}^+\left(\frac{\vec{l}^{\,2}-i0}{2l^+}\right)\right]\\
&\quad \times \bar{u}_{p_q}\frac{\gamma^+\left(p_q^+\gamma^- + \hat{p}_{q1\perp}\right)}{2p_q^+}\gamma^\mu\\
&\quad \times \left[\left(p^+\gamma^- + \frac{\vec{p}^{\,2}}{2p^+}\gamma^+ + \hat{p}_\perp\right)\left(\theta(p^+)\theta(y_{20}^+) - \theta(-p^+)\theta(y_{02}^+)\right) + i\delta\left(y_{20}^+\right)\gamma^+\right]\gamma^\alpha\\
&\quad \times \left[\left(k^+\gamma^- + \frac{\vec{k}^{\,2}}{2k^+}\gamma^+ + \hat{k}_\perp\right)\left(\theta(k^+)\theta(y_{01}^+) - \theta(-k^+)\theta(y_{10}^+)\right) + i\delta\left(y_{01}^+\right)\gamma^+\right]\\
&\quad \times \gamma^\nu\frac{\left(p_{\bar{q}}^+\gamma^- + \hat{p}_{\bar{q}2\perp}\right)}{2p_{\bar{q}}^+}\gamma^+ v_{p_{\bar{q}}}\\
&\quad \times \left[\left[\theta\left(l^+\right)\theta\left(y_{21}^+\right) - \theta\left(-l^+\right)\theta\left(y_{12}^+\right)\right]\left(g_{\perp\mu\nu} - \frac{l_{\perp\mu}n_{2\nu} + l_{\perp\nu}n_{2\mu}}{l^+} - \frac{\vec{l}^{\,2}}{\left(l^+\right)^2}n_{2\mu}n_{2\nu}\right) - \frac{2i\delta\left(y_{21}^+\right)}{l^+}\right].
\end{aligned}
$$

Integrating w.r.t. y_2^-, y_1^-, y_0^-, $\vec{y}_2$, $\vec{y}_1$ and $\vec{y}_0$ to get $+$ and transverse momentum conservation at each vertex, then after a trivial integration w.r.t. p^+, $\vec{p}$, k^+ and $\vec{k}$, one obtains :

$$
\begin{aligned}
M_2^\alpha \;=\; & \frac{iN_c e_q}{\sqrt{2p_\gamma^+}}(ig)^2\left(\frac{N_c^2-1}{2N_c\sqrt{N_c}}\right)\frac{\theta\left(p_q^+\right)\theta\left(p_{\bar q}^+\right)}{\sqrt{2p_q^+2p_{\bar q}^+}}\int\frac{d^d\vec{p}_1}{(2\pi)^d}\frac{d^d\vec{p}_2}{(2\pi)^d}\tilde{\mathcal{U}}_{12} \\
& \times\int\frac{dl^+d^d\vec{l}}{2l^+}\frac{\delta\left(p_q^+ + p_{\bar q}^+ - p_\gamma^+\right)\delta\left(\vec{p}_{q1}+\vec{p}_{\bar q 2}\right)}{2\left(p_q^+ - l^+\right)2\left(-p_{\bar q}^+ - l^+\right)} \\
& \times\int_{-\infty}^0 dy_2^+\exp\left[-iy_2^+\left(\frac{\left(\vec{p}_{q1}-\vec{l}\right)^2-i0}{2\left(p_q^+-l^+\right)}-\frac{\vec{p}_{q1}^{\,2}-i0}{2p_q^+}+\frac{\vec{l}^{\,2}-i0}{2l^+}\right)\right] \\
& \times\int_{-\infty}^0 dy_1^+\exp\left[iy_1^+\left(\frac{\vec{p}_{\bar q 2}^{\,2}-i0}{2p_{\bar q}^+}+\frac{\left(\vec{p}_{q1}-\vec{l}\right)^2-i0}{2\left(-p_{\bar q}^+-l^+\right)}+\frac{\vec{l}^{\,2}-i0}{2l^+}\right)\right] \\
& \times\int_{-\infty}^0 dy_0^+\exp\left[-iy_0^+\left(p_\gamma^- + \frac{\left(\vec{p}_{q1}-\vec{l}\right)^2-i0}{2\left(-p_{\bar q}^+-l^+\right)}-\frac{\left(\vec{p}_{q1}-\vec{l}\right)^2-i0}{2\left(p_q^+-l^+\right)}\right)\right] \\
& \times\bar{u}_{p_q}\frac{\gamma^+\left(p_q^+\gamma^- + \hat{p}_{q1\perp}\right)}{2p_q^+}\gamma^\mu\left[\left(\left(p_q^+-l^+\right)\gamma^- + \frac{\left(\vec{p}_{q1}-\vec{l}\right)^2}{2\left(p_q^+-l^+\right)}\gamma^+ + \hat{p}_{q1\perp}-\hat{l}_\perp\right)\right. \\
& \left.\times\left(\theta(p_q^+-l^+)\theta(y_{20}^+)-\theta(l^+-p_q^+)\theta(y_{02}^+)\right)+i\delta\left(y_{20}^+\right)\gamma^+\right]\gamma^\alpha \\
& \times\left[\left(\left(-p_{\bar q}^+-l^+\right)\gamma^- + \frac{\left(\vec{p}_{q1}-\vec{l}\right)^2}{2\left(-p_{\bar q}^+-l^+\right)}\gamma^+ + \hat{p}_{q1\perp}-\hat{l}_\perp\right)\left(\theta(-p_{\bar q}^+-l^+)\theta(y_{01}^+)-\theta(p_{\bar q}^++l^+)\theta(y_{10}^+)\right)\right. \\
& \left.+i\delta\left(y_{01}^+\right)\gamma^+\right]\gamma^\nu\frac{\left(p_{\bar q}^+\gamma^- + \hat{p}_{\bar q 2\perp}\right)}{2p_{\bar q}^+}\gamma^+ v_{p_{\bar q}}\left[\left(g_{\perp\mu\nu}-\frac{l_{\perp\mu}n_{2\nu}+l_{\perp\nu}n_{2\mu}}{l^+}-\frac{\vec{l}^{\,2}}{\left(l^+\right)^2}n_{2\mu}n_{2\nu}\right)\right. \\
& \left.\times\left[\theta\left(l^+\right)\theta\left(y_{21}^+\right)-\theta\left(-l^+\right)\theta\left(y_{12}^+\right)\right]-\frac{2i\delta\left(y_{21}^+\right)}{l^+}n_{2\mu}n_{2\nu}\right].
\end{aligned}
\tag{3.32}
$$

Let us now show that, as physically expected, the cases where $y_{10}^+ < 0$ or $y_{20}^+ < 0$ (which means the gluon is emitted from the quark or the antiquark before the photon splits) cancel.

For example let us consider the case where $y_{20}^+ < 0$.

- In this case, one needs $l^+ > p_q^+$. Then $\theta\left(-l^+\right) = 0$ since $p_q^+ > 0$ so the term with $\theta\left(y_{12}^+\right)$ in the gluon numerator cancels. So does the term with $\theta\left(y_{01}^+\right)$ in the antiquark numerator, since $\theta\left(-p_{\bar q}^+ - l^+\right) = \theta\left(p_q^+ - l^+ - p_\gamma^+\right)$ and $p_\gamma^+ > 0$.
- It is also easy to cancel the term with $\delta\left(y_{12}^+\right)$in the gluon numerator :
  - Due to the presence of the square of γ^+ (which is 0), the term with $\delta\left(y_{01}^+\right)$ in the antiquark propagator then cancels.
  - The remaining term contains $\theta\left(-y_{01}^+\right) = \theta\left(y_{20}^+\right)$.
  - Thus this contribution requires both $y_{20}^+ > 0$ and $y_{20}^+ < 0$, which is impossible.
- Thus the only remaining term in the gluon numerator contains a $\theta\left(y_{21}^+\right)$ factor. Hence this term contains an overall $\theta\left(y_{21}^+\right)\theta\left(y_{02}^+\right)$. This is excluded by the antiquark numerator since we canceled the contribution where $y_1^+ < y_0^+$: everything cancels.

One can thus conclude : the term with $y_0^+ > y_2^+$ cancels. The $\theta\left(-y_{10}^+\right)$ contribution can be cancelled with a similar reasoning. Hence 5 cases remain. Let us introduce $M_2^{(1)\alpha}$, $M_2^{(2)\alpha}$, $M_2^{(3)\alpha}$, $M_2^{(4)\alpha}$ and $M_2^{(5)\alpha}$,

which will correspond respectively to the cases where $y_2^+ > y_1^+ > y_0^+$, $y_1^+ > y_2^+ > y_0^+$, $y_2^+ = y_1^+ > y_0^+$, $y_1^+ > y_2^+ = y_0^+$ and $y_2^+ > y_1^+ > y_0^+$. In lightcone perturbation theory, they would be drawn diagramatically as follows :

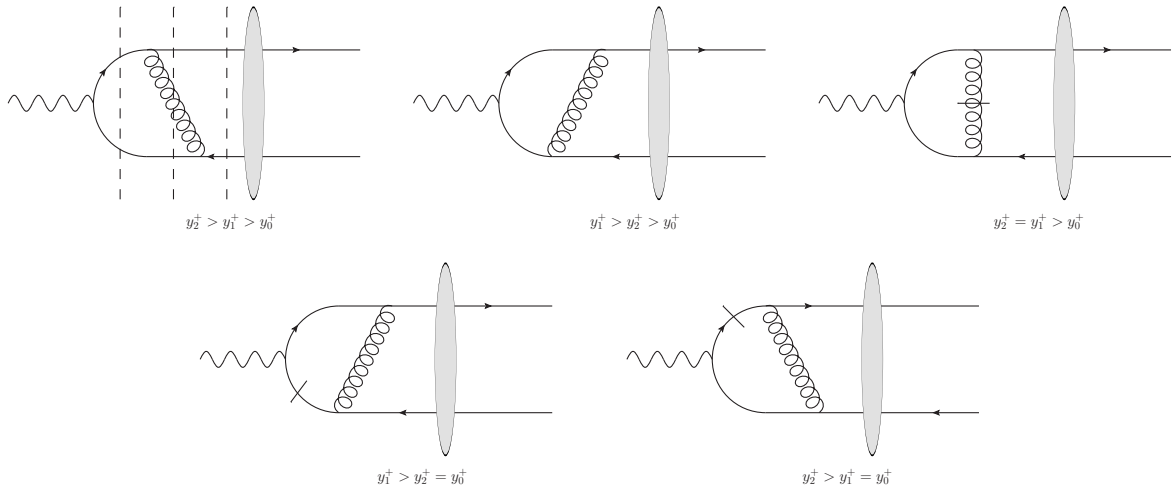

Figure 3.6: Lightcone perturbation theory description of diagram 2. In the first figure, the vertical dashed lines stand for the energy denominators, as described in the following.

The propagators which are crossed with a bar represent the *instantaneous propagator* in lightcone perturbation theory.
Let us consider the first case. We then need the following integral :

$$\begin{aligned}
&\int_{-\infty}^{0} dy_0^+ \exp\left[iy_0^+ \left(\frac{\left(\vec{p}_{q1}-\vec{l}\right)^2 - i0}{2\left(p_q^+ - l^+\right)} - \frac{\left(\vec{p}_{q1}-\vec{l}\right)^2 - i0}{2\left(p_q^+ - l^+ - p_\gamma^+\right)} - p_\gamma^- \right)\right] \\
&\times \int_{y_0^+}^{0} dy_2^+ \exp\left[iy_2^+ \left(\frac{\vec{p}_{q1}^{\,2} - i0}{2p_q^+} - \frac{\vec{l}^{\,2} - i0}{2l^+} - \frac{\left(\vec{p}_{q1}-\vec{l}\right)^2 - i0}{2\left(p_q^+ + l^+\right)} \right)\right] \\
&\times \int_{y_0^+}^{y_2^+} dy_1^+ \exp\left[iy_1^+ \left(\frac{\vec{p}_{\bar{q}2}^{\,2} - i0}{2p_{\bar{q}}^+} - \frac{\left(\vec{p}_{q1}-\vec{l}\right)^2 - i0}{2\left(p_{\bar{q}}^+ + l^+\right)} + \frac{\vec{l}^{\,2} - i0}{2l^+} \right)\right] \\
&= \frac{i}{\left(\frac{\vec{p}_{q1}^{\,2}-i0}{2p_q^+} + \frac{\vec{p}_{q1}^{\,2}-i0}{2p_{\bar{q}}^+} - p_\gamma^-\right)\left(\frac{\vec{l}^{\,2}-i0}{2l^+} + \frac{\vec{p}_{q1}^{\,2}-i0}{2p_{\bar{q}}^+} + \frac{\left(\vec{p}_{q1}-\vec{l}\right)^2-i0}{2\left(p_q^+ - l^+\right)} - p_\gamma^-\right)\left(\frac{\left(\vec{p}_{q1}-\vec{l}\right)^2-i0}{2\left(p_q^+ - l^+\right)} + \frac{\left(\vec{p}_{q1}-\vec{l}\right)^2-i0}{2\left(p_{\bar{q}}^+ + l^+\right)} - p_\gamma^-\right)}.
\end{aligned} \tag{3.33}$$

Let us consider the same contribution in lightcone perturbation theory. In this case, the denominator for the diagram is made of the so-called *energy denominators*. Such denominators can be written as

$$D_n \;=\; \left(\sum_i E_n^{(i)}\right) - E_0\,, \tag{3.34}$$

where $E_n^{(i)}$ is the lightcone energy (i.e. p^-) of the i-th particle in the n-th intermediate Fock state, and E_0 is the energy of the initial Fock state (i.e. p_γ^-). In the present case there will be 3 of them (represented by the vertical dashed lines in the first diagram in Fig. 3.6), and they will read :

$$D_1 \;=\; \frac{\left(\vec{p}_{q1}-\vec{l}\right)^2 - i0}{2\left(p_q^+ - l^+\right)} + \frac{\left(\vec{p}_{\bar{q}2}+\vec{l}\right)^2 - i0}{2\left(p_{\bar{q}}^+ + l^+\right)} - p_\gamma^-\,, \tag{3.35}$$

$$D_2 = \frac{\vec{l}^{\,2}-i0}{2l^+}+\frac{\vec{p}_{\bar{q}2}^{\,2}-i0}{2p_{\bar{q}}^+}+\frac{\left(\vec{p}_{q1}-\vec{l}\right)^2-i0}{2\left(p_q^+-l^+\right)}-p_\gamma^-\,, \tag{3.36}$$

$$D_3 = \frac{\vec{p}_{q1}^{\,2}-i0}{2p_q^+}+\frac{\vec{p}_{\bar{q}2}^{\,2}-i0}{2p_{\bar{q}}^+}-p_\gamma^-\,. \tag{3.37}$$

These are exactly the denominators in Eq. (3.33). This ends our comparison with lightcone perturbation theory. After integration w.r.t. : y_2^+, y_1^+ and y_0^+ we finally get for the 5 contributions to diagram 2 in Fig. 3.6 :

$$\begin{aligned} M_2^{(1)\alpha} &= \frac{-e_qN_c}{\sqrt{2p_\gamma^+}}(ig)^2\left(\frac{N_c^2-1}{2N_c\sqrt{N_c}}\right)\frac{\theta\left(p_q^+\right)\theta\left(p_{\bar{q}}^+\right)}{\sqrt{2p_q^+2p_{\bar{q}}^+}}\int\frac{d^d\vec{p}_1}{(2\pi)^d}\frac{d^d\vec{p}_2}{(2\pi)^d}\frac{\left(\tilde{\mathcal{U}}_{12}\right)}{\left(\frac{\vec{p}_{q1}^{\,2}-i0}{2p_q^+}+\frac{\vec{p}_{q1}^{\,2}-i0}{2p_{\bar{q}}^+}-p_\gamma^-\right)} \\ &\times\int_0^{p_q^+}\frac{dl^+}{2l^+}\frac{\delta\left(p_q^++p_{\bar{q}}^+-p_\gamma^+\right)\delta\left(\vec{p}_{q1}+\vec{p}_{\bar{q}2}\right)}{2\left(p_q^+-l^+\right)2\left(p_{\bar{q}}^++l^+\right)}\int d^d\vec{l}\,\frac{\bar{u}_{p_q}\gamma^+\left(p_q^+\gamma^-+\hat{p}_{q1\perp}\right)}{2p_q^+} \\ &\times\frac{\gamma^\mu\left[\left(p_q^+-l^+\right)\gamma^-+\frac{\left(\vec{p}_{q1}-\vec{l}\right)^2}{2\left(p_q^+-l^+\right)}\gamma^+-\left(\hat{p}_{q1\perp}-\hat{l}_\perp\right)\right]\gamma^\alpha}{\left(\frac{\vec{l}^{\,2}-i0}{2l^+}+\frac{\vec{p}_{q1}^{\,2}-i0}{2p_{\bar{q}}^+}+\frac{\left(\vec{p}_{q1}-\vec{l}\right)^2-i0}{2\left(p_q^+-l^+\right)}-p_\gamma^-\right)\left(\frac{\left(\vec{p}_{q1}-\vec{l}\right)^2-i0}{2\left(p_q^+-l^+\right)}+\frac{\left(\vec{p}_{q1}-\vec{l}\right)^2-i0}{2\left(p_{\bar{q}}^++l^+\right)}-p_\gamma^-\right)} \\ &\times\left[\left(-p_{\bar{q}}^+-l^+\right)\gamma^-+\frac{\left(\vec{p}_{q1}-\vec{l}\right)^2}{2\left(-p_{\bar{q}}^+-l^+\right)}\gamma^+-\left(\hat{p}_{q1\perp}-\hat{l}_\perp\right)\right]\gamma^\nu \\ &\times\frac{\left(p_{\bar{q}}^+\gamma^-+\hat{p}_{\bar{q}2\perp}\right)\gamma^+v_{p_{\bar{q}}}}{2p_{\bar{q}}^+}\left(g_{\perp\mu\nu}-\frac{l_{\perp\mu}n_{2\nu}+l_{\perp\nu}n_{2\mu}}{l^+}-\frac{\vec{l}^{\,2}}{\left(l^+\right)^2}n_{2\mu}n_{2\nu}\right), \end{aligned} \tag{3.38}$$

$$M_2^{(2)\alpha} = M_2^{(1)\alpha}|_{(q\leftrightarrow\bar{q})}\,, \tag{3.39}$$

where $(q\leftrightarrow\bar{q})$ stands for $(1\leftrightarrow 2,\ x_q\leftrightarrow x_{\bar{q}},\ \vec{p}_q\leftrightarrow\vec{p}_{\bar{q}})$.

$$\begin{aligned} M_2^{(3)\alpha} &= \frac{-e_qN_c}{\sqrt{2p_\gamma^+}}(ig)^2\left(\frac{N_c^2-1}{2N_c\sqrt{N_c}}\right)\frac{\theta\left(p_q^+\right)\theta\left(p_{\bar{q}}^+\right)}{\sqrt{2p_q^+2p_{\bar{q}}^+}}\int\frac{d^d\vec{p}_1}{(2\pi)^d}\frac{d^d\vec{p}_2}{(2\pi)^d}\frac{\left(\tilde{\mathcal{U}}_{12}\right)}{\left(\frac{\vec{p}_{q1}^{\,2}-i0}{2p_q^+}+\frac{\vec{p}_{\bar{q}2}^{\,2}-i0}{2p_{\bar{q}}^+}-p_\gamma^-\right)} \\ &\times\int_{-p_{\bar{q}}^+}^{p_q^+}\frac{dl^+}{\left(l^+\right)^2}\frac{\delta\left(p_q^++p_{\bar{q}}^+-p_\gamma^+\right)\delta\left(\vec{p}_{q1}+\vec{p}_{\bar{q}2}\right)}{2\left(p_q^+-l^+\right)2\left(p_{\bar{q}}^++l^+\right)}\int d^d\vec{l} \\ &\times\frac{\bar{u}_{p_q}\gamma^+\left[\left(p_q^+-l^+\right)\gamma^-+\left(\hat{p}_{q1\perp}-\hat{l}_\perp\right)\right]\gamma^\alpha\left[\left(-p_{\bar{q}}^+-l^+\right)\gamma^-+\left(\hat{p}_{q1\perp}-\hat{l}_\perp\right)\right]\gamma^+v_{p_{\bar{q}}}}{\left(-p_\gamma^--\frac{\left(\vec{p}_{q1}-\vec{l}\right)^2-i0}{2\left(-p_{\bar{q}}^+-l^+\right)}+\frac{\left(\vec{p}_{q1}-\vec{l}\right)^2-i0}{2\left(p_q^+-l^+\right)}\right)}, \end{aligned} \tag{3.40}$$

$$\begin{aligned} M_2^{(4)\alpha} &= \frac{-e_qN_c}{\sqrt{2p_\gamma^+}}(ig)^2\left(\frac{N_c^2-1}{2N_c\sqrt{N_c}}\right)\frac{\theta\left(p_q^+\right)\theta\left(p_{\bar{q}}^+\right)}{\sqrt{2p_q^+2p_{\bar{q}}^+}}\int\frac{d^d\vec{p}_1}{(2\pi)^d}\frac{d^d\vec{p}_2}{(2\pi)^d}\frac{\left(\tilde{\mathcal{U}}_{12}\right)}{\left(\frac{\vec{p}_{\bar{q}2}^{\,2}-i0}{2p_{\bar{q}}^+}+\frac{\vec{p}_{q1}^{\,2}-i0}{2p_q^+}-p_\gamma^-\right)} \\ &\times\int_{-p_{\bar{q}}^+}^0\frac{dl^+}{2l^+}\int d^d\vec{l}\frac{\delta\left(p_q^++p_{\bar{q}}^+-p_\gamma^+\right)\delta\left(\vec{p}_{q1}+\vec{p}_{\bar{q}2}\right)}{2\left(p_q^+-l^+\right)2\left(p_{\bar{q}}^++l^+\right)} \\ &\times\frac{\bar{u}_{p_q}\gamma_\perp^\mu\gamma^+\gamma^\alpha\left[-\left(p_{\bar{q}}^++l^+\right)\gamma^--\frac{\left(\vec{p}_{q1}-\vec{l}\right)^2}{2\left(p_{\bar{q}}^++l^+\right)}\gamma^++\left(\hat{p}_{q1\perp}-\hat{l}_\perp\right)\right]}{\left(-\frac{\left(\vec{p}_{q1}-\vec{l}\right)^2-i0}{2\left(-p_{\bar{q}}^+-l^+\right)}+\frac{\vec{p}_{q1}^{\,2}-i0}{2p_q^+}-\frac{\vec{l}^{\,2}-i0}{2l^+}-p_\gamma^-\right)} \\ &\times\gamma^\nu\frac{\left(p_{\bar{q}}^+\gamma^-+\hat{p}_{\bar{q}2\perp}\right)}{2p_{\bar{q}}^+}\gamma^+v_{p_{\bar{q}}}\left(g_{\perp\mu\nu}-\frac{l_{\perp\mu}n_{2\nu}}{l^+}\right), \end{aligned} \tag{3.41}$$

and finally

$$M_2^{(5)\alpha} = M_2^{(4)\alpha}|_{(q\leftrightarrow\bar{q})}\,. \tag{3.42}$$

The $l_\perp$ integration is now straightforward, we will not detail it. The integral w.r.t. l^+ is badly divergent as it is written. One has to restore the rapidity cutoff $\theta\left(|l^+|-\alpha p_\gamma^+\right)$ in the expressions above before performing this integration. After performing those two integrations and quite a bit of Dirac algebra, one can finally show that the contribution of this diagram to the $+$ impact factor reads :

$$\begin{aligned}\Phi_1^+|_2 &= \frac{1}{2}\Phi_0^+\left[2\frac{\pi^2}{3}-2\mathrm{Li}_2\left(\frac{x}{x-1}\right)-2\mathrm{Li}_2\left(\frac{\bar{x}}{\bar{x}-1}\right)-8+3\left(\frac{1}{\epsilon}-\ln\left(\frac{\mu^2}{Q^2}\right)\right)\right. \\ &\left.+-\ln^2\left(\frac{\bar{x}}{x}\right)+\ln^2\left(\frac{x\bar{x}}{\alpha^2}\right)+2\ln\left(\frac{x\bar{x}}{\alpha^2}\right)\ln\left(\frac{\mu^2}{Q^2}\right)-\frac{2}{\epsilon}\ln\left(\frac{x\bar{x}}{\alpha^2}\right)\right].\end{aligned} \tag{3.43}$$

The dilogarithms can be rewritten in terms of logarithms by using several identities :

$$\begin{aligned}\mathrm{Li}_2\left(\frac{x}{x-1}\right)+\mathrm{Li}_2\left(\frac{\bar{x}}{\bar{x}-1}\right) &= \mathrm{Li}_2\left(1-\frac{1}{\bar{x}}\right)+\mathrm{Li}_2\left(1-\frac{1}{x}\right) \\ &= -\frac{\ln^2(\bar{x})}{2}-\mathrm{Li}_2(\bar{x})-\frac{\ln^2(x)}{2}-\mathrm{Li}_2(x) \\ &= -\frac{\ln^2(\bar{x})}{2}-\frac{\ln^2(x)}{2}-\frac{\pi^2}{6}+\ln(x)\ln(\bar{x}) \\ &= -\frac{1}{2}\ln^2\left(\frac{\bar{x}}{x}\right)-\frac{\pi^2}{6}\,.\end{aligned} \tag{3.44}$$

Thus :

$$\Phi_1^+|_2 = \Phi_0^+\left[\frac{\pi^2}{2}-4+\frac{3}{2\epsilon}-\frac{3}{2}\ln\left(\frac{\mu^2}{Q^2}\right)+\frac{1}{2}\ln^2\left(\frac{x\bar{x}}{\alpha^2}\right)+\ln\left(\frac{x\bar{x}}{\alpha^2}\right)\ln\left(\frac{\mu^2}{Q^2}\right)-\frac{1}{\epsilon}\ln\left(\frac{x\bar{x}}{\alpha^2}\right)\right]. \tag{3.45}$$

Similarly one can get :

$$\begin{aligned}\Phi_1^-|_2 &= \frac{1}{2x\bar{x}}\Phi_0^-\left[-3x\bar{x}\ln\left(\frac{\vec{p}_{q1}^{\,2}+x\bar{x}Q^2}{x\bar{x}Q^2}\right)+6x\bar{x}-\frac{\pi^2}{3}\left(x\bar{x}+4\frac{\vec{p}_{q1}^{\,2}}{Q^2}\right)\right. \\ &+14\frac{\vec{p}_{q1}^{\,2}}{Q^2}-\frac{\vec{p}_{q1}^{\,2}}{Q^2}\ln^2\left(\frac{x\bar{x}}{\alpha^2}\right)+\left(\frac{\vec{p}_{q1}^{\,2}+x\bar{x}Q^2}{Q^2}\right)\ln^2\left(\frac{\bar{x}}{x}\right) \\ &+2x\bar{x}\ln\left(\frac{\vec{p}_{q1}^{\,2}+x\bar{x}Q^2}{Q^2}\right)\ln\left(\frac{x\bar{x}}{\alpha^2}\right)+\left[2\ln\left(\frac{x\bar{x}}{\alpha^2}\right)-3\right]\left(2\frac{\vec{p}_{q1}^{\,2}}{Q^2}+x\bar{x}\right)\left(\frac{1}{\epsilon}+\ln\left(\frac{\vec{p}_{q1}^{\,2}+x\bar{x}Q^2}{\mu^2}\right)\right) \\ &\left.+3\frac{\vec{p}_{q1}^{\,2}}{Q^2}\ln(x\bar{x})-2\left(\frac{\vec{p}_{q1}^{\,2}}{Q^2}+x\bar{x}\right)\ln(x\bar{x})\ln\left(\frac{x\bar{x}}{\alpha^2}\right)\right],\end{aligned} \tag{3.46}$$

and

$$\begin{aligned}\Phi_{1\perp}^i|_2 &= \Phi_{0\perp}^i\left[-4+\frac{1}{2}\ln^2\left(\frac{x\bar{x}}{\alpha^2}\right)+\frac{\pi^2}{2}-\left\{\ln\left(\frac{x\bar{x}}{\alpha^2}\right)-\frac{3}{2}\right\}\right. \\ &\left.\times\left\{\left(\frac{\vec{p}_{q1}^{\,2}+x\bar{x}Q^2}{\vec{p}_{q1}^{\,2}}\right)\ln\left(\frac{\vec{p}_{q1}^{\,2}+x\bar{x}Q^2}{x\bar{x}Q^2}\right)+\ln\left(\frac{Q^2}{\mu^2}\right)+\frac{1}{\epsilon}\right\}\right].\end{aligned} \tag{3.47}$$

3.4.4 Diagram 3 dressed quark propagator

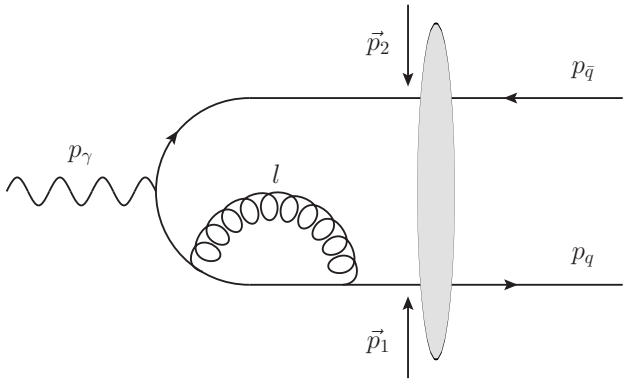

Figure 3.7: Dressed quark propagator

The contribution from diagram 3 in Fig. 3.4 reads

$$
\begin{aligned}
M_3^\alpha &= \frac{-ie_q}{\sqrt{2p_\gamma^+}}(ig)^2\int d^Dy_2d^Dy_1d^Dy_0\bar{u}_i\left(p_q,\,y_2\right)\gamma_\mu G_0\left(y_{21}\right)\gamma_\nu G_0\left(y_{10}\right)\gamma^\alpha v_m\left(p_{\bar{q}},\,y_0\right) \qquad (3.48)\\
&\quad\times G_0^{\mu\nu}\left(y_{21}\right)\frac{\delta_{im}}{\sqrt{N_c}}e^{-i(p_\gamma\cdot y_0)}\\
&= \frac{iN_ce_q}{\sqrt{2p_\gamma^+}}(ig)^2\int d^Dy_2d^Dy_1d^Dy_0\int\frac{d^d\vec{p}_1}{(2\pi)^d}\frac{d^d\vec{p}_2}{(2\pi)^d}\left(\frac{N_c^2-1}{2N_c\sqrt{N_c}}\right)\tilde{\mathcal{U}}_{12}\theta\left(-y_2^+\right)\theta\left(-y_0^+\right) \qquad (3.49)\\
&\quad\times\frac{\theta\left(p_q^+\right)\theta\left(p_{\bar{q}}^+\right)}{\sqrt{2p_q^+2p_{\bar{q}}^+}}\int\frac{dp^+d^d\vec{p}}{2p^+\left(2\pi\right)^{d+1}}\int\frac{dk^+d^d\vec{k}}{2k^+\left(2\pi\right)^{d+1}}\int\frac{dl^+d^d\vec{l}}{2l^+\left(2\pi\right)^{d+1}}\bar{u}_{p_q}\frac{\gamma^+\left(p_q^+\gamma^-+\hat{p}_{q1\perp}\right)}{2p_q^+}\gamma_\mu\\
&\quad\times\left[\left(p^+\gamma^-+\frac{\vec{p}^{\,2}}{2p^+}\gamma^++\hat{p}_\perp\right)\left(\theta(p^+)\theta(y_{21}^+)-\theta(-p^+)\theta(y_{12}^+)\right)+i\delta\left(y_{21}^+\right)\gamma^+\right]\gamma_\nu\\
&\quad\times\left[\left(k^+\gamma^-+\frac{\vec{k}^{\,2}}{2k^+}\gamma^++\hat{k}_\perp\right)\left(\theta(k^+)\theta(y_{10}^+)-\theta(-k^+)\theta(y_{01}^+)\right)+i\delta\left(y_{10}^+\right)\gamma^+\right]\gamma^\alpha\\
&\quad\times\frac{\left(p_{\bar{q}}^+\gamma^-+\hat{p}_{\bar{q}2\perp}\right)}{2p_{\bar{q}}^+}\gamma^+v_{p_{\bar{q}}}\left[\left(g_{\perp\mu\nu}-\frac{l_{\perp\mu}n_{2\nu}+l_{\perp\nu}n_{2\mu}}{l^+}-\frac{\vec{l}^{\,2}}{\left(l^+\right)^2}n_{2\mu}n_{2\nu}\right)\right.\\
&\quad\left.\times\left[\theta\left(l^+\right)\theta\left(y_{21}^+\right)-\theta\left(-l^+\right)\theta\left(y_{12}^+\right)\right]-\frac{2i\delta\left(y_{21}^+\right)}{l^+}n_{2\mu}n_{2\nu}\right]\\
&\quad\times\exp\left[i\left(p_q^+-l^+-p^+\right)y_2^-+i\left(p^++l^+-k^+\right)y_1^-+i\left(k^++p_{\bar{q}}^+-p_\gamma^+\right)y_0^-\right]\\
&\quad\times\exp\left[-i\left(\vec{p}_{q1}-\vec{l}-\vec{p}\right)\cdot\vec{y}_2+i\left(\vec{k}-\vec{l}-\vec{p}\right)\cdot\vec{y}_1-i\left(\vec{p}_{\bar{q}2}+\vec{k}\right)\cdot\vec{y}_0\right]\\
&\quad\times\exp\left[iy_2^+\left(\frac{\vec{p}_{q1}^{\,2}-i0}{2p_q^+}-\frac{\vec{l}^{\,2}-i0}{2l^+}-\frac{\vec{p}^{\,2}-i0}{2p^+}\right)+iy_1^+\left(\frac{\vec{p}^{\,2}-i0}{2p^+}+\frac{\vec{l}^{\,2}-i0}{2l^+}-\frac{\vec{k}^{\,2}-i0}{2k^+}\right)\right]\\
&\quad\times\exp\left[iy_0^+\left(\frac{\vec{p}_{\bar{q}2}^{\,2}-i0}{2p_{\bar{q}}^+}+\frac{\vec{k}^{\,2}-i0}{2k^+}-p_\gamma^-\right)\right].
\end{aligned}
$$

The expression as we wrote it might seem mathematically undefined due to the presence of products of distributions, like $\left[\delta\left(y_{21}^+\right)\right]^2$.. Let us note that it is only our compact way of writing a distinction of the cases $\left(y_2^+>y_1^+,\,y_2^+=y_1^+,\,y_2^+<y_1^+\right)$. One could perform the simultaneous Fourier transform of the two propagators between y_2 and y_1 a more careful way and obtain terms like $\delta'(y_{21}^+)$. However it is actually easy to see that when $y_2^+=y_1^+$ the gamma structure cancels and when $y_2^+<y_1^+$ one gets a contradiction

like $0 > l^+ > p_q^+ > 0$. Hence the seemingly ill-defined quantities do not contribute to our process. Integrating w.r.t. y_2^-, y_1^-, y_0^-, $\vec{y}_2$, $\vec{y}_1$ and $\vec{y}_0$ to get $+$ and transverse momentum conservation at each vertex, then after a trivial integration w.r.t. p^+, $\vec{p}$, k^+ and $\vec{k}$, one obtains :

$$
\begin{aligned}
M_3^{\alpha} \;=\; & \frac{iN_c e_q}{\sqrt{2p_\gamma^+}}\,(ig)^2 \int dy_2^+ dy_1^+ dy_0^+ \theta\left(-y_2^+\right)\theta\left(-y_0^+\right)\theta\left(y_{21}^+\right) \int \frac{d^d\vec{p}_1}{(2\pi)^d}\frac{d^d\vec{p}_2}{(2\pi)^d}\left(\frac{N_c^2-1}{2N_c\sqrt{N_c}}\right)\tilde{\mathcal{U}}_{12} \\
& \times \frac{\theta\left(p_q^+\right)\theta\left(p_{\bar{q}}^+\right)}{\sqrt{2p_q^+ 2p_{\bar{q}}^+}}\frac{1}{2p_q^+}\int_0^{p_q^+}\frac{dl^+}{2l^+ 2\left(p_q^+ - l^+\right)}\int d^d\vec{l}\,\bar{u}_{p_q}\frac{\gamma^+\left(p_q^+\gamma^- + \hat{p}_{q1\perp}\right)}{2p_q^+}\gamma_\mu \\
& \times \left[\left(p_q^+ - l^+\right)\gamma^- + \frac{\left(\vec{p}_{q1}-\vec{l}\right)^2}{2\left(p_q^+ - l^+\right)}\gamma^+ + \left(\hat{p}_{q1\perp} - \hat{l}_\perp\right)\right]\gamma_\nu \\
& \times \left[\left(p_q^+\gamma^- + \frac{\vec{p}_{q1}^{\,2}}{2p_q^+}\gamma^+ + \hat{p}_{q1\perp}\right)\theta(p_q^+)\theta(y_{10}^+) + i\delta\left(y_{10}^+\right)\gamma^+\right] \\
& \times \gamma^\alpha \frac{\left(p_{\bar{q}}^+\gamma^- + \hat{p}_{\bar{q}2\perp}\right)}{2p_{\bar{q}}^+}\gamma^+ v_{p_{\bar{q}}}\delta\left(p_q^+ + p_{\bar{q}}^+ - p_\gamma^+\right)\delta\left(\vec{p}_{q1}+\vec{p}_{\bar{q}2}\right) \\
& \times \left[g_{\perp\mu\nu} - \frac{l_{\perp\mu}n_{2\nu} + l_{\perp\nu}n_{2\mu}}{l^+} - \frac{\vec{l}^{\,2}}{\left(l^+\right)^2}n_{2\mu}n_{2\nu}\right] \\
& \times \exp\left[iy_2^+\left(\frac{\vec{p}_{q1}^{\,2}-i0}{2p_q^+} - \frac{\vec{l}^{\,2}-i0}{2l^+} - \frac{\left(\vec{p}_{q1}-\vec{l}\right)^2 - i0}{2\left(p_q^+ - l^+\right)}\right)\right] \\
& \times \exp\left[iy_1^+\left(\frac{\left(\vec{p}_{q1}-\vec{l}\right)^2 - i0}{2\left(p_q^+ - l^+\right)} + \frac{\vec{l}^{\,2}-i0}{2l^+} - \frac{\vec{p}_{q1}^{\,2}-i0}{2p_q^+}\right)\right] \\
& \times \exp\left[iy_0^+\left(\frac{\vec{p}_{\bar{q}2}^{\,2}-i0}{2p_{\bar{q}}^+} + \frac{\vec{p}_{q1}^{\,2}-i0}{2p_q^+} - p_\gamma^-\right)\right].
\end{aligned}
\tag{3.50}
$$

Distinguishing the two cases $y_1^+ > y_0^+$ and $y_1^+ = y_0^+$ gives two contributions :

$$
\begin{aligned}
M_3^{(1)\alpha} \;=\; & -\frac{N_c e_q}{\sqrt{2p_\gamma^+}}\,(ig)^2 \int \frac{d^d\vec{p}_1}{(2\pi)^d}\frac{d^d\vec{p}_2}{(2\pi)^d}\left(\frac{N_c^2-1}{2N_c\sqrt{N_c}}\right)\frac{\tilde{\mathcal{U}}_{12}}{\left(\frac{\vec{p}_{q1}^{\,2}-i0}{2p_q^+} + \frac{\vec{p}_{\bar{q}2}^{\,2}-i0}{2p_{\bar{q}}^+} - p_\gamma^-\right)} \\
& \times \frac{\theta\left(p_q^+\right)\theta\left(p_{\bar{q}}^+\right)}{\sqrt{2p_q^+ 2p_{\bar{q}}^+}}\frac{1}{2p_q^+}\int_0^{p_q^+}\frac{dl^+}{2l^+ 2\left(p_q^+ - l^+\right)}\int d^d\vec{l}\,\delta\left(p_q^+ + p_{\bar{q}}^+ - p_\gamma^+\right)\delta\left(\vec{p}_{q1}+\vec{p}_{\bar{q}2}\right) \\
& \times \bar{u}_{p_q}\frac{\gamma^+\left(p_q^+\gamma^- + \hat{p}_{q1\perp}\right)}{2p_q^+}\gamma_\mu\left[\left(p_q^+ - l^+\right)\gamma^- + \frac{\left(\vec{p}_{q1}-\vec{l}\right)^2}{2\left(p_q^+ - l^+\right)}\gamma^+ + \left(\hat{p}_{q1\perp} - \hat{l}_\perp\right)\right] \\
& \times \gamma_\nu\left(p_q^+\gamma^- + \frac{\vec{p}_{q1}^{\,2}}{2p_q^+}\gamma^+ + \hat{p}_{q1\perp}\right)\gamma^\alpha\frac{\left(p_{\bar{q}}^+\gamma^- + \hat{p}_{\bar{q}2\perp}\right)}{2p_{\bar{q}}^+}\gamma^+ v_{p_{\bar{q}}} \\
& \times \frac{g_{\perp\mu\nu} - \frac{l_{\perp\mu}n_{2\nu}+l_{\perp\nu}n_{2\mu}}{l^+} - \frac{\vec{l}^{\,2}}{(l^+)^2}n_{2\mu}n_{2\nu}}{\left(\frac{\vec{p}_{\bar{q}2}^{\,2}-i0}{2p_{\bar{q}}^+} + \frac{\vec{l}^{\,2}-i0}{2l^+} + \frac{\left(\vec{p}_{q1}-\vec{l}\right)^2-i0}{2\left(p_q^+-l^+\right)} - p_\gamma^-\right)\left(\frac{\vec{p}_{\bar{q}2}^{\,2}-i0}{2p_{\bar{q}}^+} + \frac{\vec{p}_{q1}^{\,2}-i0}{2p_q^+} - p_\gamma^-\right)},
\end{aligned}
\tag{3.51}
$$

and

$$
M_3^{(2)\alpha} \;=\; \frac{N_c e_q}{\sqrt{2p_\gamma^+}}\,(ig)^2 \int \frac{d^d\vec{p}_1}{(2\pi)^d}\frac{d^d\vec{p}_2}{(2\pi)^d}\left(\frac{N_c^2-1}{2N_c\sqrt{N_c}}\right)\frac{\tilde{\mathcal{U}}_{12}}{\left(\frac{\vec{p}_{q1}^{\,2}-i0}{2p_q^+} + \frac{\vec{p}_{\bar{q}2}^{\,2}-i0}{2p_{\bar{q}}^+} - p_\gamma^-\right)}
\tag{3.52}
$$

$$\times\frac{\theta\left(p_q^+\right)\theta\left(p_{\bar q}^+\right)}{\sqrt{2p_q^+2p_{\bar q}^+}}\frac{1}{2p_q^+}\int_0^{p_q^+}\frac{dl^+}{2l^+2\left(p_q^+-l^+\right)}\delta\left(p_q^+ + p_{\bar q}^+ - p_\gamma^+\right)\delta\left(\vec p_{q1}+\vec p_{\bar q 2}\right)$$
$$\times\int d^d\vec l\,\bar u_{p_q}\frac{\gamma^+\left(p_q^+\gamma^- + \hat p_{q1\perp}\right)}{2p_q^+}\left(\gamma_{\perp\nu}-\frac{l_{\perp\nu}}{l^+}\gamma^+\right)$$
$$\times\frac{\left[\left(p_q^+-l^+\right)\gamma^- + \left(\hat p_{q1\perp}-\hat l_\perp\right)\right]\gamma_{\perp\nu}\gamma^+\gamma^\alpha\left(p_{\bar q}^+\gamma^- + \hat p_{\bar q 2\perp}\right)\gamma^+ v_{p_{\bar q}}}{2p_{\bar q}^+\left(\frac{\vec p_{\bar q 2}^{\,2}-i0}{2p_{\bar q}^+}+\frac{\vec l^{\,2}-i0}{2l^+}+\frac{\left(\vec p_{q1}-\vec l\right)^2-i0}{2\left(p_q^+-l^+\right)}-p_\gamma^-\right)}.$$

Again the integration w.r.t. $l_\perp$ is easy and it will not be detailed. The diagram for the dressed antiquark propagator can be obtained from this one by the symmetrization $(q\leftrightarrow\bar q)$. One can finally show that diagram 3 and its symmetric contribute to Φ_1^α as :

$$\begin{aligned}\Phi_1^+|_{3+(q\leftrightarrow\bar q)} &= \Phi_0^+\left[\frac{1}{2}\ln^2\left(\frac{\bar x}{x}\right)-\frac{1}{2}\ln^2\left(\frac{x\bar x}{\alpha^2}\right)+\ln\left(x\bar x\right)\ln\left(\frac{x\bar x}{\alpha^2}\right)+7-\frac{3}{\epsilon}-2\frac{\pi^2}{3}\right.\\ &\left.+2\left\{\ln\left(\frac{\vec p_{q1}^{\,2}+x\bar xQ^2}{x\bar x\mu^2}\right)+\frac{1}{\epsilon}\right\}\ln\left(\frac{x\bar x}{\alpha^2}\right)-\frac{3}{2}\ln\left(\frac{\left(\vec p_{q1}^{\,2}+x\bar xQ^2\right)^2}{x\bar x\mu^4}\right)\right],\end{aligned}\tag{3.53}$$

$$\begin{aligned}\Phi_1^-|_{3+(q\leftrightarrow\bar q)} &= \frac{\Phi_0^-}{x\bar x}\left[-\frac{\vec p_{q1}^{\,2}}{Q^2}\left(\ln\left(\frac{\left(\vec p_{q1}^{\,2}+x\bar xQ^2\right)^2}{x\bar x\mu^4}\right)+\frac{2}{\epsilon}\right)\ln\left(\frac{x\bar x}{\alpha^2}\right)-7\frac{\vec p_{q1}^{\,2}}{Q^2}+3\frac{\vec p_{q1}^{\,2}}{Q^2}\ln\left(\frac{\vec p_{q1}^{\,2}+x\bar xQ^2}{\mu^2}\right),\right.\\ &\left.-\frac{3}{2}\frac{\vec p_{q1}^{\,2}}{Q^2}\ln\left(x\bar x\right)+\frac{3}{\epsilon}\frac{\vec p_{q1}^{\,2}}{Q^2}+2\frac{\pi^2}{3}\frac{\vec p_{q1}^{\,2}}{Q^2}\frac{1}{2}\frac{\vec p_{q1}^{\,2}}{Q^2}\ln^2\left(\frac{x\bar x}{\alpha^2}\right)-\frac{1}{2}\frac{\vec p_{q1}^{\,2}}{Q^2}\ln^2\left(\frac{\bar x}{x}\right)\right].\end{aligned}\tag{3.54}$$

$$\begin{aligned}\Phi_{1\perp}^i|_{3+(q\leftrightarrow\bar q)} &= \Phi_{0\perp}^i\left[\frac{1}{2}\ln^2\left(\frac{\bar x}{x}\right)+\left\{\ln\left(\frac{x\bar x}{\alpha^2}\right)-\frac{3}{2}\right\}\ln\left(\frac{\left(\vec p_{q1}^{\,2}+x\bar xQ^2\right)^2}{x\bar x\mu^4}\right)\right.\\ &\left.-\frac{1}{2}\ln^2\left(\frac{x\bar x}{\alpha^2}\right)+\frac{2}{\epsilon}\ln\left(\frac{x\bar x}{\alpha^2}\right)+7-\frac{3}{\epsilon}-2\frac{\pi^2}{3}\right].\end{aligned}\tag{3.55}$$

By adding Eq. (3.45) one gets the total virtual correction before the shockwave :

$$\Phi_1^+|_2+\Phi_1^+|_{3+(q\leftrightarrow\bar q)}=\Phi_0^+\left[\frac{1}{2}\ln^2\left(\frac{\bar x}{x}\right)+3-\frac{\pi^2}{6}+\left\{\ln\left(\frac{\left(\vec p_{q1}^{\,2}+x\bar xQ^2\right)^2}{x\bar x\mu^2Q^2}\right)+\frac{1}{\epsilon}\right\}\left\{\ln\left(\frac{x\bar x}{\alpha^2}\right)-\frac{3}{2}\right\}\right],\tag{3.56}$$

$$\Phi_1^-|_2+\Phi_1^-|_{3+(q\leftrightarrow\bar q)}=\Phi_0^-\left[\frac{1}{2}\ln^2\left(\frac{\bar x}{x}\right)+3-\frac{\pi^2}{6}+\left\{\ln\left(\frac{\left(\vec p_{q1}^{\,2}+x\bar xQ^2\right)^2}{x\bar x\mu^2Q^2}\right)+\frac{1}{\epsilon}\right\}\left\{\ln\left(\frac{x\bar x}{\alpha^2}\right)-\frac{3}{2}\right\}\right],\tag{3.57}$$

and

$$\begin{aligned}\Phi_{1\perp}^i|_2+\Phi_{1\perp}^i|_{3+(q\leftrightarrow\bar q)} &= \Phi_{0\perp}^i\left[\frac{1}{2}\ln^2\left(\frac{\bar x}{x}\right)-\frac{\pi^2}{6}+3+\left\{\ln\left(\frac{x\bar x}{\alpha^2}\right)-\frac{3}{2}\right\}\right.\\ &\left.\times\left\{\ln\left(\frac{\vec p_{q1}^{\,2}+x\bar xQ^2}{\mu^2}\right)-\left(\frac{x\bar xQ^2}{\vec p_{q1}^{\,2}}\right)\ln\left(\frac{\vec p_{q1}^{\,2}+x\bar xQ^2}{x\bar xQ^2}\right)+\frac{1}{\epsilon}\right\}\right].\end{aligned}\tag{3.58}$$

This set of diagrams is gauge invariant, as can be explicitly checked using the gauge invariance property of the leading order impact factor Φ_0^α in the longitudinal case.

3.4.5 Diagram 4 : final state interaction

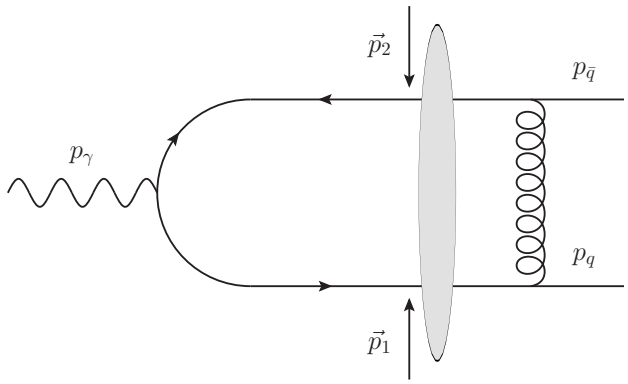

Figure 3.8: Final state interaction

The computation method is the same as before. One gets :

$$
\begin{aligned}
M_4^{\alpha} &= \frac{-ie_q}{\sqrt{2p_\gamma^+}}(ig)^2\int d^Dy_2d^Dy_1d^Dy_0\frac{\left(\bar{u}_{p_q}\right)_i}{\sqrt{2p_q^+}}e^{i(p_q\cdot y_2)}\theta\left(p_q^+\right)\gamma_\mu G\left(y_2,\,y_0\right)\gamma^\alpha e^{-i(p_\gamma\cdot y_0)} \qquad (3.59)\\
&\quad\times G\left(y_0,\,y_1\right)\gamma_\nu\frac{\left(v_{p_{\bar{q}}}\right)_m}{\sqrt{2p_{\bar{q}}^+}}e^{i(p_{\bar{q}}\cdot y_1)}\theta\left(p_{\bar{q}}^+\right)G_0^{\mu\nu}\left(y_{21}\right)\frac{\delta_{im}}{\sqrt{N_c}}\\
&= \frac{e_qN_c}{\sqrt{2p_\gamma^+}}(ig)^2\frac{\theta\left(p_q^+\right)\theta\left(p_{\bar{q}}^+\right)}{\sqrt{2p_q^+2p_{\bar{q}}^+}}\left(\frac{N_c^2-1}{2N_c\sqrt{N_c}}\right)\int\frac{d^d\vec{p}_1}{(2\pi)^d}\frac{d^d\vec{p}_2}{(2\pi)^d}\left(\tilde{\mathcal{U}}_{12}\right) \qquad (3.60)\\
&\quad\times\int\frac{dl^+d^d\vec{l}}{2l^+}\frac{\delta\left(p_q^++p_{\bar{q}}^+-p_\gamma^+\right)\delta\left(\vec{p}_{q1}+\vec{p}_{\bar{q}2}\right)}{\left(\frac{\left(\vec{p}_{q1}-\vec{l}\right)^2-i0}{2\left(p_q^+-l^+\right)}+\frac{\left(\vec{p}_{\bar{q}2}+\vec{l}\right)^2-i0}{2\left(p_{\bar{q}}^++l^+\right)}-p_\gamma^-\right)}\theta\left(p_q^+-l^+\right)\theta\left(p_{\bar{q}}^++l^+\right)\int dy_2^+dy_1^+\theta\left(y_2^+\right)\theta\left(y_1^+\right)\\
&\quad\times\bar{u}_{p_q}\gamma_\mu\frac{\gamma^-\left(p_q^+-l^+\right)+\left(\hat{p}_{q\perp}-\hat{l}_\perp\right)}{2\left(p_q^+-l^+\right)}\gamma^+\frac{\gamma^-\left(p_q^+-l^+\right)+\left(\hat{p}_{q1\perp}-\hat{l}_\perp\right)}{2\left(p_q^+-l^+\right)}\gamma^\alpha\\
&\quad\times\frac{\gamma^-\left(p_{\bar{q}}^++l^+\right)+\left(\hat{p}_{\bar{q}2\perp}+\hat{l}_\perp\right)}{2\left(p_{\bar{q}}^++l^+\right)}\gamma^+\frac{\gamma^-\left(p_{\bar{q}}^++l^+\right)+\left(\hat{p}_{\bar{q}\perp}+\hat{l}_\perp\right)}{2\left(p_{\bar{q}}^++l^+\right)}\gamma_\nu v_{p_{\bar{q}}}\\
&\quad\times\left[\left[\theta\left(l^+\right)\theta\left(y_{21}^+\right)-\theta\left(-l^+\right)\theta\left(y_{12}^+\right)\right]\left(g_{\perp\mu\nu}-\frac{l_{\perp\mu}n_{2\nu}+l_{\perp\nu}n_{2\mu}}{l^+}-\frac{\vec{l}^{\,2}}{\left(l^+\right)^2}n_{2\mu}n_{2\nu}\right)-2\frac{i\delta\left(y_{21}^+\right)}{l^+}n_{2\mu}n_{2\nu}\right]\\
&\quad\times\exp\left[iy_2^+\left(\frac{\vec{p}_q^{\,2}}{2p_q^+}-\frac{\left(\vec{p}_q-\vec{l}\right)^2-i0}{2\left(p_q^+-l^+\right)}-\frac{\vec{l}^{\,2}-i0}{2l^+}\right)+iy_1^+\left(\frac{\vec{p}_{\bar{q}}^{\,2}}{2p_{\bar{q}}^+}-\frac{\left(\vec{p}_{\bar{q}}+\vec{l}\right)^2-i0}{2\left(p_{\bar{q}}^++l^+\right)}+\frac{\vec{l}^{\,2}-i0}{2l^+}\right)\right].
\end{aligned}
$$

There are 3 contributions $M_4^{(1)\alpha}$, $M_4^{(2)\alpha}$ and $M_4^{(3)\alpha}$ corresponding respectively to $y_2^+ > y_1^+ > y_0^+$, $y_1^+ > y_2^+ > y_0^+$, $y_2^+ = y_1^+ > y_0^+$. As for the previous diagrams $M_4^{(2)\alpha} = M_1^{(1)\alpha}|_{(q\leftrightarrow\bar{q})}$. The other two read :

$$
\begin{aligned}
M_4^{(1)\alpha} &= \frac{-N_ce_q}{\sqrt{2p_\gamma^+}}(ig)^2\frac{\theta\left(p_q^+\right)\theta\left(p_{\bar{q}}^+\right)}{\sqrt{2p_q^+2p_{\bar{q}}^+}}\left(\frac{N_c^2-1}{2N_c\sqrt{N_c}}\right)\int\frac{d^d\vec{p}_1}{(2\pi)^d}\frac{d^d\vec{p}_2}{(2\pi)^d}\left(\tilde{\mathcal{U}}_{12}\right) \qquad (3.61)\\
&\quad\times\int_0^{p_q^+}\frac{dl^+}{2l^+}\int d^d\vec{l}\frac{\delta\left(p_q^++p_{\bar{q}}^+-p_\gamma^+\right)\delta\left(\vec{p}_{q1}+\vec{p}_{\bar{q}2}\right)}{\left(\frac{\left(\vec{p}_{q1}-\vec{l}\right)^2-i0}{2\left(p_q^+-l^+\right)}+\frac{\left(\vec{p}_{\bar{q}2}+\vec{l}\right)^2-i0}{2\left(p_{\bar{q}}^++l^+\right)}-p_\gamma^-\right)}
\end{aligned}
$$

$$\times\bar{u}_{p_q}\gamma_\mu\frac{\gamma^-\left(p_q^+-l^+\right)+\left(\hat{p}_{q\perp}-\hat{l}_\perp\right)}{2\left(p_q^+-l^+\right)}\gamma^+\frac{\gamma^-\left(p_q^+-l^+\right)+\left(\hat{p}_{q1\perp}-\hat{l}_\perp\right)}{2\left(p_q^+-l^+\right)}\gamma^\alpha$$
$$\times\frac{\gamma^-\left(p_{\bar{q}}^+-l^+\right)+\left(\hat{p}_{\bar{q}2\perp}+\hat{l}_\perp\right)}{2\left(p_{\bar{q}}^+-l^+\right)}\gamma^+\frac{\gamma^-\left(p_{\bar{q}}^+-l^+\right)+\left(\hat{p}_{\bar{q}\perp}+\hat{l}_\perp\right)}{2\left(p_{\bar{q}}^+-l^+\right)}\gamma_\nu v_{p_{\bar{q}}}$$
$$\times\frac{g_{\perp\mu\nu}-\frac{l_{\perp\mu}n_{2\nu}+l_{\perp\nu}n_{2\mu}}{l^+}-\frac{\vec{l}^{\,2}}{(l^+)^2}n_{2\mu}n_{2\nu}}{\left(\frac{\vec{p}_q^{\,2}}{2p_q^+}+\frac{\vec{p}_{\bar{q}}^{\,2}}{2p_{\bar{q}}^+}-\frac{\left(\vec{p}_q-\vec{l}\right)^2-i0}{2\left(p_q^+-l^+\right)}-\frac{\left(\vec{p}_{\bar{q}}+\vec{l}\right)^2-i0}{2\left(p_{\bar{q}}^+-l^+\right)}\right)\left(\frac{\vec{p}_q^{\,2}}{2p_q^+}-\frac{\left(\vec{p}_q-\vec{l}\right)^2-i0}{2\left(p_q^+-l^+\right)}-\frac{\vec{l}^{\,2}-i0}{2l^+}\right)},$$

and

$$M_4^{(3)\alpha} = \frac{N_c e_q}{\sqrt{2p_\gamma^+}}(ig)^2\frac{\theta\left(p_q^+\right)\theta\left(p_{\bar{q}}^+\right)}{\sqrt{2p_q^+2p_{\bar{q}}^+}}\left(\frac{N_c^2-1}{2N_c\sqrt{N_c}}\right)\int\frac{d^d\vec{p}_1}{(2\pi)^d}\frac{d^d\vec{p}_2}{(2\pi)^d}\left(\tilde{\mathcal{U}}_{12}\right) \tag{3.62}$$
$$\times\int\frac{dl^+d^d\vec{l}}{\left(l^+\right)^2}\frac{\delta\left(p_q^++p_{\bar{q}}^+-p_\gamma^+\right)\delta\left(\vec{p}_{q1}+\vec{p}_{\bar{q}2}\right)\theta\left(p_q^+-l^+\right)\theta\left(p_{\bar{q}}^++l^+\right)}{\left(\frac{\vec{p}_q^{\,2}}{2p_q^+}+\frac{\vec{p}_{\bar{q}}^{\,2}}{2p_{\bar{q}}^+}-\frac{\left(\vec{p}_q-\vec{l}\right)^2-i0}{2\left(p_q^+-l^+\right)}-\frac{\left(\vec{p}_{\bar{q}}+\vec{l}\right)^2-i0}{2\left(p_{\bar{q}}^++l^+\right)}\right)\left(\frac{\left(\vec{p}_{q1}-\vec{l}\right)^2-i0}{2\left(p_q^+-l^+\right)}+\frac{\left(\vec{p}_{\bar{q}2}+\vec{l}\right)^2-i0}{2\left(p_{\bar{q}}^++l^+\right)}-p_\gamma^-\right)}$$
$$\times\bar{u}_{p_q}\gamma^+\frac{\gamma^-\left(p_q^+-l^+\right)+\left(\hat{p}_{q1\perp}-\hat{l}_\perp\right)}{2\left(p_q^+-l^+\right)}\gamma^\alpha\frac{\gamma^-\left(p_{\bar{q}}^++l^+\right)+\left(\hat{p}_{\bar{q}2\perp}+\hat{l}_\perp\right)}{2\left(p_{\bar{q}}^++l^+\right)}\gamma^+v_{p_{\bar{q}}}.$$

The $l_\perp$ integral is far more complicated than the one in the previous diagrams due to the presence of 3 denominators with an $l_\perp$ dependence in $M_4^{(1)\alpha}$ and $M_4^{(2)\alpha}$. However let us note that one denominator can be reduced to $\vec{l}^{\,2}$ ater a simple shift on $\vec{l}$. Indeed :

$$\frac{\vec{p}_q^{\,2}}{2p_q^+}-\frac{\left(\vec{p}_q-\vec{l}\right)^2-i0}{2\left(p_q^+-l^+\right)}-\frac{\vec{l}^{\,2}-i0}{2l^+} = -\frac{p_q^+}{2l^+\left(p_q^+-l^+\right)}\left(\vec{l}-\frac{l^+}{p_q^+}\vec{p}_q\right)^2. \tag{3.63}$$

We will need similar integrals in most of the other diagrams, so we will define the following general integrals :

$$I_1^k(\vec{q}_1,\,\vec{q}_2,\,\Delta_1,\,\Delta_2) \equiv \frac{1}{\pi}\int\frac{d^d\vec{l}\left(l_\perp^k\right)}{\left[(\vec{l}-\vec{q}_1)^2+\Delta_1\right]\left[(\vec{l}-\vec{q}_2)^2+\Delta_2\right]\vec{l}^{\,2}}, \tag{3.64}$$

$$I_2(\vec{q}_1,\,\vec{q}_2,\,\Delta_1,\,\Delta_2) \equiv \frac{1}{\pi}\int\frac{d^d\vec{l}}{\left[(\vec{l}-\vec{q}_1)^2+\Delta_1\right]\left[(\vec{l}-\vec{q}_2)^2+\Delta_2\right]}, \tag{3.65}$$

$$I_3^k(\vec{q}_1,\,\vec{q}_2,\,\Delta_1,\,\Delta_2) \equiv \frac{1}{\pi}\int\frac{d^d\vec{l}\left(l_\perp^k\right)}{\left[(\vec{l}-\vec{q}_1)^2+\Delta_1\right]\left[(\vec{l}-\vec{q}_2)^2+\Delta_2\right]}, \tag{3.66}$$

$$I^{jk}(\vec{q}_1,\,\vec{q}_2,\,\Delta_1,\,\Delta_2) \equiv \frac{1}{\pi}\int\frac{d^d\vec{l}\left(l_\perp^jl_\perp^k\right)}{\left[(\vec{l}-\vec{q}_1)^2+\Delta_1\right]\left[(\vec{l}-\vec{q}_2)^2+\Delta_2\right]\vec{l}^{\,2}}. \tag{3.67}$$

These integrals are computed in Appendix A.1.1.

Let us start with a remark : once $\vec{l}$ has been shifted, there is no divergence when the shifted $\vec{l}$ approaches $\vec{0}$. Indeed this would correspond exactly to a divergence emerging when the gluon is collinear to the quark, which should be absent from such a diagram : collinear divergences occur when the gluon is emitted and reabsorbed by the parton to which it is collinear.

Let us rewrite the third line and the gluonic tensor in Eq. (3.60), and set $\vec{l}\to\frac{l^+}{p_q^+}\vec{p}_q$:

$$\bar{u}_{p_q}\gamma_\mu\frac{\left(\hat{p}_q-\hat{l}\right)}{2\left(p_q^+-l^+\right)}\gamma^+d_0^{\mu\nu}(l) \tag{3.68}$$
$$\to \frac{\bar{u}_{p_q}\left(\gamma_\mu\hat{p}_q\gamma^+\right)}{2p_q^+}\left(g_\perp^{\mu\nu}-\frac{p_{q\perp}^\mu n_2^\nu+p_{q\perp}^\nu n_2^\mu}{p_q^+}-\frac{\vec{p}_q^{\,2}}{\left(p_q^+\right)^2}n_2^\mu n_2^\nu\right).$$

Using the Dirac equation one can write by anticommutation of the Dirac matrices $\gamma_\mu \hat{p}_q \to 2p_{q\mu}$. Then one only has to notice that the new gluonic tensor is $d_0^{\mu\nu}(p_q)$, which is exactly canceled by $p_{q\mu}$. Thus as expected there is at least a linear dependence in $l_\perp$ in the numerator of this diagram once $l_\perp$ has been shifted, which is the reason why we will not need the integral which is similar to Eq. (3.64) but with 1 in the numerator. The only divergences from this diagram are actually soft divergences for $\alpha = +$ and $\alpha = i$. For $\alpha = -$ this diagram contains a UV divergence which should cancel when we construct a gauge invariant quantity (i.e. adding the dipole contributions of diagrams 5 and 6). However as we stated before we will not compute the $\alpha = -$ contribution. They is no way of writing the final Dirac structure and the finite result for this diagram which would be compact enough to fit in this thesis. Instead, we will present the result for the contribution of this diagram to the cross section once in Appendix A.1. We will only write explicitly the divergent part of this diagram here. One gets :

$$\begin{aligned}\left(\Phi_1^+|_4\right)_{div} &= \frac{1}{2}\Phi_0^+\left[\ln^2\left(\frac{x\bar{x}}{\alpha^2}\right) - \ln^2\left(\frac{\bar{x}}{x}\right) + 2\ln\left(\frac{x\bar{x}}{\alpha^2}\right)\left\{\ln\left(\frac{\left(\vec{p}_{q1}^{\,2} + x\bar{x}Q^2\right)^2}{Q^2\left(x\vec{p}_{\bar{q}} - \bar{x}\vec{p}_q\right)^2}\right) + i\pi\right\}\right] \qquad (3.69)\\ &+\bar{u}_{p_q} C_\parallel^4 v_{p_{\bar{q}}}\end{aligned}$$

$$\begin{aligned}\left(\Phi_{1\perp}^i|_4\right)_{div} &= \frac{1}{2}\Phi_{0\perp}^i\left[\ln^2\left(\frac{x\bar{x}}{\alpha^2}\right) - \ln^2\left(\frac{\bar{x}}{x}\right) + 2\ln\left(\frac{x\bar{x}}{\alpha^2}\right)\right. \qquad (3.70)\\ &\left.\times\left\{\ln\left(\frac{x\bar{x}\left(\vec{p}_{q1}^{\,2} + x\bar{x}Q^2\right)}{\left(x\vec{p}_{\bar{q}} - \bar{x}\vec{p}_q\right)^2}\right) - x\bar{x}\frac{Q^2}{\vec{p}_{q1}^{\,2}}\ln\left(\frac{\vec{p}_{q1}^{\,2} + x\bar{x}Q^2}{x\bar{x}Q^2}\right) + i\pi\right\}\right] + \left(\bar{u}_{p_q} C_\perp^{4i} v_{p_{\bar{q}}}\right),\end{aligned}$$

where $C_\parallel^4$ and $C_\perp^{4i}$ are finite expressions.

3.4.6 Diagram 5 : gluon exchange through the shockwave field

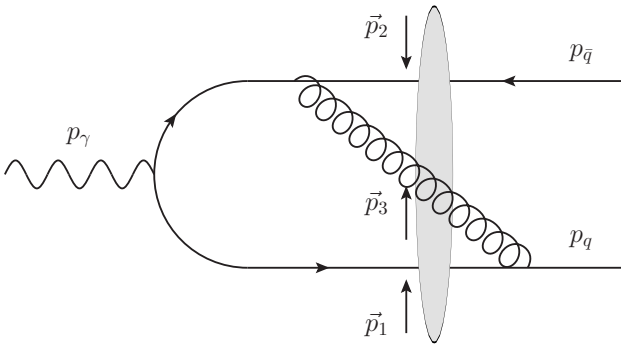

Figure 3.9: Gluon exchange through the shockwave field

This diagram reads :

$$\begin{aligned}M_5^\alpha &= \frac{-ie_q}{\sqrt{2p_\gamma^+}}(ig)^2\int d^Dy_2 d^Dy_1 d^Dy_0 \frac{\left(\bar{u}_{p_q}\right)_i}{\sqrt{2p_q^+}} e^{i(p_q\cdot y_2)}\theta\left(p_q^+\right)\gamma^\mu G\left(y_2,\, y_0\right)\gamma^\alpha e^{-i(p_\gamma\cdot y_0)} G_0\left(y_{01}\right)\gamma^\nu v_m\left(p_{\bar{q}},\, y_1\right)\\ &\times G_{\mu\nu}\left(y_{21}\right)\frac{\delta_{im}}{\sqrt{N_c}} \qquad (3.71)\\ &= \frac{-ie_q(ig)^2}{\sqrt{2p_\gamma^+}}\sqrt{N_c}\int\frac{d^dp_{1\perp}}{(2\pi)^d}\frac{d^d\vec{p}_2}{(2\pi)^d}\frac{d^d\vec{p}_3}{(2\pi)^d}\left[\frac{N_c}{2}\left(\tilde{\mathcal{U}}_{13} + \tilde{\mathcal{U}}_{32} - \tilde{\mathcal{U}}_{12} - \widetilde{\mathcal{U}_{13}\mathcal{U}_{32}}\right) + (2\pi)^d\left(\frac{N_c^2-1}{2N_c}\right)\tilde{\mathcal{U}}_{12}\delta\left(\vec{p}_3\right)\right]\\ &\times\frac{\theta\left(p_q^+\right)\theta\left(p_{\bar{q}}^+\right)}{\sqrt{2p_q^+ 2p_{\bar{q}}^+}}\int dy_1^+ dy_0^+\theta\left(-y_1^+\right)\theta\left(-y_0^+\right)\delta\left(p_q^+ + p_{\bar{q}}^+ - p_\gamma^+\right)\delta\left(\vec{p}_{q1} + \vec{p}_{\bar{q}2} - \vec{p}_3\right) \qquad (3.72)\\ &\times\int_0^{p_q^+}\frac{dl^+}{2l^+}\int d^d\vec{l}\,\bar{u}_{p_q}\gamma^\mu\frac{\gamma^-\left(p_q^+ - l^+\right) + \hat{p}_{q\perp} - \hat{l}_\perp}{2\left(p_q^+ - l^+\right)}\gamma^+\frac{\gamma^-\left(p_q^+ - l^+\right) + \left(\hat{p}_{q1\perp} - \hat{l}_\perp\right)}{2\left(p_q^+ - l^+\right)}\gamma^\alpha\end{aligned}$$

$$\times\left[\left(\left(p_{\bar{q}}^{+}+l^{+}\right)\gamma^{-}+\frac{\left(\vec{p}_{q1}-\vec{l}\right)^{2}}{2\left(p_{\bar{q}}^{+}+l^{+}\right)}\gamma^{+}-\hat{p}_{q1\perp}+\hat{l}_{\perp}\right)\theta(y_{10}^{+})+i\delta\left(y_{10}^{+}\right)\gamma^{+}\right]\gamma^{\nu}$$
$$\times\frac{\left(p_{\bar{q}}^{+}\gamma^{-}+\hat{p}_{\bar{q}2\perp}\right)}{2p_{\bar{q}}^{+}}\gamma^{+}v_{p_{\bar{q}}}\frac{1}{2\left(p_{\bar{q}}^{+}+l^{+}\right)}\left(g_{\perp\mu\beta}-\frac{l_{\perp}^{\beta}}{l^{+}}n_{2\mu}\right)\left(g_{\perp\nu}^{\beta}-\frac{l_{\perp}^{\beta}-p_{3\perp}^{\beta}}{l^{+}}n_{2\nu}\right)$$
$$\times\frac{i}{\left(p_{q}^{-}-\frac{\vec{l}^{\,2}-i0}{2l^{+}}-\frac{\left(\vec{p}_{q}-\vec{l}\right)^{2}-i0}{2\left(p_{q}^{+}-l^{+}\right)}\right)}\exp\left[iy_{0}^{+}\left(\frac{\left(\vec{p}_{q1}-\vec{l}\right)^{2}-i0}{2\left(p_{q}^{+}-l^{+}\right)}-\frac{\left(\vec{p}_{q1}-\vec{l}\right)^{2}-i0}{2\left(-p_{\bar{q}}^{+}-l^{+}\right)}-p_{\gamma}^{-}\right)\right]$$
$$\times\exp\left[iy_{1}^{+}\left(\frac{\vec{p}_{\bar{q}2}^{\,2}-i0}{2p_{\bar{q}}^{+}}+\frac{\left(\vec{p}_{q1}-\vec{l}\right)^{2}-i0}{2\left(-p_{\bar{q}}^{+}-l^{+}\right)}+\frac{\left(\vec{l}-\vec{p}_{3}\right)^{2}-i0}{2l^{+}}\right)\right].$$

There are two contributions :

$$\begin{aligned}
M_{5}^{(1)\alpha} &= \int\frac{d^{d}p_{1\perp}}{(2\pi)^{d}}\frac{d^{d}\vec{p}_{2}}{(2\pi)^{d}}\frac{d^{d}\vec{p}_{3}}{(2\pi)^{d}}\left[\frac{N_{c}}{2}\left(\tilde{\mathcal{U}}_{13}+\tilde{\mathcal{U}}_{32}-\tilde{\mathcal{U}}_{12}-\widetilde{\mathcal{U}_{13}\mathcal{U}_{32}}\right)+(2\pi)^{d}\left(\frac{N_{c}^{2}-1}{2N_{c}}\right)\tilde{\mathcal{U}}_{12}\delta\left(\vec{p}_{3}\right)\right]\\
&\times\frac{-(ig)^{2}e_{q}}{\sqrt{2p_{\gamma}^{+}}}\sqrt{N_{c}}\frac{\theta\left(p_{q}^{+}\right)\theta\left(p_{\bar{q}}^{+}\right)}{\sqrt{2p_{q}^{+}2p_{\bar{q}}^{+}}}\delta\left(p_{q}^{+}+p_{\bar{q}}^{+}-p_{\gamma}^{+}\right)\delta\left(\vec{p}_{q1}+\vec{p}_{\bar{q}2}-\vec{p}_{3}\right)\int_{0}^{p_{q}^{+}}\frac{dl^{+}}{2l^{+}}\int d^{d}\vec{l}\\
&\times\bar{u}_{p_{q}}\gamma^{\mu}\frac{\gamma^{-}\left(p_{q}^{+}-l^{+}\right)+\hat{p}_{q\perp}-\hat{l}_{\perp}}{2\left(p_{q}^{+}-l^{+}\right)}\gamma^{+}\frac{\gamma^{-}\left(p_{q}^{+}-l^{+}\right)+\left(\hat{p}_{q1\perp}-\hat{l}_{\perp}\right)}{2\left(p_{q}^{+}-l^{+}\right)}\gamma^{\alpha}\\
&\times\left[\left(p_{\bar{q}}^{+}+l^{+}\right)\gamma^{-}+\frac{\left(\vec{p}_{q1}-\vec{l}\right)^{2}}{2\left(p_{\bar{q}}^{+}+l^{+}\right)}\gamma^{+}-\hat{p}_{q1\perp}+\hat{l}_{\perp}\right]\gamma^{\nu}\frac{\left(p_{\bar{q}}^{+}\gamma^{-}+\hat{p}_{\bar{q}2\perp}\right)}{2p_{\bar{q}}^{+}}\gamma^{+}v_{p_{\bar{q}}}\frac{1}{2\left(p_{\bar{q}}^{+}+l^{+}\right)}\\
&\times\frac{\left(g_{\perp\mu\beta}-\frac{l_{\perp}^{\beta}}{l^{+}}n_{2\mu}\right)\left(g_{\perp\nu}^{\beta}-\frac{l_{\perp}^{\beta}-p_{3\perp}^{\beta}}{l^{+}}n_{2\nu}\right)}{\left(p_{q}^{-}-\frac{\vec{l}^{\,2}-i0}{2l^{+}}-\frac{\left(\vec{p}_{q}-\vec{l}\right)^{2}-i0}{2\left(p_{q}^{+}-l^{+}\right)}\right)\left(\frac{\left(\vec{p}_{q1}-\vec{l}\right)^{2}-i0}{2\left(p_{q}^{+}-l^{+}\right)}-\frac{\left(\vec{p}_{q1}-\vec{l}\right)^{2}-i0}{2\left(-p_{\bar{q}}^{+}-l^{+}\right)}-p_{\gamma}^{-}\right)}\\
&\times\frac{1}{\left(\frac{\vec{p}_{\bar{q}2}^{\,2}-i0}{2p_{\bar{q}}^{+}}+\frac{\left(\vec{l}-\vec{p}_{3}\right)^{2}-i0}{2l^{+}}+\frac{\left(\vec{p}_{q1}-\vec{l}\right)^{2}-i0}{2\left(p_{q}^{+}-l^{+}\right)}-p_{\gamma}^{-}\right)},
\end{aligned}\tag{3.73}$$

and

$$\begin{aligned}
M_{5}^{(2)\alpha} &= \int\frac{d^{d}p_{1\perp}}{(2\pi)^{d}}\frac{d^{d}\vec{p}_{2}}{(2\pi)^{d}}\frac{d^{d}\vec{p}_{3}}{(2\pi)^{d}}\left[\frac{N_{c}}{2}\left(\tilde{\mathcal{U}}_{13}+\tilde{\mathcal{U}}_{32}-\tilde{\mathcal{U}}_{12}-\widetilde{\mathcal{U}_{13}\mathcal{U}_{32}}\right)+(2\pi)^{d}\left(\frac{N_{c}^{2}-1}{2N_{c}}\right)\tilde{\mathcal{U}}_{12}\delta\left(\vec{p}_{3}\right)\right]\\
&\times\frac{(ig)^{2}e_{q}}{\sqrt{2p_{\gamma}^{+}}}\sqrt{N_{c}}\frac{\theta\left(p_{q}^{+}\right)\theta\left(p_{\bar{q}}^{+}\right)}{\sqrt{2p_{q}^{+}2p_{\bar{q}}^{+}}}\delta\left(p_{q}^{+}+p_{\bar{q}}^{+}-p_{\gamma}^{+}\right)\delta\left(\vec{p}_{q1}+\vec{p}_{\bar{q}2}-\vec{p}_{3}\right)\\
&\times\int_{0}^{p_{q}^{+}}\frac{dl^{+}}{2l^{+}}\int d^{d}\vec{l}\bar{u}_{p_{q}}\gamma^{\mu}\frac{\gamma^{-}\left(p_{q}^{+}-l^{+}\right)+\hat{p}_{q\perp}-\hat{l}_{\perp}}{2\left(p_{q}^{+}-l^{+}\right)}\gamma^{+}\frac{\gamma^{-}\left(p_{q}^{+}-l^{+}\right)+\left(\hat{p}_{q1\perp}-\hat{l}_{\perp}\right)}{2\left(p_{q}^{+}-l^{+}\right)}\gamma^{\alpha}\\
&\times\frac{\gamma^{+}\left(\gamma_{\perp\mu}-\frac{\hat{l}_{\perp}}{l^{+}}n_{2\mu}\right)v_{p_{\bar{q}}}}{\left(\frac{\vec{p}_{q}^{\,2}}{2p_{q}^{+}}-\frac{\vec{l}^{\,2}-i0}{2l^{+}}-\frac{\left(\vec{p}_{q}-\vec{l}\right)^{2}-i0}{2\left(p_{q}^{+}-l^{+}\right)}\right)\left(\frac{\left(\vec{p}_{q1}-\vec{l}\right)^{2}-i0}{2\left(p_{q}^{+}-l^{+}\right)}+\frac{\vec{p}_{\bar{q}2}^{\,2}-i0}{2p_{\bar{q}}^{+}}+\frac{\left(\vec{l}-\vec{p}_{3}\right)^{2}-i0}{2l^{+}}-p_{\gamma}^{-}\right)}\frac{1}{2\left(p_{\bar{q}}^{+}+l^{+}\right)}.
\end{aligned}\tag{3.74}$$

Similarly to diagram 4, the $l_{\perp}$ integration requires quite some work. However it will involve the same type of integrals as before. Indeed by performing the shift $\vec{l}\rightarrow\vec{l}-\frac{l^{+}}{p_{q}^{+}}\vec{p}_{q}$, one can reduce one of the denominators to $\vec{l}^{\,2}$. Then using the same arguments as before one can show that there is at least a linear dependence in $l_{\perp}$ in the numerator. The explicit finite result for this diagram can be found in

Appendix A.1. After adding the diagram which is symmetric to this one w.r.t. the exchange of the quark and the antiquark, the contributions to Φ_1^α and Φ_2^α read :

$$\left(\Phi_1^+|_5\right)_{div} = -\frac{1}{2}\Phi_0^+\left[\ln^2\left(\frac{x\bar{x}}{\alpha^2}\right)-\ln^2\left(\frac{\bar{x}}{x}\right)+2\ln\left(\frac{x\bar{x}}{\alpha^2}\right)\ln\left(\frac{\left(\vec{p}_{q1}^{\,2}+x\bar{x}Q^2\right)^2}{x\bar{x}Q^4}\right)\right]+\bar{u}_{p_q}C_{1\|}^5 v_{p_{\bar{q}}}\,, \tag{3.75}$$

$$\begin{aligned}\left(\Phi_{1\perp}^i|_5\right)_{div} &= -\frac{1}{2}\Phi_{0\perp}^i\left[\ln^2\left(\frac{x\bar{x}}{\alpha^2}\right)-\ln^2\left(\frac{\bar{x}}{x}\right)+2\ln\left(\frac{x\bar{x}}{\alpha^2}\right)\left(-2x\bar{x}\frac{Q^2}{\vec{p}_{q1}^{\,2}}\ln\left(\frac{\vec{p}_{q1}^{\,2}+x\bar{x}Q^2}{x\bar{x}Q^2}\right)+\ln\left(x\bar{x}\right)\right)\right]\\ &\quad+\bar{u}_{p_q}C_{1\perp}^{5i}v_{p_{\bar{q}}}\,,\end{aligned} \tag{3.76}$$

$$\begin{aligned}\left(\Phi_2^+|_5\right)_{div} &= \frac{2x\bar{x}p_\gamma^+\left(\bar{u}_{p_q}\gamma^+v_{p_{\bar{q}}}\right)\left(\vec{p}_3^{\,2}-\vec{p}_{\bar{q}2}^{\,2}-\vec{p}_{q1}^{\,2}-2x\bar{x}Q^2\right)}{\left(\vec{p}_{q1}^{\,2}+x\bar{x}Q^2\right)\left(\vec{p}_{\bar{q}2}^{\,2}+x\bar{x}Q^2\right)-x\bar{x}Q^2\vec{p}_3^{\,2}}\ln\left(\frac{x\bar{x}}{\alpha^2}\right)\ln\left[\frac{\left(\vec{p}_{q1}^{\,2}+x\bar{x}Q^2\right)\left(\vec{p}_{\bar{q}2}^{\,2}+x\bar{x}Q^2\right)}{x\bar{x}Q^2\vec{p}_3^{\,2}}\right]\\ &\quad+\bar{u}_{p_q}C_{2\|}^5 v_{p_{\bar{q}}}\,,\end{aligned} \tag{3.77}$$

$$\begin{aligned}\left(\Phi_{2\perp}^i|_5\right)_{div} &= =\ln\left(\frac{x\bar{x}}{\alpha^2}\right)\left\{\overline{u}_{p_q}(p_{q1\perp}^i(1-2x)+\frac{1}{2}[\hat{p}_{q1\perp},\,\gamma_\perp^i])\gamma^+v_{p_{\bar{q}}}\right.\\ &\quad\times\left[\frac{1}{\vec{p}_{q1}^{\,2}}\ln\left(\frac{\vec{p}_{q1}^{\,2}+x\bar{x}Q^2}{x\bar{x}Q^2}\right)-\frac{\vec{p}_{\bar{q}2}^{\,2}+x\bar{x}Q^2}{\left(\vec{p}_{q1}^{\,2}+x\bar{x}Q^2\right)\left(\vec{p}_{\bar{q}2}^{\,2}+x\bar{x}Q^2\right)-x\bar{x}Q^2\vec{p}_3^{\,2}}\right.\\ &\quad\left.\left.\times\ln\left(\frac{\left(\vec{p}_{q1}^{\,2}+x\bar{x}Q^2\right)\left(\vec{p}_{\bar{q}2}^{\,2}+x\bar{x}Q^2\right)}{x\bar{x}Q^2\vec{p}_3^{\,2}}\right)\right]+(q\leftrightarrow\bar{q})\right\}+\bar{u}_{p_q}C_{2\perp}^{5i}v_{p_{\bar{q}}}\,,\end{aligned} \tag{3.78}$$

where $C_{2\|}^5$ and $C_{2\perp}^{5i}$ are finite and so are $C_{1\|}^5\equiv C_{2\|}^5|_{\vec{p}_3\to\vec{0}}$ and $C_{1\perp}^{5i}\equiv C_{2\perp}^{5i}|_{\vec{p}_3\to\vec{0}}$.

3.4.7 Diagram 6 : dressed quark line through the shockwave field

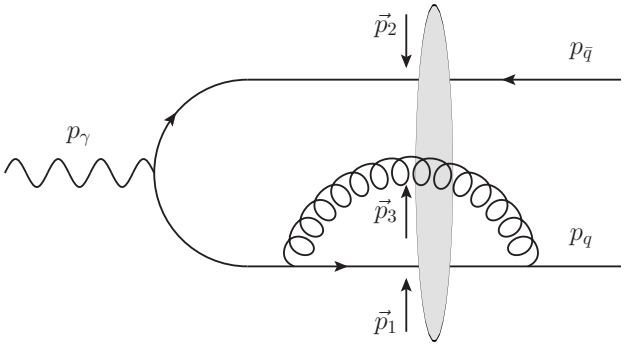

Figure 3.10: Dressed quark line through the shockwave field

With the usual computation method we get :

$$\begin{aligned}M_6^\alpha &= \frac{-ie_q}{\sqrt{2p_\gamma^+}}(ig)^2\int d^Dy_2d^Dy_1d^Dy_0\frac{\left(\bar{u}_{p_q}\right)_i\theta\left(p_q^+\right)}{\sqrt{2p_q^+}}e^{i(p_q\cdot y_2)-i(p_\gamma\cdot y_0)}\gamma^\mu G\left(y_2,\,y_1\right)\gamma^\nu G_0\left(y_{10}\right)\gamma^\alpha v_m\left(p_{\bar{q}},\,y_0\right)\\ &\quad\times\frac{\delta_{im}}{\sqrt{N_c}}G_{\mu\nu}\left(y_2,\,y_1\right)\end{aligned} \tag{3.79}$$

$$\begin{aligned}&= \frac{ie_q(ig)^2}{\sqrt{2p_\gamma^+}}\sqrt{N_c}\int\frac{d^d\vec{p}_1}{(2\pi)^d}\frac{d^d\vec{p}_2}{(2\pi)^d}\frac{d^d\vec{p}_3}{(2\pi)^d}\left[\frac{N_c}{2}\left(\tilde{\mathcal{U}}_{13}+\tilde{\mathcal{U}}_{32}-\tilde{\mathcal{U}}_{12}-\widetilde{\mathcal{U}_{13}\mathcal{U}_{32}}\right)+(2\pi)^d\left(\frac{N_c^2-1}{2N_c}\right)\tilde{\mathcal{U}}_{12}\delta\left(\vec{p}_3\right)\right]\\ &\quad\times\frac{\theta\left(p_q^+\right)\theta\left(p_{\bar{q}}^+\right)}{\sqrt{2p_q^+2p_{\bar{q}}^+}}\delta\left(p_q^++p_{\bar{q}}^+-p_\gamma^+\right)\delta\left(\vec{p}_{q1}+\vec{p}_{\bar{q}2}-\vec{p}_3\right)\int dy_1^+dy_0^+\theta\left(-y_1^+\right)\theta\left(-y_0^+\right)\end{aligned} \tag{3.80}$$

$$
\begin{aligned}
&\times\frac{1}{2p_q^+}\int_0^{p_q^+}\frac{dl^+}{2l^+}\int d^d\vec{l}\bar{u}_{p_q}\gamma^\mu\frac{\gamma^-\left(p_q^+-l^+\right)+\left(\hat{p}_{q\perp}-\hat{l}_\perp\right)}{2\left(p_q^+-l^+\right)}\gamma^+\frac{\gamma^-\left(p_q^+-l^+\right)+\left(\hat{p}_{q1\perp}-\hat{l}_\perp\right)}{2\left(p_q^+-l^+\right)}\gamma^\nu\\
&\times\left[\left(p_q^+\gamma^-+\frac{\vec{p}_{\bar{q}2}^{\,2}}{2p_q^+}\gamma^+-\hat{p}_{\bar{q}2\perp}\right)\theta(y_{10}^+)+i\delta\left(y_{10}^+\right)\gamma^+\right]\gamma^\alpha\frac{p_{\bar{q}}^+\gamma^-+\hat{p}_{\bar{q}2\perp}}{2p_{\bar{q}}^+}\gamma^+v_{p_{\bar{q}}}\\
&\times\frac{i}{\left(p_q^--\frac{\vec{l}^{\,2}-i0}{2l^+}-\frac{\left(\vec{p}_q-\vec{l}\right)^2-i0}{2\left(p_q^+-l^+\right)}\right)}\exp\left[iy_1^+\left(\frac{\left(\vec{p}_{q1}-\vec{l}\right)^2-i0}{2\left(p_q^+-l^+\right)}+\frac{\left(\vec{l}-\vec{p}_3\right)^2-i0}{2l^+}-\frac{\vec{p}_{\bar{q}2}^{\,2}-i0}{2p_q^+}\right)\right]\\
&\times\exp\left[iy_0^+\left(\frac{\vec{p}_{\bar{q}2}^{\,2}-i0}{2p_q^+}+\frac{\vec{p}_{\bar{q}2}^{\,2}-i0}{2p_{\bar{q}}^+}-p_\gamma^+\right)\right]\left(g_{\perp\mu\beta}-\frac{l_{\perp\beta}}{l^+}n_{2\mu}\right)\left(g_{\perp\mu}^\beta-\frac{l_{\perp\beta}-p_{3\perp\beta}}{l^+}\right).
\end{aligned}
$$

There are two contributions :

$$
\begin{aligned}
M_6^{(1)\alpha} &= \frac{e_q}{\sqrt{2p_\gamma^+}}(ig)^2\sqrt{N_c}\int\frac{d^d\vec{p}_1}{(2\pi)^d}\frac{d^d\vec{p}_2}{(2\pi)^d}\frac{d^d\vec{p}_3}{(2\pi)^d}\\
&\times\left[\frac{N_c}{2}\left(\tilde{\mathcal{U}}_{13}+\tilde{\mathcal{U}}_{32}-\tilde{\mathcal{U}}_{12}-\widetilde{\mathcal{U}_{13}\mathcal{U}_{32}}\right)+(2\pi)^d\left(\frac{N_c^2-1}{2N_c}\right)\tilde{\mathcal{U}}_{12}\delta\left(\vec{p}_3\right)\right]\\
&\times\frac{\theta\left(p_q^+\right)\theta\left(p_{\bar{q}}^+\right)}{\sqrt{2p_q^+2p_{\bar{q}}^+}}\frac{\delta\left(p_q^++p_{\bar{q}}^+-p_\gamma^+\right)\delta\left(\vec{p}_{q1}+\vec{p}_{\bar{q}2}-\vec{p}_3\right)}{\left(\frac{\vec{p}_{\bar{q}2}^{\,2}-i0}{2p_q^+}+\frac{\vec{p}_{\bar{q}2}^{\,2}-i0}{2p_{\bar{q}}^+}-p_\gamma^-\right)}\\
&\times\frac{1}{2p_q^+}\int_0^{p_q^+}\frac{dl^+}{2l^+}\int d^d\vec{l}\bar{u}_{p_q}\gamma^\mu\frac{\gamma^-\left(p_q^+-l^+\right)+\left(\hat{p}_{q\perp}-\hat{l}_\perp\right)}{2\left(p_q^+-l^+\right)}\gamma^+\frac{\gamma^-\left(p_q^+-l^+\right)+\left(\hat{p}_{q1\perp}-\hat{l}_\perp\right)}{2\left(p_q^+-l^+\right)}\gamma^\nu\\
&\times\left(p_q^+\gamma^-+\frac{\vec{p}_{\bar{q}2}^{\,2}}{2p_q^+}\gamma^+-\hat{p}_{\bar{q}2\perp}\right)\gamma^\alpha\frac{p_{\bar{q}}^+\gamma^-+\hat{p}_{\bar{q}2\perp}}{2p_{\bar{q}}^+}\gamma^+v_{p_{\bar{q}}}\\
&\times\frac{\left(g_{\perp\mu\beta}-\frac{l_{\perp\beta}}{l^+}n_{2\mu}\right)\left(g_{\perp\nu}^\beta-\frac{l_{\perp\beta}-p_{3\perp\beta}}{l^+}n_{2\nu}\right)}{\left(p_q^--\frac{\vec{l}^{\,2}-i0}{2l^+}-\frac{\left(\vec{p}_q-\vec{l}\right)^2-i0}{2\left(p_q^+-l^+\right)}\right)\left(\frac{\left(\vec{p}_{q1}-\vec{l}\right)^2-i0}{2\left(p_q^+-l^+\right)}+\frac{\left(\vec{l}-\vec{p}_3\right)^2-i0}{2l^+}+\frac{\vec{p}_{\bar{q}2}^{\,2}-i0}{2p_{\bar{q}}^+}-p_\gamma^-\right)},
\end{aligned}
\tag{3.81}
$$

and

$$
\begin{aligned}
M_6^{(2)\alpha} &= i\frac{ie_q}{\sqrt{2p_\gamma^+}}(ig)^2\sqrt{N_c}\int\frac{d^d\vec{p}_1}{(2\pi)^d}\frac{d^d\vec{p}_2}{(2\pi)^d}\frac{d^d\vec{p}_3}{(2\pi)^d}\\
&\times\left[\frac{N_c}{2}\left(\tilde{\mathcal{U}}_{13}+\tilde{\mathcal{U}}_{32}-\tilde{\mathcal{U}}_{12}-\widetilde{\mathcal{U}_{13}\mathcal{U}_{32}}\right)+(2\pi)^d\left(\frac{N_c^2-1}{2N_c}\right)\tilde{\mathcal{U}}_{12}\delta\left(\vec{p}_3\right)\right]\\
&\times\frac{\theta\left(p_q^+\right)\theta\left(p_{\bar{q}}^+\right)}{\sqrt{2p_q^+2p_{\bar{q}}^+}}\delta\left(p_q^++p_{\bar{q}}^+-p_\gamma^+\right)\delta\left(\vec{p}_{q1}+\vec{p}_{\bar{q}2}-\vec{p}_3\right)\frac{1}{2p_q^+}\int_0^{p_q^+}\frac{dl^+}{2l^+}\int d^d\vec{l}\\
&\times\bar{u}_{p_q}\gamma^\mu\frac{\gamma^-\left(p_q^+-l^+\right)+\left(\hat{p}_{q\perp}-\hat{l}_\perp\right)}{2\left(p_q^+-l^+\right)}\gamma_\perp^\nu\gamma^+\gamma^\alpha\frac{p_{\bar{q}}^+\gamma^-+\hat{p}_{\bar{q}2\perp}}{2p_{\bar{q}}^+}\gamma^+v_{p_{\bar{q}}}\left(g_{\perp\mu\nu}-\frac{l_{\perp\nu}}{l^+}n_{2\mu}\right)\\
&\times\frac{1}{\left(p_q^--\frac{\vec{l}^{\,2}-i0}{2l^+}-\frac{\left(\vec{p}_q-\vec{l}\right)^2-i0}{2\left(p_q^+-l^+\right)}\right)\left(\frac{\left(\vec{p}_{q1}-\vec{l}\right)^2-i0}{2\left(p_q^+-l^+\right)}+\frac{\left(\vec{l}-\vec{p}_3\right)^2-i0}{2l^+}+\frac{\vec{p}_{\bar{q}2}^{\,2}-i0}{2p_{\bar{q}}^+}-p_\gamma^-\right)}.
\end{aligned}
\tag{3.82}
$$

The $l_\perp$ integration is a usual straightforward 2-denominator integration, then the l^+ integral can be performed, distinguishing the cases with or without $\delta\left(\vec{p}_3\right)$.

The contribution of this diagram and its symmetric w.r.t. the exchange of the quark and the antiquark

to Φ_1^α and Φ_2^α reads :

$$\begin{aligned}\left(\Phi_1^+|_6\right)_{div} &= \frac{x\bar{x}p_\gamma^+(\bar{u}_{p_q}\gamma^+ v_{p_{\bar{q}}})}{\vec{p}_{q1}^{\,2}+x\bar{x}Q^2}\left[\ln^2\left(\frac{x\bar{x}}{\alpha^2}\right)-\ln^2\left(\frac{\bar{x}}{x}\right)-2\ln\left(\frac{x\bar{x}}{\alpha^2}\right)\left(\ln\left(\frac{\left(\vec{p}_{q1}^{\,2}+x\bar{x}Q^2\right)^2}{x\bar{x}\mu^4}\right)+\frac{2}{\epsilon}\right)+\frac{6}{\epsilon}\right] \\ &\quad +\bar{u}_{p_q}C_{1\|}^6 v_{p_{\bar{q}}}\,, \end{aligned} \tag{3.83}$$

$$\begin{aligned}\left(\Phi_{1\perp}^i|_6\right)_{div} &= \frac{1}{2}\Phi_{0\perp}^i\left[\ln^2\left(\frac{x\bar{x}}{\alpha^2}\right)-\ln^2\left(\frac{\bar{x}}{x}\right)-2\ln\left(\frac{x\bar{x}}{\alpha^2}\right)\left(\ln\left(\frac{\left(\vec{p}_{q1}^{\,2}+x\bar{x}Q^2\right)^2}{x\bar{x}\mu^4}\right)+\frac{2}{\epsilon}\right)+\frac{6}{\epsilon}\right] \\ &\quad +\bar{u}_{p_q}C_{1\perp}^{6i} v_{p_{\bar{q}}}\,, \end{aligned} \tag{3.84}$$

$$\left(\Phi_2^+|_6\right)_{div} = -\frac{x\bar{x}p_\gamma^+(\bar{u}_{p_q}\gamma^+ v_{p_{\bar{q}}})}{\vec{p}_{q1}^{\,2}+x\bar{x}Q^2}\left[4\ln\left(\frac{\bar{x}}{\alpha}\right)\left(\frac{1}{\epsilon}+\ln\left(\frac{\vec{p}_3^{\,2}}{\mu^2}\right)\right)-\frac{3}{\epsilon}\right]+\bar{u}_{p_q}C_{2\|}^6 v_{p_{\bar{q}}}+(q\leftrightarrow\bar{q})\,, \tag{3.85}$$

$$\begin{aligned}\left(\Phi_{2\perp}^i|_6\right)_{div} &= -\frac{\overline{u}_{p_q}(p_{q1\perp}^i(1-2x)+\frac{1}{2}[\hat{p}_{q1\perp},\gamma_\perp^i])\gamma^+ v_{p_{\bar{q}}}}{\vec{p}_{q1}^{\,2}+x\bar{x}Q^2}\left[2\ln\left(\frac{\bar{x}}{\alpha}\right)\left(\frac{1}{\epsilon}+\ln\left(\frac{\vec{p}_3^{\,2}}{\mu^2}\right)\right)-\frac{3}{2\epsilon}\right] \\ &\quad +\bar{u}_{p_q}C_{2\perp}^{6i} v_{p_{\bar{q}}}+(q\leftrightarrow\bar{q})\,, \end{aligned} \tag{3.86}$$

where $C_{2\|}^6$ and $C_{2\perp}^{6i}$ are finite, and so are $C_{1\|}^6 \equiv C_{2\|}^6|_{\vec{p}_3\to\vec{0}}$ and $C_{1\perp}^{6i} \equiv C_{2\perp}^{6i}|_{\vec{p}_3\to\vec{0}}$.

3.4.8 Total dipole contribution

Summing the contributions from all diagrams involving $\mathcal{U}_{12}$ finally gives :

$$\Phi_1^\alpha = \frac{S_V}{2}\Phi_0^\alpha + \Phi_{1R}^\alpha\,, \tag{3.87}$$

where the singular term reads

$$\frac{S_V}{2} = \left[\ln\left(\frac{x\bar{x}}{\alpha^2}\right)-\frac{3}{2}\right]\left[\ln\left(\frac{x\bar{x}\mu^2}{(x\vec{p}_{\bar{q}}-\bar{x}\vec{p}_q)^2}\right)-\frac{1}{\epsilon}\right]+i\pi\ln\left(\frac{x\bar{x}}{\alpha^2}\right)+\frac{1}{2}\ln^2\left(\frac{x\bar{x}}{\alpha^2}\right)-\frac{\pi^2}{6}+3\,, \tag{3.88}$$

and the regular terms read

$$\Phi_{1R}^+ = \frac{3}{2}\Phi_0^+\ln\left(\frac{x^2\bar{x}^2\mu^4Q^2}{(x\vec{p}_{\bar{q}}-\bar{x}\vec{p}_q)^2\left(\vec{p}_{q1}^{\,2}+x\bar{x}Q^2\right)^2}\right)+\bar{u}_{p_q}(C_\|^4+C_{1\|}^5+C_{1\|}^6)v_{p_{\bar{q}}}\,, \tag{3.89}$$

and

$$\begin{aligned}\Phi_{1R}^i &= \frac{3}{2}\Phi_0^i\left[\ln\left(\frac{x\bar{x}\mu^4}{(x\vec{p}_{\bar{q}}-\bar{x}\vec{p}_q)^2(\vec{p_{q1}}^{\,2}+x\bar{x}Q^2)}\right)-\frac{x\bar{x}Q^2}{\vec{p}_{q1}^{\,2}}\ln\left(\frac{x\bar{x}Q^2}{\vec{p}_{q1}^{\,2}+x\bar{x}Q^2}\right)\right] \\ &\quad +\bar{u}_{p_q}(C_\perp^{4i}+C_{1\perp}^{5i}+C_{1\perp}^{6i})v_{p_{\bar{q}}}\,. \end{aligned} \tag{3.90}$$

Note that the $i\pi\ln\left(\frac{x\bar{x}}{\alpha^2}\right)$ term will never contribute, since in the cross sections $\frac{S_V}{2}$ will actually always appear as $\frac{1}{2}(S_V+S_V^*)$. In appendix A we will write the expressions for $C_\|^4$ and $C_\perp^{4i}$, and for $C_{2\|}^5$, $C_{2\perp}^{5i}$, $C_{2\|}^6$ and $C_{2\perp}^{6i}$. The corresponding C_1 coefficients are trivial to obtain by writing $C_{1\|,\perp}^n = C_{2\|,\perp}^n|_{\vec{p}_3\to\vec{0}}$.

3.4.9 Total double-dipole contribution

Cancelling the rapidity divergence : B-JIMWLK dipole evolution The divergent part of the virtual amplitude contains a rapidity divergence of the form $\ln(\alpha)$ in the double-dipole contribution of diagrams 5 and 6. Such terms have to be absorbed into the renormalized Wilson operators with the help of the BK equation. Indeed the LO contribution as defined in Eq. (3.12) involves the Wilson line operators at rapidity $\ln(\alpha)$. We thus have to use the B-JIMWLK evolution for these operators from the non-physical cutoff α to the rapidity divide e^η, by writing

$$U_{\vec{x}}^{e^\eta} = U_{\vec{x}}^\alpha + \int_\alpha^{e^\eta} d\rho\left(\frac{\partial U_{\vec{x}}^\rho}{\partial\rho}\right). \tag{3.91}$$

Let us note that the B-JIMWLK equation is of order α_s so $U^{\alpha}_{\vec{x}}$ can be directly replaced by $U^{e^\eta}_{\vec{x}}$ in NLO corrections to impact factors without concern. Plugging this Eq. (3.91) into Eq. (3.12) and using the dipole B-JIMWLK equation (2.106) allows one to evolve the LO dipole contribution into an NLO double-dipole contribution. This contribution reads :

$$\begin{aligned}
\langle T_0^\alpha\rangle^\eta &= \int d^dp_{1\perp}d^dp_{2\perp}\delta(p_{q1\perp}+p_{\bar{q}2\perp}-p_{\gamma\perp})\Phi_0^\alpha(p_{1\perp},p_{2\perp})\\
&\times \ln(\frac{e^\eta}{\alpha})\delta(k_{1\perp}+k_{2\perp}+k_{3\perp}-p_{1\perp}-p_{2\perp})2\alpha_s\mu^{2-d}\int\frac{d^dk_{1\perp}d^dk_{2\perp}d^dk_{3\perp}}{(2\pi)^{2d}}\\
&\times\left[-\frac{2(k_{1\perp}-p_{1\perp})\cdot(k_{2\perp}-p_{2\perp})}{(k_1-p_1)^2_\perp(k_2-p_2)^2_\perp}\right.\\
&\left.+\frac{\pi^{\frac{d}{2}}\Gamma(1-\frac{d}{2})\Gamma(\frac{d}{2})^2}{\Gamma(d-1)}\left(\frac{\delta(k_{2\perp}-p_{2\perp})}{(-(k_1-p_1)^2_\perp)^{1-\frac{d}{2}}}+\frac{\delta(k_{1\perp}-p_{1\perp})}{(-(k_2-p_2)^2_\perp)^{1-\frac{d}{2}}}\right)\right]\\
&\times[\mathrm{Tr}(U_1U_3^\dagger)\mathrm{Tr}(U_3U_2^\dagger)-N_c\mathrm{Tr}(U_1U_2^\dagger)](k_{1\perp},k_{2\perp},k_{3\perp}).
\end{aligned}\tag{3.92}$$

After integrating w.r.t. $p_{2\perp}$ and renaming the variables, we get

$$\begin{aligned}
\langle T_0^\alpha\rangle^\eta &= \int\frac{d^dp_{1\perp}d^dp_{2\perp}d^dp_{3\perp}}{(2\pi)^d}\delta(p_{q1\perp}+p_{\bar{q}2\perp}-p_{3\perp}-p_{\gamma\perp})\\
&\times\ln(\frac{e^\eta}{\alpha})2\alpha_s\mu^{2-d}\int\frac{d^dp_\perp}{(2\pi)^d}\Phi_0^\alpha(p_{1\perp}+p_\perp,p_{2\perp}+p_{3\perp}-p_\perp)\\
&\times\left[\frac{2(p_\perp\cdot(p_\perp-p_{3\perp}))}{p_\perp^2(p-p_3)^2_\perp}+\frac{\pi^{\frac{d}{2}}\Gamma(1-\frac{d}{2})\Gamma(\frac{d}{2})^2}{\Gamma(d-1)}\left(\frac{\delta(p_\perp-p_{3\perp})}{(-p_\perp^2)^{1-\frac{d}{2}}}+\frac{\delta(p_\perp)}{(-(p-p_3)^2_\perp)^{1-\frac{d}{2}}}\right)\right]\\
&\times[\mathrm{Tr}(U_1U_3^\dagger)\mathrm{Tr}(U_3U_2^\dagger)-N_c\mathrm{Tr}(U_1U_2^\dagger)](p_{1\perp},p_{2\perp},p_{3\perp}).
\end{aligned}\tag{3.93}$$

Integrating w.r.t. $p_\perp$, one can get the contribution from this convolution :

$$\begin{aligned}
\Phi^+_{BK}(p_{1\perp},p_{2\perp},p_{3\perp}) &= -4x\bar{x}p_\gamma^+(\bar{u}_{p_q}\gamma^+v_{p_{\bar{q}}})\ln\left(\frac{e^\eta}{\alpha}\right)\\
&\times\left[\left(\ln\left(\frac{\vec{p}_3^{\,2}}{\mu^2}\right)+\frac{1}{\epsilon}\right)\left(\frac{-1}{\vec{p}_{q1}^{\,2}+x\bar{x}Q^2}+\frac{-1}{\vec{p}_{\bar{q}2}^{\,2}+x\bar{x}Q^2}\right)\right.\\
&\left.+\frac{\vec{p}_3^{\,2}-\vec{p}_{q1}^{\,2}-\vec{p}_{\bar{q}2}^{\,2}-2x\bar{x}Q^2}{(\vec{p}_{q1}^{\,2}+x\bar{x}Q^2)(\vec{p}_{\bar{q}2}^{\,2}+x\bar{x}Q^2)-x\bar{x}\vec{p}_3^{\,2}Q^2}\ln\left(\frac{(\vec{p}_{q1}^{\,2}+x\bar{x}Q^2)(\vec{p}_{\bar{q}2}^{\,2}+x\bar{x}Q^2)}{x\bar{x}\vec{p}_3^{\,2}Q^2}\right)\right]
\end{aligned}\tag{3.94}$$

in the longitudinal case, and

$$\begin{aligned}
\Phi^i_{BK} &= -2\ln\left(\frac{e^\eta}{\alpha}\right)\left\{\bar{u}_{p_q}\left((1-2x)p^i_{q1\perp}+\frac{1}{2}[\hat{p}_{q1\perp},\gamma^i_\perp]\right)\gamma^+v_{p_{\bar{q}}}\right.\\
&\times\left[\frac{-1}{\vec{p}_{q1}^{\,2}+x\bar{x}Q^2}\left(\ln\left(\frac{\vec{p}_3^{\,2}}{\mu^2}\right)+\frac{1}{\epsilon}\right)+\frac{1}{\vec{p}_{q1}^{\,2}}\ln\left(\frac{\vec{p}_{q1}^{\,2}+x\bar{x}Q^2}{x\bar{x}Q^2}\right)\right.\\
&-\frac{\vec{p}_{\bar{q}2}^{\,2}+x\bar{x}Q^2}{(\vec{p}_{q1}^{\,2}+x\bar{x}Q^2)(\vec{p}_{\bar{q}2}^{\,2}+x\bar{x}Q^2)-x\bar{x}\vec{p}_3^{\,2}Q^2}\\
&\left.\left.\times\ln\left(\frac{(\vec{p}_{q1}^{\,2}+x\bar{x}Q^2)(\vec{p}_{\bar{q}2}^{\,2}+x\bar{x}Q^2)}{x\bar{x}\vec{p}_3^{\,2}Q^2}\right)\right]+(q\leftrightarrow\bar{q})\right\}
\end{aligned}\tag{3.95}$$

in the transverse case. Combining this subtraction term with the results from diagrams 5 and 6 in Eqs. (3.77-3.78) and (3.85-3.86), we can cancel the $\ln\alpha$ rapidity divergence and obtain the actual double-

dipole part $\Phi_2' = \Phi_2 + \Phi_{BK}$ of the impact factor :

$$\begin{aligned}\Phi_2'^{+} = 2p_\gamma^+(\bar{u}_{p_q}\gamma^+ v_{p_{\bar{q}}}) \Bigg\{ & \frac{x\bar{x}(\vec{p}_3^{\,2} - \vec{p}_{\bar{q}2}^{\,2} - \vec{p}_{q1}^{\,2} - 2x\bar{x}Q^2)}{(\vec{p}_{\bar{q}2}^{\,2} + x\bar{x}Q^2)\left(\vec{p_{q1}}^{\,2} + x\bar{x}Q^2\right) - x\bar{x}Q^2\vec{p}_3^{\,2}} \\ & \times \ln\left(\frac{x\bar{x}}{e^{2\eta}}\right) \ln\left(\frac{(\vec{p}_{\bar{q}2}^{\,2} + x\bar{x}Q^2)\left(\vec{p}_{q1}^{\,2} + x\bar{x}Q^2\right)}{x\bar{x}Q^2\vec{p}_3^{\,2}}\right) \\ & - \left(\frac{x\bar{x}}{\vec{p}_{q1}^{\,2} + x\bar{x}Q^2}\left[2\ln\left(\frac{\bar{x}}{e^\eta}\right)\left(\frac{1}{\epsilon} + \ln\left(\frac{\vec{p}_3^{\,2}}{\mu^2}\right)\right) - \frac{3}{2\epsilon}\right] + (q \leftrightarrow \bar{q})\right)\Bigg\} \\ & + \bar{u}_{p_q}(C_{2\|}^5 + C_{2\|}^6)v_{p_{\bar{q}}}\end{aligned} \tag{3.96}$$

in the longitudinal case, or

$$\begin{aligned}\Phi_2'^{i} = \Bigg\{ & \overline{u}_{p_q}(p_{q1\perp}^i(1-2x) + \frac{1}{2}[\hat{p}_{q1\perp}, \gamma_\perp^i])\gamma^+ v_{p_{\bar{q}}} \left(\frac{-1}{\vec{p}_{q1}^{\,2} + x\bar{x}Q^2}\right. \\ & \times \left[2\ln\left(\frac{\bar{x}}{e^\eta}\right)\left(\frac{1}{\epsilon} + \ln\left(\frac{\vec{p}_3^{\,2}}{\mu^2}\right)\right) - \frac{3}{2\epsilon}\right] + \ln\left(\frac{x\bar{x}}{e^{2\eta}}\right) \\ & \times \left[\frac{1}{\vec{p}_{q1}^{\,2}}\ln\left(\frac{\vec{p}_{q1}^{\,2} + x\bar{x}Q^2}{x\bar{x}Q^2}\right) - \frac{\vec{p}_{\bar{q}2}^{\,2} + x\bar{x}Q^2}{(\vec{p}_{q1}^{\,2} + x\bar{x}Q^2)(\vec{p}_{\bar{q}2}^{\,2} + x\bar{x}Q^2 - x\bar{x}Q^2\vec{p}_3^{\,2})}\right. \\ & \left.\left.\times \ln\left(\frac{(\vec{p}_{q1}^{\,2} + x\bar{x}Q^2)(\vec{p}_{\bar{q}2}^{\,2} + x\bar{x}Q^2)}{x\bar{x}Q^2\vec{p}_3^{\,2}}\right)\right]\right) + (q \leftrightarrow \bar{q})\Bigg\} + \bar{u}_{p_q}(C_{2\perp}^{5i} + C_{2\perp}^{6i})v_{p_{\bar{q}}}\end{aligned} \tag{3.97}$$

in the transverse case. These impact factors still contain $\frac{1}{\epsilon}$ terms, although by construction they should not have any IR, UV or collinear singularity. These poles are artificial UV poles and already appear in the momentum representation of the B-JIMWLK equation for the dipole operator (2.106). They originate from the fact that when we define the Fourier transform of the double-dipole Wilson line operator into its momentum space representation straightforwardly in Eq. (2.101), we do not take into account its property of vanishing when $r_3 = r_2$ or $r_3 = r_1$. This property reveals in the convolution of the impact factor and the operator (2.101) killing all the artificial singularities. Indeed, the divergent terms depend only on $\vec{p}_1$ and are independent of $\vec{p}_3$ and $\vec{p}_2$ (up to a (1↔2) permutation). Writing those terms as $F(p_{1\perp})$ and convoluting them as in Eq. (3.26) gives

$$\begin{aligned} & \int d^d p_{1\perp} d^d p_{2\perp} d^d p_{3\perp} \delta(p_{q1} + p_{\bar{q}2} - p_{\gamma\perp} - p_{3\perp}) F(p_{1\perp}) \\ & \times [tr(U_1U_3^\dagger)tr(U_3U_2^\dagger) - N_c tr(U_1U_2^\dagger)](p_{1\perp}, p_{2\perp}, p_{3\perp}) \\ = & \int d^d p_{1\perp} d^d p_{3\perp} d^d r_{1\perp} d^d r_{2\perp} d^d r_{3\perp} \\ & \times F(p_{1\perp})\, e^{i(r_{1\perp}\cdot p_{1\perp}) + ir_{2\perp}\cdot(p_{q1\perp} + p_{\bar{q}\gamma\perp}) + i(p_{3\perp}\cdot r_{32\perp})}[tr(U_1U_3^\dagger)tr(U_3U_2^\dagger) - N_c tr(U_1U_2^\dagger)] \\ \sim & \int d^d p_{1\perp} d^d r_{1\perp} d^d r_{2\perp} F(p_{1\perp})\, e^{i(r_{1\perp}\cdot p_{1\perp}) + ir_{2\perp}\cdot(p_{q1\perp} + p_{\bar{q}\gamma\perp})} \\ & \times \int d^d r_{3\perp} \delta(r_{32\perp})[tr(U_1U_3^\dagger)tr(U_3U_2^\dagger) - N_c tr(U_1U_2^\dagger)] = 0. \end{aligned} \tag{3.98}$$

Thus the artificially divergent part

$$F(p_{1\perp}) = \frac{x\bar{x}}{\vec{p}_{q1}^{\,2} + x\bar{x}Q^2}\left[2\ln\left(\frac{\bar{x}}{e^\eta}\right)\frac{1}{\epsilon} - \frac{3}{2\epsilon}\right] \tag{3.99}$$

will cancel once convoluted, so it can be omitted. For a more involved discussion about such terms, see Ref. [87]. The same computation can allow one to omit the $\ln(\mu^2)$ contribution. However, we will keep it so that no dimensional log appears, keeping in mind that there is no actual μ dependence. Therefore

hereafter we will use

$$\begin{aligned}\Phi_2'^{+} = 2p_\gamma^+(\bar{u}_{p_q}\gamma^+ v_{p_{\bar{q}}})\Bigg\{ & \frac{x\bar{x}(\vec{p}_3^{\,2}-\vec{p}_{\bar{q}2}^{\,2}-\vec{p}_{q1}^{\,2}-2x\bar{x}Q^2)}{(\vec{p}_{\bar{q}2}^{\,2}+x\bar{x}Q^2)\left(\vec{p}_{q1}^{\,2}+x\bar{x}Q^2\right)-x\bar{x}Q^2\vec{p}_3^{\,2}} \\ & \times \ln\left(\frac{x\bar{x}}{e^{2\eta}}\right)\ln\left(\frac{(\vec{p}_{\bar{q}2}^{\,2}+x\bar{x}Q^2)\left(\vec{p}_{q1}^{\,2}+x\bar{x}Q^2\right)}{x\bar{x}Q^2\vec{p}_3^{\,2}}\right) \\ & + \left(\frac{-2x\bar{x}}{\vec{p}_{q1}^{\,2}+x\bar{x}Q^2}\ln\left(\frac{\bar{x}}{e^{\eta}}\right)\ln\left(\frac{\vec{p}_3^{\,2}}{\mu^2}\right)+(q\leftrightarrow\bar{q})\right)\Bigg\} \\ & + \bar{u}_{p_q}(C_{2\|}^5+C_{2\|}^6)v_{p_{\bar{q}}}\,,\end{aligned} \tag{3.100}$$

and

$$\begin{aligned}\Phi_2'^{i} = \Bigg\{ & \overline{u}_{p_q}(p_{q1\perp}^i(1-2x)+\frac{1}{2}[\hat{p}_{q1\perp},\,\gamma_\perp^i])\gamma^+ v_{p_{\bar{q}}}\left(\frac{-2}{\vec{p}_{q1}^{\,2}+x\bar{x}Q^2}\ln\left(\frac{\bar{x}}{e^{\eta}}\right)\ln\left(\frac{\vec{p}_3^{\,2}}{\mu^2}\right)\right. \\ & + \ln\left(\frac{x\bar{x}}{e^{2\eta}}\right)\left[\frac{1}{\vec{p}_{q1}^{\,2}}\ln\left(\frac{\vec{p}_{q1}^{\,2}+x\bar{x}Q^2}{x\bar{x}Q^2}\right)-\frac{\vec{p}_{\bar{q}2}^{\,2}+x\bar{x}Q^2}{\left(\vec{p}_{q1}^{\,2}+x\bar{x}Q^2\right)\left(\vec{p}_{\bar{q}2}^{\,2}+x\bar{x}Q^2\right)-x\bar{x}Q^2\vec{p}_3^{\,2}}\right. \\ & \left.\left.\times\ \ln\left(\frac{\left(\vec{p}_{q1}^{\,2}+x\bar{x}Q^2\right)\left(\vec{p}_{\bar{q}2}^{\,2}+x\bar{x}Q^2\right)}{x\bar{x}Q^2\vec{p}_3^{\,2}}\right)\right]\right)+(q\leftrightarrow\bar{q})\Bigg\}+\bar{u}_{p_q}(C_{2\perp}^{5i}+C_{2\perp}^{6i})v_{p_{\bar{q}}}\,.\end{aligned} \tag{3.101}$$

3.4.10 Cancelling the UV divergence : renormalization

The virtual correction as we computed it contains both UV and IR divergences. The usual way of canceling them is to first use the renormalization of the colored fields in the NLO amplitude to cancel the UV divergence and then build an infrared and collinearly safe observable by adding the appropriate real corrections to cancel the IR divergence.

In this section, we will show how renormalization is not actually needed when the external lines are massless quarks, even in non-covariant gauges. In this case, the UV divergence in the NLO amplitude will be canceled by IR divergences in the real correction.

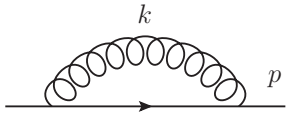

Figure 3.11: Quark self energy

Let us compute a quark self energy diagram, keeping in mind that we want to apply it to an external massless quark later on. It reads

$$\hat{\Sigma}(p) = (ig)^2\left(\frac{N_c^2-1}{2}\right)\int d^Dk\frac{\gamma^\mu\left(\hat{p}-\hat{k}\right)\gamma^\nu}{(k^2+i0)\left[(p-k)^2+i0\right]}\left[g_{\mu\nu}-\frac{k_\mu n_{2\nu}+k_\nu n_{2\mu}}{k^+}\theta\left(k_0^+-\left|k^+\right|\right)\right], \tag{3.102}$$

where we introduced a general cutoff k_0^+ to deal with the spurious lightcone gauge pole $(k^+)^{-1}$.
There are only two vectors to project the result on. Let us write :

$$\hat{\Sigma}(p) \equiv \Sigma_p\hat{p}+\Sigma_n\hat{n}_2\,. \tag{3.103}$$

Then one has

$$\frac{1}{4}\mathrm{Tr}\left[\hat{p}\hat{\Sigma}(p)\right] = \Sigma_p p^2+\Sigma_n p^+ \tag{3.104}$$

$$\frac{1}{4}\mathrm{Tr}\left[\gamma^+\hat{\Sigma}(p)\right] = \Sigma_p p^+. \tag{3.105}$$

Thus after a trivial evaluation of Dirac traces and using Feynman's trick, one gets :

$$\begin{aligned}\Sigma_p &= (ig)^2 (2-D)\left(\frac{N_c^2-1}{2p^+}\right)\int \frac{d^Dk\,(p^2-p.k)}{(k^2+i0)\left[(p-k)^2+i0\right]} \\ &= (ig)^2 (2-D)\left(\frac{N_c^2-1}{2p^+}\right)\int_0^1 d\alpha \int \frac{d^Dk\,(p^2-p.k)}{\left[(k-\alpha p)^2+\alpha\bar{\alpha}p^2+i0\right]^2}\,. \end{aligned} \tag{3.106}$$

For an on-shell quark after performing a shift on k the integral becomes a scaleless integral $\propto \int \frac{d^Dk}{(-k^2-i0)^2}$. In dimensional regularization such an integral is set by zero as follows. Let us first perform the right Wick rotation to go to Euclidean space :

$$\begin{aligned}\int \frac{d^Dk}{(-k^2-i0)^2} &= i\int \frac{d^Dk_E}{(k_E^2)^2} \\ &= iS_{D-1}\int_0^{+\infty} dk_E\,(k_E)^{D-5}\,, \end{aligned} \tag{3.107}$$

where $S_{D-1}=\frac{2\pi^{\frac{D}{2}}}{\Gamma\left(\frac{D}{2}\right)}$ is the surface of the D-sphere. Let us separate the IR sector and the UV sector by introducing an arbitrary cutoff Λ :

$$\int_0^{+\infty} dk_E\,(k_E)^{D-5} = \lim_{k_{IR}\to 0,\,k_{UV}\to+\infty}\left[\int_{k_{IR}}^{\Lambda} dk_E\,(k_E)^{D-5}+\int_{\Lambda}^{k_{UV}}(k_E)^{D-5}\right]. \tag{3.108}$$

In dimension $D=4+2\epsilon$, one needs ϵ to be positive in the IR sector and negative in the UV sector. Let us then introduce $\epsilon_{IR}>0$ and $\epsilon_{UV}<0$. Then :

$$\begin{aligned}\int_0^{+\infty} dk_E\,(k_E)^{D-5} &= \lim_{k_{IR}\to 0,\,k_{UV}\to+\infty}\left[\frac{1}{2\epsilon_{IR}}\left(\Lambda^{2\epsilon_{IR}}-k_{IR}^{2\epsilon_{IR}}\right)+\frac{1}{2\epsilon_{UV}}\left(k_{UV}^{2\epsilon_{UV}}-\Lambda^{2\epsilon_{UV}}\right)\right] \\ &= \frac{\Lambda^{2\epsilon_{IR}}}{2\epsilon_{IR}}-\frac{\Lambda^{2\epsilon_{UV}}}{2\epsilon_{UV}}\,. \end{aligned} \tag{3.109}$$

Now we want to take the $\epsilon_{UV/IR}\to 0$ limit, getting the pole

$$\int_0^{+\infty} dk_E\,(k_E)^{D-5} \to \frac{1}{2\epsilon_{IR}}-\frac{1}{2\epsilon_{UV}}\,. \tag{3.110}$$

The mere principle of dimensional regularization is to find the analytic continuation for any expression at $\epsilon=0$. The constraints $\epsilon_{IR}>0$ and $\epsilon_{UV}<0$ can then be dropped, and we will write $\epsilon_{IR}=\epsilon_{UV}=\epsilon$. Then our scaleless integral can be set to 0. We conclude :

$$\Sigma_p = 0\,. \tag{3.111}$$

The gauge term is cancelled using the same principle except for one term. From Eq. (3.104) one gets :

$$\begin{aligned}\Sigma_n &= (ig)^2\left(\frac{N_c^2-1}{2p^+}\right)\int \frac{d^Dk}{(k^2+i0)\left[(p-k)^2+i0\right]} \\ &\times\left[(2-D)\left(p^2-p.k\right)-\frac{2p^+(p.k)-2k^+p^2+2(p.k)p^+-2k^2p^+}{k^+}\theta\left(k_0^+-\left|k^+\right|\right)\right]. \end{aligned} \tag{3.112}$$

Using the exact same argument as before for scaleless integrals, one can cancel any term without k^+ in the denominator. Thus we can write :

$$\Sigma_n = (ig)^2\left(N_c^2-1\right)\int \frac{d^Dk}{(k^2+i0)\left[(p-k)^2+i0\right]}\left[\frac{k^2-2(p.k)}{k^+}\right]\theta\left(k_0^+-\left|k^+\right|\right). \tag{3.113}$$

Writing the numerator in the brackets as $(p-k)^2 - p^2$ and dropping the p^2 term since we want to put the quark on the mass shell at the end, we get :

$$\Sigma_n = (ig)^2 \left(N_c^2 - 1\right) \int \frac{d^D k}{k^+ \left(k^2 + i0\right)} \theta\left(k_0^+ - \left|k^+\right|\right). \tag{3.114}$$

This is a scaleless (tadpole) integral so it has to cancel. The previous argument based on dimensional regularization is however not sufficient due to the spurious $\frac{1}{k^+}$ pole. The trick is now to perform the transverse integration first :

$$\begin{aligned}\Sigma_n &= (ig)^2 \left(N_c^2 - 1\right) \int \frac{dk^+}{k^+} \theta\left(k_0^+ - \left|k^+\right|\right) \int dk^- \, (-1) \int \frac{d^d \vec{k}}{\left[\vec{k}^2 - 2k^+k^- - i0\right]} \\ &= (ig)^2 \left(N_c^2 - 1\right) \int \frac{dk^+}{k^+} \theta\left(k_0^+ - \left|k^+\right|\right) \int dk^- \, (-1) \, \Gamma\left(1 - \frac{d}{2}\right) \frac{\pi^{\frac{d}{2}-1}}{\left[-2k^+k^- - i0\right]^{1-\frac{d}{2}}}\end{aligned} \tag{3.115}$$

Now let us separate the 4 different cases for the signs of k^+ and k^- :

$$\begin{aligned}\Sigma_n = {} & g^2 \left(N_c^2 - 1\right) \Gamma\left(1 - \frac{d}{2}\right) \pi^{\frac{d}{2}-1} \\ & \times \left[\int_{k_0^+}^{+\infty} \frac{dk^+}{k^+} \int_0^{+\infty} dk^- \left(2k^+k^-\right)^{\frac{d}{2}-1} e^{-i\pi\left(\frac{d}{2}-1\right)} \right. \\ & + \int_{k_0^+}^{+\infty} \frac{dk^+}{k^+} \int_{-\infty}^{0} dk^- \left(-2k^+k^-\right)^{\frac{d}{2}-1} \\ & + \int_{-\infty}^{-k_0^+} \frac{dk^+}{k^+} \int_0^{+\infty} dk^- \left(-2k^+k^-\right)^{\frac{d}{2}-1} \\ & \left. + \int_{-\infty}^{-k_0^+} \frac{dk^+}{k^+} \int_{-\infty}^{0} dk^- \left(2k^+k^-\right)^{\frac{d}{2}-1} e^{-i\pi\left(\frac{d}{2}-1\right)} \right].\end{aligned} \tag{3.116}$$

By performing the right changes of variables to get the final integration over $(k^+, k^-) \in \left[k_0^+, +\infty\right] \times [0, +\infty]$ for every term, one can easily see that those terms will cancel two by two. This way one can cancel the spurious tadpole integral.

The conclusion is now that one can completely cancel the quark self energy in the case of a massless on-shell quark, by setting $\epsilon_{IR} = \epsilon_{UV}$. Thus throughout our computation we will set $Z_2 = 1$, i.e. we will not renormalize the quarks. Our statement will be that the UV divergence in the virtual amplitude is then canceled by the IR divergence in the real amplitude, which is unusual but exactly equivalent to keeping $Z_2 \neq 1$ and by its action turning the $\frac{1}{\epsilon_{UV}}$ divergence into a $\frac{1}{\epsilon_{IR}}$, then canceling $\frac{1}{\epsilon_{IR}}$ with actual IR divergences.

3.5 The $\gamma^* \to q\bar{q}g$ impact factor

We will now derive the $\gamma^* \to q\bar{q}g$ impact factor. Later in this thesis it will be used to construct a well defined cross section for dijet production, free of the soft and the collinear singularities. The IR finiteness of the cross-section is discussed in details in Section 3.8. The complete expression for the $\gamma^* \to q\bar{q}g$ cross section is included in Appendix A.2. The computation of this impact factor in dimension 4 was already presented in [74]. For the purpose of the present study we need its divergent part in dimension D, therefore we will rewrite our results for an arbitrary value of D. The corresponding matrix element for the EM current in the shockwave background reads

$$\tilde{M}'^{\alpha} = -ie_q \int d^D y_0 \frac{e^{-i(p_\gamma \cdot y_0)}}{\sqrt{2p_\gamma^+}} \sqrt{\frac{2}{N_c^2 - 1}} (t^r)_l^n \langle 0 | T(b^l_{p_{\bar{q}}}(a_{p_q})_n c^r_{p_g} \overline{\psi}(y_0) \gamma^\alpha \psi(y_0) \, e^{i \int \mathcal{L}_i(z) dz}) | 0 \rangle_{sw}, \tag{3.117}$$

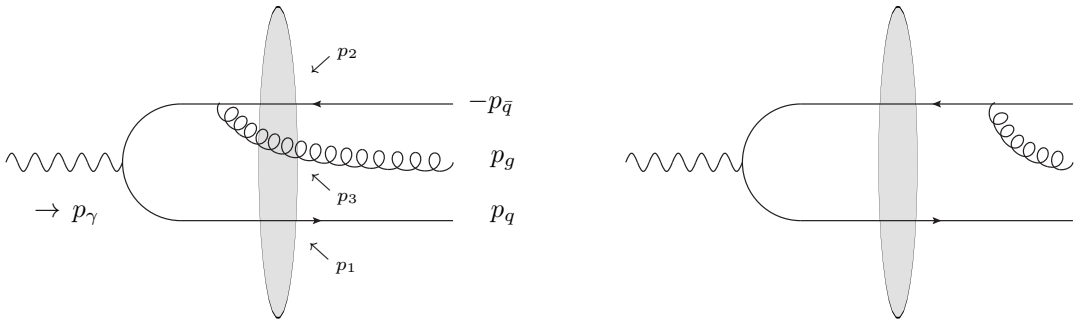

Figure 3.12: Diagrams for the $\gamma^* \to q\bar{q}g$ amplitude. The momenta p_1, p_2 and p_3 go from the shockwave to the quark, antiquark and gluon.

where c is the gluon annihilation operator and $\sqrt{\frac{2}{N_c^2-1}}(t^r)^n_l$ is the projector on the color singlet. We label the emitted gluon momentum as

$$p_g^\mu = x_g p_\gamma^+ n_1^\mu + \frac{-p_{g\perp}^2}{2x_g p_\gamma^+} n_2^\mu + p_{g\perp}^\mu. \tag{3.118}$$

Again, we will work with the reduced matrix element $\tilde{T}'^\alpha$

$$\tilde{M}'^\alpha = \frac{-ie_q}{\sqrt{2p_\gamma^+}} \sqrt{\frac{2}{N_c^2-1}} \frac{-i\delta(p_q^+ + p_{\bar{q}}^+ + p_g^+ - p_\gamma^+)}{(2\pi)^{D-3}\sqrt{2p_{\bar{q}}^+}\sqrt{2p_q^+}\sqrt{2p_g^+}} \tilde{T}'^\alpha, \tag{3.119}$$

which after subtraction of the noninteracting part can be parametrized as

$$\begin{aligned} T'^\alpha &= -g\mu^{-\epsilon} N_c \int d^d p_{1\perp} d^d p_{2\perp} \left\{ \delta(p_{q1\perp} + p_{\bar{q}2\perp} + p_{g\perp}) \left(\frac{N_c^2-1}{N_c}\right) \tilde{\mathcal{U}}_{12} \Phi_3^\alpha \right. \\ &+ \left. N_c \int \frac{d^d p_{3\perp}}{(2\pi)^d} \delta(p_{q1\perp} + p_{\bar{q}2\perp} + p_{g3\perp}) \left[\tilde{\mathcal{U}}_{13} + \tilde{\mathcal{U}}_{32} - \tilde{\mathcal{U}}_{12} - \widetilde{\mathcal{U}_{13}\mathcal{U}_{32}}\right] \Phi_4^\alpha \right\}. \end{aligned} \tag{3.120}$$

There are four diagrams contributing to the matrix element T'. Two of them are shown in Fig. 3.12, the remaining one are obtained from them by the substitution $p_q \leftrightarrow p_{\bar{q}}$, $\bar{u}_q \leftrightarrow v_{\bar{q}}$, $p_1 \leftrightarrow p_2$ and the reversal of the order of the gamma matrices, which we will denote $(q \leftrightarrow \bar{q})$. The expressions for the amplitudes in D-dimensional space with a longitudinal photon read

$$\Phi_4^+ = \frac{p_\gamma^+ \overline{u}_{p_q} [2x_q g_\perp^{\mu\nu} + x_g(\gamma_\perp^\nu \gamma_\perp^\mu)] \gamma^+ v_{p_{\bar{q}}} \varepsilon^*_{g\perp\mu} (x_g p_{q1\nu\perp} - x_q p_{g3\nu\perp})}{x_q x_g (x_q + x_g) \left(Q^2 + \frac{\vec{p}_{\bar{q}2}^{\,2}}{x_{\bar{q}}(1-x_{\bar{q}})}\right) \left(Q^2 + \frac{\vec{p}_{q1}^{\,2}}{x_q} + \frac{\vec{p}_{\bar{q}2}^{\,2}}{x_{\bar{q}}} + \frac{\vec{p}_{g3}^{\,2}}{x_g}\right)} - (q \leftrightarrow \bar{q}), \tag{3.121}$$

and

$$\begin{aligned} \Phi_3^+ &= \Phi_4^+|_{p_3=0} + \left[-\frac{x_g p_\gamma^+ \overline{u}_{p_q} \hat{\varepsilon}_g^* (\hat{p}_q + \hat{p}_g) \gamma^+ v_{p_{\bar{q}}}}{x_q (\vec{p}_g - \frac{x_g}{x_q}\vec{p}_q)^2 \left(Q^2 + \frac{\vec{p}_{\bar{q}2}^{\,2}}{x_{\bar{q}}(1-x_{\bar{q}})}\right)} + (q \leftrightarrow \bar{q}) \right] \\ &\equiv \Phi_4^+|_{p_3=0} + \tilde{\Phi}_3^+ . \end{aligned} \tag{3.122, 3.123}$$

For a transverse photon, they read

$$\begin{aligned} \Phi_{4\perp}^i &= \frac{\epsilon^*_{g\perp\mu} \overline{u}_{p_q} \gamma^+}{2x_q x_{\bar{q}} (x_q + x_g) \left(Q^2 + \frac{\vec{p}_{\bar{q}2}^{\,2}}{x_{\bar{q}}(1-x_{\bar{q}})}\right) \left(Q^2 + \frac{\vec{p}_{q1}^{\,2}}{x_q} + \frac{\vec{p}_{\bar{q}2}^{\,2}}{x_{\bar{q}}} + \frac{\vec{p}_{g3}^{\,2}}{x_g}\right)} \\ &\times \left[x_q x_{\bar{q}} Q^2 (\gamma_\perp^\mu \gamma_\perp^i) + (\hat{p}_{q1\perp} \gamma_\perp^\mu \gamma_\perp^i \hat{p}_{\bar{q}2\perp}) + 4\frac{x_q}{x_g} p_{\bar{q}2\perp}^i (x_{\bar{q}} p_{g3\perp}^\mu - x_g p_{\bar{q}2\perp}^\mu) \right. \\ &\left. -2\frac{x_q}{x_g} p_{g3\perp}^\mu (\gamma_\perp^i \hat{p}_{\bar{q}2\perp}) + 2x_q p_{\bar{q}2\perp}^i (\hat{p}_{\bar{q}2\perp} \gamma_\perp^\mu) - 2x_{\bar{q}} p_{\bar{q}2\perp}^i (\hat{p}_{q1\perp} \gamma_\perp^\mu) \right] v_{p_{\bar{q}}} - (q \leftrightarrow \bar{q}) , \end{aligned} \tag{3.124}$$

and

$$\Phi_3^i = \Phi_4^i|_{p_3=0} + \left[-\frac{x_g \overline{u}_{p_q} \hat{\varepsilon}_g^* (\hat{p}_q + \hat{p}_g)\gamma^+ (\gamma_\perp^i \hat{p}_{\bar{q}2\perp} - 2x_{\bar{q}} p_{\bar{q}2\perp}^i) v_{p_{\bar{q}}}}{2x_q x_{\bar{q}} (1-x_{\bar{q}}) (\vec{p}_g - \frac{x_g}{x_q}\vec{p}_q)^2 \left(Q^2 + \frac{\vec{p}_{\bar{q}2}^{\,2}}{x_{\bar{q}}(1-x_{\bar{q}})} \right)} + (q \leftrightarrow \bar{q}) \right] \tag{3.125}$$

$$\equiv \Phi_4^i|_{p_3=0} + \tilde{\Phi}_3^i \,. \tag{3.126}$$

3.6 Construction of the $\gamma^* P \to q\bar{q}P'$ cross section

Let us define the reduced matrix element A_3 such that the $\gamma^* P \to q\bar{q}P'$ cross section reads

$$d\sigma = \frac{1}{4s}(2\pi)^D \delta^{(D)}(p_\gamma + p_0 - p_q - p_{\bar{q}} - p_0') |A_3|^2 d\rho_3. \tag{3.127}$$

We will need the parametrization of the proton matrix elements in the shockwave background

$$\langle P'(p_0')|T(tr(U_{\frac{z_\perp}{2}} U^\dagger_{-\frac{z_\perp}{2}}) - N_c)|P(p_0)\rangle \equiv 2\pi\delta(p^-_{00'}) F_{p_{0\perp} p'_{0\perp}}(z_\perp) \equiv 2\pi\delta(p^-_{00'}) F(z_\perp), \tag{3.128}$$

$$\begin{aligned} &\langle P'(p_0')|T(tr(U_{\frac{z}{2}} U_x^\dagger) tr(U_x U^\dagger_{-\frac{z}{2}}) - N_c tr(U_{\frac{z}{2}} U^\dagger_{-\frac{z}{2}}))|P(p_0)\rangle \\ &\equiv 2\pi\delta(p^-_{00'}) \tilde{F}_{p_{0\perp} p'_{0\perp}}(z_\perp, x_\perp) \equiv 2\pi\delta(p^-_{00'}) \tilde{F}(z_\perp, x_\perp). \end{aligned} \tag{3.129}$$

We dropped the dependence on the proton transverse momenta $p_{0\perp}$ and $p'_{0\perp}$ for convenience, and we assumed the following proton state normalization :

$$\langle P'(p_0')|P(p_0)\rangle = (2\pi)^{D-1} \delta(p^-_{00'}) \delta_\perp^{D-2}(p_{00'\perp}) \delta_{s_P s_{P'}} \tag{3.130}$$

The corresponding Fourier transforms read

$$\int d^d z_\perp e^{i(z_\perp \cdot p_\perp)} F(z_\perp) \equiv \mathbf{F}(p_\perp), \tag{3.131}$$

$$\int d^d z_\perp d^d x_\perp e^{i(p_\perp \cdot x_\perp) + i(z_\perp \cdot q_\perp)} \tilde{F}(z_\perp, x_\perp) \equiv \tilde{\mathbf{F}}(q_\perp, p_\perp). \tag{3.132}$$

These hadronic matrix elements naturally appear when we insert the Wilson line operators between the proton states and we extract the overall momentum conservation delta functions. The matrix element for the dipole operator reads

$$\begin{aligned} &\langle P'(p_0')|T(tr(U_1 U_2^\dagger) - N_c)[p_{1\perp}, p_{2\perp}]|P(p_0)\rangle \\ &= (2\pi)^d \delta(p_{1\perp} + p_{2\perp} + p_{0'0\perp}) \int d^d z_\perp e^{i\frac{(z_\perp \cdot p_{12\perp})}{2}} \langle P'(p_0')|T(tr(U_{\frac{z_\perp}{2}} U^\dagger_{-\frac{z_\perp}{2}}) - N_c)|P(p_0)\rangle. \end{aligned} \tag{3.133}$$

For the double dipole operator the analogous formula has the form :

$$\begin{aligned} &\langle P'(p_0')|T(tr(U_1 U_3^\dagger) tr(U_3 U_2^\dagger) - N_c tr(U_1 U_2^\dagger))[p_{1\perp}, p_{2\perp}, p_{3\perp}]|P(p_0)\rangle \\ &= (2\pi)^d \delta(p_{1\perp} + p_{2\perp} + p_{3\perp} + p_{0'0\perp}) \\ &\times \int d^d z_\perp d^d x_\perp e^{i\frac{(z_\perp \cdot p_{12\perp})}{2} + i(p_{3\perp} \cdot x_\perp)} \langle P'(p_0')|T(tr(U_{\frac{z}{2}} U_x^\dagger) tr(U_x U^\dagger_{-\frac{z}{2}}) - N_c tr(U_{\frac{z}{2}} U^\dagger_{-\frac{z}{2}}))|P(p_0)\rangle. \end{aligned} \tag{3.134}$$

In our kinematics, momentum conservation reads

$$\delta^{(D)}(p_\gamma + p_0 - p_q - p_{\bar{q}} - p_0') = \delta(p^-_{00'}) \delta(p_q^+ + p_{\bar{q}}^+ - p_\gamma^+) \delta^{(d)}(p_{q\perp} + p_{\bar{q}\perp} - p_{\gamma\perp} + p_{0'0\perp}), \tag{3.135}$$

with the phase space measure

$$d\rho_3 = \frac{dp_q^+ d^d p_{q\perp}}{2p_q^+ (2\pi)^{d+1}} \frac{dp_{\bar{q}}^+ d^d p_{\bar{q}\perp}}{2p_{\bar{q}}^+ (2\pi)^{d+1}} \frac{dp_0'^- d^d p'_{0\perp}}{2p_0'^- (2\pi)^{d+1}} \,. \tag{3.136}$$

The reduced matrix element A_3 includes the LO and NLO dipole contributions and the NLO double dipole contribution, as defined in section 3. It reads :

$$\begin{aligned} A_3 = & \frac{-2p_0^- e_q \varepsilon_\alpha}{\sqrt{N_c}\,(2\pi)^{D-4}} \int d^d p_{1\perp} d^d p_{2\perp} \\ & \times \left[\delta(p_{q1\perp} + p_{\bar{q}2\perp} - p_{\gamma\perp}) \left\{ \Phi_0^\alpha + \alpha_s \frac{\Gamma(1-\epsilon)}{(4\pi)^{1+\epsilon}} \frac{N_c^2-1}{N_c} \Phi_1^\alpha \right\} \mathbf{F}\left(\frac{p_{12\perp}}{2}\right) \right. \\ & \left. + \alpha_s \frac{\Gamma(1-\epsilon)}{(4\pi)^{1+\epsilon}} \int \frac{d^d p_{3\perp}}{(2\pi)^d} \delta(p_{q1\perp} + p_{\bar{q}2\perp} - p_{\gamma\perp} - p_{3\perp}) \Phi_2^\alpha \tilde{\mathbf{F}}\left(\frac{p_{12\perp}}{2}, p_{3\perp}\right) \right]. \end{aligned} \tag{3.137}$$

Since the photon in the initial state can appear with different polarizations, we construct the density matrix from the cross sections

$$d\sigma_{JI} = \begin{pmatrix} d\sigma_{LL} & d\sigma_{LT} \\ d\sigma_{TL} & d\sigma_{TT} \end{pmatrix}, \qquad d\sigma_{TL} = d\sigma_{LT}^*. \tag{3.138}$$

Each element of this matrix has an LO contribution $d\sigma_0$, an NLO contribution $d\sigma_1$ involving two dipole operators and an NLO contribution $d\sigma_2$ involving a dipole operator and a double-dipole operator.

$$d\sigma_{JI} = d\sigma_{0JI} + d\sigma_{1JI} + d\sigma_{2JI}. \tag{3.139}$$

The leading order cross section can be written as

$$\begin{aligned} d\sigma_{0JI} &= \frac{\alpha_{\rm em} Q_q^2}{(2\pi)^{4(d-1)} N_c} \frac{\left(p_0^-\right)^2}{2x\bar{x}s^2} dx d\bar{x} d^d p_{q\perp} d^d p_{\bar{q}\perp} \delta\left(1-x-\bar{x}\right) \left(\varepsilon_{I\beta} \varepsilon_{J\gamma}^*\right) \\ &\times \int d^d p_{1\perp} d^d p_{2\perp} d^d p_{1'\perp} d^d p_{2'\perp} \delta\left(p_{q1\perp} + p_{\bar{q}2\perp}\right) \delta\left(p_{11'\perp} + p_{22'\perp}\right) \\ &\times \Phi_0^\beta\left(p_{1\perp}, p_{2\perp}\right) \Phi_0^{\gamma *}\left(p_{1'\perp}, p_{2'\perp}\right) \mathbf{F}\left(\frac{p_{12\perp}}{2}\right) \mathbf{F}^*\left(\frac{p_{1'2'\perp}}{2}\right). \end{aligned} \tag{3.140}$$

The dipole $\times$ dipole NLO cross section is given by

$$\begin{aligned} d\sigma_{1JI} &= \alpha_s \frac{\Gamma\left(1-\epsilon\right)}{(4\pi)^{1+\epsilon}} \left(\frac{N_c^2-1}{N_c}\right) \frac{\alpha_{\rm em} Q_q^2}{(2\pi)^{4(d-1)} N_c} \frac{\left(p_0^-\right)^2}{2x\bar{x}s^2} dx d\bar{x} d^d p_{q\perp} d^d p_{\bar{q}\perp} \delta\left(1-x-\bar{x}\right) \left(\varepsilon_{I\beta} \varepsilon_{J\gamma}^*\right) \\ &\times \int d^d p_{1\perp} d^d p_{2\perp} d^d p_{1'\perp} d^d p_{2'\perp} \delta\left(p_{q1\perp} + p_{\bar{q}2\perp}\right) \delta\left(p_{11'\perp} + p_{22'\perp}\right) \mathbf{F}\left(\frac{p_{12\perp}}{2}\right) \mathbf{F}^*\left(\frac{p_{1'2'\perp}}{2}\right) \\ &\times \left[\Phi_1^\beta\left(p_{1\perp}, p_{2\perp}\right) \Phi_0^{\gamma *}\left(p_{1'\perp}, p_{2'\perp}\right) + \Phi_0^\beta\left(p_{1\perp}, p_{2\perp}\right) \Phi_1^{\gamma *}\left(p_{1'\perp}, p_{2'\perp}\right)\right]. \end{aligned} \tag{3.141}$$

We can separate this cross section into its divergent part and its convergent part. To get the convergent part, one only has to replace Φ_1 in Eq. (3.141) by Φ_{1R} from Eq. (3.87) and to set ϵ to 0. The remaining divergent part reads

$$\left(d\sigma_{1JI}\right)_{div} = \alpha_s \frac{\Gamma(1-\epsilon)}{(4\pi)^{1+\epsilon}} \left(\frac{N_c^2-1}{2N_c}\right) \left(S_V + S_V^*\right) d\sigma_{0JI}. \tag{3.142}$$

Replacing Φ_2 by the contribution Φ_2' from Eqs. (3.100, 3.101) which includes the B-JIMWLK evolution (see the discussion in Section 3.4.9), one gets a non-divergent dipole $\times$ double dipole NLO contribution, which reads

$$\begin{aligned} d\sigma_{2JI} &= \alpha_s \frac{\Gamma\left(1-\epsilon\right)}{(4\pi)^{1+\epsilon}} \frac{\alpha_{\rm em} Q_q^2}{(2\pi)^{4(d-1)} N_c} \frac{\left(p_0^-\right)^2}{2x\bar{x}s^2} dx d\bar{x} d^d p_{q\perp} d^d p_{\bar{q}\perp} \delta\left(1-x-\bar{x}\right) \left(\varepsilon_{I\beta} \varepsilon_{J\gamma}^*\right) \\ &\times \int d^d p_{1\perp} d^d p_{2\perp} d^d p_{1'\perp} d^d p_{2'\perp} \frac{d^d p_{3\perp} d^d p_{3'\perp}}{(2\pi)^d} \delta\left(p_{q1\perp} + p_{\bar{q}2\perp} - p_{3\perp}\right) \delta\left(p_{11'\perp} + p_{22'\perp} + p_{33'\perp}\right) \\ &\times \left[\Phi_2'^\beta\left(p_{1\perp}, p_{2\perp}, p_{3\perp}\right) \Phi_0^{\gamma *}\left(p_{1'\perp}, p_{2'\perp}\right) \mathbf{F}^*\left(\frac{p_{1'2'\perp}}{2}\right) \tilde{\mathbf{F}}\left(\frac{p_{12\perp}}{2}, p_{3\perp}\right) \delta\left(p_{3'\perp}\right) \right. \\ &\quad \left. + \Phi_2'^{\gamma *}\left(p_{1'\perp}, p_{2'\perp}, p_{3'\perp}\right) \Phi_0^\beta\left(p_{1\perp}, p_{2\perp}\right) \mathbf{F}\left(\frac{p_{12\perp}}{2}\right) \tilde{\mathbf{F}}^*\left(\frac{p_{1'2'\perp}}{2}, p_{3'\perp}\right) \delta\left(p_{3\perp}\right)\right]. \end{aligned} \tag{3.143}$$

This expression is now finite so one can set $\epsilon = 0$.

3.6.1 Results for the Born cross section

Using Eqs. (3.15) and (3.16) and summing over helicities of the quark and the antiquark, one gets

$$\sum_{helicities} \Phi_0^+(p_{1\perp}, p_{2\perp})\Phi_0^+(p'_{1\perp}, p'_{2\perp}) = \frac{32(p_\gamma^+)^4 x^3 \bar{x}^3}{(\vec{p}_{q1}^{\,2} + x\bar{x}Q^2)(\vec{p}_{q1'}^{\,2} + x\bar{x}Q^2)}, \tag{3.144}$$

$$\sum_{helicities} \Phi_0^+(p_{1\perp}, p_{2\perp})\Phi_0^i(p'_{1\perp}, p_{2'\perp})^* = \frac{16(p_\gamma^+)^3 x^2 \bar{x}^2 p^i_{q1'\perp}(1-2x)}{(\vec{p}_{q1}^{\,2} + x\bar{x}Q^2)(\vec{p}_{q1'}^{\,2} + x\bar{x}Q^2)}, \tag{3.145}$$

and

$$\sum_{helicities} \Phi_0^i(p_{1\perp}, p_{2\perp})\Phi_0^k(p'_{1\perp}, p_{2'\perp})^* = \frac{8(p_\gamma^+)^2 x\bar{x}[(1-2x)^2 g_\perp^{ri} g_\perp^{lk} - g_\perp^{rk} g_\perp^{li} + g_\perp^{rl} g_\perp^{ik}] p_{q1\perp r} p_{q1'\perp l}}{(\vec{p}_{q1}^{\,2} + x\bar{x}Q^2)(\vec{p}_{q1'}^{\,2} + x\bar{x}Q^2)}. \tag{3.146}$$

As a result, the LO density matrix elements read

$$\begin{aligned} d\sigma_{0LL} &= \frac{4\alpha_{\rm em} Q_q^2}{(2\pi)^4 N_c} dx d\bar{x} d^2p_{q\perp} d^2p_{\bar{q}\perp} \delta(1-x-\bar{x}) x^2\bar{x}^2 Q^2 \\ &\times \left| \int \frac{d^2p_{1\perp}}{\vec{p}_{q1}^{\,2} + x\bar{x}Q^2} \mathbf{F}(p_{1q\perp} + \frac{p_{q\bar{q}\perp}}{2}) \right|^2, \end{aligned} \tag{3.147}$$

$$\begin{aligned} d\sigma_{0TL} &= \frac{2\alpha_{\rm em} Q_q^2}{(2\pi)^4 N_c} dx d\bar{x} d^2p_{q\perp} d^2p_{\bar{q}\perp} \delta(1-x-\bar{x}) x\bar{x}(1-2x) Q \\ &\times \left[\int \frac{d^2p_{1\perp}}{\vec{p}_{q1}^{\,2} + x\bar{x}Q^2} \mathbf{F}(p_{1q\perp} + \frac{p_{q\bar{q}\perp}}{2}) \right] \left[\int \frac{d^2p'_{1\perp}(\varepsilon_\perp \cdot p_{q1'\perp})}{\vec{p}_{q1'}^{\,2} + x\bar{x}Q^2} \mathbf{F}(p_{1'q\perp} + \frac{p_{q\bar{q}\perp}}{2}) \right]^*, \end{aligned} \tag{3.148}$$

and

$$\begin{aligned} d\sigma_{0TT} &= \frac{\alpha_{\rm em} Q_q^2}{(2\pi)^4 N_c} dx d\bar{x} d^2p_{q\perp} d^2p_{\bar{q}\perp} \delta(1-x-\bar{x}) [(1-2x)^2 g_\perp^{ki} g_\perp^{lj} - g_\perp^{kj} g_\perp^{li} + g_\perp^{kl} g_\perp^{ij}] \\ &\times \left[\int \frac{d^2p_{1\perp}(\varepsilon_{\perp i} p_{q1\perp k})}{\vec{p}_{q1}^{\,2} + x\bar{x}Q^2} \mathbf{F}(p_{1q\perp} + \frac{p_{q\bar{q}\perp}}{2}) \right] \left[\int \frac{d^2p'_{1\perp}(\varepsilon_{\perp j} p_{q1'\perp l})}{\vec{p}_{q1'}^{\,2} + x\bar{x}Q^2} \mathbf{F}(p_{1'q\perp} + \frac{p_{q\bar{q}\perp}}{2}) \right]^*. \end{aligned} \tag{3.149}$$

3.6.2 Dipole - dipole NLO cross section $d\sigma_1$

LL photon transition

Combining Eqs. (3.141), (3.87) and (3.15), and summing over the polarization components $\varepsilon^+\Phi_0^- + \varepsilon^-\Phi_0^+$ with the help of the gauge invariance relation $\Phi_0^- = \frac{Q^2}{2(p_\gamma^+)^2}\Phi_0^+$, we get

$$\begin{aligned} d\sigma_{1LL} &= \alpha_s \frac{\Gamma(1-\epsilon)}{(4\pi)^{1+\epsilon}} \left(\frac{N_c^2 - 1}{2N_c} \right) (S_V + S_V^*) d\sigma_{0LL} \\ &+ \frac{\alpha_s Q^2}{4\pi} \left(\frac{N_c^2 - 1}{N_c} \right) \frac{\alpha_{\rm em} Q_q^2}{(2\pi)^4 N_c} dx d\bar{x} d^2p_{q\perp} d^2p_{\bar{q}\perp} \delta(1-x-\bar{x}) \\ &\times \int d^2p_{1\perp} d^2p_{2\perp} d^2p'_{1\perp} d^2p'_{2\perp} \delta(p_{q1\perp} + p_{\bar{q}2\perp}) \frac{\delta(p_{11'\perp} + p_{22'\perp})}{\vec{p}_{q1'}^{\,2} + x\bar{x}Q^2} \mathbf{F}\left(\frac{p_{12\perp}}{2}\right) \mathbf{F}^*\left(\frac{p_{1'2'\perp}}{2}\right) \\ &\times \left[\frac{6x^2\bar{x}^2}{\vec{p}_{q1}^{\,2} + x\bar{x}Q^2} \ln\left(\frac{x^2\bar{x}^2\mu^4 Q^2}{(x\vec{p}_{\bar{q}} - \bar{x}\vec{p}_q)^2 (\vec{p}_{q1}^{\,2} + x\bar{x}Q^2)^2} \right) \right. \\ &\left. + \frac{(p_0^-)^2}{s^2 p_\gamma^+} tr((C_\parallel^4 + C_{1\parallel}^5 + C_{1\parallel}^6) \hat{p}_{\bar{q}} \gamma^+ \hat{p}_q) \right] + h.c. \end{aligned} \tag{3.150}$$

We will parametrize the finite contribution of the C functions using the $+$ prescription as defined in Eq. 3.29 :

$$\frac{(p_0^-)^2}{s^2 p_\gamma^+} tr(C^4_{||}\hat{p}_{\bar{q}}\gamma^+\hat{p}_q) = \int_0^x dz\,[(\phi_4)_{LL}]_+ + (q \leftrightarrow \bar{q})\,, \tag{3.151}$$

and

$$\frac{(p_0^-)^2}{s^2 p_\gamma^+} tr(C^n_{1||}\hat{p}_{\bar{q}}\gamma^+\hat{p}_q) = \int_0^x dz\,[(\phi_n)_{LL}]_+ \,|_{\vec{p}_3=\vec{0}} + (q \leftrightarrow \bar{q})\,, \tag{3.152}$$

where $n = 5$ or 6. The expressions for $(\phi_n)_{LL}$ are given in Appendix A.1. For $n = 6$ the integral can be performed analytically to the end, so that :

$$\begin{aligned}\frac{(p_0^-)^2}{s^2 p_\gamma^+} tr(C^6_{1||}\hat{p}_{\bar{q}}\gamma^+\hat{p}_q) &= \frac{-2x^2\bar{x}^3\vec{p}_1^{\,2}}{(\vec{p}_{q1}^{\,2} + x\bar{x}Q^2 - \bar{x}\vec{p}_1^{\,2})^2}\ln\left(\frac{x\bar{x}Q^2 + \vec{p}_{q1}^{\,2}}{\bar{x}\vec{p}_1^{\,2}}\right)\\ &+\frac{2x^2\bar{x}^2}{\vec{p}_{q1}^{\,2} + x\bar{x}Q^2}\left[4\,\mathrm{Li}_2\left(\frac{\vec{p}_{q1}^{\,2} + x\bar{x}Q^2 - \bar{x}\vec{p}_1^{\,2}}{\vec{p}_{q1}^{\,2} + x\bar{x}Q^2}\right) + 3\ln\left(\frac{\vec{p}_1^{\,2}}{\mu^2}\right) - 8\right]\\ &+\frac{2x^2\bar{x}^2}{\vec{p}_{q1}^{\,2} + x\bar{x}Q^2 - \bar{x}\vec{p}_1^{\,2}}\left[3\ln\left(\frac{\vec{p}_{q1}^{\,2} + x\bar{x}Q^2}{\bar{x}\vec{p}_1^{\,2}}\right) + 1\right] + (q \leftrightarrow \bar{q}).\end{aligned} \tag{3.153}$$

LT photon transition

Using the same method as for the LL component, we get

$$\begin{aligned} d\sigma_{1TL} &= \alpha_s\frac{\Gamma(1-\epsilon)}{(4\pi)^{1+\epsilon}}\left(\frac{N_c^2-1}{2N_c}\right)(S_V + S_V^*)\,d\sigma_{0TL}\\ &+ \frac{\alpha_s Q}{(4\pi)}\left(\frac{N_c^2-1}{N_c}\right)\frac{\alpha_{\mathrm{em}}Q_q^2}{(2\pi)^4 N_c}dx d\bar{x} d^2p_{q\perp}d^2p_{\bar{q}\perp}\delta(1-x-\bar{x})\varepsilon^*_{Ti}\\ &\times \int d^2p_{1\perp}d^2p_{2\perp}d^2p'_{1\perp}d^2p_{2'\perp}\delta(p_{q1\perp}+p_{\bar{q}2\perp})\delta(p_{11'\perp}+p_{22'\perp})\mathbf{F}\left(\frac{p_{12\perp}}{2}\right)\mathbf{F}^*\left(\frac{p_{1'2'\perp}}{2}\right)\\ &\times \left[\frac{(p_0^-)^2}{s^2}\frac{tr((C'^{4i}_\perp + C'^{5i}_{1\perp} + C'^{6i}_{1\perp})\hat{p}_{\bar{q}}\gamma^+\hat{p}_q)^\dagger}{\vec{p}_{q1}^{\,2} + x\bar{x}Q^2} + \frac{3x\bar{x}(1-2x)p^i_{q1'\perp}}{(\vec{p}_{q1}^{\,2} + x\bar{x}Q^2)(\vec{p}_{q1'}^{\,2} + x\bar{x}Q^2)}\right.\\ &\times \left(\ln\left(\frac{x^3\bar{x}^3\mu^8Q^2(x\vec{p}_{\bar{q}} - \bar{x}\vec{p}_q)^{-4}}{(\vec{p}_{q1}^{\,2} + x\bar{x}Q^2)^2(\vec{p}_{q1'}^{\,2} + x\bar{x}Q^2)}\right) - \frac{x\bar{x}Q^2}{\vec{p}_{q1'}^{\,2}}\ln\left(\frac{x\bar{x}Q^2}{\vec{p}_{q1'}^{\,2} + x\bar{x}Q^2}\right)\right)\\ &+ \left.\frac{(p_0^-)^2}{s^2}\frac{tr((C^4_\parallel + C^5_{1\parallel} + C^6_{1\parallel})\hat{p}_{\bar{q}}(\gamma^i\hat{p}_{q1'\perp} - 2xp^i_{q1'\perp})\gamma^+\hat{p}_q)}{2p_\gamma^+ x\bar{x}\left(\vec{p}_{q1'}^{\,2} + x\bar{x}Q^2\right)}\right]. \end{aligned} \tag{3.154}$$

Once more we will parametrize the contributions from the C functions, as

$$\frac{(p_0^-)^2 tr(C^4_{||}\hat{p}_{\bar{q}}((1-2x)p^i_{q1'\perp} - \frac{1}{2}[\hat{p}_{q1'\perp},\gamma^i_\perp])\gamma^+\hat{p}_q)}{s^2 p_\gamma^+} = \int_0^x dz[(\phi_4)^i_{LT}]_+ + (q \leftrightarrow \bar{q})\,, \tag{3.155}$$

$$\frac{(p_0^-)^2 tr(C^n_{1||}\hat{p}_{\bar{q}}((1-2x)p^i_{q1'\perp} - \frac{1}{2}[\hat{p}_{q1'\perp},\gamma^i_\perp])\gamma^+\hat{p}_q)}{s^2 p_\gamma^+} = \int_0^x dz[(\phi_n)^i_{LT}]_+|_{\vec{p}_3=\vec{0}} + (q \leftrightarrow \bar{q})\,, \tag{3.156}$$

and

$$\frac{(p_0^-)^2}{s^2} tr(C^{4i}_\perp \hat{p}_{\bar{q}}\gamma^+\hat{p}_q) = \int_0^x dz[(\phi_4)^i_{TL}]_+ + (q \leftrightarrow \bar{q})\,, \tag{3.157}$$

$$\frac{(p_0^-)^2}{s^2} tr(C^{ni}_{1\perp}\hat{p}_{\bar{q}}\gamma^+\hat{p}_q) = \int_0^x dz[(\phi_n)^i_{TL}]_+|_{\vec{p}_3=\vec{0}} + (q \leftrightarrow \bar{q})\,, \tag{3.158}$$

with $n = 5,\,6$. The values for (ϕ_n) are given in Appendix A.1. The contribution from diagram 6 can be computed to the end :

$$\frac{(p_0^-)^2 tr(C^6_{1||}\hat{p}_{\bar{q}}((1-2x)p^i_{q1'\perp} - \frac{1}{2}[\hat{p}_{q1'\perp},\gamma^i_\perp])\gamma^+\hat{p}_q)}{s^2 p_\gamma^+} = (1-2x)p^i_{q1'\perp}\frac{(p_0^-)^2}{s^2 p_\gamma^+} tr(C^6_{1||}\hat{p}_{\bar{q}}\gamma^+\hat{p}_q), \tag{3.159}$$

and

$$\begin{aligned}
&\frac{(p_0^-)^2}{s^2} tr(C_{1\perp}^{6i}\hat{p}_{\bar{q}}\gamma^+\hat{p}_q) = \frac{-x\bar{x}(1-2x)p_{q1\perp}^i}{\vec{p}_{q1}^{\,2}+x\bar{x}Q^2-\bar{x}\vec{p}_1^{\,2}}\ln\left(\frac{\bar{x}\vec{p}_1^{\,2}}{\vec{p}_{q1}^{\,2}+x\bar{x}Q^2}\right)\\
+\;&\frac{x\bar{x}(1-2x)p_{q1\perp}^i}{\vec{p}_{q1}^{\,2}+x\bar{x}Q^2}\left[4\mathrm{Li}_2\left(\frac{\bar{x}\vec{p}_1^{\,2}}{\vec{p}_{q1}^{\,2}+x\bar{x}Q^2}+1\right)+3\ln\left(\frac{\vec{p}_1^{\,2}}{\mu^2}\right)-8\right]\\
+\;&\frac{-x\bar{x}p_{1\perp}^i}{3\vec{p}_1^{\,2}}\left[\pi^2-6\mathrm{Li}_2\left(\frac{\bar{x}\vec{p}_1^{\,2}}{\vec{p}_{q1}^{\,2}+x\bar{x}Q^2}+1\right)\right]+x\bar{x}\left(xp_{q1\perp}^i-\bar{x}p_{q\perp}^i\right)\\
\times\;&\left(\frac{-\bar{x}\vec{p}_1^{\,2}}{(\vec{p}_{q1}^{\,2}+x\bar{x}Q^2-\bar{x}\vec{p}_1^{\,2})^2}\ln\left(\frac{\bar{x}\vec{p}_1^{\,2}}{\vec{p}_{q1}^{\,2}+x\bar{x}Q^2}\right)\right.\\
&\left.+\frac{1}{(\vec{p}_{q1}^{\,2}+x\bar{x}Q^2-\bar{x}\vec{p}_1^{\,2})}\left[2\ln\left(\frac{\bar{x}\vec{p}_1^{\,2}}{\vec{p}_{q1}^{\,2}+x\bar{x}Q^2}\right)-1\right]\right)+(q\leftrightarrow\bar{q}).
\end{aligned}\tag{3.160}$$

TT photon transition

The cross section for the TT transition reads

$$\begin{aligned}
d\sigma_{1TT} &= \alpha_s\frac{\Gamma(1-\epsilon)}{(4\pi)^{1+\epsilon}}\left(\frac{N_c^2-1}{2N_c}\right)(S_V+S_V^*)\,d\sigma_{0TT}\\
&+\frac{\alpha_s}{4\pi}\left(\frac{N_c^2-1}{N_c}\right)\frac{\alpha_{\mathrm{em}}Q_q^2}{(2\pi)^4\,N_c}dxd\bar{x}d^2p_{q\perp}d^2p_{\bar{q}\perp}\delta(1-x-\bar{x})(\varepsilon_{Ti}\varepsilon_{Tk}^*)\\
&\times\int d^2p_{1\perp}d^2p_{2\perp}d^2p'_{1\perp}d^2p'_{2\perp}\delta(p_{q1\perp}+p_{\bar{q}2\perp})\delta(p_{11'\perp}+p_{22'\perp})\mathbf{F}\left(\frac{p_{12\perp}}{2}\right)\mathbf{F}^*\left(\frac{p_{1'2'\perp}}{2}\right)\\
&\times\left\{\frac{3}{2}\frac{p_{q1\perp r}p_{q1'\perp l}}{(\vec{p}_{q1}^{\,2}+x\bar{x}Q^2)(\vec{p}_{q1'}^{\,2}+x\bar{x}Q^2)}[(1-2x)^2g_\perp^{ri}g_\perp^{lk}-g_\perp^{rk}g_\perp^{li}+g_\perp^{rl}g_\perp^{ik}]\right.\\
&\times\left[\ln\left(\frac{x\bar{x}\mu^4}{(x\vec{p}_{\bar{q}}-\bar{x}\vec{p}_q)^2(\vec{p}_{q1}^{\,2}+x\bar{x}Q^2)}\right)-\frac{x\bar{x}Q^2}{\vec{p}_{q1}^{\,2}}\ln\left(\frac{x\bar{x}Q^2}{\vec{p}_{q1}^{\,2}+x\bar{x}Q^2}\right)\right]\\
&+\left.\frac{(p_0^-)^2}{2s^2x\bar{x}}\frac{tr[(C_\perp^{4i}+C_{1\perp}^{5i}+C_{1\perp}^{6i})\hat{p}_{\bar{q}}(p_{q1'\perp}^j(1-2x)-\frac{1}{2}[\hat{p}_{q1'\perp},\gamma^j]\gamma^+\hat{p}_q]}{\vec{p}_{q1'}^{\,2}+x\bar{x}Q^2}+h.c.|_{\substack{p_1\leftrightarrow p'_1\\ i\leftrightarrow k}}\right\}.
\end{aligned}\tag{3.161}$$

The C functions are given by :

$$\frac{(p_0^-)^2}{2s^2}tr(C_\perp^{4i}\hat{p}_{\bar{q}}(p_{q1'\perp}^j(1-2x)-\frac{1}{2}[\hat{p}_{q1'\perp},\gamma_\perp^j])\gamma^+\hat{p}_q)=\int_0^x dz\left[(\phi_4^{ij})_{TT}\right]_+ +(q\leftrightarrow\bar{q}),\tag{3.162}$$

and

$$\frac{(p_0^-)^2}{2s^2}tr(C_{1\perp}^{ni}\hat{p}_{\bar{q}}(p_{q1'\perp}^j(1-2x)-\frac{1}{2}[\hat{p}_{q1'\perp},\gamma_\perp^j])\gamma^+\hat{p}_q)=\int_0^x dz\left[(\phi_n^{ij})_{TT}\right]_+|_{\vec{p}_3=\vec{0}}+(q\leftrightarrow\bar{q}),\tag{3.163}$$

with $n=5\,,\,6$. The values for ϕ_n are given in Appendix A.1. The contribution from diagram 6 finally reads :

$$\begin{aligned}
&\frac{(p_0^-)^2}{s^2}tr(C_{1\perp}^{6i}\hat{p}_{\bar{q}}(p_{q1'\perp}^k(1-2x)-\frac{1}{2}[\hat{p}_{q1'\perp},\gamma_\perp^k])\gamma^+\hat{p}_q)\\
&=x\bar{x}\left[g_\perp^{ik}(\vec{p}_1\cdot\vec{p}_{q1'})+p_{1\perp}^kp_{q1'\perp}^i+(2x-1)p_{1\perp}^ip_{q1'\perp}^k\right]\\
&\times\left[\frac{-\bar{x}^2\vec{p}_1^{\,2}}{(\vec{p}_{q1}^{\,2}+x\bar{x}Q^2-\bar{x}\vec{p}_1^{\,2})^2}\ln\left(\frac{\bar{x}\vec{p}_1^{\,2}}{\vec{p}_{q1}^{\,2}+x\bar{x}Q^2}\right)\right.\\
&\left.+\frac{\bar{x}}{\vec{p}_{q1}^{\,2}+x\bar{x}Q^2-\bar{x}\vec{p}_1^{\,2}}\left[2\ln\left(\frac{\bar{x}\vec{p}_1^{\,2}}{\vec{p}_{q1}^{\,2}+x\bar{x}Q^2}\right)-1\right]\right.
\end{aligned}$$

$$
\begin{aligned}
&+\frac{2}{\vec{p}_1^{\,2}}\left(\frac{\pi^2}{6}-\mathrm{Li}_2\left(\frac{\vec{p}_{q1}^{\,2}+x\bar{x}Q^2-\bar{x}\vec{p}_1^{\,2}}{\vec{p}_{q1}^{\,2}+x\bar{x}Q^2}\right)\right)\Bigg]\\
&-x\bar{x}\left[p^i_{q1\perp}p^k_{q1'\perp}(1-2x)^2-g^{ik}_{\perp}(\vec{p}_{q1}\cdot\vec{p}_{q1'})-p^k_{q1\perp}p^i_{q1'\perp}\right]\\
&\times\left[\frac{-1}{\vec{p}_{q1}^{\,2}+x\bar{x}Q^2-\bar{x}\vec{p}_1^{\,2}}\left(1-3\ln\left(\frac{\bar{x}\vec{p}_1^{\,2}}{\vec{p}_{q1}^{\,2}+x\bar{x}Q^2}\right)\right)\right.\\
&-\frac{1}{\vec{p}_{q1}^{\,2}+x\bar{x}Q^2}\left(3\ln\left(\frac{\vec{p}_1^{\,2}}{\mu^2}\right)+4\mathrm{Li}_2\left(\frac{\vec{p}_{q1}^{\,2}+x\bar{x}Q^2-\bar{x}\vec{p}_1^{\,2}}{\vec{p}_{q1}^{\,2}+x\bar{x}Q^2}\right)-8\right)\\
&\left.+\frac{-\bar{x}\vec{p}_1^{\,2}}{(\vec{p}_{q1}^{\,2}+x\bar{x}Q^2-\bar{x}\vec{p}_1^{\,2})^2}\ln\left(\frac{\bar{x}\vec{p}_1^{\,2}}{\vec{p}_{q1}^{\,2}+x\bar{x}Q^2}\right)\right]+(q\leftrightarrow\bar{q})\,. \qquad (3.164)
\end{aligned}
$$

3.6.3 Dipole - double dipole cross section $d\sigma_2$

LL photon transition

$$
\begin{aligned}
d\sigma_{2LL} &= \frac{\alpha_s Q^2}{4\pi}\frac{\alpha_{\mathrm{em}}Q_q^2}{(2\pi)^4 N_c}dxd\bar{x}d^2p_{q\perp}d^2p_{\bar{q}\perp}\delta(1-x-\bar{x})\\
&\times\int d^2p_{1\perp}d^2p_{2\perp}d^2p'_{1\perp}d^2p'_{2\perp}\int\frac{d^2p_{3\perp}}{(2\pi)^2}\delta(p_{q1\perp}+p_{\bar{q}2\perp}-p_{3\perp})\delta(p_{11'\perp}+p_{22'\perp}+p_{3\perp})\\
&\times\frac{1}{\vec{p}_{q1'}^{\,2}+x\bar{x}Q^2}\tilde{\mathbf{F}}\left(\frac{p_{12\perp}}{2},p_{3\perp}\right)\int\mathbf{F}^*\left(\frac{p_{1'2'\perp}}{2}\right)\\
&\times\left(4x\bar{x}\left\{\frac{x\bar{x}(\vec{p}_3^{\,2}-\vec{p}_{\bar{q}2}^{\,2}-\vec{p}_{q1}^{\,2}-2x\bar{x}Q^2)}{(\vec{p}_{\bar{q}2}^{\,2}+x\bar{x}Q^2)(\vec{p}_{q1}^{\,2}+x\bar{x}Q^2)-x\bar{x}Q^2\vec{p}_3^{\,2}}\right.\right.\\
&\times\ln\left(\frac{x\bar{x}}{e^{2\eta}}\right)\ln\left(\frac{(\vec{p}_{q2}^{\,2}+x\bar{x}Q^2)\left(\vec{p}_{q1}^{\,2}+x\bar{x}Q^2\right)}{x\bar{x}Q^2\vec{p}_3^{\,2}}\right)\\
&-\left.\left.\left(\frac{2x\bar{x}}{\vec{p}_{q1}^{\,2}+x\bar{x}Q^2}\ln\left(\frac{x}{e^{\eta}}\right)\ln\left(\frac{\vec{p}_3^{\,2}}{\mu^2}\right)+(q\leftrightarrow\bar{q})\right)\right\}\right.\\
&+\left.\frac{Q^2(p_0^-)^2}{p_\gamma^+ s^2}tr((C^5_{2\|}+C^6_{2\|})\hat{p}_{\bar{q}}\gamma^+\hat{p}_q)\right)+h.c. \qquad (3.165)
\end{aligned}
$$

We will write

$$
\frac{(p_0^-)^2}{s^2p_\gamma^+}tr(C^n_{2||}\hat{p}_{\bar{q}}\gamma^+\hat{p}_q)=\int_0^x dz\left[(\phi_n)_{LL}\right]_+ +(q\leftrightarrow\bar{q})\,, \qquad (3.166)
$$

with $n=5,\,6$. The values for ϕ_n are given in Appendix A.1.

LT photon transition

$$
\begin{aligned}
d\sigma_{2TL} &= \frac{\alpha_s Q}{4\pi}\frac{\alpha_{\mathrm{em}}Q_q^2}{(2\pi)^4 N_c}dxd\bar{x}d^2p_{q\perp}d^2p_{\bar{q}\perp}\delta(1-x-\bar{x})\int d^2p_{1\perp}d^2p_{2\perp}d^2p'_{1\perp}d^2p'_{2\perp} \qquad (3.167)\\
&\times\int\frac{d^2p_{3\perp}d^2p'_{3\perp}}{(2\pi)^2}\delta(p_{q1\perp}+p_{\bar{q}2\perp}+p_{g3\perp})\delta(p_{11'\perp}+p_{22'\perp}+p_{33'\perp})\\
&\times\varepsilon^*_{Ti}\left[\frac{\delta(p'_{3\perp})}{\vec{p}_{q1'}^{\,2}+x\bar{x}Q^2}\tilde{\mathbf{F}}\left(\frac{p_{12\perp}}{2},p_{3\perp}\right)\mathbf{F}^*\left(\frac{p_{1'2'\perp}}{2}\right)\right.\\
&\times\left(2(1-2x)p^i_{q1'\perp}\left\{\frac{x\bar{x}(\vec{p}_3^{\,2}-\vec{p}_{\bar{q}2}^{\,2}-\vec{p}_{q1}^{\,2}-2x\bar{x}Q^2)}{(\vec{p}_{\bar{q}2}^{\,2}+x\bar{x}Q^2)(\vec{p}_{q1}^{\,2}+x\bar{x}Q^2)-x\bar{x}Q^2\vec{p}_3^{\,2}}\right.\right.\ln\left(\frac{x\bar{x}}{e^{2\eta}}\right)\\
&\times\left.\left.\ln\left(\frac{(\vec{p}_{\bar{q}2}^{\,2}+x\bar{x}Q^2)\left(\vec{p}_{q1}^{\,2}+x\bar{x}Q^2\right)}{x\bar{x}Q^2\vec{p}_3^{\,2}}\right)\right.\right.
\end{aligned}
$$

$$
\begin{aligned}
&- \quad \left(\frac{2x\bar{x}}{\vec{p}_{q1}^{\,2} + x\bar{x}Q^2} \ln\left(\frac{x}{e^\eta}\right) \ln\left(\frac{\vec{p}_3^{\,2}}{\mu^2}\right) + (q \leftrightarrow \bar{q}) \right) \Bigg\} \\
&+ \quad \frac{(p_0^-)^2}{2s^2 x\bar{x} p_\gamma^+} tr[(C^5_{2\|} + C^6_{2\|}) \hat{p}_{\bar{q}} (p^i_{q1'\perp}(1-2x) - \frac{1}{2}[\hat{p}_{q1'\perp}\,,\,\gamma^i])\gamma^+ \hat{p}_q] \Big) \\
&+ \quad \frac{\delta(p_{3\perp})}{\vec{p}_{q1}^{\,2} + x\bar{x}Q^2} \mathbf{F}\left(\frac{p_{12\perp}}{2}\right) \tilde{\mathbf{F}}^*\left(\frac{p_{1'2'\perp}}{2}, p_{3'\perp}\right) \\
&\times \quad \Bigg(\Bigg\{ 2x\bar{x}(1-2x) p^i_{q1'\perp} \left(\frac{-2}{Q^2 + x\bar{x}\vec{p}_{q1'}^{\,2}} \ln\left(\frac{x}{e^\eta}\right) \ln\left(\frac{\vec{p}_{3'}^{\,2}}{\mu^2}\right) \right. \\
&+ \quad \ln\left(\frac{x\bar{x}}{e^{2\eta}}\right) \left[- \frac{\vec{p}_{\bar{q}2'}^{\,2} + x\bar{x}Q^2}{(\vec{p}_{q1'}^{\,2} + x\bar{x}Q^2)(\vec{p}_{\bar{q}2'}^{\,2} + x\bar{x}Q^2) - x\bar{x}Q^2\vec{p}_{3'}^{\,2}} \right. \\
&\times \quad \left. \ln\left(\frac{(\vec{p}_{q1'}^{\,2} + x\bar{x}Q^2)(\vec{p}_{\bar{q}2'}^{\,2} + x\bar{x}Q^2)}{x\bar{x}Q^2\vec{p}_{3'}^{\,2}} \right) \right. \\
&+ \quad \left. \left. \frac{1}{\vec{p}_{q1'}^{\,2}} \ln\left(\frac{\vec{p}_{q1'}^{\,2} + x\bar{x}Q^2}{x\bar{x}Q^2} \right) \right] \right) + (q \leftrightarrow \bar{q}) \Bigg\} + \frac{(p_0^-)^2}{s^2} tr((C'^{5i}_{2\perp} + C'^{6i}_{2\perp}) \hat{p}_{\bar{q}} \gamma^+ \hat{p}_q)^* \Big) \Big] .
\end{aligned}
$$

Again we will write

$$
\frac{(p_0^-)^2}{s^2} tr(C^{ni}_{2\perp} \hat{p}_{\bar{q}} \gamma^+ \hat{p}_q) = \int_0^x dz \left[(\phi^i_n)_{LT} \right]_+ dz + (q \leftrightarrow \bar{q}) \,, \tag{3.168}
$$

and

$$
\frac{(p_0^-)^2}{s^2 p_\gamma^+} tr(C^n_{2||} \hat{p}_{\bar{q}} (p^i_{q1'\perp}(1-2x) - \frac{1}{2}[\hat{p}_{q1'\perp}, \gamma^i_\perp])\gamma^+ \hat{p}_q) = \int_0^x dz \left[(\phi^i_n)_{TL} \right]_+ + (q \leftrightarrow \bar{q}) \,. \tag{3.169}
$$

The values for $(\phi_{5,6})_{LT}$ and $(\phi_{5,6})_{TL}$ are given in Appendix A.1.

TT photon transition

$$
\begin{aligned}
& d\sigma_{2TT} = \frac{\alpha_s}{4\pi} \frac{\alpha_{\rm em} Q_q^2}{(2\pi)^4 N_c} dx d\bar{x} d^2p_{q\perp} d^2p_{\bar{q}\perp} \delta(1-x-\bar{x}) \int d^2p_{1\perp} d^2p_{2\perp} d^2p'_{1\perp} d^2p'_{2\perp} \int \frac{d^2p_{3\perp}}{(2\pi)^d} \\
\times \quad & \frac{(\varepsilon_{Ti} \varepsilon^*_{Tj})}{\vec{p}_{q1'}^{\,2} + x\bar{x}Q^2} \left[\tilde{\mathbf{F}}\left(\frac{p_{12\perp}}{2}, p_{3\perp}\right) \mathbf{F}^*\left(\frac{p_{1'2'\perp}}{2}\right) \delta(p_{q1\perp} + p_{\bar{q}2\perp} - p_{3\perp}) \delta(p_{11'\perp} + p_{22'\perp} + p_{3\perp}) \right. \\
\times \quad & \Bigg(\Bigg\{ p_{q1'\perp l} p_{q1\perp k} [(1-2x)^2 g_\perp^{ki} g_\perp^{lj} - g_\perp^{kj} g_\perp^{li} + g_\perp^{kl} g_\perp^{ij}] \left(\frac{-2}{\vec{p}_{q1}^{\,2} + x\bar{x}Q^2} \ln\left(\frac{x}{e^\eta}\right) \ln\left(\frac{\vec{p}_3^{\,2}}{\mu^2}\right) \right. \\
+ \quad & \ln\left(\frac{x\bar{x}}{e^{2\eta}}\right) \left[\frac{1}{\vec{p}_{q1}^{\,2}} \ln\left(\frac{\vec{p}_{q1}^{\,2} + x\bar{x}Q^2}{x\bar{x}Q^2} \right) - \frac{\vec{p}_{\bar{q}2}^{\,2} + x\bar{x}Q^2}{(\vec{p}_{q1}^{\,2} + x\bar{x}Q^2)(\vec{p}_{\bar{q}2}^{\,2} + x\bar{x}Q^2) - x\bar{x}Q^2\vec{p}_3^{\,2}} \right. \\
\times \quad & \left. \left. \ln\left(\frac{(\vec{p}_{q1}^{\,2} + x\bar{x}Q^2)(\vec{p}_{\bar{q}2}^{\,2} + x\bar{x}Q^2)}{x\bar{x}Q^2\vec{p}_3^{\,2}} \right) \right] \right) + (q \leftrightarrow \bar{q}) \Bigg\} \\
+ \quad & \left. \frac{(p_0^-)^2}{2s^2 x\bar{x}} tr((C^{5i}_{2\perp} + C^{6i}_{2\perp}) \hat{p}_{\bar{q}} [p^j_{q1'\perp}(1-2x) - \frac{1}{2}[\hat{p}_{q1'\perp}\,,\,\gamma^j])\gamma^+ \hat{p}_q] \Big) + h.c.|_{\substack{p_1, p_3 \leftrightarrow p'_1, p'_3 \\ i \leftrightarrow j}} \right] .
\end{aligned} \tag{3.170}
$$

As for the other contributions, we will write

$$
\frac{(p_0^-)^2}{2s^2} tr(C^{ni}_{2\perp} \hat{p}_{\bar{q}} (p^j_{q1'\perp}(1-2x) - \frac{1}{2}[\hat{p}_{q1'\perp}, \gamma^j_\perp])\gamma^+ \hat{p}_q) = \int_0^x dz \left[(\phi^{ij}_n)_{TT} \right]_+ dz + (q \leftrightarrow \bar{q}) \,. \tag{3.171}
$$

The expressions of $(\phi^{ij}_5)_{TT}$ and $(\phi^{ij}_6)_{TT}$ can be found in Appendix A.1.

3.7 Cross section for the $\gamma^* P \to q\bar{q}gP'$ transition

As in Section 3.6 we define a reduced matrix element A_4 such that the $\gamma^* P \to q\bar{q}gP'$ cross section reads

$$d\sigma_{(q\bar{q}g)} = \frac{1}{4s}(2\pi)^D \delta^{(D)}(p_\gamma + p_0 - p_q - p_{\bar{q}} - p_g - p_0')|A_4|^2 d\rho_4\,, \tag{3.172}$$

where

$$\begin{aligned}\delta^{(D)}(p_\gamma + p_0 - p_q - p_{\bar{q}} - p_g - p_0') = \delta(p_{00'}^-)\delta(p_q^+ + p_{\bar{q}}^+ + p_g^+ - p_\gamma^+) \\ \times \delta^{(d)}(p_{q\perp} + p_{\bar{q}\perp} + p_{g\perp} - p_{\gamma\perp} + p_{0'0\perp})\,,\end{aligned} \tag{3.173}$$

with the 4-body phase space measure

$$d\rho_4 = \frac{dp_q^+ d^d p_{q\perp}}{2p_q^+(2\pi)^{d+1}} \frac{dp_{\bar{q}}^+ d^d p_{\bar{q}\perp}}{2p_{\bar{q}}^+(2\pi)^{d+1}} \frac{dp_g^+ d^d p_{g\perp}}{2p_g^+(2\pi)^{d+1}} \frac{dp_0'^- d^d p_{0\perp}'}{2p_0'^-(2\pi)^{d+1}}\,. \tag{3.174}$$

The reduced matrix element can be derived from Section 3.5 and reads

$$\begin{aligned}A_4 = \frac{-e_q 2p_0^- \varepsilon_\alpha}{(2\pi)^{D-4}} \sqrt{\frac{2}{N_c^2-1}} g\mu^{-\epsilon} \int d^d p_{1\perp} d^d p_{2\perp} \left\{ \delta(p_{q1\perp} + p_{\bar{q}2\perp} + p_{g\perp}) \left(\frac{N_c^2-1}{N_c}\right) \mathbf{F}(\frac{p_{12\perp}}{2}) \Phi_3^\alpha \right. \\ \left. + \int \frac{d^d p_{3\perp}}{(2\pi)^d} \delta(p_{q1\perp} + p_{\bar{q}2\perp} + p_{g3\perp}) \tilde{\mathbf{F}}(\frac{p_{12\perp}}{2}, p_{3\perp}) \Phi_4^\alpha \right\}\,.\end{aligned} \tag{3.175}$$

This cross section has a contribution $d\sigma_3$ with 2 dipole operators, a contribution $d\sigma_4$ with a dipole operator and a double dipole operator, and a contribution $d\sigma_5$ with 2 double dipole operators,

$$d\sigma_{(q\bar{q}g)} = d\sigma_3 + d\sigma_4 + d\sigma_5. \tag{3.176}$$

The dipole $\times$ dipole contribution reads

$$\begin{aligned}d\sigma_{3JI} &= \frac{\alpha_s}{\mu^{2\epsilon}} \left(\frac{N_c^2-1}{N_c}\right) \frac{\alpha_{\rm em} Q_q^2}{(2\pi)^{4(d-1)} N_c} \frac{(p_0^-)^2}{s^2 x_q x_{\bar{q}}} (\varepsilon_{I\alpha} \varepsilon_{J\beta}^*) \\ &\times dx_q\, dx_{\bar{q}}\, d^d p_{q\perp}\, d^d p_{\bar{q}\perp} \frac{dx_g d^d p_{g\perp}}{x_g (2\pi)^d} \delta(1 - x_q - x_{\bar{q}} - x_g) \\ &\times \int d^d p_{1\perp} d^d p_{2\perp} d^d p_{1\perp}' d^d p_{2\perp}' \delta(p_{q1\perp} + p_{\bar{q}2\perp} + p_{g\perp}) \delta(p_{11'\perp} + p_{22'\perp}) \\ &\times \Phi_3^\alpha(p_{1\perp}, p_{2\perp}) \Phi_3^{\beta *}(p_{1\perp}', p_{2\perp}') \mathbf{F}\left(\frac{p_{12\perp}}{2}\right) \mathbf{F}^*\left(\frac{p_{1'2'\perp}}{2}\right)\,.\end{aligned} \tag{3.177}$$

The dipole $\times$ double dipole contribution reads

$$\begin{aligned}d\sigma_{4JI} &= \frac{\alpha_s}{\mu^{2\epsilon}} \frac{\alpha_{\rm em} Q_q^2}{(2\pi)^{4(d-1)} N_c} \frac{(p_0^-)^2}{s^2 x_q x_{\bar{q}}} (\varepsilon_{I\alpha} \varepsilon_{J\beta}^*) dx_q dx_{\bar{q}} d^d p_{q\perp} d^d p_{\bar{q}\perp} \frac{dz d^d p_{g\perp}}{z(2\pi)^d} \delta(1 - x_q - x_{\bar{q}} - x_g) \\ &\times \int d^d p_{1\perp} d^d p_{2\perp} d^d p_{1\perp}' d^d p_{2\perp}' \frac{d^d p_{3\perp} d^d p_{3\perp}'}{(2\pi)^d} \delta(p_{q1\perp} + p_{\bar{q}2\perp} + p_{g3\perp}) \delta(p_{11'\perp} + p_{22'\perp} + p_{33'\perp}) \\ &\times \left[\Phi_3^\alpha(p_{1\perp}, p_{2\perp}) \Phi_4^{\beta *}(p_{1\perp}', p_{2\perp}', p_{3\perp}') \mathbf{F}\left(\frac{p_{12\perp}}{2}\right) \tilde{\mathbf{F}}^*\left(\frac{p_{1'2'\perp}}{2}, p_{3\perp}'\right) \delta(p_{3\perp}) \right. \\ &\left. + \Phi_4^\alpha(p_{1\perp}, p_{2\perp}, p_{3\perp}) \Phi_3^{\beta *}(\frac{p_{1'2'\perp}}{2}) \tilde{\mathbf{F}}\left(\frac{p_{12\perp}}{2}, p_{3\perp}\right) \mathbf{F}^*\left(\frac{p_{1'2'\perp}}{2}\right) \delta(p_{3\perp}') \right],\end{aligned} \tag{3.178}$$

and the double dipole $\times$ double dipole contribution is given by

$$\begin{aligned}d\sigma_{5JI} = \frac{\alpha_s}{\mu^{2\epsilon}} \frac{\alpha_{\rm em} Q_q^2}{(2\pi)^{4(d-1)}} \frac{(p_0^-)^2}{s^2 x_q x_{\bar{q}}} \frac{(\varepsilon_{I\alpha} \varepsilon_{J\beta}')}{N_c^2 - 1} dx_q dx_{\bar{q}} d^d p_{q\perp} d^d p_{\bar{q}\perp} \frac{dz d^d p_{g\perp}}{z(2\pi)^d} \delta(1 - x_q - x_{\bar{q}} - x_g) \\ \times \int d^d p_{1\perp} d^d p_{2\perp} d^d p_{1\perp}' d^d p_{2\perp}' \frac{d^d p_{3\perp} d^d p_{3\perp}'}{(2\pi)^{2d}} \delta(p_{q1\perp} + p_{\bar{q}2\perp} + p_{g3\perp}) \delta(p_{11'\perp} + p_{22'\perp} + p_{33'\perp}) \\ \times \Phi_4^\alpha(p_{1\perp}, p_{2\perp}, p_{3\perp}) \Phi_4^{\beta *}(p_{1\perp}', p_{2\perp}', p_{3\perp}') \tilde{\mathbf{F}}\left(\frac{p_{12\perp}}{2}, p_{3\perp}\right) \tilde{\mathbf{F}}^*\left(\frac{p_{1'2'\perp}}{2}, p_{3\perp}'\right).\end{aligned} \tag{3.179}$$

We present the results for the products $\Phi_a \Phi_b^*$ in Appendix B in D-dimensional space. They can be used directly in dimension 4 to describe the exclusive production of 3 jets. The cross sections here seem to have a singularity for $x_g = 0$. The dipole dipole part $d\sigma_3$ describes gluon emission after the shockwave. Therefore it is natural for this term to have soft and collinear divergences as will be discussed in the next section. However, each $d\sigma_{3,4,5}$ also gets logarithmically large terms from the gluons with fixed transverse momenta integrated over a large area $\frac{\vec{p}^{\,2}}{s} \ll x_g \ll 1$. To apply these formulas for the exclusive production of 3 jets one has to restrict the x_g integration with the rapidity cutoff $\theta(x_g - e^{\eta})$ from the definition of the impact factor and use it only for the fast gluons (jets). As a result, the cross section gets an explicit dependence on the rapidity cutoff of the 3 observed jets. The situation is different in more inclusive cases when one has to integrate over the produced gluon. Since the x_g integration gives a $\ln(s)$ factor, one has to resum all such contributions. One can do it via the evolution equation for the double dipole operator with a color singlet projector following the logic of [88]. However, since the main motivation of the present thesis is to study the production of a dijet with NLO accuracy, in the next section we will only extract the soft and collinear divergences in these real terms to construct a well defined cross section for this process.

3.8 Cross section for the $\gamma^* P \to 2jets\, P'$ exclusive transition

The expressions for $\gamma^* \to q\bar{q}$ and $\gamma^* \to q\bar{q}g$ impact factors can be used to construct IR stable cross sections for dijet production. Whatever the experimental conditions are, one has to combine the $q\bar{q}$ and $q\bar{q}g$ production cross sections obtained above to cancel the soft and collinear singularities in the virtual part. They cancel with the singular contribution of $q\bar{q}g$ production arising from the emitted gluon phase space area where the gluon is soft or collinear to the quark or the antiquark. We will explicitly show this cancellation on the example of the $\gamma^* P \to 2jets P'$ exclusive production cross section experimentally studied in [86]. By exclusive production we understand that only two jets and the scattered proton are seen in the detector and there is nothing else. Since we want our result for the cross section to be differential only in the jet momenta, we integrate over the transverse momentum of the outgoing proton as before. We define jets using the small cone algorithm, as in [89].

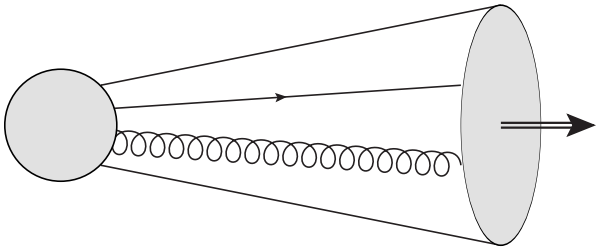

Figure 3.13: Jet formed by a quark and a gluon

Let us define a jet cone radius R^2. For convenience, we will assume that $R^2 \ll 1$. Two given partons i, k with respective momenta p_i and p_k will form a jet with a momentum equal to the sum of their momenta if they both satisfy the following condition :

$$\Delta\phi_{i,k}^2 + \Delta Y_{i,k}^2 < R^2\,, \tag{3.180}$$

where $\Delta\phi_{i,k}$ is the azimuthal angle difference between parton i (resp. k) and the jet, and $\Delta Y_{i,k}$ is the rapidity difference between the parton and the jet. The jet momentum will be given by

$$p_J = x_J p_\gamma^+ n_1^\mu + \left(p_i^- + p_k^-\right) n_2^\mu + p_{J\perp}^\mu, \qquad x_J = x_i + x_k, \quad \vec{p}_J = \vec{p}_i + \vec{p}_k\,. \tag{3.181}$$

In the small cone limit, $p_i^- + p_k^- \sim \frac{\vec{p}_J^{\,2}}{2p_\gamma^+ x_J}$ up to a $O(R)$ correction so the jet is on-shell in this approximation. The azimuthal angle and rapidity differences read :

$$\Delta\phi_{i,k} = \arccos\frac{(\vec{p}_J \cdot \vec{p}_{i,k})}{|\vec{p}_J|\,|\vec{p}_{i,k}|}, \quad \Delta Y_{i,k} = \frac{1}{2}\ln\frac{x_J^2 \vec{p}_{i,k}^{\,2}}{x_{i,k}^2 \vec{p}_J^{\,2}}\,. \tag{3.182}$$

Introducing the variable

$$\vec{\Delta}_{ik} = \frac{x_i \vec{p}_k - x_k \vec{p}_i}{x_i + x_k}\,, \tag{3.183}$$

which approaches 0 when the partons are collinear, expanding Eq. (3.182) in terms of $\vec{\Delta}_{ik}$, we get the condition for the partons to be inside the cone :

$$\vec{\Delta}_{ik}^2 < R^2 \min\left(\frac{x_i^2}{x_J^2}, \frac{x_k^2}{x_J^2}\right) \vec{p}_J^{\,2}\,. \tag{3.184}$$

We are now studying the exclusive production of dijets, thus there are only two kinds of contributions : either one of the jets contains two of the produced partons, or the gluon is too soft to be detected. Let us now focus on the first kind of contributions.

First let us note that any non-collinearly divergent diagram will be subdominant in terms of the R expansion. Indeed the way we will obtain the first kind of contribution is the following : if particles i and j constitute the first jet J and particle k constitutes the second jet K, we will make the following change of variables :

$$dx_i dx_j dx_k d^d\vec{p}_i d^d\vec{p}_j d^d\vec{p}_k \quad \to \quad dx_i d^d\vec{\Delta}_{ij} \left(dx_J d^d\vec{p}_J dx_K d^d\vec{p}_K\right)\,, \tag{3.185}$$

$$\left(x_J,\, \vec{p}_J,\, x_K,\, \vec{p}_K,\, \vec{\Delta}_{ij}\right) \quad \equiv \quad \left(x_i + x_j,\, \vec{p}_i + \vec{p}_j,\, x_k,\, \vec{p}_k,\, \frac{x_i}{x_J}\vec{p}_j - \frac{x_j}{x_J}\vec{p}_i\right)\,. \tag{3.186}$$

The Jacobian for this transformation is 1. The condition for particles i and j to be in the cone of J in Eq. (3.184) will restrict the integration w.r.t. $\vec{\Delta}_{ij}$, so what one gets will have the form :

$$\left(\Phi^{\alpha}_{n_1} \Phi^{\beta *}_{n_2}\right) \propto \int d^d\vec{\Delta}_{ij}\theta \left[R^2 \min\left(\frac{x_i^2}{x_J^2}, \frac{x_j^2}{x_J^2}\right) \vec{p}_J^{\,2} - \vec{\Delta}_{ij}^2\right] \left[F^{\alpha\beta}_{n_1 n_2}(\vec{\Delta}_{ij})\right]\,. \tag{3.187}$$

The generic function F will then be expanded around $\vec{\Delta}_{ij} = \vec{0}$ by writing

$$F^{\alpha\beta}_{n_1 n_2}(\vec{\Delta}_{ij}) \equiv \frac{\left[F^{\alpha\beta}_{n_1 n_2}(\vec{\Delta}_{ij})\right]_{col}}{\vec{\Delta}_{ij}^2} + \left[F^{\alpha\beta}_{n_1 n_2}(\vec{\Delta}_{ij})\right]_0 + O(\vec{\Delta}_{ij}). \tag{3.188}$$

Then the integral becomes :

$$\left(\Phi^{\alpha}_{n_1} \Phi^{\beta *}_{n_2}\right) \propto \frac{2\pi^{\frac{d}{2}}}{\Gamma\left(\frac{d}{2}\right)} \left[\frac{\left[F^{\alpha\beta}_{n_1 n_2}(\vec{\Delta}_{ij})\right]_{col}}{d-2} + \frac{\left[F^{\alpha\beta}_{n_1 n_2}(\vec{\Delta}_{ij})\right]_0}{d} \min\left(\frac{x_i^2}{x_J^2}, \frac{x_j^2}{x_J^2}\right) \vec{p}_J^{\,2} R^2\right] \left[R^2 \min\left(\frac{x_i^2}{x_J^2}, \frac{x_j^2}{x_J^2}\right) \vec{p}_J^{\,2}\right]^{\frac{d}{2}-1} \tag{3.189}$$

Thus the diagram combinations with $\left(F^{\alpha\beta}_{n_1 n_2}\right)_{col} = 0$ are always suppressed by a factor R^2.

3.8.1 Jet cone algorithm and the soft and collinear divergence

To clarify how the cone algorithm allows one to cancel the soft and collinear divergence for our process, let us consider a more general algorithm. Let us define a jet distribution $\mathcal{J}\left(p_J,\, p_K\right)$, where p_J and p_K are the jet momenta. The cross section for the production of jets can be written as the convolution of the jet distribution and the differential cross section for the production of partons. For example when the first jet is made of a gluon and a quark, we can write

$$d\sigma^{(qg,\,\bar{q})}_{jets} \quad = \quad \int dx_q dx_{\bar{q}} dx_g d^d\vec{p}_q d^d\vec{p}_{\bar{q}} d^d\vec{p}_g \mathcal{J}\left(p_q + p_g,\, p_{\bar{q}}\right) d\sigma_{partons}\left(p_q,\, p_{\bar{q}},\, p_g\right)\,. \tag{3.190}$$

Let us define Ω_q and $\Omega_{\bar{q}}$ the areas of integration w.r.t. p_g where the gluon is collinear respectively to the quark or the antiquark, and Ω_s the area of integration where the gluon is soft. Then the jet cross section

can be rewritten using the simple remark $\Omega_s \cap \overline{\Omega_q} \cap \overline{\Omega_{\bar{q}}} = \Omega_s \setminus ((\Omega_s \cap \Omega_q) \cup (\Omega_s \cap \Omega_{\bar{q}}))$:

$$\begin{aligned} d\sigma_{jets} = & \int dx_q dx_{\bar{q}} d^d\vec{p}_q d^d\vec{p}_{\bar{q}} \left\{ \int_{\Omega_q} dx_g d^d\vec{p}_g \left[\mathcal{J}\left(p_q + p_g,\, p_{\bar{q}}\right) + \mathcal{J}\left(p_{\bar{q}},\, p_q + p_g\right)\right] \right. \\ & + \int_{\Omega_{\bar{q}}} dx_g d^d\vec{p}_g \left[\mathcal{J}\left(p_q,\, p_{\bar{q}} + p_g\right) + \mathcal{J}\left(p_{\bar{q}} + p_g,\, p_q\right)\right] \\ & \left. + \int_{\Omega_s \cap \overline{\Omega_q} \cap \overline{\Omega_{\bar{q}}}} dx_g d^d\vec{p}_g \left[\mathcal{J}\left(p_q,\, p_{\bar{q}}\right) + \mathcal{J}\left(p_{\bar{q}},\, p_q\right)\right] \right\} d\sigma_{partons}\left(p_q,\, p_{\bar{q}},\, p_g\right) . \end{aligned} \tag{3.191}$$

$$\begin{aligned} = & \int dx_q dx_{\bar{q}} d^d\vec{p}_q d^d\vec{p}_{\bar{q}}\, d\sigma_{partons}\left(p_q,\, p_{\bar{q}},\, p_g\right) \left\{ \int_{\Omega_s} dx_g d^d\vec{p}_g \left[\mathcal{J}\left(p_q,\, p_{\bar{q}}\right) + \mathcal{J}\left(p_{\bar{q}},\, p_q\right)\right] \right. \\ & + \int_{\Omega_q} dx_g d^d\vec{p}_g \left[\mathcal{J}\left(p_q + p_g,\, p_{\bar{q}}\right) - \theta(p_g \in \Omega_s)\mathcal{J}\left(p_q,\, p_{\bar{q}}\right) + \mathcal{J}\left(p_{\bar{q}},\, p_q + p_g\right) - \theta(p_g \in \Omega_s)\mathcal{J}\left(p_{\bar{q}},\, p_q\right)\right] \\ & \left. + \int_{\Omega_{\bar{q}}} dx_g d^d\vec{p}_g \left[\mathcal{J}\left(p_q,\, p_{\bar{q}} + p_g\right) - \theta(p_g \in \Omega_s)\mathcal{J}\left(p_q,\, p_{\bar{q}}\right) + \mathcal{J}\left(p_{\bar{q}} + p_g,\, p_q\right) - \theta(p_g \in \Omega_s)\mathcal{J}\left(p_{\bar{q}},\, p_q\right)\right] \right\} . \end{aligned} \tag{3.192}$$

One can now easily see that the divergence arising when the gluon is both soft and collinear to the quark or the antiquark is canceled by the use of the jet algorithm through the cancellation of terms like $\mathcal{J}\left(p_q + p_g,\, p_{\bar{q}}\right) - \theta(p_g \in \Omega_s)\mathcal{J}\left(p_q,\, p_{\bar{q}}\right)$ in the soft limit. We will show this cancellation explicitely in the following pages in our formalism.

3.8.2 Preliminary remark

To obtain the $\gamma^* P \to 2jets\, P'$ cross section from the $\gamma^* P \to q\bar{q}\, P'$ cross section, one only have to make the change of variables $(p_q,\, p_{\bar{q}}) \to (p_J,\, p_K)$, where p_J and p_K are the jet momenta, and then apply the $(J \leftrightarrow K)$ symmetry.

We will show in the following pages that the divergent terms in the real part only arise from the square of $\tilde{\Phi}_3^{\alpha}$. However for completeness we computed all the contributions to the cross section from the real diagrams. Such contributions can be used to go beyond the small cone approximation in our computation, or to compute other cross sections, e.g. for the exclusive production of a trijet among other possibilities. Obtaining the squared real part is a fastidious but straightforward task. It can be done with the massive use of the following remark :

$$\mathrm{Tr}\left(\gamma^{n_1}\gamma^{n_2}...\gamma^{n_p}\right) = g^{n_1 n_2}\mathrm{Tr}\left(\gamma^{n_3}...\gamma^{n_p}\right) - g^{n_1 n_3}\mathrm{Tr}\left(\gamma^{n_2}\gamma^{n_4}...\gamma^{n_p}\right) + ... + g^{n_1 n_p}\mathrm{Tr}\left(\gamma^{n_2}\gamma^{n_3}...\gamma^{n_{p-1}}\right) . \tag{3.193}$$

Given that $g^{++} = g^{+i} = g^{--} = g^{-i} = 0$ and that all the outgoing partons are on-shell and the t-channel momenta are purely transverse, most of the terms in the right-hand side of Eq. (3.193) will cancel until everything is reduced to a sum of traces of 4 and 6 transverse gamma matrices. Then those are taken explicitely and recombined. In this work, this task was done by hand then checked using FeynCalc to compute the exclusively transverse traces. Independently, it was computed using Mathematica and it was checked that all the results coincide. All the expressions for the traces are in Appendix A.2 of this thesis, but in this part we will need the expressions for the square of $\tilde{\Phi}_3^{\alpha}$, which are given below :

$$\begin{aligned} & \sum_{\lambda_q,\, \lambda_{\bar{q}},\, s_g} \left[\tilde{\Phi}_3^{+}\left(\vec{p}_1,\, \vec{p}_2\right) \tilde{\Phi}_3^{+*}\left(\vec{p}_{1'},\, \vec{p}_{2'}\right)\right] \\ & = \frac{8 x_q x_{\bar{q}} \left(p_\gamma^+\right)^4 \left(dx_g^2 + 4x_q\left(x_q + x_g\right)\right)}{\left(x_q + x_g\right)^2 \left(Q^2 + \frac{\vec{p}_{\bar{q}2}^{\,2}}{x_{\bar{q}}(1-x_{\bar{q}})}\right)\left(Q^2 + \frac{\vec{p}_{\bar{q}2'}^{\,2}}{x_{\bar{q}}(1-x_{\bar{q}})}\right)\vec{\Delta}_{qg}^2} \\ & - \frac{8 x_q x_{\bar{q}} \left(p_\gamma^+\right)^4 \left(2x_g - dx_g^2 + 4x_q x_{\bar{q}}\right)}{\left(x_q + x_g\right)\left(x_{\bar{q}} + x_g\right)\left(Q^2 + \frac{\vec{p}_{\bar{q}2'}^{\,2}}{x_{\bar{q}}(1-x_{\bar{q}})}\right)\left(Q^2 + \frac{\vec{p}_{q1}^{\,2}}{x_q(1-x_q)}\right)} \left(\frac{\vec{\Delta}_{qg}\cdot\vec{\Delta}_{\bar{q}g}}{\vec{\Delta}_{qg}^2\vec{\Delta}_{\bar{q}g}^2}\right) + \left(q \leftrightarrow \bar{q}\right), \end{aligned} \tag{3.194}$$

$$\sum_{\lambda_q,\,\lambda_{\bar q},\,s_g}\left[\tilde\Phi_3^i\left(\vec p_1,\,\vec p_2\right)\tilde\Phi_3^{+*}\left(\vec p_{1'},\,\vec p_{2'}\right)\right] \tag{3.195}$$
$$=\frac{4x_q\left(p_\gamma^+\right)^3}{\left(x_q+x_g\right)^2\left(x_{\bar q}+x_g\right)\left(Q^2+\frac{\vec p_{\bar q2}^{\,2}}{x_{\bar q}(1-x_{\bar q})}\right)\left(Q^2+\frac{\vec p_{q1'}^{\,2}}{x_q(1-x_q)}\right)}\left(\frac{\Delta_{qg\perp\mu}\Delta_{\bar qg\perp\nu}}{\vec\Delta_{qg}^2\vec\Delta_{\bar qg}^2}\right)$$
$$\times\left[x_g\left(4x_{\bar q}+x_gd-2\right)\left(p_{\bar q2\perp}^\mu g_\perp^{i\nu}-p_{\bar q2\perp}^\nu g_\perp^{\mu i}\right)-\left(2x_{\bar q}-1\right)\left(4x_qx_{\bar q}+x_g(2-x_gd)\right)g_\perp^{\mu\nu}p_{\bar q2\perp}^i\right]$$
$$-\frac{4x_q\left(p_\gamma^+\right)^3\left(2x_{\bar q}-1\right)\left(x_g^2d+4x_q\left(x_q+x_g\right)\right)p_{\bar q2\perp}^i}{\left(x_q+x_g\right)^3\left(Q^2+\frac{\vec p_{\bar q2}^{\,2}}{x_{\bar q}(1-x_{\bar q})}\right)\left(Q^2+\frac{\vec p_{\bar q2'}^{\,2}}{x_{\bar q}(1-x_{\bar q})}\right)\vec\Delta_{qg}^2}+\left(q\leftrightarrow\bar q\right),$$

and finally

$$\sum_{\lambda_q,\,\lambda_{\bar q},\,s_g}\left[\tilde\Phi_3^i\left(\vec p_1,\,\vec p_2\right)\tilde\Phi_3^{k*}\left(\vec p_{1'},\,\vec p_{2'}\right)\right] \tag{3.196}$$
$$=\frac{-2\left(p_\gamma^+\right)^2}{\left(x_q+x_g\right)^2\left(x_{\bar q}+x_g\right)^2\left(Q^2+\frac{\vec p_{\bar q2}^{\,2}}{x_{\bar q}(1-x_{\bar q})}\right)\left(Q^2+\frac{\vec p_{q1'}^{\,2}}{x_q(1-x_q)}\right)}\left(\frac{\Delta_{qg\perp\mu}\Delta_{\bar qg\perp\nu}}{\vec\Delta_{qg}^2\vec\Delta_{\bar qg}^2}\right)\{x_g((d-4)x_g-2)$$
$$\times\left[p_{q1'\perp}^\nu\left(p_{\bar q2\perp}^\mu g_\perp^{ik}+p_{\bar q2\perp}^k g_\perp^{\mu i}\right)+g_\perp^{\mu\nu}\left((\vec p_{q1'}\cdot\vec p_{\bar q2})g_\perp^{ik}+p_{q1'\perp}^i p_{\bar q2\perp}^k\right)\right.$$
$$\left.-\,g_\perp^{\nu k}p_{q1'\perp}^i p_{\bar q2\perp}^\mu-g_\perp^{\mu i}g_\perp^{\nu k}(\vec p_{q1'}\cdot\vec p_{\bar q2})\right]-g_\perp^{\mu\nu}$$
$$\times\left[(2x_q-1)\left(2x_{\bar q}-1\right)p_{q1'\perp}^k p_{\bar q2\perp}^i\left(4x_qx_{\bar q}+x_g(2-x_gd)\right)+4x_qx_{\bar q}\left((\vec p_{q1'}\cdot\vec p_{\bar q2})g_\perp^{ik}+p_{q1'\perp}^i p_{\bar q2\perp}^k\right)\right]$$
$$+\left(p_{q1'\perp}^\mu p_{\bar q2\perp}^\nu g_\perp^{ik}-p_{q1'\perp}^\mu p_{\bar q2\perp}^k g_\perp^{\nu i}-p_{q1'\perp}^i p_{\bar q2\perp}^\nu g_\perp^{\mu k}-g_\perp^{\mu k}g_\perp^{\nu i}(\vec p_{q1'}\cdot\vec p_{\bar q2})\right)$$
$$\times x_g((d-4)x_g+2)+x_g\left(2x_{\bar q}-1\right)\left(x_gd+4x_q-2\right)\left(g_\perp^{\mu k}p_{q1'\perp}^\nu-g_\perp^{\nu k}p_{q1'\perp}^\mu\right)p_{\bar q2\perp}^i$$
$$+\,x_g\left(2x_q-1\right)p_{q1'\perp}^k\left(4x_{\bar q}+x_gd-2\right)\left(g_\perp^{\nu i}p_{\bar q2\perp}^\mu-g_\perp^{\mu i}p_{\bar q2\perp}^\nu\right)\Big\}$$
$$-\frac{2x_q\left(p_\gamma^+\right)^2\left(x_g^2d+4x_q\left(x_q+x_g\right)\right)\left((\vec p_{\bar q2}\cdot\vec p_{\bar q2'})g_\perp^{ik}-\left(1-2x_{\bar q}\right)^2p_{\bar q2\perp}^i p_{\bar q2'\perp}^k+p_{\bar q2'\perp}^i p_{\bar q2\perp}^k\right)}{x_{\bar q}\left(x_q+x_g\right)^4\left(Q^2+\frac{\vec p_{\bar q2}^{\,2}}{x_{\bar q}(1-x_{\bar q})}\right)\left(Q^2+\frac{\vec p_{\bar q2'}^{\,2}}{x_{\bar q}(1-x_{\bar q})}\right)\vec\Delta_{qg}^2}+\left(q\leftrightarrow\bar q\right).$$

3.8.3 Collinear contribution

Considering expressions (3.121), (3.122), (3.124), and (3.125) for the impact factors and the remark in (3.189) one can now see that only the square of diagrams without the gluon crossing the shockwave will contribute in the small cone approximation. Indeed if the gluon is collinear to the emitter before they both cross the shockwave, the interaction with the shockwave will spoil their collinearity before the gluon is reabsorbed. The diagrams giving the first kind of real contributions to the cross section will thus be the ones in Fig. 3.14.

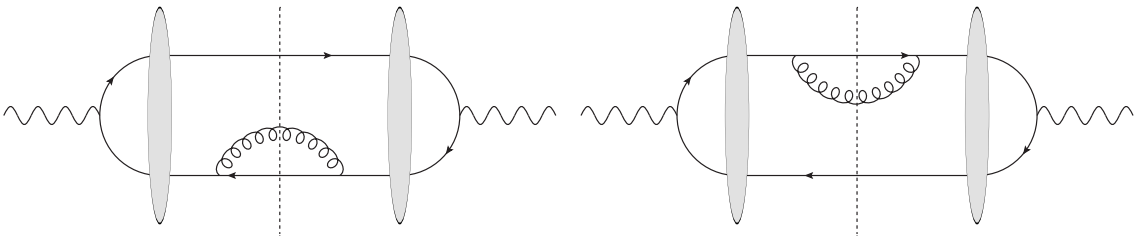

Figure 3.14: Small-R contributions to the cross section

Additionally the contribution where the gluon constitutes a jet by itself and the quark-antiquark pair constitutes the second jet, as in Fig. 3.15, is also suppressed since it is not collinearly divergent.

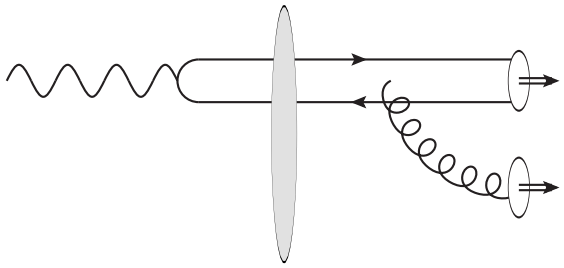

Figure 3.15: R-suppressed contribution

When the first jet J is formed by the quark and the gluon and the second jet K is formed by the antiquark, using the jet variables (3.185) and the small cone limit the collinearly divergent squared impact factor reads :

$$\sum_{\lambda_q,\,\lambda_{\bar{q}},\,s_g}\left[\tilde{\Phi}_3^{+}\left(\vec{p}_1,\,\vec{p}_2\right)\tilde{\Phi}_3^{+*}\left(\vec{p}_{1'},\,\vec{p}_{2'}\right)\right]_{col}\to\frac{8x_K\left(p_\gamma^+\right)^4\left(x_J-x_g\right)\left[x_g^2 d+4\left(x_J-x_g\right)x_J\right]}{x_J^2\left(Q^2+\frac{\vec{p}_{K2}^{\,2}}{x_J x_K}\right)\left(Q^2+\frac{\vec{p}_{K2'}^{\,2}}{x_J x_K}\right)\vec{\Delta}_{qg}^2}\,, \tag{3.197}$$

$$\sum_{\lambda_q,\,\lambda_{\bar{q}},\,s_g}\left[\tilde{\Phi}_3^{i}\left(\vec{p}_1,\,\vec{p}_2\right)\tilde{\Phi}_3^{+*}\left(\vec{p}_{1'},\,\vec{p}_{2'}\right)\right]_{col}=\frac{4\left(x_J-x_K\right)\left(p_\gamma^+\right)^3 p_{K2\perp}^{i}\left(x_J-x_g\right)\left[x_g^2 d+4\left(x_J-x_g\right)x_J\right]}{x_J^3\left(Q^2+\frac{\vec{p}_{K2}^{\,2}}{x_J x_K}\right)\left(Q^2+\frac{\vec{p}_{K2'}^{\,2}}{x_J x_K}\right)\vec{\Delta}_{qg}^2}\,, \tag{3.198}$$

and

$$\sum_{\lambda_q,\,\lambda_{\bar{q}},\,s_g}\left[\tilde{\Phi}_3^{i}\left(\vec{p}_1,\,\vec{p}_2\right)\tilde{\Phi}_3^{k*}\left(\vec{p}_{1'},\,\vec{p}_{2'}\right)\right]_{col} \tag{3.199}$$

$$=-\frac{2\left(p_\gamma^+\right)^2\left[\left(\vec{p}_{K2}\cdot\vec{p}_{K2'}\right)g_\perp^{ik}-\left(x_J-x_K\right)^2 p_{K2\perp}^{i}p_{K2'\perp}^{k}+p_{K2'\perp}^{i}p_{K2\perp}^{k}\right]\left(x_J-x_g\right)\left[x_g^2 d+4\left(x_J-x_g\right)x_J\right]}{x_K x_J^4\left(Q^2+\frac{\vec{p}_{K2}^{\,2}}{x_J x_K}\right)\left(Q^2+\frac{\vec{p}_{K2'}^{\,2}}{x_J x_K}\right)\vec{\Delta}_{qg}^2}\,.$$

The other contributions can be obtained by the $(q\leftrightarrow\bar{q})$ and $(J\leftrightarrow K)$ symmetries. It is easy to see that the LO contribution can can be factorized in these results, as follows :

$$\sum_{\lambda_q,\,\lambda_{\bar{q}},\,s_g}\left[\tilde{\Phi}_3^{\alpha}\left(\vec{p}_1,\,\vec{p}_2\right)\tilde{\Phi}_3^{\beta*}\left(\vec{p}_{1'},\,\vec{p}_{2'}\right)\right]_{col}=\frac{\left(x_J-x_g\right)\left[x_g^2 d+4\left(x_J-x_g\right)x_J\right]}{4x_J^3\vec{\Delta}_{qg}^2}\sum_{helicities}\Phi_0^{\alpha}(\vec{p}_1,\,\vec{p}_2)\Phi_0^{\alpha}(\vec{p}_{1'},\,\vec{p}_{2'})\,. \tag{3.200}$$

Adding the phase space factors and integrating, one obtains :

$$d\sigma'_{3JI}|_{\rm col}=\alpha_s\frac{\Gamma(1-\epsilon)}{(4\pi)^{1+\epsilon}}\left(\frac{N_c^2-1}{2N_c}\right)\left(n_J+n_K\right)d\sigma'_{0JI}\,, \tag{3.201}$$

where n_J is proportional to the "number of jets in the quark" :

$$\begin{aligned}n_J&\equiv\frac{(4\pi)^{1+\epsilon}}{\Gamma(1-\epsilon)}\int_\alpha^{x_J}\frac{dx_g}{2x_g}\int_{\vec{\Delta}_{qg}^{\,2}<\frac{R^2\vec{p}_J^{\,2}}{x_J^2}\min(x_g^2,(x_J-x_g)^2)}\frac{d^d\vec{\Delta}_{qg}}{(2\pi)^d}\frac{\mu^{-2\epsilon}}{2p_J^+2p_q^+}\frac{tr(\hat{p}_q\gamma^\mu\hat{p}_J\gamma^\nu)d_{\mu\nu}(p_g)}{(p_q^-+p_g^-p_J^-)^2}\\&=4\int_\alpha^{x_J}\frac{x_J dx_g}{x_g(x_J-x_g)}\frac{\mu^{-2\epsilon}}{\Gamma(1-\epsilon)\pi^{\frac{d}{2}}}\int_{\vec{\Delta}_{qg}^{\,2}<\frac{R^2\vec{p}_J^{\,2}}{x_J^2}\min(x_g^2,(x_J-x_g)^2)}d^d\vec{\Delta}_{qg}\\&\times\frac{1}{4}\frac{\left(x_J-x_g\right)\left[x_g^2 d+4x_J\left(x_J-x_g\right)\right]}{x_J^3\vec{\Delta}_{qg}^2}\,.\end{aligned} \tag{3.202}$$

n_K is obtained through the $(J\leftrightarrow K)$ symmetry. After a straightforward integration, one can show :

$$\begin{aligned}n_J+n_K=4\Bigg[&\left\{\ln\left(\frac{x_J x_K}{\alpha^2}\right)-\frac{3}{2}\right\}\left\{\frac{1}{2}\ln\left(\frac{R^4\vec{p}_J^{\,2}\vec{p}_K^{\,2}}{\mu^4}\right)+\frac{1}{\epsilon}\right\}\\&-\frac{1}{2}\ln^2\left(\frac{x_J x_K}{\alpha^2}\right)+\frac{1}{2}\ln\left(\frac{x_J}{x_K}\right)\ln\left(\frac{x_K\vec{p}_J^{\,2}}{x_J\vec{p}_K^{\,2}}\right)-\frac{\pi^2}{3}+\frac{7}{2}+\ln(8)\Bigg]\,.\end{aligned} \tag{3.203}$$

3.8.4 Soft contribution

Similarly to the collinear divergence, the soft divergence arises from the diagrams where the gluon is emitted after the $z^+ = 0$ line. Indeed if a soft gluon is emitted before the shockwave, its energy is not sufficient for it to reach the $z^+ = 0$ before being reabsorbed. Thus such a contribution belongs to the virtual dipole term. Hence the real diagrams contributing to the soft divergence are those in Fig. 3.16.

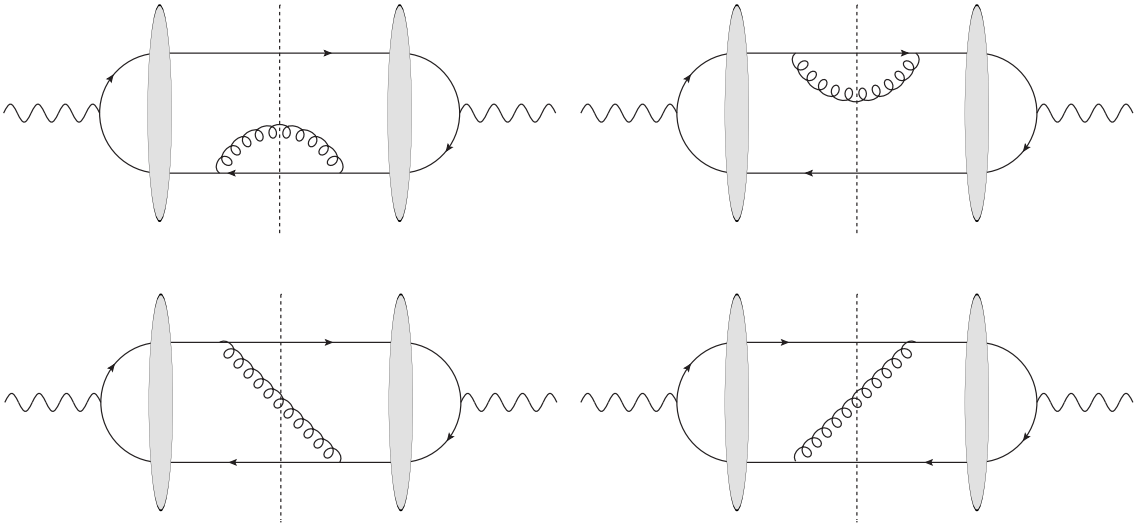

Figure 3.16: Soft contribution to the cross section

The soft limit can be taken by writing

$$p_g = x_g u\,, \tag{3.204}$$

where u is of order unity and $|x_g| \ll x_q,\, x_{\bar{q}}$ is small. Then Eqs. (3.194), (3.195) and (3.196) become respectively :

$$\sum_{\lambda_q,\,\lambda_{\bar{q}},\,s_g} \left[\tilde{\Phi}_3^{+}\left(\vec{p}_1,\,\vec{p}_2\right)\tilde{\Phi}_3^{+*}\left(\vec{p}_{1'},\,\vec{p}_{2'}\right)\right] \tag{3.205}$$

$$= \frac{32 x_J x_K \left(p_\gamma^+\right)^4}{\left(Q^2+\frac{\vec{p}_{K2}^{\,2}}{x_J x_K}\right)\left(Q^2+\frac{\vec{p}_{K2'}^{\,2}}{x_J x_K}\right)} \frac{\left(\frac{\vec{p}_J}{x_J}-\frac{\vec{p}_K}{x_K}\right)^2}{x_g^2\left(\vec{u}-\frac{\vec{p}_J}{x_J}\right)^2\left(\vec{u}-\frac{\vec{p}_K}{x_K}\right)^2}\,,$$

$$\sum_{\lambda_q,\,\lambda_{\bar{q}},\,s_g} \left[\tilde{\Phi}_3^{i}\left(\vec{p}_1,\,\vec{p}_2\right)\tilde{\Phi}_3^{+*}\left(\vec{p}_{1'},\,\vec{p}_{2'}\right)\right] \tag{3.206}$$

$$= \frac{16\left(x_J - x_K\right)\left(p_\gamma^+\right)^3 p_{K2\perp}^i}{\left(Q^2+\frac{\vec{p}_{K2}^{\,2}}{x_J x_K}\right)\left(Q^2+\frac{\vec{p}_{K2'}^{\,2}}{x_J x_K}\right)} \frac{\left(\frac{\vec{p}_J}{x_J}-\frac{\vec{p}_K}{x_K}\right)^2}{x_g^2\left(\vec{u}-\frac{\vec{p}_J}{x_J}\right)^2\left(\vec{u}-\frac{\vec{p}_K}{x_K}\right)^2}\,,$$

and

$$\sum_{\lambda_q,\,\lambda_{\bar{q}},\,s_g} \left[\tilde{\Phi}_3^{i}\left(\vec{p}_1,\,\vec{p}_2\right)\tilde{\Phi}_3^{k*}\left(\vec{p}_{1'},\,\vec{p}_{2'}\right)\right] \tag{3.207}$$

$$= -\frac{8\left(p_\gamma^+\right)^2\left[\left(\vec{p}_{K2}\cdot\vec{p}_{K2'}\right)g_\perp^{ik} - \left(x_J - x_K\right)^2 p_{K2\perp}^i p_{K2'\perp}^k + p_{K2'\perp}^i p_{K2\perp}^k\right]}{x_J x_K\left(Q^2+\frac{\vec{p}_{K2}^{\,2}}{x_J x_K}\right)\left(Q^2+\frac{\vec{p}_{K2'}^{\,2}}{x_J x_K}\right)} \frac{\left(\frac{\vec{p}_J}{x_J}-\frac{\vec{p}_K}{x_K}\right)^2}{x_g^2\left(\vec{u}-\frac{\vec{p}_J}{x_J}\right)^2\left(\vec{u}-\frac{\vec{p}_K}{x_K}\right)^2}\,.$$

It is now easy to extract the leading order cross section by writing :

$$\sum_{\lambda_q,\,\lambda_{\bar{q}},\,s_g} \left[\tilde{\Phi}_3^{\alpha}\left(\vec{p}_1,\,\vec{p}_2\right)\tilde{\Phi}_3^{\beta*}\left(\vec{p}_{1'},\,\vec{p}_{2'}\right)\right] = \frac{\left(\frac{\vec{p}_J}{x_J}-\frac{\vec{p}_K}{x_K}\right)^2}{x_g^2\left(\vec{u}-\frac{\vec{p}_J}{x_J}\right)^2\left(\vec{u}-\frac{\vec{p}_K}{x_K}\right)^2} \sum_{helicities} \Phi_0^{\alpha}(\vec{p}_1,\,\vec{p}_2)\Phi_0^{\beta}(\vec{p}_{1'},\,\vec{p}_{2'})\,. \tag{3.208}$$

By adding the phase space factors, one can then rewrite the soft cross section as :

$$d\sigma'_{3JI}|_{soft} = d\sigma'_{0JI}\alpha_s \frac{N_c^2-1}{2N_c}\frac{\Gamma(1-\epsilon)}{(4\pi)^{1+\epsilon}} S, \quad S \equiv \frac{(4\pi)^{1+\epsilon}}{\Gamma(1-\epsilon)} \int dx_g \left(x_g^{d-3}\right) \int \frac{d^d\vec{u}}{(2\pi)^d} \frac{4\left(\frac{\vec{p}_J}{x_J}-\frac{\vec{p}_K}{x_K}\right)^2}{\left(\vec{u}-\frac{\vec{p}_J}{x_J}\right)^2\left(\vec{u}-\frac{\vec{p}_K}{x_K}\right)^2}, \tag{3.209}$$

or with a more explicit physical meaning :

$$S \equiv \frac{(4\pi)^{1+\epsilon}}{\Gamma(1-\epsilon)} \int \left|\frac{p_q^\mu}{(p_q\cdot p_g)} - \frac{p_{\bar{q}}^\mu}{(p_{\bar{q}}\cdot p_g)}\right|^2 \frac{dx_g}{x_g}\frac{d^d\vec{p}_g}{(2\pi)^d}.$$

To describe an exclusive quantity, we need to introduce an energy resolution E and integrate out the gluons with an energy too small for it to be detected. Thus the soft gluon integration region consists in :

$$\omega_g = \frac{1}{2}\left(p_g^+ + p_g^-\right) < E \ll p_\gamma^+, \tag{3.210}$$

so that

$$x_g\left(1+\frac{\vec{u}^{\,2}}{(p_\gamma^+)^2}\right) < \frac{2E}{p_\gamma^+} \ll 1. \tag{3.211}$$

Thus :

$$S = \int_\alpha^{\frac{2E}{p_\gamma^+}} dx_g \left(x_g^{d-3}\right) \int_{\vec{u}^{\,2}<(p_\gamma^+)^2(\frac{2E}{x_g p_\gamma^+}-1)} \frac{\mu^{-2\epsilon}d^d\vec{u}}{\Gamma(1-\epsilon)\pi^{\frac{d}{2}}} \frac{4\left(\frac{\vec{p}_J}{x_J}-\frac{\vec{p}_K}{x_K}\right)^2}{\left(\vec{u}-\frac{\vec{p}_J}{x_J}\right)^2\left(\vec{u}-\frac{\vec{p}_K}{x_K}\right)^2}. \tag{3.212}$$

We have restored the rapidity cutoff α which will of course play a role to regularize the soft divergence. However, in the sum $n_J + n_K + S$ the region with a gluon both soft and collinear to the quark or to the antiquark is calculated twice. To avoid double counting we restrict the integration in S so that the gluons sit outside the cones (3.184). The integration region then reads

$$\Omega = \left\{\vec{u}^{\,2} < (p_\gamma^+)^2\left(\frac{2E}{x_g p_\gamma^+}-1\right)\right\} \cap \Omega_{nc}, \tag{3.213}$$

$$\Omega_{nc} \equiv \left\{\left(\vec{u}-\frac{\vec{p}_J}{x_J}\right)^2 > \frac{R^2\vec{p}_J^{\,2}}{x_J^2}\right\} \cap \left\{\left(\vec{u}-\frac{\vec{p}_K}{x_K}\right)^2 > \frac{R^2\vec{p}_K^{\,2}}{x_K^2}\right\}. \tag{3.214}$$

Let us denote S' the new definition of S with this integration area :

$$\begin{aligned} S' &\equiv 4\int_\alpha^{\frac{2E}{p_\gamma^+}} \frac{dx_g}{x_g}\int_\Omega \frac{d\vec{u}}{\pi} \frac{4\left(\frac{\vec{p}_J}{x_J}-\frac{\vec{p}_K}{x_K}\right)^2}{\left(\vec{u}-\frac{\vec{p}_J}{x_J}\right)^2\left(\vec{u}-\frac{\vec{p}_K}{x_K}\right)^2} \\ &= 4\int_\alpha^{\frac{2E}{p_\gamma^+}} \frac{dx_g}{x_g}\int_{\Omega_{nc}} \frac{d\vec{u}}{\pi} \frac{4\left(\frac{\vec{p}_J}{x_J}-\frac{\vec{p}_K}{x_K}\right)^2}{\left(\vec{u}-\frac{\vec{p}_J}{x_J}\right)^2\left(\vec{u}-\frac{\vec{p}_K}{x_K}\right)^2} + 4\,I(R,E) \\ &= 4\ln\left(\frac{2E}{\alpha p_\gamma^+}\right)\ln\left(\frac{(\vec{p}_J x_K - x_J\vec{p}_K)^4}{(R^2\vec{p}_J^{\,2}x_J^2)(R^2\vec{p}_K^{\,2}x_K^2)}\right) + 4\,I(R,E), \end{aligned} \tag{3.215}$$

where we defined

$$I(R,E) \equiv -\int_0^{\frac{2E}{p_\gamma^+}} \frac{dx_g}{x_g}\int_{\{\vec{u}^{\,2}>(p_\gamma^+)^2(\frac{2E}{x_g p_\gamma^+}-1)\}\cap\Omega_{nc}} \frac{d\vec{u}}{\pi} \frac{\left(\frac{\vec{p}_J}{x_J}-\frac{\vec{p}_K}{x_K}\right)^2}{\left(\vec{u}-\frac{\vec{p}_J}{x_J}\right)^2\left(\vec{u}-\frac{\vec{p}_K}{x_K}\right)^2}. \tag{3.216}$$

The integral $I(R,E)$ is convergent and depends neither on α nor on ϵ. In Appendix A.3, we show that this integral gives a contribution which is suppressed by a factor $1/s$. Finally,

$$S' = 4\ln\left(\frac{2E}{\alpha p_\gamma^+}\right)\ln\left(\frac{(\vec{p}_J x_K - x_J\vec{p}_K)^4}{(R^2\vec{p}_J^{\,2}x_J^2)(R^2\vec{p}_K^{\,2}x_K^2)}\right). \tag{3.217}$$

Combining Eqs. (3.203) and (3.217) we have

$$\begin{aligned} S' + n_J + n_K = \; & 2\left[\ln\left(\frac{(x_K\vec{p}_J - x_J\vec{p}_K)^4}{x_J^2 x_K^2 R^4 \vec{p}_J^{\,2}\vec{p}_K^{\,2}}\right)\ln\left(\frac{4E^2}{x_J x_K (p_\gamma^+)^2}\right)\right. \\ & + 2\ln\left(\frac{x_J x_K}{\alpha^2}\right)\left(\frac{1}{\epsilon} - \ln\left(\frac{x_J x_K \mu^2}{(x_K\vec{p}_J - x_J\vec{p}_K)^2}\right)\right) - \ln^2\left(\frac{x_J x_K}{\alpha^2}\right) \\ & \left. + \frac{3}{2}\ln\left(\frac{16\mu^4}{R^4\vec{p}_J^{\,2}\vec{p}_K^{\,2}}\right) - \ln\left(\frac{x_J}{x_K}\right)\ln\left(\frac{x_J\vec{p}_K^{\,2}}{x_K\vec{p}_J^{\,2}}\right) - \frac{3}{\epsilon} - \frac{2\pi^2}{3} + 7\right]. \end{aligned} \tag{3.218}$$

Adding the singular part of the virtual correction (3.88), one finally cancels the $\ln\alpha$ and $\frac{1}{\epsilon}$ divergences and gets :

$$\begin{aligned} S_R = S' + n_J + n_K + S_V + S_V^* = 4\left[\frac{1}{2}\ln\left(\frac{(x_K\vec{p}_J - x_J\vec{p}_K)^4}{x_J^2 x_K^2 R^4 \vec{p}_K^{\,2}\vec{p}_J^{\,2}}\right)\left(\ln\left(\frac{4E^2}{x_J x_K (p_\gamma^+)^2}\right) + \frac{3}{2}\right)\right. \\ \left. + \ln(8) - \frac{1}{2}\ln\left(\frac{x_J}{x_K}\right)\ln\left(\frac{x_J\vec{p}_K^{\,2}}{x_K\vec{p}_J^{\,2}}\right) + \frac{13-\pi^2}{2}\right]. \end{aligned} \tag{3.219}$$

This is the main result of this study : we managed to build a finite cross section for the exclusive diffractive production of a dijet at NLO accuracy and with general kinematics using the shockwave formalism in the small jet cone approximation. To get this IR-safe cross section, one has to take the $q\bar{q}$ production cross section from section 6, rename the quark momenta

$$(p_q, p_{\bar{q}}) \to (p_J, p_K),$$

and substitute $S_V + S_V^* \to S_R$ in Eq. (3.150) for the LL transition, in Eq. (3.154) for the LT transition, and in Eq. (3.161) for the TT transition.

3.8.5 Summary

Using the QCD shockwave approach [22, 90, 91], we have performed the first full computation of an exclusive cross section with NLO accuracy in the shockwave approach. We have shown in a detailed way the cancellation of UV, soft, collinear and rapidity divergences. All our results were obtained without any approximation, with general semihard kinematics: *i.e.* for nonzero incoming photon virtuality, arbitrary $t-$channel momentum transfer and invariant mass of the produced state. In the next chapter, we will present a short but detailed list of several studies which could be based on our result or on our computation methods. First, we will describe how one could give phenomenological predictions for our process, and how to extend it for other phenomenological applications. We will then give hints on how to extend or rewrite our work for more theoretical problems.

Chapter 4

Prospects

Quite a lot of phenomenological and theoretical developments can be pursued based on our study. In this chapter, we will focus on a list of some such prospects, and we will detail how we believe they could be performed. First we will discuss the possible phenomenological applications of our process. Then we will explain how to adapt our computation to the production of a light meson instead of jets, and the theoretical problem at stake. We will then focus on the NLO $\gamma^* \to \gamma^*$ impact factor. First we will explain how previous computations were done to emphasize that although some results exist, none were obtained through a completely explicit NLO computation[1]. Then we will give details on how we believe at the moment one could recover this impact factor from our results. Finally we will discuss the extensions of our computation for massive quarks with an emphasis on charmonium production. We will motivate and discuss this by summing up part of another work of ours [93] on the production of a forward J/Ψ and a backwards jet at the LHC.

4.1 Phenomenological applications

The phenomenological applications of our results are multiple, and we expect them to improve essentially the precision of models based on the k_T-factorization picture, since several observables could now be made accessible theoretically with NLO accuracy. Indeed, it is known that adding the NLO correction to Born impact factors have major effects in BFKL predictions. The only available process for which such a complete NLO description was obtained [94–99] is Mueller-Navelet dijet production [100]. In particular, the azimuthal decorrelation was recently extracted by CMS [101] and confronted with its very good theoretical description of Refs. [102, 103]. Furthermore, the fact that the state exchanged in the $t-$channel in our computation is very general allows one to study not only the linear BFKL regime, but also saturation effects in a proton or in a nucleus with NLO accuracy.

First, the NLO impact factor of the present thesis could be used as it is to describe the exclusive diffractive electroproduction of a dijet [86], and it can easily be adapted to non-exclusive dijet diffractive electroproduction by ignoring the energy resolution E when performing the integral w.r.t. the gluon momentum in the sector of the phase space where the gluon is outside the jet cones. This process was studied at HERA [104]. In the limit $Q^2 \to 0$, our general result could be also applied to the diffractive photoproduction of jets [105, 106], with a hard scale given for example by the invariant mass of the produced state. A precise comparison of the future NLO BFKL predictions with the NLO collinear factorization approach could be performed [107, 108]. More generally at future ep and eA colliders like EIC [109] and LHeC [110], a large set of observables will give a possibility to enter the saturation regime in a controllable way, since the saturation scale becomes perturbative for large center-of-mass energy and/or large values of A. This includes photoproduction of heavy quarkonia, exclusive diffractive production of light mesons, e.g. $\rho-$meson, either in electroproduction or photoproduction at large t. In particular diffractive dijet production is considered as a very promising observable to probe the color glass condensate and more generally to perform proton and nucleus tomography at low x, in connection to Wigner distributions. Our result might be a first step to go beyond the recent LO analyses [111, 112].

Second, before the advent of future high energy and high luminosity ep and eA colliders, ultraperipheral collisions (UPCs) at high energy which provide a source of photons from a projectile proton or

[1] We are however aware that such a computation was started by the author of [92]

nucleus are perfect playgrounds in order to probe the high-energy partonic content of the target proton or nucleus. These are already accessible at the LHC. In particular during the Run I of the LHC, the LHCb collaboration have measured exclusive photoproduction of J/ψ and $\psi(2S)$ mesons [113, 114] in pp collision (later extended to Υ in Ref. [115]), while the ALICE collaboration measured this process in pPb [116] and $PbPb$ [117–119] collisions. CMS very recently released a similar analysis for $PbPb$ [120]. The physics potential of UPCs will improve very significantly thanks to several very forward detectors which are installed, under test, or planned in each of the four LHC experiments, in particular the CMS-TOTEM Proton Spectrometer, AD-ALICE, HERSCHEL at LHCb and AFP at ATLAS [121]. For example, the diffractive protoproduction of a large invariant mass dijet could be studied in UPC during Run II at the LHC [2].

4.2 The $\gamma^* \to \rho$ impact factor and the BFKL/BK correspondence

After applying a suitable adaptation of our results, one can obtain the NLO impact factor for the $\gamma^*\rho$ transition in arbitrary kinematics, therefore extending the result of [123]. At leading twist, this process is dominated by the $\gamma_L \to \rho_L$ transition, transitions with other polarizations are twist-3 contributions. The impact factor for the transition $\gamma_T^* \to \rho_T$ in the forward limit was obtained at LO in Ref. [124, 125], including both the kinematical twist 3 (the so-called Wandzura Wilczek (WW) [126] contribution, where the Fock state of the produced meson is only made of a $q\bar{q}$ pair) and the genuine twist 3 contributions (*i.e.* including a $q\bar{q}g$ Fock state).
The present result opens the way to a computation of LO $\gamma^* \to \rho$ transitions for arbitrary polarizations and kinematics (using our $\gamma^{(*)} \to q\bar{q}g$ Born order result), as well as of the NLO $\gamma^{(*)} \to \rho$ impact factor in the WW approximation, using our one-loop $\gamma^{(*)} \to q\bar{q}$ result.
In the following section, we will show how to adapt our results for the leading twist $\gamma_L \to \rho_L$ transition then we will discuss a fundamental question at stake.

4.2.1 Collinear factorization for the production of a light vector meson at leading twist

Let us study the $\gamma^* gg \to \rho$ amplitude, where ρ is supposed to be longitudinally polarized and the photon has a large virtuality Q^2 which will be our hard scale. We choose the frame so that the momentum p of the ρ meson has null transverse components and is along n_1^μ :

$$p^\mu = p^+ n_1^\mu + \frac{m_\rho^2}{p^+} n_2^\mu \sim p^+ n_1^\mu. \tag{4.1}$$

The amplitude for this process reads :

$$i\,(2\pi)^D\,\delta\,(p - p_1 - p_2 - q)\,\mathcal{A} \quad = \quad \langle V\,(p)|\,\mathcal{H}_{int}\,|g\,(p_1)\,g\,(p_2)\,\gamma\,(q)\rangle\,, \tag{4.2}$$

where $\mathcal{H}_{int}$ is the interaction hamiltonian. Then :

$$\begin{aligned} &i\,(2\pi)^D\,\delta\,(p - p_1 - p_2 - q)\,\mathcal{A} \\ &= \sum_f\,(ie_f)\,(ig)^2 \int d^D z_2 d^D z_1 d^D z_0 \\ &\times \langle V(p)|\,\mathcal{P}\left[\bar{\psi}_f(z_2) t^a \hat{A}_g^a(z_2)\psi_f(z_2)\bar{\psi}_f(z_1) t^b \hat{A}_g^b(z_1)\psi_f(z_1)\bar{\psi}_f(z_0)\hat{A}_\gamma(z_0)\psi_f(z_0)\right]|g^a(p_1)g^b(p_2)\gamma(q)\rangle\,. \end{aligned} \tag{4.3}$$

Here f is a flavor index. In the following for readability we will not write it, and we will mention in the end how flavor should be included in the computation.

[2] In the usual collinear picture, a recent study of this process has been performed in Ref. [122].

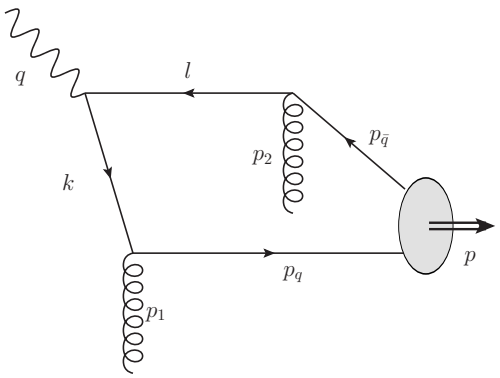

Figure 4.1: Example of one diagram for the $\gamma^* gg \to \rho$ transition. p_1 and p_2 are incoming momenta.

For example the diagram in Fig. 4.1 reads :

$$\begin{aligned} & i\left(2\pi\right)^D \delta\left(p-p_1-p_2-q\right)\mathcal{A} \\ & = \left(ie_q\right)\left(ig\right)^2 \int d^D z_2 d^D z_1 d^D z_0 e^{-i(p_1\cdot z_1)-i(p_2\cdot z_2)-i(q\cdot z_0)} \\ & \times \int \frac{d^D k}{\left(2\pi\right)^D}\frac{d^D l}{\left(2\pi\right)^D} e^{-i(k\cdot z_{10})-i(l\cdot z_{02})} \left[t^a \hat{\varepsilon}_1 G_0\left(k\right) t^b \hat{\varepsilon}_q G_0\left(l\right)\hat{\varepsilon}_2\right]^{ij}_{\alpha\beta} \left\langle V\left(p\right)\right| \bar{\psi}^i_\alpha\left(z_1\right)\psi^j_\beta\left(z_2\right)\left|0\right\rangle , \end{aligned} \tag{4.4}$$

where (i,j) are color indices and (α,β) are spinor indices. Here we assumed that the gluons are on-shell for simplicity in this toy model. In a k_t-factorization computation, the polarization vectors ε_i must be replaced by *non-sense polarizations* $\propto n_2$ of off-shell gluons.
First, let us write the Fierz identity in color space as follows :

$$\begin{aligned} & \left[t^a \hat{\varepsilon}_2 G_0\left(k\right) t^b \hat{\varepsilon}_1 G_0\left(l\right)\hat{\varepsilon}_q\right]^{mn}_{\alpha\beta} \bar{\psi}^i_\alpha\left(z_1\right)\psi^j_\beta\left(z_2\right)\delta^{im}\delta^{jn} \\ = \; & \left[t^a \hat{\varepsilon}_2 G_0\left(k\right) t^b \hat{\varepsilon}_1 G_0\left(l\right)\hat{\varepsilon}_q\right]^{mn}_{\alpha\beta} \bar{\psi}^i_\alpha\left(z_1\right)\psi^j_\beta\left(z_2\right)\left[2\left(t^c\right)_{ij}\left(t^c\right)_{nm}+\frac{1}{N_c}\delta_{ij}\delta_{mn}\right] \end{aligned} \tag{4.5}$$

Due to the color neutrality of the meson state, the first term in the right hand side of Eq. (4.5) cancels. Then one gets :

$$\begin{aligned} & \left[t^a \hat{\varepsilon}_1 G_0\left(k\right) t^b \hat{\varepsilon}_q G_0\left(l\right)\hat{\varepsilon}_2\right]^{mn}_{\alpha\beta} \bar{\psi}^i_\alpha\left(z_1\right)\psi^j_\beta\left(z_2\right)\delta^{im}\delta^{jn} \\ & = \left[\hat{\varepsilon}_1 G_0\left(k\right)\hat{\varepsilon}_q G_0\left(l\right)\hat{\varepsilon}_2\right]_{\alpha\beta}\bar{\psi}_\alpha\left(z_1\right)\psi_\beta\left(z_2\right)\frac{\delta^{ab}}{2N_c}, \end{aligned} \tag{4.6}$$

where we defined $\bar{\psi}_\alpha\left(z_1\right)\psi_\beta\left(z_2\right) \equiv \bar{\psi}^i_\alpha\left(z_1\right)\psi^i_\beta\left(z_2\right)$. The Fierz identity in spinor space relies on the decomposition of the sixteen Dirac matrices on the following basis :

$$\begin{aligned} \Gamma^S &= I, \quad \Gamma^P = i\gamma^5, \\ \Gamma^{V\mu} &= \gamma^\mu, \quad \Gamma^{A\mu} = \gamma^\mu\gamma^5, \\ \Gamma^{\mu\nu} &= \frac{i}{2}\left[\gamma^\mu,\gamma^\nu\right]. \end{aligned} \tag{4.7}$$

The elements of this basis will be written as Γ^λ, with λ a generalized index. Their inverses $\left(\Gamma^\lambda\right)^{-1} \equiv \Gamma_\lambda$ read :

$$\begin{aligned} \Gamma_S &= \Gamma^S, \quad \Gamma_P = -\Gamma^P, \\ \Gamma_{V\mu} &= \Gamma^V_\mu, \quad \Gamma_{A\mu} = \Gamma^A_\mu, \\ \Gamma_{\mu\nu} &= \Gamma^{\mu\nu}. \end{aligned} \tag{4.8}$$

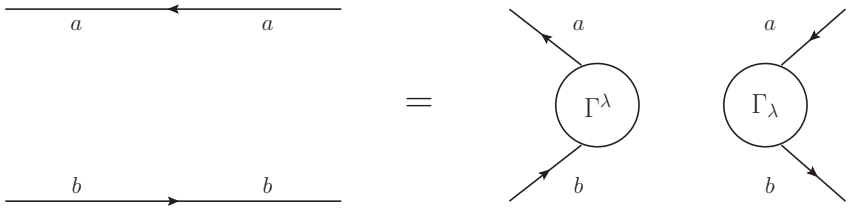

Figure 4.2: Factorization in spinor space

The Fierz identity in spinor space reads

$$\delta_{a\alpha}\delta_{b\beta} = \frac{1}{4}\left(\Gamma_\lambda\right)_{\beta\alpha}\left(\Gamma^\lambda\right)_{ab}. \tag{4.9}$$

The Fierz matrices being a basis of the spinor space, any matrix X of this space can be written as $X = x_\lambda \Gamma^\lambda$, and the previous identity allows one to check easily that

$$X = \frac{1}{4}\mathrm{Tr}\left(X\Gamma_\lambda\right)\Gamma^\lambda. \tag{4.10}$$

Applying this identity allows one to write :

$$\begin{aligned}&\left[\hat{\varepsilon}_1 G_0\left(k\right)\hat{\varepsilon}_q G_0\left(l\right)\hat{\varepsilon}_2\right]_{\alpha\beta}\bar{\psi}_\alpha\left(z_1\right)\psi_\beta\left(z_2\right)\frac{\delta^{ab}}{2N_c} \\ &= \frac{\delta^{ab}}{8N_c}\left[\bar{\psi}\left(z_1\right)\Gamma_\lambda\psi\left(z_2\right)\right]\mathrm{Tr}\left[\hat{\varepsilon}_1 G_0\left(k\right)\hat{\varepsilon}_q G_0\left(l\right)\hat{\varepsilon}_2\Gamma^\lambda\right].\end{aligned} \tag{4.11}$$

One gets :

$$\begin{aligned}&i\left(2\pi\right)^D\delta\left(p-p_1-p_2-q\right)\mathcal{A} \\ &= \frac{\delta^{ab}}{8N_c}\left(ie_q\right)\left(ig\right)^2\int d^Dz_2d^Dz_1d^Dz_0e^{-i(p_1\cdot z_1)-i(p_2\cdot z_2)-i(q\cdot z_0)}\left\langle V\left(p\right)\right|\bar{\psi}\left(z_1\right)\Gamma_\lambda\psi\left(z_2\right)\left|0\right\rangle \\ &\times\int\frac{d^Dk}{\left(2\pi\right)^D}\frac{d^Dl}{\left(2\pi\right)^D}e^{-i(k\cdot z_{10})-i(l\cdot z_{02})}\mathrm{Tr}\left[\hat{\varepsilon}_1 G_0\left(k\right)\hat{\varepsilon}_q G_0\left(l\right)\hat{\varepsilon}_2\Gamma^\lambda\right].\end{aligned} \tag{4.12}$$

Chirality conservation implies that once convoluted with the hard part, the meson matrix element will be canceled for every Fierz structure except for $\Gamma^{V\mu}$ and $\Gamma^{A\mu}$, as can be trivially seen when considering the trace in Eq. (4.12).
Collinear factorization relies on the expansion around the lightcone direction for the meson matrix element. One can show that the axial matrix element starts at the 1st order in this Q^{-1}-expansion while the vector matrix element which starts at the 0th order. For a process such as $\gamma^* gg \to \rho$ the leading contribution comes from the vector matrix element.

Thus for the production of a longitudinally polarized meson at leading twist, only the vector term $\Gamma_\lambda = \gamma_\lambda$ will contribute.
Finally, the translation invariance of such a matrix element allows one to write

$$\left\langle\rho\left(p\right)\right|\bar{\psi}\left(z_1\right)\gamma_\mu\psi\left(z_2\right)\left|0\right\rangle = e^{i(p\cdot z_2)}\left\langle\rho\left(p\right)\right|\bar{\psi}\left(z_1-z_2\right)\gamma_\mu\psi\left(0\right)\left|0\right\rangle. \tag{4.13}$$

One concludes :

$$\begin{aligned}\delta\left(p-p_1-p_2-q\right)\mathcal{A} &= -i\frac{\delta^{ab}\left(ie_q\right)\left(ig\right)^2}{8N_c\left(2\pi\right)^D}\int d^Dz_2d^Dz_1d^Dz_0e^{-i(p_1\cdot z_1)-i(p_2\cdot z_2)-i(q\cdot z_0)}e^{i(p\cdot z_2)} \\ &\times \left\langle V\left(p\right)\right|\bar{\psi}\left(z_1-z_2\right)\gamma_\mu\psi\left(0\right)\left|0\right\rangle \\ &\times \int\frac{d^Dk}{\left(2\pi\right)^D}\frac{d^Dl}{\left(2\pi\right)^D}e^{-i(k\cdot z_{10})-i(l\cdot z_{02})}\mathrm{Tr}\left[\hat{\varepsilon}_1 G_0\left(k\right)\hat{\varepsilon}_q G_0\left(l\right)\hat{\varepsilon}_2\gamma^\mu\right].\end{aligned} \tag{4.14}$$

Integrating w.r.t. z_0, performing the change of variables $(z_1,\, z_2) \to (z_1 + z_2, r \equiv z_1 - z_2)$, integrating w.r.t. $(z_1 + z_2)$ and finally w.r.t. k gives :

$$\begin{aligned}\delta\left(p - p_1 - p_2 - q\right)\mathcal{A} &= -i\frac{\delta^{ab}\left(ie_q\right)\left(ig\right)^2}{8N_c}\int d^D r\,\langle\rho\left(p\right)|\,\bar{\psi}\left(r\right)\gamma_\mu\psi\left(0\right)|0\rangle\,\delta\left(q + p_1 - p + p_2\right)\\ &\times\int\frac{d^D l}{\left(2\pi\right)^D}e^{-i\left(l+p-p_2\right)\cdot r}\mathrm{Tr}\left[\hat{\varepsilon}_1 G_0\left(l+q\right)\hat{\varepsilon}_q G_0\left(l\right)\hat{\varepsilon}_2\gamma^\mu\right].\end{aligned} \tag{4.15}$$

Let us shift l so that it represents the momentum p_q of the "external quark" : $l \to p_q \equiv l + q + p_1$.

$$\begin{aligned}\delta\left(p - p_1 - p_2 - q\right)\mathcal{A} &= -i\frac{\delta^{ab}\left(ie_q\right)\left(ig\right)^2}{8N_c}\int d^D r\,\langle\rho\left(p\right)|\,\bar{\psi}\left(r\right)\gamma_\mu\psi\left(0\right)|0\rangle\,\delta\left(q + p_1 - p + p_2\right)\\ &\times\int\frac{d^D p_q}{\left(2\pi\right)^D}e^{-i\left(p_q\cdot r\right)}\mathrm{Tr}\left[\hat{\varepsilon}_1 G_0\left(p_q - p_1\right)\hat{\varepsilon}_q G_0\left(p_q - p_1 - q\right)\hat{\varepsilon}_2\gamma^\mu\right].\end{aligned} \tag{4.16}$$

We thus managed to factorize our process into a non-perturbative bilocal meson operator

$$\langle\rho\left(p\right)|\,\bar{\psi}\left(z_1 - z_2\right)\gamma_\mu\psi\left(0\right)|0\rangle \tag{4.17}$$

and a hard part

$$H^\mu\left(p_q,\, p - p_q\right) \equiv -i\frac{\delta^{ab}\left(ie_q\right)\left(ig\right)^2}{8N_c\left(2\pi\right)^D}\mathrm{Tr}\left[\hat{\varepsilon}_1 G_0\left(p_q - p_1\right)\hat{\varepsilon}_q G_0\left(p_q - p_1 - q\right)\hat{\varepsilon}_2\gamma^\mu\right] \tag{4.18}$$

as such :

$$\begin{aligned}\delta\left(p - p_1 - p_2 - q\right)\mathcal{A} &= \int d^D r\,\langle\rho\left(p\right)|\,\bar{\psi}\left(r\right)\gamma_\mu\psi\left(0\right)|0\rangle\,\delta\left(p - p_1 - p_2 - q\right)\\ &\times\int\frac{d^D p_q}{\left(2\pi\right)^D}e^{-i\left(p_q\cdot r\right)}H^\mu\left(p_q,\, p - p_q\right).\end{aligned} \tag{4.19}$$

In the spirit of collinear factorization, one then assumes that the $-$ and transverse components of p_q are negligible in the hard part, since the hard scale Q^2 is propagating along n_1 and the quark is collinear to the meson.
Then one can trivially integrate w.r.t. p_q^- and $\vec{p}_q$ to get :

$$\begin{aligned}\delta\left(p - p_1 - p_2 - q\right)\mathcal{A} &= \int d^D r\,\langle\rho\left(p\right)|\,\bar{\psi}\left(r\right)\gamma_\mu\psi\left(0\right)|0\rangle\,\delta\left(p - p_1 - p_2 - q\right)\delta\left(r^+\right)\delta\left(\vec{r}\right)\\ &\times\int\frac{dp_q^+}{\left(2\pi\right)^D}e^{-i\left(p_q^+ r^-\right)}H^\mu\left[p_q^+ n_1,\,\left(p^+ - p_q^+\right)n_1\right].\end{aligned} \tag{4.20}$$

Thus the mesonic matrix element is evaluated in the limit where r is along the lightcone : $r \propto n_2$. Such a limit for this operator was derived in [127, 128] :

$$\langle\rho\left(p\right)|\,\bar{\psi}\left(r\right)\gamma_\mu\psi\left(0\right)|0\rangle\,|_{r^2=0} = p_\mu f_V\int_0^1 dx e^{ix\left(p\cdot r\right)}\phi_\parallel\left(x\right), \tag{4.21}$$

where $\phi_\parallel\left(x\right)$ is the Distribution Amplitude of the longitudinal meson. Then integrating w.r.t. r and w.r.t. p_q^+ gives :

$$\delta\left(p - p_1 - p_2 - q\right)\mathcal{A} = \frac{f_V}{\left(2\pi\right)^{D-1}}\delta\left(p - p_1 - p_2 - q\right)\int_0^1 dx\phi_\parallel\left(x\right)\left(p\cdot H\right)\left[xp^+ n_1,\,\left(1-x\right)p^+ n_1\right]. \tag{4.22}$$

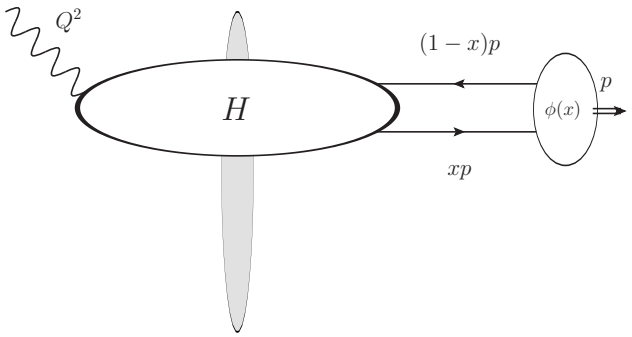

Figure 4.3: Factorization for the production of a light meson

Thus the leading twist amplitude for the production of a light longitudinal vector meson is obtained by first computing the amplitude for the production of an open $q\bar{q}$ pair with respective momenta xp and $\bar{x}p$[3] with the right Fierz projection, and integrating the result multiplied by the DA of the meson $\phi_{\parallel}(x)$ over $x \in [0,1]$. See Fig. 4.3.
This procedure must be applied for each quark flavor contributing to the meson's wavefunction, then their contributions must be combined. For example for the production of a ρ^0 meson, whose wavefunction is $\frac{|u\bar{u}\rangle - |d\bar{d}\rangle}{\sqrt{2}}$, the amplitude must be computed for $f = u$ and $f = d$, and combined with the factors $\frac{1}{\sqrt{2}}$ and $\frac{-1}{\sqrt{2}}$. For such a simple process, one can compute it once by using an effective quark charge $e_q \equiv \frac{e_u - e_d}{\sqrt{2}}$ but for more complicated processes involving several DAs or GPDs as in part 2 of this thesis, this effective charge does not exist and one must compute each contribution to the end.

4.2.2 Adapting the present results to the production of a ρ meson

Similarly to the toy model studied in the previous section, we can adapt our results for the NLO $\gamma^* p \to q\bar{q}p$ cross section to the production of a longitudinal light vector meson at leading twist by studying the limit where the quark and the antiquark are collinear, carrying the momenta xp_V and $\bar{x}p_V$, where p_V is the meson's momentum. The presence of logarithms of type

$$\ln\left[\left(x\vec{p}_{\bar{q}} - x\vec{p}_q\right)^2\right] \tag{4.23}$$

whose argument cancels exactly when the quark and the antiquark are collinear in our result is the sign that the integration w.r.t. the transverse momentum of the loop gluon should be performed *after* applying the new kinematics. Then the integral will give rise to divergent terms from the collinear limit. Such terms should then be absorbed into the ERBL evolution of the meson's DA. Apart from that, the computation is very similar to our calculation for the open $q\bar{q}$ production.

Obtaining such a result would extend the study in [123] to the non-forward case. Additionally, this would be the first impact factor known at NLO accuracy in both the BFKL and the B-JIMWLK pictures.
The correspondence between the BFKL formalism and the linearized BK formalism with NLL accuracy is a non-trivial question. The kernels for both approaches were shown to be equivalent for color neutral processes : they are formulated as different representations of the same kernel. The difference lies in the ambiguity in the definition of evolution kernels at NLO accuracy : there is always a possibility to redistribute radiative corrections between the kernel and the impact factors. Thus the equivalence must actually be true for cross sections, or for kernels and impact factors up to the action of an operator. Schematically :

$$\Phi_{BK} \otimes \mathcal{K}_{BK} \otimes \Phi'_{BK} = (\Phi_{BFKL}\mathcal{O}) \otimes \left(\mathcal{O}^\dagger \mathcal{K}_{BFKL}\mathcal{O}\right) \otimes \left(\mathcal{O}^\dagger \Phi_{BFKL}\right). \tag{4.24}$$

The operator $\mathcal{O}$ was derived for the kernel equivalence, but its action on impact factors was not checked yet[4]. Thus knowing an impact factor with NLO accuracy in both the BFKL and the B-JIMWLK approaches would allow a consistency check between the two formalisms.

[3] p in considered to be lightlike (up to a $\frac{m_\rho}{Q}$ correction) when computing the hard part.
[4] For more detailed discussions about this subject, the reader is referred to [87, 129, 130]

4.3 The NLO $\gamma^* \to \gamma^*$ cross section

DIS experiments at HERA were among the strongest motivations for the study of QCD in the Regge limit. However studies with LO accuracy in the k_t-formalism only allowed for qualitative descriptions of the DIS data : the predicted low x evolution seems to be faster than the observed evolution[5] Thus higher order corrections to the $\gamma^* p \to \gamma^* p$ cross section should be computed.
The photon impact factor was derived in the shockwave approach [90, 91], then the DIS cross section was obtained based on this result [133] and a phenomenological study [134] based on this cross section seemed to fail to describe LEP2 data.
We believe that one could recover the NLO $\gamma^* \to \gamma^*$ impact factor from our results. Such a computation would be a useful consistency check of the previous results for this impact factor, in particular for the dipole contribution, which was obtained indirectly in [90, 91]. In this section, we will carefully describe the method used in [90, 91], then we will show how to adapt our results to check its validity range.
The first step is to separate the dipole and double dipole contributions.

First computation : the double dipole contribution

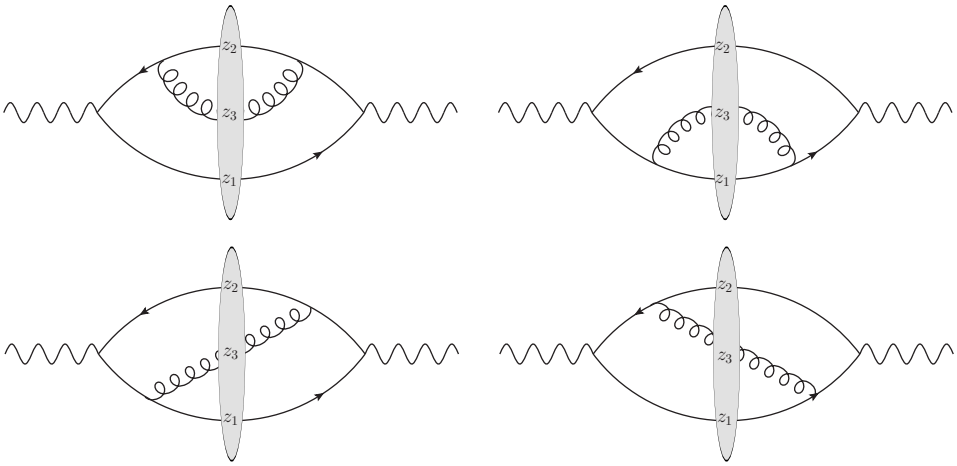

Figure 4.4: Double dipole contribution to the $\gamma^* \to \gamma^*$ cross section at NLO

Like for our computation, using color neutrality in t-channel and subtracting the non-interacting part allows one to write the double-dipole contribution, consisting of the diagrams in Fig. 4.4, as

$$\begin{aligned}\sigma_2^{\mu\nu} &= \int d^d\vec{z}_1 d^d\vec{z}_2 d^d\vec{z}_3 \mathcal{I}_2^{\mu\nu}\left(\vec{z}_1,\,\vec{z}_2,\,\vec{z}_3\right)\left[\mathrm{Tr}\left(U_{\vec{z}_1}U^\dagger_{\vec{z}_3}\right)\mathrm{Tr}\left(U_{\vec{z}_3}U^\dagger_{\vec{z}_2}\right) - N_c\mathrm{Tr}\left(U_{\vec{z}_1}U^\dagger_{\vec{z}_2}\right)\right] \\ &+ \int d^d\vec{z}_1 d^d\vec{z}_2\left[\int d^d\vec{z}_3\left(\frac{N_c^2-1}{N_c}\right)\mathcal{I}_2^{\mu\nu}\left(\vec{z}_1,\,\vec{z}_2,\,\vec{z}_3\right)\right]\left[\mathrm{Tr}\left(U_{\vec{z}_1}U^\dagger_{\vec{z}_2}\right) - N_c\right].\end{aligned} \tag{4.25}$$

For this computation too one can separate this quantity into two contributions by introducing

$$\tilde{\mathcal{I}}_1^{\mu\nu}\left(\vec{z}_1,\,\vec{z}_2\right) \equiv \left[\int d^d\vec{z}_3\left(\frac{N_c^2-1}{N_c}\right)\mathcal{I}_2^{\mu\nu}\left(\vec{z}_1,\,\vec{z}_2,\,\vec{z}_3\right)\right]. \tag{4.26}$$

The first term in Eq. (4.25) will be the full double dipole contribution, while Eq. (4.26) will be included in the single dipole contribution.
For the same physical reasons as in the previous chapter, the only divergence which appears in the double dipole contribution is the rapidity divergence. Thus computing the diagrams above does not require dimensional regularization, only the rapidity regulator must be kept.

[5] Although recent studies [131, 132] involving collinearly resummed versions of the B-JIMLWK kernel give more optimistic results.

In 4 dimensions, the gluon propagator can be written a convenient way as follows :

$$G_{\mu\nu}\left(z_2,\, z_0\right)|_{z_2^+>0>z_0^+} \;=\; \frac{8}{i}\int \frac{d^4z_1}{\left(2\pi\right)^4}\delta\left(z_1^+\right)\frac{g_{\perp\mu}^{\alpha}z_{21}^+ - z_{21\perp}^{\alpha}n_{2\mu}}{\left(z_{21}^2-i0\right)^2}U_{\vec{z}_1}\frac{1}{\frac{\partial}{\partial z_0^-}}\frac{z_{10}^+ g_{\perp\alpha\nu} - z_{10\perp}^{\alpha}n_{2\nu}}{\left(z_{10}^2-i0\right)^2}\,, \tag{4.27}$$

where

$$\frac{1}{\frac{\partial}{\partial z_0^-}}f\left(z_0^-\right) \;\equiv\; \int\frac{dk^+}{2\pi}\theta\left(\sigma-k^+\right)\int du\frac{e^{-ik^+\left(z_0^- - u\right)}}{-ik^+}f\left(z_0^+\right)\,. \tag{4.28}$$

In this formula, k is the actual physical momentum of the gluon and σ is the rapidity cutoff. Given the definitions in Section 2.2 and Eq. (4.27) one can now easily isolate the vertex integrations. Let us consider one of the two qqg vertices :

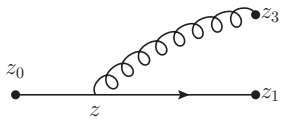

Figure 4.5: qqg vertex

The integration w.r.t. the coordinate of the vertex in Fig. 4.5 is proportional to

$$J^{\alpha} \;\equiv\; \int d^4z\, G_0\left(z_1-z\right)\gamma^{\mu}\, G_0\left(z-z_0\right)\frac{g_{\perp\mu}^{\alpha} - \left(z_3-z\right)_{\perp}^{\alpha}n_{2\mu}}{\left[\left(z_3-z\right)^2-i0\right]^2} \tag{4.29}$$

$$\propto \int d^4z\frac{\hat{z}_1-\hat{z}}{\left[\left(z_1-z\right)^2-i0\right]^2}\left(\frac{\left(z_3^+-z^+\right)\gamma_{\perp}^{\alpha}}{\left[\left(z_3-z\right)^2-i0\right]^2} - \frac{\left(z_3-z\right)_{\perp}^{\alpha}\gamma^+}{\left[\left(z_3-z\right)^2-i0\right]^2}\right)\frac{\hat{z}-\hat{z}_0}{\left[\left(z-z_0\right)^2-i0\right]^2} \tag{4.30}$$

Thus with a change of variable, one can reduce this vertex integral to the following quantity :

$$\mathcal{J}^{\mu\nu}\left(x,\, y\right) \;\equiv\; \int d^4z\frac{\hat{x}-\hat{z}}{\left(x-z\right)^4}\left[\gamma^{\mu}\frac{z^{\nu}}{z^4} - \gamma^{\nu}\frac{z^{\mu}}{z^4}\right]\frac{\hat{z}-\hat{y}}{\left(z-y\right)^4}\,. \tag{4.31}$$

The way this integral is computed in [90, 91] relies heavily on the dimension : in 4 dimensions one can use the conformal transformation $z^{\mu}\to z'^{\mu}\equiv\frac{z^{\mu}}{z^2}$ to get rid of one denominator. Indeed if one defines $x'\equiv\frac{x}{x^2}$ and $y'\equiv\frac{y}{y^2}$, J becomes :

$$\mathcal{J}^{\mu\nu}\left(x,\, y\right) \;=\; x'^4y'^4\int d^4z'\frac{z'^2}{\left(x'-z'\right)^4\left(z'-y'\right)^4}\left(\frac{\hat{x}'}{x'^2}-\frac{\hat{z}'}{z'^2}\right)\left(\gamma^{\mu}z'^{\nu}-\gamma^{\nu}z'^{\mu}\right)\left(\frac{\hat{z}'}{z'^2}-\frac{\hat{y}'}{y'^2}\right) \tag{4.32}$$

Such an integral can now be taken with the usual computation methods. It can be done to the end in dimension 4 and without any regulator by cancelling potentially divergent terms through the $(\mu\leftrightarrow\nu)$ antisymmetry property. Finally we obtain[6] :

$$\begin{aligned}\mathcal{J}^{\mu\nu}\left(x,\, y\right) \;=\; & \frac{-i\pi^2}{x^2y^2\left(x-y\right)^2}\left[\hat{x}\left(\frac{x^{\mu}}{x^2}\gamma^{\nu}-\frac{x^{\nu}}{x^2}\gamma^{\mu}\right)\hat{y}+\hat{x}\left(\frac{y^{\mu}}{y^2}\gamma^{\nu}-\frac{y^{\nu}}{y^2}\gamma^{\mu}\right)\hat{y}\right.\\ & \left.+\frac{1}{2}\hat{x}\left(\gamma^{\mu}\gamma^{\nu}-\gamma^{\nu}\gamma^{\mu}\right)-\frac{1}{2}\left(\gamma^{\mu}\gamma^{\nu}-\gamma^{\nu}\gamma^{\mu}\right)\hat{y}+2\frac{x^{\mu}y^{\nu}-y^{\mu}x^{\nu}}{\left(x-y\right)^2}\left(\hat{x}-\hat{y}\right)\right]\,.\end{aligned}$$

This integral was used in our first paper [74] to obtain the amplitude for the diffractive production of a quark, an antiquark and a gluon, which was also computed in [135] to construct the cross section for the exclusive production of 3 partons.
In [90, 91], the authors use this integral twice then integrate w.r.t. the $^+$-momentum of the gluon with the rapidity cutoff, then use one step of B-JIMWLK evolution to get a finite expression for the double dipole contribution to the $\gamma^*\to\gamma^*$ impact factor.
The single dipole contribution is then obtained indirectly.

[6] The -i factor corrects a misprint in [90].

Single dipole contribution

The total dipole contribution reads

$$\sigma_1^{\mu\nu} = \int d^d\vec{z}_1 d^d\vec{z}_2 \left[\mathcal{I}_1^{\mu\nu}(\vec{z}_1,\vec{z}_2) + \tilde{\mathcal{I}}_1^{\mu\nu}(\vec{z}_1,\vec{z}_2)\right]\left[\mathrm{Tr}\left(U_{\vec{z}_1}U^\dagger_{\vec{z}_2}\right) - N_c\right]. \tag{4.33}$$

It contains the contribution $\tilde{\mathcal{I}}$ in which the gluon crosses the external field but does not interact, and the one $\mathcal{I}$ in which the gluon does not cross the $z^+ = 0$ line, such as the diagrams in Fig. 4.6 and their complex conjugates.

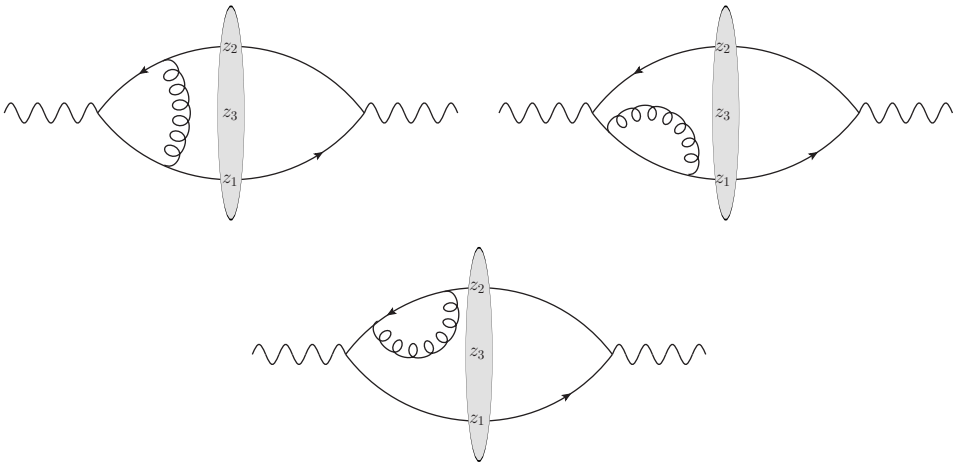

Figure 4.6: Dipole contribution to the $\gamma^* \to \gamma^*$ cross section at NLO

The trick used in [90, 91] is now to study the non-interacting term which was subtracted before. Indeed the sum of all diagrams must reduce, when the shockwaves are set to identity, to the 2-loops correction to the gluon polarization tensor, which happens to be proportional to its 1-loop correction :

$$\int d^d\vec{z}_1 d^d\vec{z}_2 \left[\mathcal{I}_1^{\mu\nu}(\vec{z}_1,\vec{z}_2) + \tilde{\mathcal{I}}_1^{\mu\nu}(\vec{z}_1,\vec{z}_2)\right] = \Pi^{\mu\nu}_{2-loop}. \tag{4.34}$$

$$= \frac{3\alpha_s}{4\pi} C_F \Pi^{\mu\nu}_{1-loop} \tag{4.35}$$

$$= \frac{3\alpha_s}{4\pi} C_F \int d^d\vec{z}_1 d^d\vec{z}_2\, \mathcal{I}_0^{\mu\nu}(\vec{z}_1,\vec{z}_2), \tag{4.36}$$

where $\mathcal{I}_0^{\mu\nu}$ is the leading order contribution to the process.
From this, the authors deduce that

$$\sigma_1^{\mu\nu} = \int d^d\vec{z}_1 d^d\vec{z}_2 \left[\mathcal{I}_1^{\mu\nu}(\vec{z}_1,\vec{z}_2) + \tilde{\mathcal{I}}_1^{\mu\nu}(\vec{z}_1,\vec{z}_2)\right]\left[\mathrm{Tr}\left(U_{\vec{z}_1}U^\dagger_{\vec{z}_2}\right) - N_c\right] \tag{4.37}$$

$$= \frac{3\alpha_s}{4\pi} C_F \int d^d\vec{z}_1 d^d\vec{z}_2\, \mathcal{I}_0^{\mu\nu}(\vec{z}_1,\vec{z}_2)\left[\mathrm{Tr}\left(U_{\vec{z}_1}U^\dagger_{\vec{z}_2}\right) - N_c\right]. \tag{4.38}$$

It would be interesting to check the validity of this method with a more completely explicit NLO calculation for the $\gamma^* \to \gamma^*$ impact factor. We are not aware of any such computation available at the moment. There was another attempt at computing it in [136] using lightcone perturbation theory. However the author of [136] also used an indirect method to obtain the dipole contribution and this method turned out to be incomplete, as explained by the author himself in [92].
A new calculation was started by the same author and some preliminary results were discussed.
It would be interesting to obtain this result and to check the methods used in [90, 91] by adapting our computation to the $\gamma^* \to \gamma^*$ impact factor.

4.3.1 Adapting our results to the $\gamma^* \to \gamma^*$impact factor

Wilson line operators

With open quark and antiquark color indices i and j , the leading order amplitude involves

$$\left(\tilde{C}_0\right)_{ij} = \left(U_1 U_2^\dagger\right)_{ij} . \tag{4.39}$$

Let us consider the dipole and double dipole contributions to the NLO amplitude and to the real correction with open color indices :

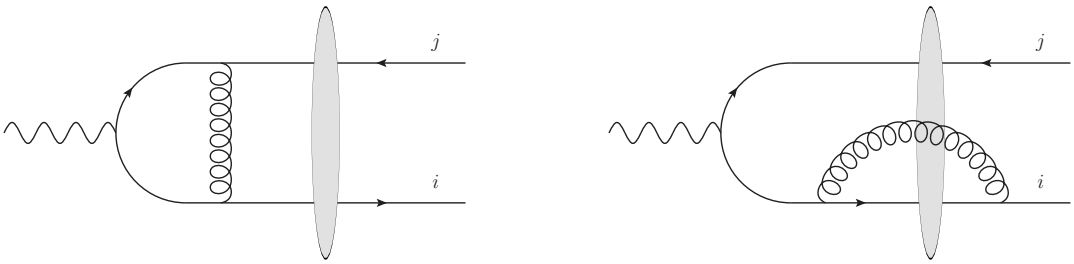

Figure 4.7: Example of two non-singlet virtual contributions

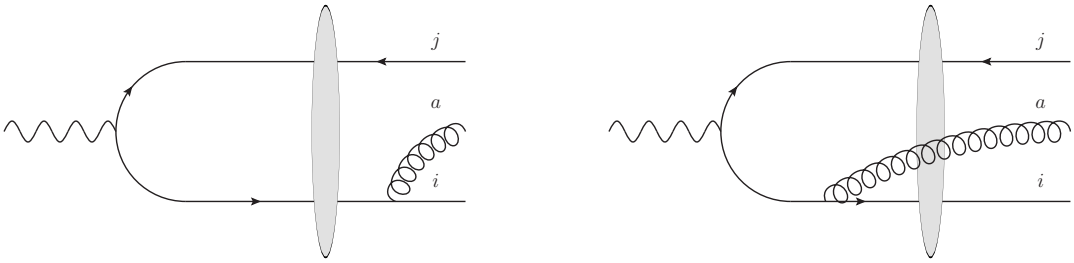

Figure 4.8: Example of two non-singlet real contributions

The virtual and real color factors now read :

$$\left(\tilde{C}_1^V\right)_{ij} = \left(\frac{N_c^2-1}{2N_c}\right)\left(\tilde{C}_0\right)_{ij} , \tag{4.40}$$

$$\left(\tilde{C}_2^V\right)_{ij} = \frac{1}{2}\left[\mathrm{Tr}\left(U_1 U_3^\dagger\right)\left(U_3 U_2^\dagger\right)_{ij} - N_c\left(U_1 U_2^\dagger\right)_{ij}\right] + \left(\tilde{C}_1^V\right)_{ij} , \tag{4.41}$$

$$\left(\tilde{C}_1^R\right)^a_{ij} = \left(t^a U_1 U_2^\dagger\right)_{ij} , \tag{4.42}$$

$$\left(\tilde{C}_2^R\right)^a_{ij} = \left(U_1 U_3^\dagger t^a U_3 U_2^\dagger\right)_{ij} \tag{4.43}$$

It is easy to check that by subtracting the non-interacting term and adding the projections on the color singlet one would recover Eqs. (3.22) and (3.24). We will subtract the non-interacting term for each diagram and study the parts with and without the shockwave separately. Schematically we will write the non-interacting term with a double dashed line. For example instead of diagram 2 we will compute the difference in Fig. 4.9.

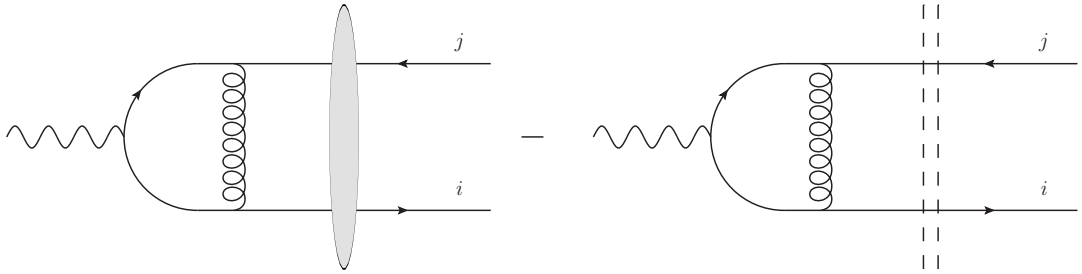

Figure 4.9: Contribution from diagram 2

4.3.2 Contribution without vertices between two shockwaves

Let us consider a contribution with two shockwaves and without a vertex between the shockwaves.

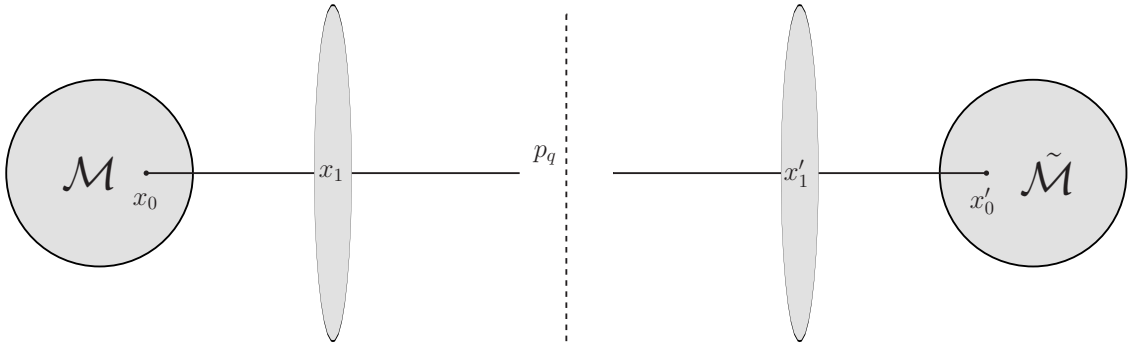

Figure 4.10: Shockwave merging

Using the expressions for the quark lines through the shockwave field, one obtains for this contribution :

$$I_0 = \sum_{\lambda_q} \int \frac{dp_q^+ d^d\vec{p}_q}{(2\pi)^{d+1}} \left[\int d^D x_0 \bar{u}\left(p_q,\, x_0\right) \mathcal{M}\left(x_0\right)\right] \left[\int d^D x_0' \bar{u}\left(p_q,\, x_0'\right) \tilde{\mathcal{M}}\left(x_0'\right)\right]^* \tag{4.44}$$

$$\begin{aligned} = & \int d^D x_0' d^D x_0 \theta\left(-x_0^+\right) \theta\left(-x_0'\right) \int d^d\vec{x}_1 d^d\vec{x}_1' \left(U_{\vec{x}_1} U^\dagger_{\vec{x}_1'}\right) \\ & \times \int \frac{dp_q^+ d^d\vec{p}_q}{(2\pi)^{d+1}} \theta\left(p_q^+\right) \frac{1}{4\left(2\pi\right)^d} \left(\frac{p_q^+}{-x_0^+}\right)^{\frac{d}{2}} \left(\frac{p_q^+}{-x_0'^+}\right)^{\frac{d}{2}} \\ & \times \mathrm{Tr}\left[\tilde{\mathcal{M}}^*\left(x_1\right) \frac{-x_0'^+\gamma^- + \hat{x}_{1'0'\perp}}{-x_0'^+} \gamma^+ \frac{\hat{p}_q}{2p_q^+} \gamma^+ \frac{-x_0^+\gamma^- + \hat{x}_{10\perp}}{-x_0^+} \mathcal{M}\left(x_0\right)\right] \\ & \times \exp\left[ip_q^+\left(x_0^- - \frac{\vec{x}_{10}^{\,2}}{2x_0^+} + i0\right) - ip_q^+\left(x_0'^- - \frac{\vec{x}_{1'0'}^{\,2}}{2x_0'^+} + i0\right) + i\left(\vec{p}_q \cdot \vec{x}_{1'}\right) - i\left(\vec{p}_q \cdot \vec{x}_1\right)\right]. \end{aligned} \tag{4.45}$$

The only dependence on $\vec{p}_q$ is in the exponential given that $\gamma^+ \frac{\hat{p}_q}{2p_q^+} \gamma^+ = \gamma^+$. Then integrating w.r.t. $\vec{p}_q$ gives a $\delta\left(\vec{x}_1 - \vec{x}_1'\right)$. Using the same argument for the antiquark lines, one also gets a $\delta\left(\vec{x}_2 - \vec{x}_2'\right)$. Thus by unitarity of the Wilson lines this contribution reduces to the non-interacting one so it does not need to be computed.

4.3.3 Contribution with a vertex between the shockwaves

Let us consider a general inclusive cross section with a quark-gluon vertex between two shockwaves with the non-interacting term taken out. We will show that the virtual and the real contributions cancel exactly

each other.
The virtual correction reads :

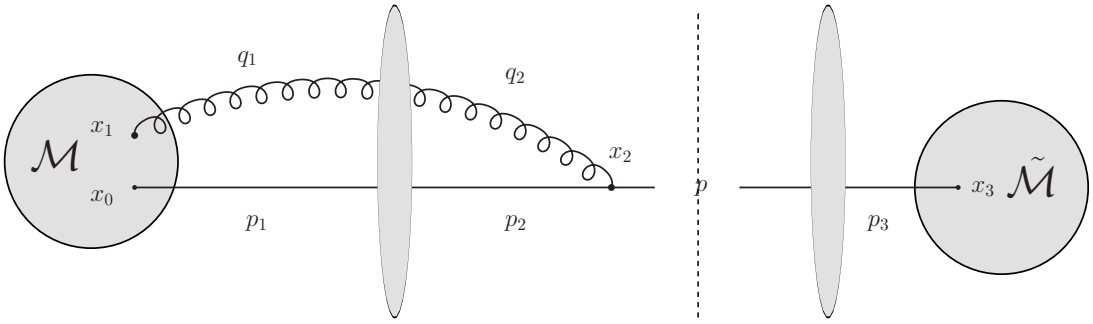

Figure 4.11: Virtual contribution

$$
\begin{aligned}
I_V &= \sum_{\lambda_p} \int \frac{dp^+ d^d\vec{p}}{(2\pi)^{d+1}} \left[(ig) \int d^D x_2 d^D x_1 d^D x_0 \mathcal{M}^\nu (x_1,\, x_0) \frac{\bar{u}_p}{\sqrt{2p^+}} \theta\left(p^+\right) e^{i(p\cdot x_2)} \gamma^\mu G (x_2,\, x_0)\, G_{\mu\nu} (x_2,\, x_1) \right] \\
&\quad \times \left[\int d^D x_3 \bar{u} (p,\, x_3)\, \tilde{\mathcal{M}} (x_3) \right]^* . \qquad (4.46)
\end{aligned}
$$

Using the expressions for Feynman rules in the shockwave field and after a few straightforward integrations, one can get :

$$
\begin{aligned}
I_V &= \int d^D x_3 d^D x_1 d^D x_0 \int \frac{d^d\vec{p}_3}{(2\pi)^d} \frac{d^d\vec{p}_1}{(2\pi)^d} \frac{d^d\vec{p}_2}{(2\pi)^d} \frac{d^d\vec{q}_1}{(2\pi)^{d+1}} \qquad (4.47) \\
&\quad \times \int \frac{dp^+ d^d\vec{p}}{(2\pi)^{d+1}} \left[U\left(\vec{p}-\vec{p}_3\right)\right]^* \left[U\left(\vec{p}_{21}\right)\right] \left[U\left(\vec{p}-\vec{p}_2-\vec{q}_1\right)\right] \theta\left(p^+\right) \\
&\quad \times \int dp_2^+ \int dx_2^+ \theta\left(-x_0^+\right) \theta\left(-x_1^+\right) \theta\left(x_2^+\right) \theta\left(-x_3^+\right) \theta\left(p^+ - p_2^+\right) \theta\left(p_2^+\right) \\
&\quad \times \frac{-(ig)}{\left(2p^+\right)^2 \left(2p_2^+\right)^2 2\left(p^+ - p_2^+\right)} \mathrm{Tr}\left[\hat{p} \gamma^\mu \hat{p}_2 \gamma^+ \left(p_2^+ \gamma^- + \hat{p}_{1\perp}\right) \mathcal{M}^\nu (x_1,\, x_0)\, \tilde{\mathcal{M}}^* (x_3) \left(p^+ \gamma^- + \hat{p}_{3\perp}\right) \gamma^+ \right] \\
&\quad \times d_{0\mu\alpha_\perp} \left(p^+ - p_2^+,\, \vec{p} - \vec{p}_2\right) d_{0\nu}^{\alpha_\perp} \left(p^+ - p_2^+,\, \vec{q}_1\right) \\
&\quad \times \exp\left[i x_2^+ \left(\frac{\vec{p}^2}{2p^+} - \frac{\vec{p}_2^2 - i0}{2p_2^+} - \frac{\left(\vec{p}-\vec{p}_2\right)^2 - i0}{2\left(p^+ - p_2^+\right)} \right) + i x_0^+ \frac{\vec{p}_1^2 - i0}{2p_2^+} + i x_1^+ \frac{\vec{q}_1^2 - i0}{2\left(p^+ - p_2^+\right)} - i x_3^+ \left(\frac{\vec{p}_3^2 - i0}{2p^+} \right) \right] \\
&\quad \times \exp\left[i p^+ x_{13}^- - i p_2^+ x_{10}^- - i\left(\vec{p}_1 \cdot \vec{x}_0\right) - i\left(\vec{q}_1 \cdot \vec{x}_1\right) + i\left(\vec{p}_3 \cdot \vec{x}_3\right) \right] .
\end{aligned}
$$

The real contribution reads :

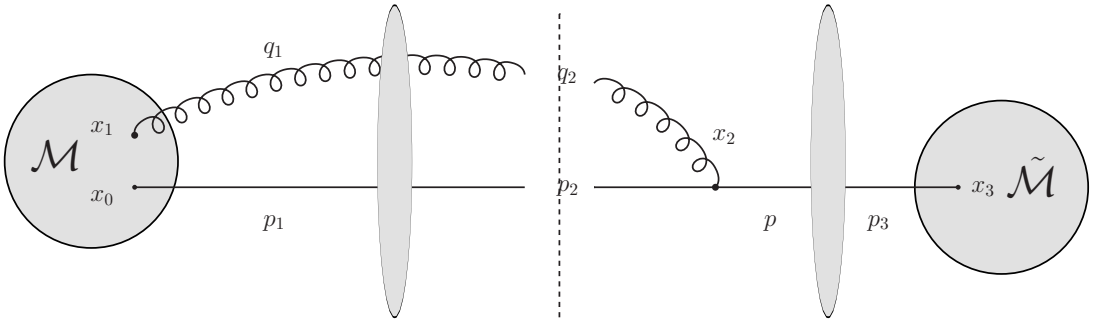

Figure 4.12: Real contribution

$$
\begin{aligned}
I_R \;=\; & \sum_{\lambda_p,\, s_{q_2}} \int \frac{dp_2^+ d^d\vec{p}_2}{(2\pi)^{d+1}} \frac{dq_2^+ d^d\vec{q}_2}{(2\pi)^{d+1}} \left[\int d^D x_1 d^D x_0 \bar{u}\left(p_2,\, x_0\right) \mathcal{M}^{\mu}\left(x_1,\, x_0\right) \epsilon_{\nu}^{*}\left(q_2,\, x_1\right) \right] \\
& \times \left[(ig) \int d^D x_3 d^D x_2 \frac{\bar{u}_{p_2}}{\sqrt{2p_2^+}} \gamma^{\mu} e^{i(p_2 \cdot x_2)} \theta\left(p_2^+\right) \frac{\epsilon^*_{q_2\mu}}{\sqrt{2q_2^+}} e^{i(q_2 . x_2)} \theta\left(q_2^+\right) G\left(x_2,\, x_3\right) \tilde{\mathcal{M}}\left(x_3\right) \right]^* .
\end{aligned}
\tag{4.48}
$$

Again after a couple straightforward manipulations, we can show :

$$
\begin{aligned}
I_R \;=\; & \int d^D x_3 d^D x_1 d^D x_0 \int \frac{d^d\vec{p}_3}{(2\pi)^d} \frac{d^d\vec{p}_2}{(2\pi)^d} \frac{d^d\vec{p}_1}{(2\pi)^d} \frac{d^d\vec{q}_1}{(2\pi)^{d+1}} \\
& \times \int \frac{dp^+ d^d\vec{p}}{(2\pi)^{d+1}} \left[U\left(\vec{p}-\vec{p}_3\right)\right]^* \left[U\left(\vec{p}_{21}\right)\right] \left[U\left(\vec{p}-\vec{p}_2-\vec{q}_1\right)\right] \theta\left(p^+\right) \\
& \times \int dp_2^+ \int dx_2^+ \theta\left(-x_0^+\right) \theta\left(-x_1^+\right) \theta\left(x_2^+\right) \theta\left(-x_3^+\right) \theta\left(p^+ - p_2^+\right) \theta\left(p_2^+\right) \\
& \times \frac{(ig)}{\left(2p^+\right)^2 \left(2p_2^+\right)^2 2\left(p^+ - p_2^+\right)} \mathrm{Tr}\left[\tilde{\mathcal{M}}^*\left(x_3\right) \left(p^+\gamma^- + \hat{p}_{3\perp}\right) \gamma^+ \hat{p} \gamma^{\mu} \hat{p}_2 \gamma^+ \left(p_2^+\gamma^- + \hat{p}_{1\perp}\right) \mathcal{M}^{\nu}\left(x_1,\, x_0\right) \right] \\
& \times \left(g_{\perp\mu\sigma} + \frac{p_{\perp\sigma} - p_{2\perp\sigma}}{p^+ - p_2^+} n_{2\mu} \right) \left(g^{\sigma}_{\perp\nu} - \frac{q^{\sigma}_{1\perp}}{p^+ - p_2^+} n_{2\nu} \right) \\
& \times \exp\left[i x_2^+ \left(\frac{\vec{p}^{\,2} - i0}{2p^+} - \frac{\vec{p}_2^{\,2}}{2p_2^+} - \frac{\left(\vec{p}-\vec{p}_2\right)^2}{2\left(p^+ - p_2^+\right)} \right) \right] \\
& \times \exp\left[i x_0^+ \left(\frac{\vec{p}_1^{\,2} - i0}{2p_2^+} \right) + i x_1^+ \left(\frac{\vec{q}_1^{\,2}}{2\left(p^+ - p_2^+\right)} \right) - i x_3^+ \left(\frac{\vec{p}_3^{\,2} - i0}{2p^+} \right) \right] \\
& \times \exp\left[i p^+ x_{13}^- - i p_2^+ x_{10}^- - i\left(\vec{p}_1 \cdot \vec{x}_0\right) - i\left(\vec{q}_1 \cdot \vec{x}_1\right) + i\left(\vec{p}_3 \cdot \vec{x}_3\right) \right] .
\end{aligned}
\tag{4.49}
$$

By cyclicity of the trace and using the explicit expressions for the gluonic tensors in Eq. (4.47), one can now see that

$$
I_R \;=\; -I_V \,. \tag{4.50}
$$

This is a very general result : in an inclusive cross section the vertices which are after the shockwave in the amplitude will only contribute when one of the shockwaves around the vertex is set to identity, either in the amplitude or in the complex conjugate amplitude. For our process, there is an additional line which does not have a vertex between its two shockwave interactions. Using the previous results, one can conclude that it will contribute to the non-interacting part. As a conclusion, one gets that contributions with a vertex between the shockwaves must only be taken into account when the shockwaves are set to identity in the amplitude or in the complex conjugate amplitude.

4.3.4 Conclusion : computation method

One can use the remarks in the two previous subsections to conclude that we only have to compute the contributions with all the shockwaves in the amplitude or in the complex conjugate amplitude set to identity. For example, diagrams 2 and 5 will contribute as shown in Fig. 4.13.

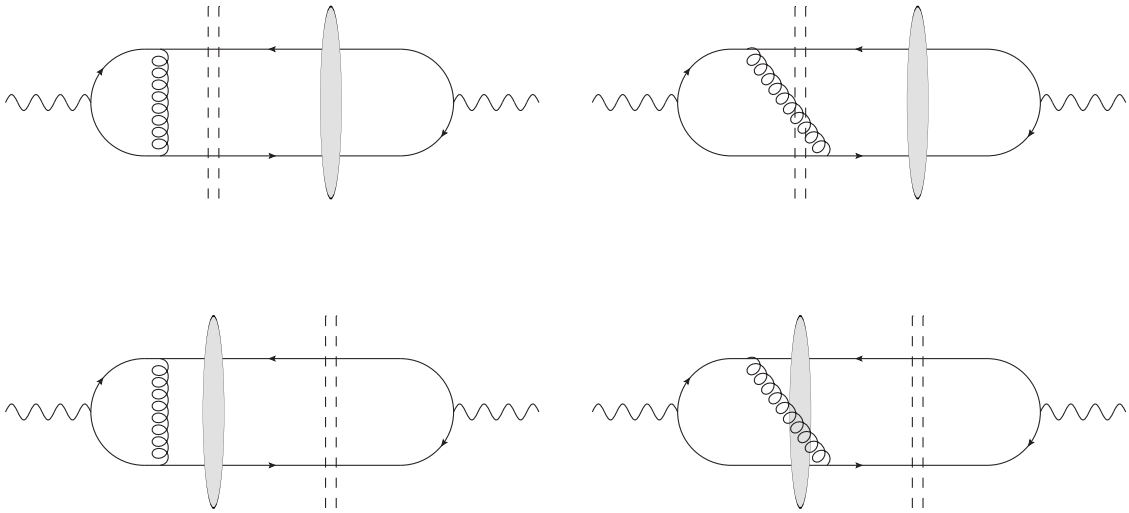

Figure 4.13: Contributions from diagram 2 and diagram 5 to NLO DIS

In practice setting the shockwaves to identity on one side means projecting the Wilson line operators on the other side on the color singlet state (without the additional $\frac{1}{\sqrt{N_c}}$ factor). This is coherent with the fact that $\gamma^* \to \gamma^*$ is of course a color neutral process. As a result of this remark, the operators involved in such a computation are the same as those involved in ours at the level of the amplitude. To obtain the $\gamma^* \to \gamma^*$ at NLO accuracy in the shockwave formalism, one should then take our results for the $\gamma^* \to q\bar{q}$ impact factor in Section 3.6 and for the $\Gamma^* \to q\bar{q}g$ impact factor in Section 3.7, set all the Wilson line operators to identity either in the amplitude or in the complex conjugate amplitude, and integrate over the phase space of the produced particles.

4.3.5 Open charm and charmonium production

Adding a mass : open charm production

Adapting the Feynman rules with the shockwave field from Section 2.2 to the case of massive quarks is actually a straightforward task in mixed space and in momentum space representations of the building blocks. For example the quark propagator in mixed space given by Eq. (2.56) becomes

$$\begin{aligned}\hat{G}\left(x_2,\, x_0\right)|_{x_2^+>0>x_0^+} \;=\; & \int \frac{dp_1^+ d^d p_{1\perp}}{(2\pi)^{d+1}} \int \frac{dp_2^+ d^d p_{2\perp}}{(2\pi)^{d+1}} e^{-ix_2^- p_2^+ - i(p_{2\perp}\cdot x_{2\perp})} e^{ix_0^- p_1^+ + i(p_{1\perp}\cdot x_{0\perp})} 2\pi\delta(p_{12}^+)\theta(p_2^+) \\ & \times e^{ix_2^+ \frac{p_{2\perp}^2 - m^2 + i0}{2p_2^+}} \; e^{-ix_0^+ \frac{p_{1\perp}^2 - m^2 + i0}{2p_1^+}} \frac{\gamma^- p_2^+ + \hat{p}_{2\perp} + m}{2p_2^+} \gamma^+ U(p_{21\perp}) \frac{\gamma^- p_1^+ + \hat{p}_{1\perp} + m}{2p_1^+}.\end{aligned} \tag{4.51}$$

Then every step until the evaluation of integrals (3.64-3.67) can be adapted without any concern. The integrals, however, become more complicated. We believe that contrary to our result, which is written as a finite integral over one real parameter, the result in the massive case will finally be written as a finite integral over two real parameters. The cancellation of divergences will be different due to the absence of collinear divergences and to the presence of quark mass renormalization terms.

Apart from these remarks, the main computation steps are the same for massive quarks. By adding a mass to our result for the NLO $q\bar{q}$ production impact factor, one immediately gets the impact factor for the production of massive quarks. With further adjustments, one could also get the NLO impact factor for the production of a charmonium, for example a J/ψ meson.

Charmonium production

Although J/ψ mesons were first observed more than 40 years ago, the theoretical mechanism for their production is still to be fully understood and the validity of some models remains a subject of discussions[7].

[7]For recent reviews see for example [137, 138]

The two main competing models for charmonium production are the Color Evaporation Model (CEM) and the Non-Relativistic QCD (NRQCD) formalism.

The Color Evaporation Model relies on the *local duality hypothesis*, which states that a heavy quark pair $Q\bar{Q}$ with an invariant mass below the threshold for the production of a pair of the lightest meson which contains Q will eventually produce a bound $Q\bar{Q}$ state after a series of randomized soft interactions between its production and its confinement in $\frac{1}{N_c^2}$ cases, independently of its color and spin. The $\frac{1}{N_c^2}$ factor corresponds to the probability for the pair to be in a color singlet state after such a series of randomized color rotations. It is assumed that the distribution between all possible charmonium states is universal.

Thus the way one should compute the cross section for J/ψ production in the CEM consists in computing all Feynman diagrams for the production of an open $c\bar{c}$ pair, summing over all spins and colors, and integrating w.r.t. the invariant mass of the pair from the $(2m_c)^2$ threshold to the D meson mass threshold $(2m_D)^2$. Then one must add the supposedly universal fraction $F_{J/\psi}$ which corresponds to the factor $\frac{1}{N_c^2}$ times the probability for the charmonium state to be a J/ψ among all the possible charmonium states. This assertion relies on the additional hypothesis that the number of J/ψ mesons produced above the $(2m_D)^2$ threshold is negligible when compared to the quantity produced below it. To sum up, in the CEM the cross section for the production of a J/ψ is related to the cross section for the production of a $c\bar{c}$ pair via :

$$\sigma_{J/\psi} = F_{J/\psi} \int_{4m_c^2}^{4m_D^2} dM^2 \frac{d\sigma_{c\bar{c}}}{dM^2}, \tag{4.52}$$

where M^2 is the invariant mass of the $c\bar{c}$ pair and the value for the fraction $F_{J/\psi}$ must be taken from previous data fits, see for example [139].

As a conclusion if one relies on the CEM, one could directly obtain the cross section for J/ψ production from the massive extension of our results by integrating w.r.t. the invariant mass of the charm pair.

Adapting our results to an NRQCD computation requires more involved steps. This formalism relies on the expansion of the onium wavefunction w.r.t. the velocity of its constituents :

$$|J/\psi\rangle = O(1) \left| Q\bar{Q}[^3S_1^{(1)}] \right\rangle + O(v) \left| Q\bar{Q}[^3S_1^{(8)}]g \right\rangle + O(v^2). \tag{4.53}$$

It is assumed that all the non-perturbative physics is encoded in this wavefunction. Note that there is no rigorous proof of NRQCD factorization between a hard part and the wavefunction at all orders, and the general relative importance of the terms in the expansion of the wavefunction remains unknown.
The NRQCD formalism is quite similar to the collinear factorization framework. One computes the hard part for the production of a collinear quark-antiquark pair with the right quantum numbers and uses the corresponding effective vertices, obtained from the NRQCD expansion. For example the effective vertex for the first term in Eq. 4.53 reads :

$$v_\beta^j(q_2)\bar{u}_\alpha^i(q_1) \to \frac{\delta^{ij}}{4N_c} \left(\frac{\langle \mathcal{O}_1 \rangle_{J/\psi}}{m} \right)^{\frac{1}{2}} \left[\hat{\varepsilon}^*_{J/\psi} (\hat{k}_{J/\psi} + M) \right]_{\alpha\beta}, \tag{4.54}$$

which corresponds the transition from a quark and an antiquark of mass m with respective Lorentz indices α and β, respective colors i and j and respective momenta q_1 and q_2 to a J/ψ with momentum $k_{J/\psi}$, polarization $\varepsilon_{J/\psi}$ and mass M. In the lowest orders in the NRQCD expansion, one can use $M = 2m$ and $k_{J/\psi} = 2q_1 = 2q_2 \equiv 2q$. The operator $\mathcal{O}_1$ arises from the non relativistic hamiltonian, and its vacuum expectation value can be fitted to data, for example via its contribution to the $J/\psi \to \mu^+\mu^-$ decay rate.
Similarly the effective vertex for the second term in Eq. 4.53 reads :

$$\left[v_\beta^j(q_2)\bar{u}_\alpha^i(q_1) \right]^a \to \frac{t^a_{ji}}{4N_c} \left(\frac{\langle \mathcal{O}_8 \rangle_{J/\psi}}{m} \right)^{\frac{1}{2}} \left[\hat{\varepsilon}^*_{J/\psi} (\hat{k}_{J/\psi} + M) \right]_{\alpha\beta}. \tag{4.55}$$

For example if one considers a process like $\gamma^* p \to J/\psi p$, charge parity conservation implies that there are two types of hard parts to compute. The first term in Eq. 4.53 (to which we will refer as the color singlet contribution) must be convoluted with the hard part for the production of a quark-antiquark pair in the color singlet state and a gluon, and the second term in Eq. 4.53 (to which we will refer as the color singlet contribution) must be convoluted with the hard part for the production of a quark-antiquark pair in the color octet state without the additional gluon.

As stated before, there is no general estimate of the relative importance of the color singlet contribution and the color octet contribution once convoluted with the hard part.
In a work in progress[8], we have been studying the production of a forward J/ψ and a backward jet at the LHC. The description we used for this process is very similar to the BFKL description of Mueller-Navelet jets, as shown by squaring the amplitude in Fig. 4.14 : one collinear parton is extracted from each hadron through a PDF, and the hard part is factorized using the usual k_t-factorization picture : two impact factors and a BFKL Green's function linked via off-shell *non-sense* gluons with non-zero transverse momenta.

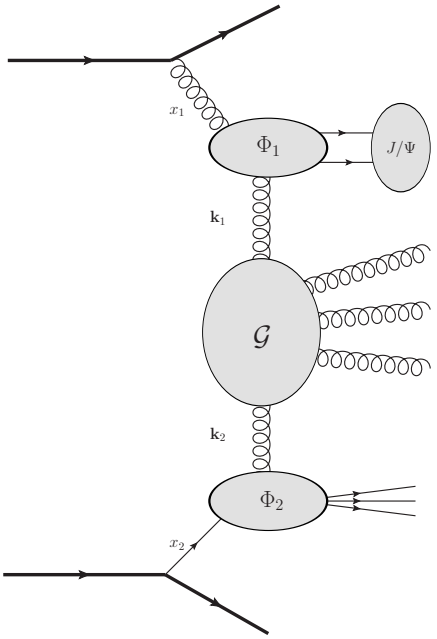

Figure 4.14: The k_t-factorized amplitude for the production of a forward J/ψ meson and a backward jet.

The so-called *production vertex* for the J/ψ (which once squared and integrated becomes the upper impact factor) can be described via NRQCD, in which case both the color singlet and the color octet contribution must be taken into account. Our present results for this study, which incorporate the NLO jet production vertex the NLL BFKL Green's function and the J/ψ production vertex at LO accuracy, tend to show that the color octet contribution (hence the second term in the wavefunction expansion 4.53) dominates the process. This can be seen by considering the diagrams involved for each contribution as shown in Figs. 4.16 and 4.15.

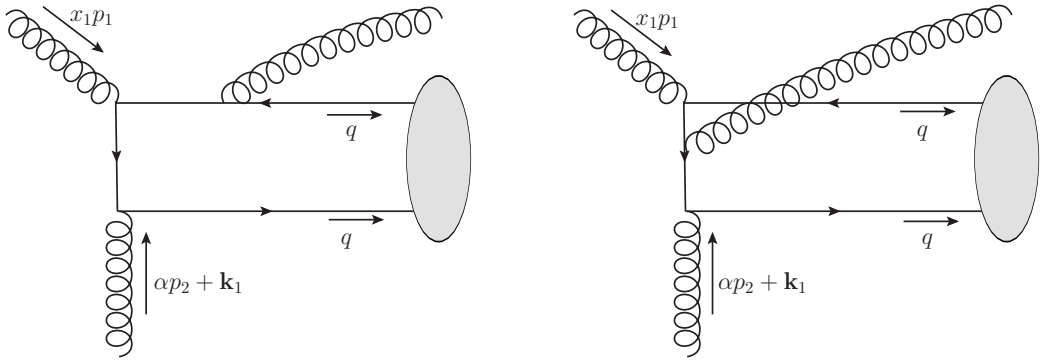

Figure 4.15: Two examples out of the six diagrams contributing to J/ψ production from a $c\bar{c}$ pair in the color singlet state.

[8]see [93] for a preview

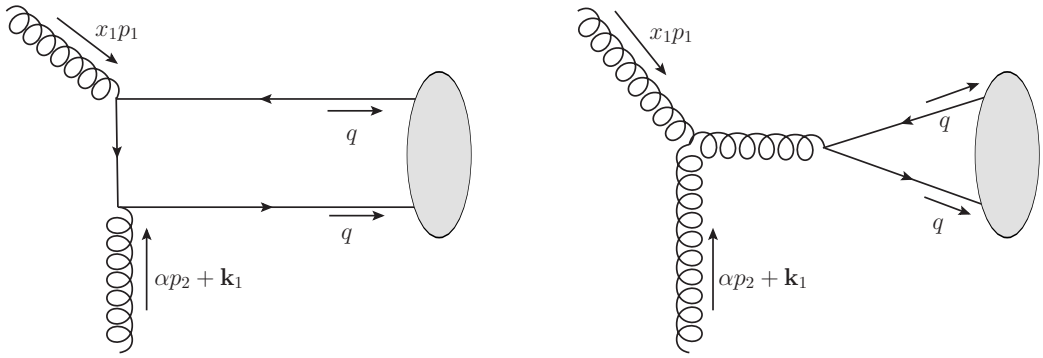

Figure 4.16: Two examples out of the three diagrams contributing to J/ψ production from a $c\bar{c}$ pair in the color octet state.

If one considers a process where the transverse momentum of the J/ψ meson is rather large, it is easy to see that the diagram with the triple gluon vertex will dominate the whole process : the other contributions are suppressed by a $\frac{1}{\vec{k}^2_{J/\psi}}$ factor when compared to this one.

Thus there are processes where the color octet contribution may be sufficient to describe the data. Let us note that for a process involving on-shell gluons in t-channel, the triple-gluon-vertex diagram is excluded by the Landau-Yang theorem, which is the reason why the color singlet contribution will not be subdominating.

While fully adapting the NLO computation described in the first part of this thesis to the production of a J/ψ meson using NRQCD would be impossible due to the presence of the additional gluon in the color singlet contribution, by selecting a process in which the color octet contribution is expected to dominate one should be able to give a good estimate of the J/ψ impact factor. For example if one wants to adapt the computation in this thesis to the process studied in [93], one should add a mass to the quarks and make them collinear, and replace the incoming virtual photon by an on-shell gluon. Such an adaptation is non-straightforward and the required B-JIMWLK evolution will not be the dipole evolution anymore, yet it should be feasible from our results.

Part III

Probing GPDs through the photoproduction of a ρ meson and a photon

4.4 Introduction

The near forward photoproduction of a pair of particles with a large invariant mass is a case for a natural extension of collinear QCD factorization theorems which have been much studied for near forward deeply virtual Compton scattering (DVCS) and deeply virtual meson production [140–145]. In the present chapter, we study the case where a wide angle Compton scattering subprocess $\gamma(q\bar{q}) \to \gamma\rho$ characterized by the large scale $M_{\gamma\rho}$ (the invariant mass of the final state) factorizes from generalized parton distributions. This large scale $M_{\gamma\rho}$ is related to the large transverse momenta transmitted to the final photon and to the final meson, the pair having an overall small transverse momentum. This opens a new way to the extraction of these GPDs and thus to check their universality.

The study of such processes was initiated in Ref. [146, 147], where the process under study was the high energy diffractive photo- (or electro-) production of two vector mesons, the hard probe being the virtual "Pomeron" exchange (and the hard scale being the virtuality of this pomeron), in analogy with the virtual photon exchange occuring in the deep inelastic electroproduction of a meson. A similar strategy has also been advocated in Ref. [148–150] to enlarge the number of processes which could be used to extract information on GPDs.

The process we study here[9]

$$\gamma^{(*)}(q) + N(p_1) \to \gamma(k) + \rho^0(p_\rho, \varepsilon_\rho) + N'(p_2)\,, \tag{4.56}$$

is sensitive to both chiral-even and chiral-odd GPDs due to the chiral-even (resp. chiral-odd) character of the leading twist distribution amplitude (DA) of ρ_L (resp. ρ_T).

Its experimental study should not present major difficulties to large acceptance detectors such as those developed for the 12 GeV upgrade of JLab. The estimated rate depends of course much on the magnitude of the generalized parton distributions, but we show that the experiment is feasible under reasonable assumptions based on their relations to usual parton distributions and to lattice [153–156] calculations.

Let us briefly comment on the extension of the existing factorization proofs in the framework of QCD to our process. The argument is two-folded.

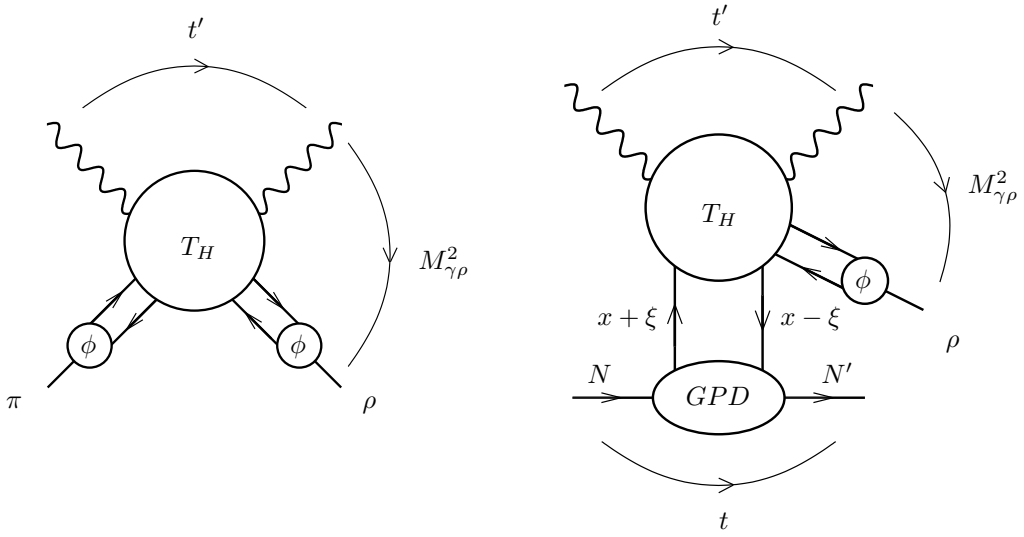

Figure 4.17: a) Factorization of the amplitude for the process $\gamma + \pi \to \gamma + \rho$ at large s and fixed angle (i.e. fixed ratio t'/s); b) replacing one DA by a GPD leads to the factorization of the amplitude for $\gamma + N \to \gamma + \rho + N'$ at large $M^2_{\gamma\rho}$.

The now classical proof of factorization of exclusive scattering at fixed angle and large energy [157] allows to write the leading twist amplitude for the process $\gamma + \pi \to \gamma + \rho$ as the convolution of a mesonic distribution amplitude and a hard scattering subprocess amplitude $\gamma + (q + \bar{q}) \to \gamma + (q + \bar{q})$ with the meson state replaced by a collinear quark-antiquark pair. This is described in Fig. 4.17a. The

[9] Some of the results presented here have been reported previously [151, 152].

demonstration of the absence of any pinch singularity (which is the weak point of the proof for the generic case $A + B \to C + D$) has been proven in the case of interest here [158].

We extract from the factorization procedure of the exclusive meson electroproduction amplitude near the forward region [15] the right to replace in Fig. 4.17a the lower left meson distribution amplitude by a $N \to N'$ GPD, and thus get Fig. 4.17b. Indeed the same collinear factorization property bases the validity of the leading twist approximation which replaces either the meson wave function by its distribution amplitude or the $N \to N'$ transition to its GPDs. A slight difference is that light cone fractions $(z, 1-z)$ leaving the DA are positive, but the corresponding fractions $(x+\xi, \xi - x)$ may be positive or negative in the case of the GPD. Our calculation will show that this difference does not spoil the factorization property, at least at the (leading) order at which we are working here.

The analogy to the timelike Compton scattering process [159–161]:

$$\gamma^{(*)} N \to \gamma^* N' \to \mu^+ \mu^- N' \,, \tag{4.57}$$

where the lepton pair has a large squared invariant mass Q^2, is quite instructive. Although the photon-meson pair in our process (4.56) has a more complex momentum flow, one may draw on this analogy to ascribe the role of the hard scale to the photon-meson pair invariant mass.

In order for the factorization of a partonic amplitude to be legitimate, one should avoid the dangerous kinematical regions where a small momentum transfer is exchanged in the upper blob, namely small $t' = (k-q)^2$ or small $u' = (p_\rho - q)^2$, and the region where strong final state interactions between the ρ meson and the nucleon are dominated by resonance effects, namely where the invariant mass $M^2_{\rho N'} = (p_\rho + p_{N'})^2$ is not large enough.

This chapter is organized as follows. In Section 4.5, we clarify the kinematics we are interested in and set our conventions. Section 4.6 is devoted to the presentation of our model for DAs and GPDs. Then, in Section 4.7, we describe the scattering amplitude of the process under study in the framework of QCD factorization. Section 4.8 presents our results for the unpolarized differential cross section in the kinematics of quasi-real photon beams at JLab where $S_{\gamma N} \sim$ 6-22 GeV^2 . Finally, in Section 4.9 we give estimates of expected rates at JLab. In appendices, we describe several technical details required by analytical and numerical aspects of our calculations.

As a final remark in this introduction, let us stress that our discussion applies as well to the case of electroproduction where a moderate virtuality of the initial photon may help to access the perturbative domain with a lower value of the hard scale $M_{\gamma\rho}$.

4.5 Kinematics

We study the exclusive photoproduction of a vector meson ρ^0 and a real photon on a polarized or unpolarized proton or neutron target

$$\gamma(q, \varepsilon_q) + N(p_1, \lambda) \to \gamma(k, \varepsilon_k) + \rho^0(p_\rho, \varepsilon_\rho) + N'(p_2, \lambda') \,, \tag{4.58}$$

in the kinematical regime of large invariant mass $M_{\gamma\rho}$ of the final photon and meson pair and small momentum transfer $t = (p_2 - p_1)^2$ between the initial and the final nucleons. Roughly speaking, these kinematics mean moderate to large, and approximately opposite, transverse momenta of the final photon and meson. Our conventions are the following. We define

$$P^\mu = \frac{p_1^\mu + p_2^\mu}{2} \,, \; \Delta^\mu = p_2^\mu - p_1^\mu \,, \tag{4.59}$$

and decompose momenta on a Sudakov basis as

$$v^\mu = a\, n^\mu + b\, p^\mu + v_\perp^\mu \,, \tag{4.60}$$

with p and n the lightcone vectors

$$p^\mu = \frac{\sqrt{s}}{2}(1,0,0,1) \qquad n^\mu = \frac{\sqrt{s}}{2}(1,0,0,-1) \qquad p \cdot n = \frac{s}{2} \,, \tag{4.61}$$

and

$$v_\perp^\mu = (0, v^x, v^y, 0) \,, \qquad v_\perp^2 = -\vec{v}_t^{\,2} \,. \tag{4.62}$$

The particle momenta read

$$p_1^\mu = (1+\xi)\,p^\mu + \frac{M^2}{s(1+\xi)}\,n^\mu\,, \quad p_2^\mu = (1-\xi)\,p^\mu + \frac{M^2+\vec{\Delta}_t^{\,2}}{s(1-\xi)}n^\mu + \Delta_\perp^\mu\,, \quad q^\mu = n^\mu\,, \tag{4.63}$$

$$\begin{aligned} k^\mu &= \alpha\,n^\mu + \frac{(\vec{p}_t - \vec{\Delta}_t/2)^2}{\alpha s}\,p^\mu + p_\perp^\mu - \frac{\Delta_\perp^\mu}{2}\,, \\ p_\rho^\mu &= \alpha_\rho\,n^\mu + \frac{(\vec{p}_t + \vec{\Delta}_t/2)^2 + m_\rho^2}{\alpha_\rho s}\,p^\mu - p_\perp^\mu - \frac{\Delta_\perp^\mu}{2}\,, \end{aligned} \tag{4.64}$$

with M, m_ρ the masses of the nucleon and the ρ meson. From these kinematical relations it follows that

$$2\,\xi = \frac{(\vec{p}_t - \frac{1}{2}\vec{\Delta}_t)^2}{s\,\alpha} + \frac{(\vec{p}_t + \frac{1}{2}\vec{\Delta}_t)^2 + m_\rho^2}{s\,\alpha_\rho} \tag{4.65}$$

and

$$1 - \alpha - \alpha_\rho = \frac{2\,\xi\,M^2}{s\,(1-\xi^2)} + \frac{\vec{\Delta}_t^{\,2}}{s\,(1-\xi)}\,. \tag{4.66}$$

The total squared center-of-mass energy of the γ-N system is

$$S_{\gamma N} = (q+p_1)^2 = (1+\xi)s + M^2\,. \tag{4.67}$$

On the nucleon side, the squared transferred momentum is

$$t = (p_2 - p_1)^2 = -\frac{1+\xi}{1-\xi}\vec{\Delta}_t^{\,2} - \frac{4\xi^2 M^2}{1-\xi^2}\,. \tag{4.68}$$

The other useful Mandelstam invariants read

$$s' = (k+p_\rho)^2 = M_{\gamma\rho}^2 = 2\xi\,s\left(1 - \frac{2\,\xi\,M^2}{s(1-\xi^2)}\right) - \vec{\Delta}_t^{\,2}\frac{1+\xi}{1-\xi}\,, \tag{4.69}$$

$$-t' = -(k-q)^2 = \frac{(\vec{p}_t - \vec{\Delta}_t/2)^2}{\alpha}\,, \tag{4.70}$$

$$-u' = -(p_\rho - q)^2 = \frac{(\vec{p}_t + \vec{\Delta}_t/2)^2 + (1-\alpha_\rho)\,m_\rho^2}{\alpha_\rho}\,, \tag{4.71}$$

and

$$M_{\rho N'}^2 = s\left(1 - \xi + \frac{(\vec{p}_t + \vec{\Delta}_t/2)^2 + m_\rho^2}{s\,\alpha_\rho}\right)\left(\alpha_\rho + \frac{M^2 + \vec{\Delta}_t^{\,2}}{s\,(1-\xi)}\right) - \left(\vec{p}_t - \frac{1}{2}\vec{\Delta}_t\right)^2\,. \tag{4.72}$$

The hard scale $M_{\gamma\rho}^2$ is the invariant squared mass of the $(\gamma\,\rho^0)$ system. The leading twist calculation of the hard part only involves the approximated kinematics in the generalized Bjorken limit: neglecting $\vec{\Delta}_t$ in front of $\vec{p}_t$ as well as hadronic masses, it amounts to

$$M_{\gamma\rho}^2 \approx \frac{\vec{p}_t^{\,2}}{\alpha\bar{\alpha}}\,, \tag{4.73}$$

$$\alpha_\rho \approx 1 - \alpha \equiv \bar{\alpha}\,, \tag{4.74}$$

$$\xi = \frac{\tau}{2-\tau} \quad , \quad \tau \approx \frac{M_{\gamma\rho}^2}{S_{\gamma N} - M^2}\,, \tag{4.75}$$

$$-t' \approx \bar{\alpha}\,M_{\gamma\rho}^2 \quad , \quad -u' \approx \alpha\,M_{\gamma\rho}^2\,. \tag{4.76}$$

For further details on kinematics, we refer to Appendix B.3.

The typical cuts that one should apply are $-t', -u' > \Lambda^2$ and $M_{\rho N'}^2 = (p_\rho + p_{N'})^2 > M_R^2$ where $\Lambda \gg \Lambda_{QCD}$ and M_R is a typical baryonic resonance mass. This amounts to cuts in α and $\bar{\alpha}$ at fixed

$M^2_{\gamma\rho}$, which can be translated in terms of u' at fixed $M^2_{\gamma\rho}$ and t. These conditions boil down to a safe kinematical domain $(-u')_{min} \leqslant -u' \leqslant (-u')_{max}$ which we will discuss in more details in Section 4.8.

In the following, we will choose as independent kinematical variables $t, u', M^2_{\gamma\rho}$.

Due to electromagnetic gauge invariance, the scattering amplitude for the production of a ρ_T meson with chiral-odd GPDs and the scattering amplitude for the production of a ρ_L meson with chiral-even GPDs are separately gauge invariant, up to the well known corrections of order $\frac{\Delta_T}{\sqrt{s}}$ which have been much studied for the DVCS case [162, 163]. We choose the axial gauge $p_\mu \, \varepsilon^\mu_k = 0$ and parametrize the polarization vector of the final photon in terms of its transverse components

$$\varepsilon^\mu_k = \varepsilon^\mu_{k\perp} - \frac{\varepsilon_{k\perp} \cdot k_\perp}{p \cdot k} p^\mu \,, \tag{4.77}$$

while the initial photon polarization is simply written as

$$\varepsilon^\mu_q = \varepsilon^\mu_{q\perp} \,. \tag{4.78}$$

We will use the transversity relation $p_\rho \cdot \varepsilon_\rho = 0$ to express the polarization of the ρ meson in terms of only its transverse components and its component along n, using

$$n \cdot \varepsilon_\rho = \frac{1}{\alpha_\rho} \left[\frac{p^2_\perp}{\alpha_\rho s} (p \cdot \varepsilon_\rho) + (p_\perp \cdot \varepsilon_{\rho\perp}) \right] . \tag{4.79}$$

4.6 Non-perturbative ingredients: DAs and GPDs

In this section, we describe the way the non-perturbative quantities which enter the scattering amplitude are parametrized.

4.6.1 GPD factorization

GPDs are the non-forward extensions of PDFs. The way one factorizes a process with a GPD is very similar to the DA factorization scheme we introduced in 4.2.1 : the hard part and the non-perturbative part are factorized in spinor space and in color space using Fierz identities. Factorization in the space of momenta is a bit more involved. It can be shown that such a process can be written as the convolution of a hard part, computed with a pair of collinear on-shell partons carrying respective momenta $(x+\xi)p$ (incoming) and $(x-\xi)p$ (outgoing), where ξ is the skewness parameter, and a GPD, integrated over $x \in [-1, 1]$. See figure 4.18.

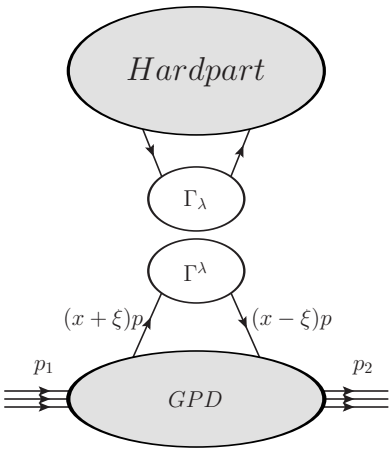

Figure 4.18: Collinear factorization involving a GPD

Thus for our process which combines the factorization of a DA and of a GPD, the amplitude is written as the integral over $(x, z) \in [-1, 1] \times [0, 1]$ of the product of the hart part, a GPD (depending on x and ξ) and a DA (depending on z). The exact formulae can be found in section 4.7.
We will now describe the expressions used for the non-perturbative matrix elements, and extract our parameterization for the GPDs and the DAs.

4.6.2 Distribution amplitudes for the ρ meson

The chiral-even lightcone DA for a longitudinally polarized vector meson ρ_L^0 is defined, at the leading twist 2, by the matrix element [127]

$$\langle 0|\bar{u}(0)\gamma^\mu u(x)|\rho^0(p_\rho,\varepsilon_{\rho L})\rangle = \frac{1}{\sqrt{2}} p_\rho^\mu f_{\rho^0} \int_0^1 dz\; e^{-izp_\rho\cdot x}\; \phi_\parallel(z), \tag{4.80}$$

with $f_{\rho^0} = 216\,\text{MeV}$, while the chiral-odd lightcone DA for the transversely polarized meson vector ρ_T^0 is defined as:

$$\langle 0|\bar{u}(0)\sigma^{\mu\nu} u(x)|\rho^0(p_\rho,\varepsilon_{\rho\pm})\rangle = \frac{i}{\sqrt{2}}(\varepsilon_{\rho\pm}^\mu p_\rho^\nu - \varepsilon_{\rho\pm}^\nu p_\rho^\mu) f_\rho^\perp \int_0^1 dz\; e^{-izp_\rho\cdot x}\; \phi_\perp(z), \tag{4.81}$$

where $\varepsilon_{\rho\pm}^\mu$ is the ρ-meson transverse polarization and with $f_\rho^\perp$ = 160 MeV. The factor $\frac{1}{\sqrt{2}}$ takes into account the quark structure of the ρ^0-meson: $|\rho^0\rangle = \frac{1}{\sqrt{2}}(|u\bar{u}\rangle - |d\bar{d}\rangle)$. We shall use the asymptotic form for the normalized functions $\phi_\parallel$ and $\phi_\perp$

$$\begin{aligned} \phi_\parallel(z) &= 6z(1-z)\,, \\ \phi_\perp(z) &= 6z(1-z)\,. \end{aligned} \tag{4.82}$$

4.6.3 Generalized parton distributions

The chiral-even generalized parton distributions of a parton q (here $q = u,\ d$) in the nucleon target (λ and λ' are the lightcone helicities of the nucleons with respective momenta p_1 and p_2) are defined by [164]:

$$\begin{aligned} &\langle p(p_2,\lambda')|\,\bar{q}\left(-\frac{y}{2}\right)\,\gamma^+ q\left(\frac{y}{2}\right)|p(p_1,\lambda)\rangle \\ &= \int_{-1}^1 dx\; e^{-\frac{i}{2}x(p_1^+ + p_2^+)y^-}\,\bar{u}(p_2,\lambda')\,\left[\gamma^+ H^q(x,\xi,t) + \frac{i}{2m}\sigma^{+\,\alpha}\Delta_\alpha\, E^q(x,\xi,t)\right] u(p_1,\lambda)\,, \end{aligned} \tag{4.83}$$

and

$$\begin{aligned} &\langle p(p_2,\lambda')|\,\bar{q}\left(-\frac{y}{2}\right)\,\gamma^+\gamma^5 q\left(\frac{y}{2}\right)|p(p_1,\lambda)\rangle \\ &= \int_{-1}^1 dx\; e^{-\frac{i}{2}x(p_1^+ + p_2^+)y^-}\,\bar{u}(p_2,\lambda')\,\left[\gamma^+\gamma^5 \tilde{H}^q(x,\xi,t) + \frac{1}{2m}\gamma^5\Delta^+\,\tilde{E}^q(x,\xi,t)\right] u(p_1,\lambda)\,. \end{aligned} \tag{4.84}$$

The transversity generalized parton distribution of a quark q is defined by:

$$\begin{aligned} &\langle p(p_2,\lambda')|\,\bar{q}\left(-\frac{y}{2}\right)\,i\,\sigma^{+j} q\left(\frac{y}{2}\right)|p(p_1,\lambda)\rangle \\ &= \int_{-1}^1 dx\; e^{-\frac{i}{2}x(p_1^+ + p_2^+)y^-}\,\bar{u}(p_2,\lambda')\,\left[i\,\sigma^{+j} H_T^q(x,\xi,t) + \ldots\right] u(p_1,\lambda)\,, \end{aligned} \tag{4.85}$$

where $\ldots$ denote the remaining three chiral-odd GPDs which contributions are omitted in the present analysis.

We parametrize the GPDs in terms of double distributions (DDs) [165]

$$H^q(x,\xi,t=0) = \int_\Omega d\beta\, d\alpha\; \delta(\beta + \xi\alpha - x)\, \mathcal{F}^q(\beta,\alpha,t=0)\,, \tag{4.86}$$

where $\mathcal{F}^q$ is a generic quark DD and $\Omega = \{|\beta| + |\alpha| \leqslant 1\}$ is its support domain. A D-term contribution, necessary to be completely general while fulfilling the polynomiality constraints, could be added. In our parameterization, we do not include such an arbitrary term. Note that similar GPD parameterizations have been used in Ref. [166].

As shown in Section 4.7.2, with a good approximation we will only use the three GPDs H, $\tilde{H}$ and H_T. We adhere on Radyushkin-type parameterization and write the unpolarized DD f^q and the transversity DD f_T^q in the form

$$f^q(\beta,\alpha,t=0) = \Pi(\beta,\alpha)\, q(\beta)\Theta(\beta) - \Pi(-\beta,\alpha)\,\bar{q}(-\beta)\,\Theta(-\beta)\,, \tag{4.87}$$

and [148]

$$f_T^q(\beta,\alpha,t=0) = \Pi(\beta,\alpha)\,\delta q(\beta)\,\Theta(\beta) - \Pi(-\beta,\alpha)\,\delta\bar{q}(-\beta)\,\Theta(-\beta)\,, \tag{4.88}$$

while the polarized DD $\tilde{f}^q$ reads

$$\tilde{f}^q(\beta,\alpha,t=0) = \Pi(\beta,\alpha)\,\Delta q(\beta)\,\Theta(\beta) + \Pi(-\beta,\alpha)\,\Delta\bar{q}(-\beta)\,\Theta(-\beta)\,, \tag{4.89}$$

where $\Pi(\beta,\alpha) = \frac{3}{4}\frac{(1-\beta)^2-\alpha^2}{(1-\beta)^3}$ is a profile function and q, $\bar{q}$ are the quark and antiquark unpolarized parton distribution functions (PDFs), Δq, $\Delta\bar{q}$, are the quark and antiquark polarized PDFs and δq, $\delta\bar{q}$ are the quark and antiquark transversity PDFs.

We now give specific formulas for the three GPDs which will be used in the present study. The GPD H^q reads

$$\begin{aligned}
H^q(x,\xi,t=0) &= \Theta(x>\xi)\int_{\frac{-1+x}{1+\xi}}^{\frac{1-x}{1-\xi}} dy\,\frac{3}{4}\frac{(1-x+\xi y)^2-y^2}{(1-x+\xi y)^3}q(x-\xi y) \\
&+ \Theta(\xi>x>-\xi)\left[\int_{\frac{-1+x}{1+\xi}}^{\frac{x}{\xi}} dy\,\frac{3}{4}\frac{(1-x+\xi y)^2-y^2}{(1-x+\xi y)^3}q(x-\xi y)\right. \\
&- \left.\int_{\frac{x}{\xi}}^{\frac{1+x}{1+\xi}} dy\,\frac{3}{4}\frac{(1+x-\xi y)^2-y^2}{(1+x-\xi y)^3}\bar{q}(-x+\xi y)\right] \\
&- \Theta(-\xi>x)\int_{-\frac{1+x}{1-\xi}}^{\frac{1+x}{1+\xi}} dy\,\frac{3}{4}\frac{(1+x-\xi y)^2-y^2}{(1+x-\xi y)^3}\bar{q}(-x+\xi y)\,.
\end{aligned} \tag{4.90}$$

Similarly, the transversity GPD H_T^q reads

$$\begin{aligned}
H_T^q(x,\xi,t=0) &= \Theta(x>\xi)\int_{\frac{-1+x}{1+\xi}}^{\frac{1-x}{1-\xi}} dy\,\frac{3}{4}\frac{(1-x+\xi y)^2-y^2}{(1-x+\xi y)^3}\delta q(x-\xi y) \\
&+ \Theta(\xi>x>-\xi)\left[\int_{\frac{-1+x}{1+\xi}}^{\frac{x}{\xi}} dy\,\frac{3}{4}\frac{(1-x+\xi y)^2-y^2}{(1-x+\xi y)^3}\delta q(x-\xi y)\right. \\
&- \left.\int_{\frac{x}{\xi}}^{\frac{1+x}{1+\xi}} dy\,\frac{3}{4}\frac{(1+x-\xi y)^2-y^2}{(1+x-\xi y)^3}\delta\bar{q}(-x+\xi y)\right] \\
&- \Theta(-\xi>x)\int_{-\frac{1+x}{1-\xi}}^{\frac{1+x}{1+\xi}} dy\,\frac{3}{4}\frac{(1+x-\xi y)^2-y^2}{(1+x-\xi y)^3}\delta\bar{q}(-x+\xi y)\,,
\end{aligned} \tag{4.91}$$

while the $\tilde{H}^q$ GPD reads

$$\begin{aligned}
\tilde{H}^q(x,\xi,t=0) &= \Theta(x>\xi)\int_{\frac{-1+x}{1+\xi}}^{\frac{1-x}{1-\xi}} dy\,\frac{3}{4}\frac{(1-x+\xi y)^2-y^2}{(1-x+\xi y)^3}\Delta q(x-\xi y) \\
&+ \Theta(\xi>x>-\xi)\left[\int_{\frac{-1+x}{1+\xi}}^{\frac{x}{\xi}} dy\,\frac{3}{4}\frac{(1-x+\xi y)^2-y^2}{(1-x+\xi y)^3}\Delta q(x-\xi y)\right. \\
&+ \left.\int_{\frac{x}{\xi}}^{\frac{1+x}{1+\xi}} dy\,\frac{3}{4}\frac{(1+x-\xi y)^2-y^2}{(1+x-\xi y)^3}\Delta\bar{q}(-x+\xi y)\right] \\
&+ \Theta(-\xi>x)\int_{-\frac{1+x}{1-\xi}}^{\frac{1+x}{1+\xi}} dy\,\frac{3}{4}\frac{(1+x-\xi y)^2-y^2}{(1+x-\xi y)^3}\Delta\bar{q}(-x+\xi y)\,.
\end{aligned} \tag{4.92}$$

Since our process selects the exchange of charge conjugation $C=-1$ in the $t-$channel, we now consider the corresponding valence GPDs

$$H^{q(-)}(x,\xi,t) = H^q(x,\xi,t) + H^q(-x,\xi,t) \tag{4.93}$$

and

$$H_T^{q(-)}(x,\xi,t) = H_T^q(x,\xi,t) + H_T^q(-x,\xi,t) \tag{4.94}$$

which have the symmetry properties $H^{q(-)}(x,\xi,t) = H^{q(-)}(-x,\xi,t)$ and $H_T^{q(-)}(x,\xi,t) = H_T^{q(-)}(-x,\xi,t)$, as well as the valence GPD

$$\tilde{H}^{q(-)}(x,\xi,t) = \tilde{H}^{q}(x,\xi,t) - \tilde{H}^{q}(-x,\xi,t)\,, \tag{4.95}$$

which has the antisymmetry property $\tilde{H}^{q(-)}(x,\xi,t) = -\tilde{H}^{q(-)}(-x,\xi,t)\,.$

Introducing the symmetric valence distributions

$$q_{\rm val}(x) = \theta(x)[q(x) - \bar{q}(x)] + \theta(-x)[q(-x) - \bar{q}(-x)] \tag{4.96}$$

and

$$\delta q_{\rm val}(x) = \theta(x)[\delta q(x) - \delta\bar{q}(x)] + \theta(-x)[\delta q(-x) - \delta\bar{q}(-x)]\,, \tag{4.97}$$

and the antisymmetric valence distribution

$$\Delta q_{\rm val}(x) = \theta(x)[\Delta q(x) - \Delta\bar{q}(x)] - \theta(-x)[\Delta q(-x) - \Delta\bar{q}(-x)]\,, \tag{4.98}$$

the set of GPDs which we use in our computation of the scattering amplitude reads

$$\begin{aligned}\frac{1}{2}H^{q(-)}(x,\xi,t=0) &= \frac{1}{2}\left[\left(\Theta(x>\xi)\int_{\frac{-1+x}{1+\xi}}^{\frac{1-x}{1-\xi}} dy\ \frac{3}{4}\frac{(1-x+\xi y)^2-y^2}{(1-x+\xi y)^3} q_{\rm val}(x-\xi y)\right.\right.\\ &+ \left.\left.\Theta(\xi>x>-\xi)\int_{\frac{-1+x}{1+\xi}}^{\frac{x}{\xi}} dy\ \frac{3}{4}\frac{(1-x+\xi y)^2-y^2}{(1-x+\xi y)^3}\, q_{\rm val}(x-\xi y)\right)\right.\\ &+ \left.(x\leftrightarrow -x)\right]\,,\end{aligned} \tag{4.99}$$

$$\begin{aligned}\frac{1}{2}H_T^{q(-)}(x,\xi,t=0) &= \frac{1}{2}\left[\left(\Theta(x>\xi)\int_{\frac{-1+x}{1+\xi}}^{\frac{1-x}{1-\xi}} dy\ \frac{3}{4}\frac{(1-x+\xi y)^2-y^2}{(1-x+\xi y)^3}\delta q_{\rm val}(x-\xi y)\right.\right.\\ &+ \left.\left.\Theta(\xi>x>-\xi)\int_{\frac{-1+x}{1+\xi}}^{\frac{x}{\xi}} dy\ \frac{3}{4}\frac{(1-x+\xi y)^2-y^2}{(1-x+\xi y)^3}\, \delta q_{\rm val}(x-\xi y)\right)\right.\\ &+ \left.(x\leftrightarrow -x)\right]\,,\end{aligned} \tag{4.100}$$

and

$$\begin{aligned}\frac{1}{2}\tilde{H}^{q(-)}(x,\xi,t=0) &= \frac{1}{2}\left[\left(\Theta(x>\xi)\int_{\frac{-1+x}{1+\xi}}^{\frac{1-x}{1-\xi}} dy\ \frac{3}{4}\frac{(1-x+\xi y)^2-y^2}{(1-x+\xi y)^3}\Delta q_{\rm val}(x-\xi y)\right.\right.\\ &+ \left.\left.\Theta(\xi>x>-\xi)\int_{\frac{-1+x}{1+\xi}}^{\frac{x}{\xi}} dy\ \frac{3}{4}\frac{(1-x+\xi y)^2-y^2}{(1-x+\xi y)^3}\, \Delta q_{\rm val}(x-\xi y)\right)\right.\\ &- \left.(x\leftrightarrow -x)\right]\,.\end{aligned} \tag{4.101}$$

4.6.4 Numerical modeling

For the various PDFs, we neglect any QCD evolution (in practice, we take a fixed factorization scale $\mu_F^2 = 10\ {\rm GeV}^2$) and we use the following models:

- For $xq(x)$, we rely on the GRV-98 parameterization [167], as made available from the Durham database. We neglect the uncertainty of this parameterization, considering only the central value set of parameters.

  In Fig. 4.19, we show the resulting GPDs $H^{u(-)}$ and $H^{d(-)}$ for $\xi = .1$ corresponding in our process to the typical value $S_{\gamma N} = 20\ {\rm GeV}^2$ and $M_{\gamma\rho}^2 = 3.5\ {\rm GeV}^2$.

- For $x\Delta q(x)$, we rely on the GRSV-2000 parameterization [168], as made available from the Durham database. Two scenarios are proposed in this parameterization: the "standard", *i.e.* with flavor-symmetric light sea quark and antiquark distributions, and the "valence" scenario with completely flavor-asymmetric light sea densities. We use both of them in order to evaluate the order of magnitude of the theoretical uncertainty.

  In Fig. 4.20, we show the resulting GPDs $\tilde{H}^{u(-)}$ and $\tilde{H}^{u(-)}$ for $\xi = .1$ corresponding in our process to the typical value $S_{\gamma N} = 20\ {\rm GeV}^2$ and $M_{\gamma\rho}^2 = 3.5\ {\rm GeV}^2$.

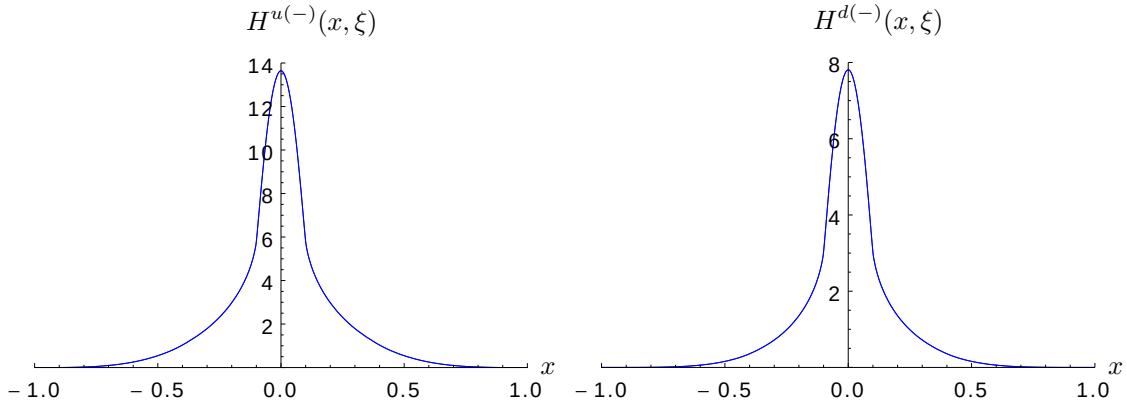

Figure 4.19: Models for the GPDs $H^{u(-)}$ and $H^{d(-)}$ for $\xi = .1$, a value corresponding to $S_{\gamma N} = 20$ GeV^2 and $M^2_{\gamma\rho} = 3.5$ GeV^2.

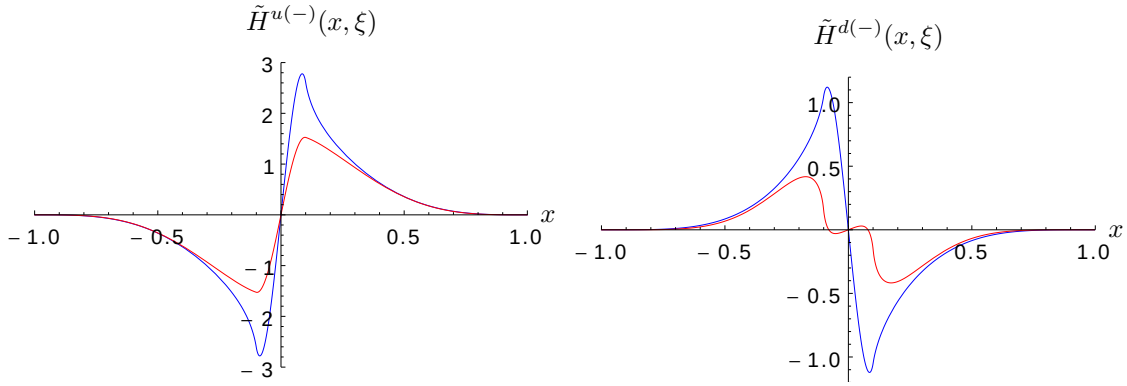

Figure 4.20: Models for the GPDs $\tilde{H}^{u(-)}$ and $\tilde{H}^{d(-)}$ for $\xi = .1$, a value corresponding to $S_{\gamma N} = 20$ GeV^2 and $M^2_{\gamma\rho} = 3.5$ GeV^2.

- For $x\delta q(x)$ we rely on a parameterization performed for TMDs (based on a fit of azimuthal asymmetries in semi-inclusive deep inelastic scattering), from which the transversity PDFs $x\delta q(x)$ are obtained as a limiting case [169]. These transversity PDFs are parametrized as

$$\delta q(x) = \frac{1}{2}\mathcal{N}_q^T(x)[q(x) + \Delta(x)] \tag{4.102}$$

with

$$\mathcal{N}_q^T(x) = N_q^T x^\alpha (1-x)^\beta \frac{(\alpha+\beta)^{(\alpha+\beta)}}{\alpha^\alpha \beta^\beta}. \tag{4.103}$$

Since this parameterization itself relies on the knowledge of $xq(x)$ and $x\Delta q(x)$, we will evaluate the uncertainty on these PDFs by two means: first by passing from the "standard" to the "valence" polarized PDFs (see above), second by performing a variation of the set of parameters N_q^T, α, β, using the χ^2 distribution of these parameters as used in Ref. [169][10]. We further discuss our procedure in Section 4.8.6.

In Fig. 4.21, we show the resulting GPDs $H_T^{u(-)}$ and $H_T^{d(-)}$ for $\xi = .1$ corresponding in our process to the typical value $S_{\gamma N} = 20$ GeV^2 and $M^2_{\gamma\rho} = 3.5$ GeV^2.

[10] We thank S. Melis for providing us the complete set of parameters with the corresponding χ^2 distribution.

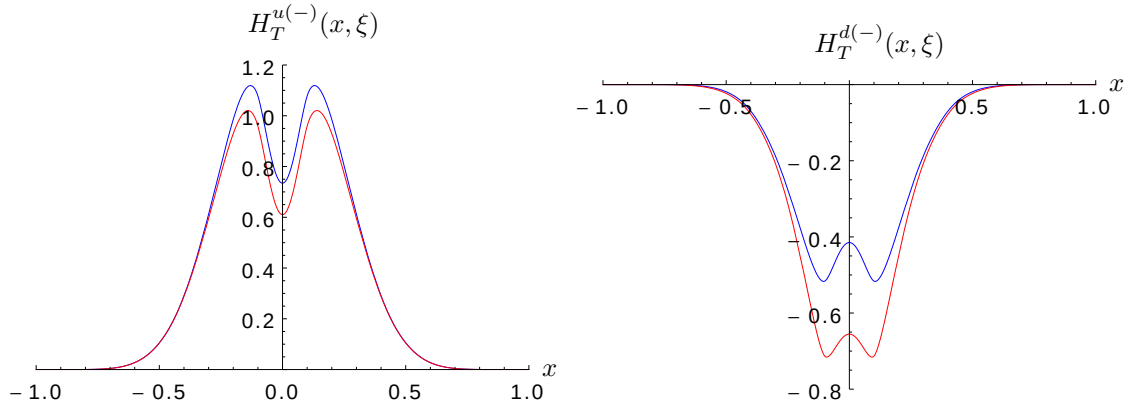

Figure 4.21: Models for the GPDs $H_T^{u(-)}$ and $H_T^{d(-)}$ for $\xi = .1$, a value corresponding to $S_{\gamma N} = 20$ GeV^2 and $M^2_{\gamma\rho} = 3.5$ GeV^2.

In order to evaluate the scattering amplitudes of our process, we calculate, for each of the above three types of GPDs, sets of u and d quarks GPDs indexed by $M^2_{\gamma\rho}$, *i.e.* ultimately by ξ given by

$$\xi = \frac{M^2_{\gamma\rho}}{2(S_{\gamma N} - M^2) - M^2_{\gamma\rho}} \tag{4.104}$$

We vary $M^2_{\gamma\rho}$ from 2.2 GeV ^{2} up to 10 GeV ^{2}, with a step of 0.1 GeV ^{2}, in order to have a full coverage of $M^2_{\gamma\rho}$ for the case $S_{\gamma N} = 20$ GeV ^{2}, see Appendix B.4.

For each $M^2_{\gamma\rho}$, the GPDs are computed as tables of 1000 values for x from -1 to 1. Figs. 4.19, 4.20 and 4.21 are examples of these sets.

4.7 The Scattering Amplitude

4.7.1 Analytical part

Let us now consider the computation of the scattering amplitude of our process (4.58). When the hard scale is large enough, it is possible to study it in the framework of collinear QCD factorization, where the squared invariant mass of the (γ, ρ^0) system $M^2_{\gamma\rho}$ is taken as the factorization scale. We write the scattering amplitude of our process (4.58), taking into account the fact that the ρ^0 meson is described as $\frac{u\bar{u}-d\bar{d}}{\sqrt{2}}$:

$$\mathcal{M}_{\parallel,\perp}(t, M^2_{\gamma\rho}, u') = \frac{1}{\sqrt{2}}(\mathcal{M}^u_{\parallel,\perp} - \mathcal{M}^d_{\parallel,\perp}) \tag{4.105}$$

where $\mathcal{M}^u_{\parallel,\perp}$ and $\mathcal{M}^d_{\parallel,\perp}$ are expressed in terms of form factors $\mathcal{H}^q, \mathcal{E}, \tilde{\mathcal{H}}^q, \tilde{\mathcal{E}}^q$ and $\mathcal{H}^q_{T\perp j}, \tilde{\mathcal{H}}^q_{T\perp j}, \mathcal{E}^q_{T\perp j}, \tilde{\mathcal{E}}^q_{T\perp j}$, analogous to Compton form factors in DVCS, in the factorized form and read

$$\mathcal{M}^q_{\parallel} \equiv \frac{1}{n\cdot p}\bar{u}(p_2,\lambda')\Big[\hat{n}\mathcal{H}^q(\xi,t) + \frac{i\,\sigma^{n\,\alpha}\Delta_\alpha}{2m}\mathcal{E}^q(\xi,t) + \hat{n}\gamma^5\tilde{\mathcal{H}}^q(\xi,t) + \frac{n\cdot\Delta}{2m}\gamma^5\,\tilde{\mathcal{E}}^q(\xi,t)\Big]u(p_1,\lambda) \tag{4.106}$$

in the chiral-even case, and

$$\begin{aligned}\mathcal{M}^q_{\perp} \;\equiv\; & \frac{1}{n\cdot p}\,\bar{u}(p_2,\lambda')\,\Big[i\,\sigma^{nj}\mathcal{H}^q_{T\perp j}(\xi,t) + \frac{P\cdot n\,\Delta^j - \Delta\cdot n\,P^j}{m^2}\tilde{\mathcal{H}}^q_{T\perp j}(\xi,t) \\ & + \frac{\gamma\cdot n\,\Delta^j - \Delta\cdot n\,\gamma^j}{2m}\mathcal{E}^q_{T\perp j}(\xi,t) + \frac{\gamma\cdot n\,P^j - P\cdot n\,\gamma^j}{m}\tilde{\mathcal{E}}^q_{T\perp j}(\xi,t)\Big]\,u(p_1,\lambda)\end{aligned} \tag{4.107}$$

in the chiral-odd case.

For convenience, we now define

$$\mathcal{M}^q(t, M^2_{\gamma\rho}, p_T) = \equiv \int_{-1}^{1} dx \int_0^1 dz\, T^q(t, M^2_{\gamma\rho}, p_T, x, z)\,. \tag{4.108}$$

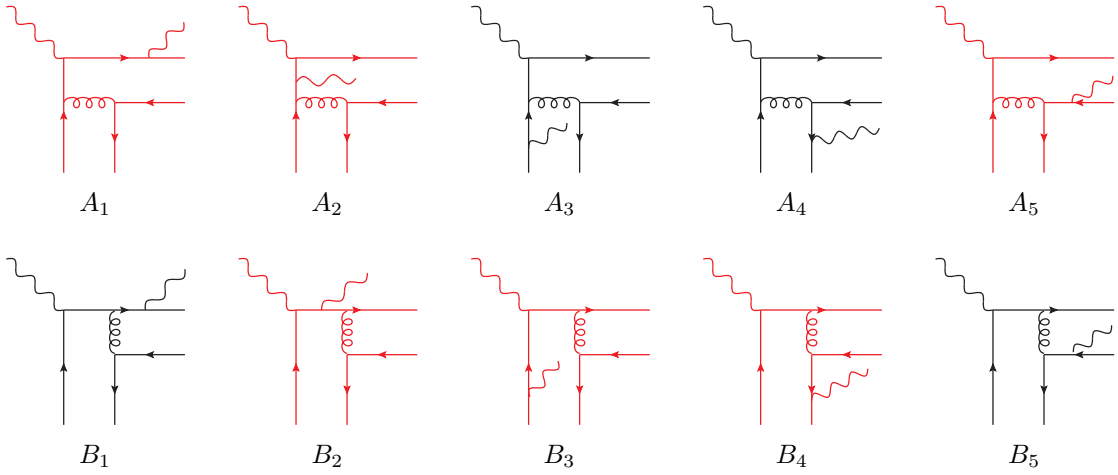

Figure 4.22: Half of the Feynman diagrams contributing to the hard amplitude. In the chiral-odd case, A_3, A_4 and B_1, B_5 are the only contributing diagrams (the red diagrams cancel in this case).

The scattering sub-process is described at lower twist by 20 Feynman diagrams, but using the $q \leftrightarrow \bar{q}$ (anti)symmetry properties allows one to compute only 10 of them, shown in Fig. 4.22, then deduce the remaining contributions by substituting $(x, z) \leftrightarrow (-x, 1 - z)$.
In the case of (γ, ρ_L) production all the diagrams contribute. In the case of $(\gamma, \rho_\perp)$ production, due to the chiral-odd structure of DAs and GPDs, there are only 8 non-vanishing diagrams, out of which one only needs to compute B_1, A_3, A_4 and B_5.

We now discuss diagram B_1 in some details, and give the results for the other diagrams in Appendix B.1.

The chiral-even scattering amplitudes for longitudinally polarized ρ^0 described by the DA (4.80) involve both the vector GPDs (4.84) and the axial GPDs (4.85). We now give the detailed expressions for $T_V^{q\,CE}(B_1)$, $T_A^{q\,CE}(B_1)$, for a quark with flavor q and for diagram B_1 in Feynman gauge. The vector amplitude reads

$$\begin{aligned}
T_V^{q\,CE}(B_1) &= \frac{1}{i}\,\frac{tr(t^a t^a)}{(4N)^2}\, f_\rho\, \phi_{||}(z)\, (-ieQ_q)^2\, (-ig)^2\, i^2\, (-i) \\
&\times tr_D \left[\hat{p}_\rho \hat{\varepsilon}^*_k \frac{\hat{k} + z\hat{p}_\rho}{(k + zp_\rho)^2 + i\epsilon} \gamma^\mu \frac{\hat{q} + (x + \xi)p}{(q + (x + \xi)p)^2 + i\epsilon}\, \hat{\varepsilon}_q\, \hat{p}\, \gamma_\mu\, \frac{1}{(\bar{z}p_\rho + (x - \xi)p)^2 + i\epsilon} \right] \\
&\times \frac{2}{s}\, \bar{u}(p_2, \lambda') \left[\hat{n} H^q(x, \xi, t) + \frac{i}{2m} \sigma^{n\,\alpha} \Delta_\alpha\, E^q(x, \xi, t) \right] u(p_1, \lambda) \\
&= C^{q\,CE}\, tr_D^V\, [B_1]\; \phi_{||}(z)\, \frac{2}{s}\, \bar{u}(p_2, \lambda') \left[\hat{n}\, H^q(x, \xi, t) + \frac{i}{2m} \sigma^{n\,\alpha} \Delta_\alpha\, E^q(x, \xi, t) \right] u(p_1, \lambda)\,,
\end{aligned} \tag{4.109}$$

which includes all non trivial factors (vertices as well as quark and gluon propagators) of the hard part of diagram B_1. Here, $C^{q\,CE}$ is a common coefficient for all diagrams involving vector and axial GPDs, reading

$$C^{q\,CE} = \frac{4}{9}\, f_\rho\, \alpha_{em}\, \alpha_s\, \pi^2\, Q_q^2\,. \tag{4.110}$$

The trace reads:

$$\begin{aligned} tr_D^V[B_1] &= tr_D\left[\hat{p}_\rho\hat{\varepsilon}_k^*\frac{\hat{k}+z\hat{p}_\rho}{(k+zp_\rho)^2+i\epsilon}\gamma^\mu\frac{\hat{q}+(x+\xi)p}{(q+(x+\xi)p)^2+i\epsilon}\,\hat{\varepsilon}_q\,\hat{p}\,\gamma_\mu\,\frac{1}{(\bar{z}p_\rho+(x-\xi)p)^2+i\epsilon}\right] \\ &= \frac{8s\left[-s\xi\alpha\,(\varepsilon_{q\perp}\cdot\varepsilon_{k\perp}^*)+\frac{z}{\alpha}\,(\varepsilon_{q\perp}\cdot p_{\rho\perp})\,(\varepsilon_{k\perp}^*\cdot p_{\rho\perp})\right]}{((k+zp_\rho)^2+i\epsilon)((q+(x+\xi)p)^2+i\epsilon)((\bar{z}p_\rho+(x-\xi)p)^2+i\epsilon)}\,, \\ &= \frac{4\left[-\alpha^2\xi sT_A+zT_B\right]}{\alpha\bar{\alpha}\xi s^2z\bar{z}\,(x-\xi+i\epsilon)\,(x+\xi+i\epsilon)}. \end{aligned} \tag{4.111}$$

We introduced the two tensor structures that will appear in chiral-even diagrams in the vector sector:

$$\begin{aligned} T_A &= (\varepsilon_{q\perp}\cdot\varepsilon_{k\perp}^*)\,, \\ T_B &= (\varepsilon_{q\perp}\cdot p_\perp)(p_\perp\cdot\varepsilon_{k\perp}^*). \end{aligned} \tag{4.112}$$

Similarly one can write in the axial sector:

$$\begin{aligned} T_A^{q\,CE}(B_1) &= \frac{1}{i}\,\frac{tr(t^at^a)}{(4N)^2}\,f_\rho\,\phi_{||}(z)\,(-ieQ_q)^2\,(-ig)^2\,i^2\,(-i) \\ &\times tr_D\left[\hat{p}_\rho\hat{\varepsilon}_k^*\frac{\hat{k}+z\hat{p}_\rho}{(k+zp_\rho)^2+i\epsilon}\gamma^\mu\frac{\hat{q}+(x+\xi)p}{(q+(x+\xi)p)^2+i\epsilon}\,\hat{\varepsilon}_q\,\hat{p}\,\gamma^5\,\gamma_\mu\,\frac{1}{(\bar{z}p_\rho+(x-\xi)p)^2+i\epsilon}\right] \\ &\times\frac{2}{s}\,\bar{u}(p_2,\lambda')\,\left[\gamma^5\,\hat{n}\,\tilde{H}^q(x,\xi,t)-\frac{n\cdot\Delta}{2m}\gamma^5\,\tilde{E}^q(x,\xi,t)\right]u(p_1,\lambda) \\ &= C^{q\,CE}\,tr_D^A[B_1]\;\phi_{||}(z)\,\frac{2}{s}\,\bar{u}(p_2,\lambda')\,\left[\gamma^5\,\hat{n}\,\tilde{H}^q(x,\xi,t)-\frac{n\cdot\Delta}{2m}\gamma^5\,\tilde{E}^q(x,\xi,t)\right]u(p_1,\lambda)\,, \end{aligned} \tag{4.113}$$

with

$$\begin{aligned} tr_D^A[B_1] &= tr_D\left[\hat{p}_\rho\hat{\varepsilon}_k^*\frac{\hat{k}+z\hat{p}_\rho}{(k+zp_\rho)^2+i\epsilon}\gamma^\mu\frac{\hat{q}+(x+\xi)p}{(q+(x+\xi)p)^2+i\epsilon}\,\hat{\varepsilon}_q\,\hat{p}\,\gamma^5\,\gamma_\mu\,\frac{1}{(\bar{z}p_\rho+(x-\xi)p)^2+i\epsilon}\right] \\ &= -\frac{8i}{\alpha\alpha_\rho}\,\frac{\left[\alpha\,(\varepsilon_{q\perp}\cdot p_{\rho\perp})\,\epsilon^{p\,n\,p_{\rho\perp}\,\varepsilon_{k\perp}^*}-(\alpha+2z\alpha_\rho)\,(\varepsilon_{k\perp}^*\cdot p_{\rho\perp})\,\epsilon^{p\,n\,p_{\rho\perp}\,\varepsilon_{q\perp}}\right]}{((k+zp_\rho)^2+i\epsilon)((q+(x+\xi)p)^2+i\epsilon)((\bar{z}p_\rho+(x-\xi)p)^2+i\epsilon)} \\ &= \frac{-4i\left[(\alpha+2\bar{\alpha}z)\,T_{A_5}-\alpha T_{B_5}\right]}{\alpha\bar{\alpha}^2\xi s^3z\bar{z}\,(x-\xi+i\epsilon)\,(x+\xi+i\epsilon)}, \end{aligned} \tag{4.114}$$

where we introduced the two tensor structures which will appear in chiral-even diagrams in the axial sector:

$$\begin{aligned} T_{A_5} &= (p_\perp\cdot\varepsilon_{k\perp}^*)\,\epsilon^{n\,p\,\varepsilon_{q\perp}\,p_\perp}\,, \\ T_{B_5} &= (p_\perp\cdot\varepsilon_{q\perp})\,\epsilon^{n\,p\varepsilon_{k\perp}^*\,p_\perp}. \end{aligned} \tag{4.115}$$

The chiral-odd (CO) scattering amplitude involving quark of flavor q ($q=u,d$) corresponding to diagram B_1 in Feynman gauge has the form:

$$\begin{aligned} &T^{q\,CO}(B_1) = -\frac{1}{i}\,\frac{tr(t^at^a)}{(8N)^2}\,i\,2f_\rho^\perp\,\phi_\perp(z)\,(-ieQ_q)^2\,(-ig)^2\,i^2\,(-i) \\ &tr_D\left[\hat{p}_\rho\hat{\varepsilon}_\rho^*\hat{\varepsilon}_k^*\frac{(\hat{k}+z\hat{p}_\rho)}{(k+zp_\rho)^2+i\epsilon}\gamma^\mu\frac{\hat{q}+(x+\xi)p}{(q+(x+\xi)p)^2+i\epsilon}\,\hat{\varepsilon}_q\,\hat{p}\,\gamma_{\perp j}\,\gamma_\mu\,\frac{1}{(\bar{z}p_\rho+(x-\xi)p)^2+i\epsilon}\right] \\ &\frac{2}{s}\,\bar{u}(p_2,\lambda')\,\left[\sigma^{nj}H_T^q(x,\xi,t)\right]u(p_1,\lambda) \\ &=\; C^{q\,CO}\,tr_D^{CO}[B_1]_j\;\phi_\perp(z)\,\frac{2}{s}\,\bar{u}(p_2,\lambda')\,\left[i\sigma^{nj}H_T^q(x,\xi,t)\right]u(p_1,\lambda), \end{aligned} \tag{4.116}$$

where

$$C^{q\,CO} = -\frac{2}{9}\,f_\rho^\perp\,\alpha_{em}\,\alpha_s\,\pi^2\,Q_q^2 \tag{4.117}$$

is a common coefficient for all diagrams involving chiral-odd DA and GPD, and

$$tr_D^{CO}[B_1]_j = \tag{4.118}$$
$$tr_D\left[\hat{p}_\rho \hat{\varepsilon}^*_\rho \hat{\varepsilon}^*_k \frac{(\hat{k}+z\hat{p}_\rho)}{(k+zp_\rho)^2+i\epsilon}\gamma^\mu \frac{\hat{q}+(x+\xi)p}{(q+(x+\xi)p)^2+i\epsilon}\,\hat{\varepsilon}_q\,\hat{p}\,\gamma_{\perp j}\,\gamma_\mu\,\frac{1}{(\bar{z}p_\rho+(x-\xi)p)^2+i\epsilon}\right]$$

includes all non trivial factors (vertices as well as quark and gluon propagators) of the hard part of diagram B_1. The calculation of traces over γ-matrices leads to the expression

$$\begin{aligned} tr_D^{CO}[B_1]_j &= \frac{8s\left[(q\cdot p)\varepsilon_{q\perp\, j}\left(p_\rho\cdot\varepsilon^*_k\,\varepsilon^*_\rho\cdot k - s\xi\,\varepsilon^*_k\cdot\varepsilon^*_\rho\right) - \epsilon^{k\,\varepsilon^*_k\,p_\rho\,\varepsilon^*_\rho}\,\epsilon^{q\,\varepsilon_q\,p\,\nu}g_{\perp\nu j}\right]}{((k+zp_\rho)^2+i\epsilon)\,((\bar{z}p_\rho+(x-\xi)p)^2+i\epsilon)((q+(x+\xi)p)^2+i\epsilon)} \\ &= \frac{T_{B\perp j}}{2\bar{\alpha}\xi s^3 z\bar{z}\,(x+\xi+i\epsilon)\,(x-\xi+i\epsilon)}\,. \end{aligned} \tag{4.119}$$

Here $T_{B\perp j}$ is one of the two tensor structures which will appear in chiral-odd diagrams,

$$\begin{aligned} T^i_{A\perp} &\equiv (p\cdot k)\,\varepsilon^{i*}_{k\perp}\left[(\varepsilon_q\cdot p_\rho)\,(q\cdot\varepsilon^*_\rho) - (q\cdot p_\rho)\,(\varepsilon_q\cdot\varepsilon^*_\rho)\right] - \epsilon^{p_\rho\,\varepsilon^*_\rho\,q\,\varepsilon_q}\,\epsilon^{p\,\nu\,k\,\varepsilon^*_k}g^i_{\perp\nu} \\ &= \frac{-8s}{\bar{\alpha}}\left\{\alpha\varepsilon^{i*}_{k\perp}\left[-2\alpha\xi\left(p\cdot\epsilon^*_\rho\right)\left(p_\perp\cdot\varepsilon_{q\perp}\right) + \left(p_\perp\cdot\varepsilon_{q\perp}\right)\left(p_\perp\cdot\varepsilon^*_{\rho\perp}\right) + \alpha\bar{\alpha}\xi s\left(\varepsilon_{q\perp}\cdot\varepsilon^*_{\rho\perp}\right)\right]\right. \\ &\quad -\bar{\alpha}\varepsilon^{i*}_{\rho\perp}\left[\alpha\,(\alpha-2)\,\xi s\,(\varepsilon_{q\perp}\cdot\varepsilon^*_{k\perp}) - (p_\perp\cdot\varepsilon_{q\perp})\,(p_\perp\cdot\varepsilon^*_{k\perp})\right] \\ &\quad +p^i_\perp\left[-2\alpha^2\xi p^i_\perp\left(p\cdot\epsilon^*_\rho\right)(\varepsilon_{q\perp}\cdot\varepsilon^*_{k\perp}) + \left(p_\perp\cdot\varepsilon^*_{\rho\perp}\right)(\varepsilon_{q\perp}\cdot\varepsilon^*_{k\perp}) - \bar{\alpha}\left(\varepsilon^*_{k\perp}\cdot\varepsilon^*_{\rho\perp}\right)(p_\perp\cdot\varepsilon_{q\perp})\right] \\ &\quad \left.+\varepsilon^i_{q\perp}\left[2\alpha^2\xi\left(p\cdot\epsilon^*_\rho\right)(p_\perp\cdot\varepsilon^*_{k\perp}) - \left(p_\perp\cdot\varepsilon^*_{\rho\perp}\right)(p_\perp\cdot\varepsilon^*_{k\perp}) + \alpha\bar{\alpha}\,(\alpha-2)\,\xi s\left(\varepsilon^*_{k\perp}\cdot\varepsilon^*_{\rho\perp}\right)\right]\right\}\,, \end{aligned} \tag{4.120}$$

the other one being

$$\begin{aligned} T^i_{B\perp} &\equiv (q\cdot p)\,\varepsilon^i_{q\perp}\left[(p_\rho\cdot\varepsilon^*_k)\,(\varepsilon^*_\rho\cdot k) - s\xi\,(\varepsilon^*_k\cdot\varepsilon^*_\rho)\right] - \epsilon^{k\,\varepsilon^*_k\,p_\rho\,\varepsilon^*_\rho}\,\epsilon^{q\,\varepsilon_q\,p\,\nu}g^i_{\perp\nu} \\ &= \frac{8s}{\alpha\bar{\alpha}}\left\{\bar{\alpha}\varepsilon^{i*}_{\rho\perp}\left[(p_\perp\cdot\varepsilon_{q\perp})\,(p_\perp\cdot\varepsilon^*_{k\perp}) - \alpha\,(2\alpha-1)\,\xi s\,(\varepsilon_{q\perp}\cdot\varepsilon^*_{k\perp})\right]\right. \\ &\quad +\alpha\varepsilon^{i*}_{k\perp}\left[\bar{\alpha}\,(2\alpha-1)\,\xi s\left(\varepsilon_{q\perp}\cdot\varepsilon^*_{\rho\perp}\right) + 2\xi\left(p\cdot\epsilon^*_\rho\right)(p_\perp\cdot\varepsilon_{q\perp}) + (p_\perp\cdot\varepsilon_{q\perp})\left(p_\perp\cdot\varepsilon^*_{\rho\perp}\right)\right] \\ &\quad +\varepsilon^i_{q\perp}\left[2\alpha\xi\left(p\cdot\epsilon^*_\rho\right)(p_\perp\cdot\varepsilon^*_{k\perp}) - \left(p_\perp\cdot\varepsilon^*_{\rho\perp}\right)(p_\perp\cdot\varepsilon^*_{k\perp}) - \alpha\bar{\alpha}\xi s\left(\varepsilon^*_{k\perp}\cdot\varepsilon^*_{\rho\perp}\right)\right] \\ &\quad \left.+p^i_\perp\left[2\alpha\xi\left(p\cdot\epsilon^*_\rho\right)(\varepsilon_{q\perp}\cdot\varepsilon^*_{k\perp}) - \alpha\left(p_\perp\cdot\varepsilon^*_{\rho\perp}\right)(\varepsilon_{q\perp}\cdot\varepsilon^*_{k\perp}) - \bar{\alpha}\left(\varepsilon_{q\perp}\cdot\varepsilon^*_{\rho\perp}\right)(p_\perp\cdot\varepsilon^*_{k\perp})\right]\right\}\,. \end{aligned} \tag{4.121}$$

Here, we expressed these two tensor structures in terms of the transverse polarization vectors and of $(p\cdot\varepsilon_\rho)$, using Eqs. (4.77-4.79), for later convenience.

At the dominant twist, the sum over the transverse polarizations of the rho meson can be written as

$$\sum_{pol}\varepsilon^\mu_\rho\varepsilon^{\nu*}_\rho = -g^{\mu\nu} + \frac{p^\mu_\rho p^\nu_\rho}{m^2_\rho}, \tag{4.122}$$

when computing the square of the chiral odd amplitude. The second term of this sum, which arises mainly from the longitudinal polarization, does not contribute at leading twist. We thus note that $(p\cdot\varepsilon_\rho)$ terms in the tensor structures will not contribute to the cross section since when summed over the transverse polarizations at the dominant twist they will produce terms involving the scalar product of p either with a transverse vector or with itself, which is null in both cases.

In a similar way we obtain the expressions for the remaining independent diagrams: A_1, A_2, A_3, A_4, A_5, B_2, B_3, B_4, B_5 in the chiral-even sector and A_3, A_4 and B_5 in the chiral-odd sector. We show these results in Appendix B.1.

The integral with respect to z is trivially performed in the case of a DA expanded in the basis of Gegenbauer polynomials. The expressions for the case of two asymptotical DAs $\phi_\parallel$ and $\phi_\perp$, which we only consider in the present article, are given explicitly in Appendix B.2, and expressed as linear combination of building blocks.

The integration with respect to x, for a given set of GPDs, (which can be our model described in Section 4.6 or any other model), is then reduced to the numerical evaluation of these building block integrals.

4.7.2 Square of $\mathcal{M}_\parallel$ and $\mathcal{M}_\perp$

In the forward limit $\Delta_\perp = 0 = P_\perp$, one can show that the squares of $\mathcal{M}_\parallel$ and of $\mathcal{M}_\perp$ read after summing over nucleon helicities:

$$\begin{aligned}
\mathcal{M}^q_\parallel \mathcal{M}^{q'*}_\parallel &\equiv \sum_{\lambda',\,\lambda} \mathcal{M}^q_\parallel(\lambda,\lambda')\,\mathcal{M}^{q'*}_\parallel(\lambda,\lambda') \qquad (4.123)\\
&= 8(1-\xi^2)\left(\mathcal{H}^q(\xi,t)\mathcal{H}^{q'*}(\xi,t) + \tilde{\mathcal{H}}^q(\xi,t)\tilde{\mathcal{H}}^{q'*}(\xi,t)\right)\\
&- 4\,\xi^2\left(\mathcal{E}^q(\xi,t)\mathcal{E}^{q'*}(\xi,t) + \tilde{\mathcal{E}}^q(\xi,t)\tilde{\mathcal{E}}^{q'*}(\xi,t)\right)\\
&- 8\,\xi^2\left(\mathcal{H}^q(\xi,t)\mathcal{E}^{q'*}(\xi,t) + \mathcal{H}^{q'*}(\xi,t)\mathcal{E}^q(\xi,t) + \tilde{\mathcal{H}}^q(\xi,t)\tilde{\mathcal{E}}^{q'*}(\xi,t) + \tilde{\mathcal{H}}^{q'*}(\xi,t)\tilde{\mathcal{E}}^q(\xi,t)\right),
\end{aligned}$$

and

$$\begin{aligned}
\mathcal{M}^q_\perp \mathcal{M}^{q'*}_\perp &\equiv \sum_{\lambda',\,\lambda} \mathcal{M}^q_\perp(\lambda,\lambda')\,\mathcal{M}^{q'*}_\perp(\lambda,\lambda') \qquad (4.124)\\
= \; 8\Bigg[&-(1-\xi^2)\mathcal{H}^{q\,i}_T(\xi,t)\mathcal{H}^{q'\,j\,*}_T(\xi,t) - \frac{\xi^2}{1-\xi^2}[\xi\,\mathcal{E}^{q\,i}_T(\xi,t) - \tilde{\mathcal{E}}^{q\,i}_T(\xi,t)][\xi\,\mathcal{E}^{q'\,j*}_T(\xi,t) - \tilde{\mathcal{E}}^{q'\,j*}_T(\xi,t)]\\
&+\xi\left\{\mathcal{H}^{qi}_T(\xi,t)[\xi\,\mathcal{E}^{q'\,j}_T(\xi,t) - \tilde{\mathcal{E}}^{q'\,j}_T(\xi,t)]^* + \mathcal{H}^{q'i*}_T(\xi,t)[\xi\,\mathcal{E}^{qj}_T(\xi,t) - \tilde{\mathcal{E}}^{qj}_T(\xi,t)]\right\}\Bigg]\, g_{\perp ij}.
\end{aligned}$$

For moderately small values of ξ, these become:

$$\mathcal{M}^q_\parallel \mathcal{M}^{q'*}_\parallel = 8\left(\mathcal{H}^q(\xi,t)\,\mathcal{H}^{q'*}(\xi,t) + \tilde{\mathcal{H}}^q(\xi,t)\,\tilde{\mathcal{H}}^{q'*}(\xi,t)\right), \qquad (4.125)$$

$$\mathcal{M}^q_\perp \mathcal{M}^{q'*}_\perp = -8\,\mathcal{H}^{q\,i}_T(\xi,t)\,\mathcal{H}^{q'\,j\,*}_T(\xi,t)\,g_{\perp ij}\,. \qquad (4.126)$$

Hence we will restrict ourselves to H^q, $\tilde{H}^q$ and H^q_T to perform our estimates of the cross section[11].

4.8 Unpolarized Differential Cross Section and Rate Estimates

4.8.1 From amplitudes to cross sections

We isolate the tensor structures of the form factors as

$$\mathcal{H}^q(\xi,t) = \mathcal{H}^q_A(\xi,t)T_A + \mathcal{H}^q_B(\xi,t)T_B\,, \qquad (4.127)$$

$$\tilde{\mathcal{H}}^q(\xi,t) = \tilde{\mathcal{H}}^q_A(\xi,t)T_{A_5} + \tilde{\mathcal{H}}^q_B(\xi,t)T_{B_5}\,, \qquad (4.128)$$

$$\mathcal{H}^{q\,i}_T(\xi,t) = \mathcal{H}^q_{T_A}(\xi,t)T^i_{A\perp} + \mathcal{H}^q_{T_B}(\xi,t)T^i_{B\perp}. \qquad (4.129)$$

These coefficients can be expressed in terms of the sum over diagrams of the integral of the product of their traces, of GPDs and DAs, as defined and given explicitly in Appendix B.2. They read :

$$\mathcal{H}^q_A = \frac{1}{s}C^{q\,CE}N^q_A\,, \qquad (4.130)$$

$$\mathcal{H}^q_B = \frac{1}{s^2}C^{q\,CE}N^q_B\,, \qquad (4.131)$$

$$\tilde{\mathcal{H}}^q_{A_5} = \frac{1}{s^3}C^{q\,CE}N^q_{A_5}\,, \qquad (4.132)$$

$$\mathcal{H}^q_{B_5} = \frac{1}{s^3}C^{q\,CE}N^q_{B_5}\,, \qquad (4.133)$$

and

$$\mathcal{H}^q_{T\,A} = \frac{1}{s^3}C^{q\,CO}N^q_{T\,A}\,, \qquad (4.134)$$

$$\mathcal{H}^q_{T\,B} = \frac{1}{s^3}C^{q\,CO}N^q_{T\,B}\,. \qquad (4.135)$$

[11] In practice, we keep the first line in the r.h.s. of Eq. (4.123) and the first term in the r.h.s of Eq. (4.124).

For the specific case of our process, it is convenient to define the total form factors as follows:

$$\mathcal{H}(\xi,t) \equiv \mathcal{H}^u(\xi,t) - \mathcal{H}^d(\xi,t)\,, \tag{4.136}$$
$$\tilde{\mathcal{H}}(\xi,t) \equiv \tilde{\mathcal{H}}^u(\xi,t) - \tilde{\mathcal{H}}^d(\xi,t)\,, \tag{4.137}$$
$$\mathcal{H}^i_T(\xi,t) \equiv \mathcal{H}^{u\,i}_T(\xi,t) - \mathcal{H}^{d\,i}_T(\xi,t)\,, \tag{4.138}$$

from which we isolate the tensor structures

$$\mathcal{H}(\xi,t) = \mathcal{H}_A(\xi,t)\,T_A + \mathcal{H}_B(\xi,t)\,T_B\,, \tag{4.139}$$
$$\tilde{\mathcal{H}}(\xi,t) = \tilde{\mathcal{H}}_{A_5}(\xi,t)\,T_{A_5} + \tilde{\mathcal{H}}_{B_5}(\xi,t)\,T_{B_5}\,, \tag{4.140}$$
$$\mathcal{H}^i_T(\xi,t) = \mathcal{H}_{T_A}(\xi,t)\,T^i_{A\perp} + \mathcal{H}_{T_B}(\xi,t)\,T^i_{B\perp}. \tag{4.141}$$

In this study, we are interested in the unpolarized cross section. As a result, we will need the squared form factors after summation over all the polarizations (outgoing γ and ρ, incoming γ):

$$|\mathcal{H}(\xi,t)|^2 \equiv \sum_{\lambda_k\lambda_q} \mathcal{H}(\xi,t,\lambda_k,\lambda_q)\,\mathcal{H}(\xi,t,\lambda_k,\lambda_q) \tag{4.142}$$
$$= 2|\mathcal{H}_A(\xi,t)|^2 + p_\perp^4|\mathcal{H}_B(\xi,t)|^2 + p_\perp^2\left[\mathcal{H}_A(\xi,t)\mathcal{H}^*_B(\xi,t) + \mathcal{H}^*_A(\xi,t)\mathcal{H}_B(\xi,t)\right],$$

$$|\tilde{\mathcal{H}}(\xi,t)|^2 \equiv \sum_{\lambda_k\lambda_q} \tilde{\mathcal{H}}(\xi,t,\lambda_k,\lambda_q)\,\tilde{\mathcal{H}}^*(\xi,t,\lambda_k,\lambda_q) \tag{4.143}$$
$$= \frac{s^2p_\perp^4}{4}|\tilde{\mathcal{H}}_{A_5}(\xi,t)|^2 + |\tilde{\mathcal{H}}_{B_5}(\xi,t)|^2,$$

$$|\mathcal{H}_T(\xi,t)|^2 \equiv -g_{\perp i\,j}\sum_{\lambda_k\lambda_q\lambda_\rho} \mathcal{H}^i_T(\xi,t,\lambda_k,\lambda_q,\lambda_\rho)\mathcal{H}^{j*}_T(\xi,t,\lambda_k,\lambda_q,\lambda_\rho) \tag{4.144}$$
$$= 512\xi^2s^4\left(\alpha^4|\mathcal{H}_{T_A}(\xi,t)|^2 + |\mathcal{H}_{T_B}(\xi,t)|^2\right).$$

We now define the averaged squared amplitude $|\overline{\mathcal{M}}|^2$, which includes the factor 1/4 coming from the averaging over the polarizations of the initial particles. Collecting all the prefactors (including a factor of 2^2 for the missing half of the set of diagrams and a factor of 1/2 from the square of the ρ^0 wave function, see Eq. (4.105)), which reads

$$\frac{1}{s^2}2^2 8(1-\xi^2)\left(C^{q\,CE(OD)}\right)^2\frac{1}{2^3}\,,$$

we have the net result (factorizing out the coefficient for the $u-$quark), for the chiral-even case

$$|\overline{\mathcal{M}}^{CE}|^2 = \frac{4}{s^2}(1-\xi^2)\left(C^{u\,CE}\right)^2\left\{2\left|N^u_A - \frac{1}{4}N^d_A\right|^2 + \frac{p_\perp^4}{s}^2\left|N^u_B - \frac{1}{4}N^d_B\right|^2\right. \tag{4.145}$$
$$\left. + \frac{p_\perp^2}{s}\left(\left[N^u_A - \frac{1}{4}N^d_A\right]\left[N^u_B - \frac{1}{4}N^d_B\right]^* + c.c.\right) + \frac{p_\perp^4}{4s^2}\left|\tilde{N}^u_A - \frac{1}{4}\tilde{N}^d_A\right|^2 + \frac{p_\perp^4}{4s^2}\left|\tilde{N}^u_B - \frac{1}{4}\tilde{N}^d_B\right|^2\right\},$$

while for the chiral-odd case, we get

$$|\overline{\mathcal{M}}^{CO}|^2 = \frac{2048}{s^2}\xi^2(1-\xi^2)\left(C^{u\,CO}\right)^2\left\{\alpha^4\left|N^u_{T\,A} - \frac{1}{4}N^d_{T\,A}\right|^2 + \left|N^u_{T\,B} - \frac{1}{4}N^d_{T\,B}\right|^2\right\}. \tag{4.146}$$

The differential cross section as a function of t, $M^2_{\gamma\rho}$, $-u'$ then reads

$$\left.\frac{d\sigma}{dt\,du'\,dM^2_{\gamma\rho}}\right|_{-t=(-t)_{min}} = \frac{|\overline{\mathcal{M}}|^2}{32S^2_{\gamma N}M^2_{\gamma\rho}(2\pi)^3}\,. \tag{4.147}$$

4.8.2 Numerical evaluation of the scattering amplitudes and of cross sections

Above, we have reduced the calculation of the cross sections, see Eq. (4.147), to the numerical evaluation of the coefficients (B.62), (B.63), (B.43), (B.44), (B.45), (B.46). These coefficients are expressed as linear combinations of numerical integrals, listed in Appendix B.2.

Our central set of curves, displayed below, is obtained for $S_{\gamma N} = 20$ GeV^2, with $M^2_{\gamma\rho}$ varying in the range $2.10\ \text{GeV}^2 < M^2_{\gamma\rho} < 9.47\ \text{GeV}^2$ (this latter value comes from the vanishing of the phase-space in $-t$, as shown in Appendix B.4, see Eq. (B.115)) with a 0.1 GeV^2 step.

For each of these values of $M^2_{\gamma\rho}$, we chose 100 values of $-u'$, linearly varying from $(-u')_{min} = 1\ \text{GeV}^2$ up to $(-u')_{maxMax}$ as defined by Eq. (B.111).

For each of these couples of values of $(M^2_{\gamma\rho}, -u',)$ we compute each of the numerical coefficients N^u_A, N^d_A, N^u_B, N^d_B and $\tilde{N}^u_A$, $\tilde{N}^d_A$, $\tilde{N}^u_B$, $\tilde{N}^d_B$ for the chiral-even case, as well as the coefficients $N^u_{T\,A}$, $N^d_{T\,A}$, $N^u_{T\,B}$, $N^d_{T\,B}$ for the chiral-odd case, using the sets of GPDs indexed by $M^2_{\gamma\rho}$ and computed as explained in Section 4.6.3.

This whole set of dimensionless numerical coefficients allows us to perform the various phenomenological studies discussed in the next subsections.

4.8.3 Fully differential cross sections

Let us first discuss chiral-even results, showing in parallel the proton and neutron target cases.

We first analyze the various contributions to the differential cross section in the specific kinematics: $M^2_{\gamma\rho} = 4$ GeV^2, $S_{\gamma N} = 20\ \text{GeV}^2$, $-t = (-t)_{min}$ as a function of $-u'$. The dependency with respect to $S_{\gamma N}$ will be discussed in Section 4.8.5.

In Fig. 4.23, we show the relative contributions of the $u-$ and $d-$quark GPDs (adding the vector and axial contributions), which interfere in a destructive way because of the flavor structure of the $\rho^0 = \frac{u\bar{u}-d\bar{d}}{\sqrt{2}}$. The $d-$quark contribution is of course more important for the neutron target case.

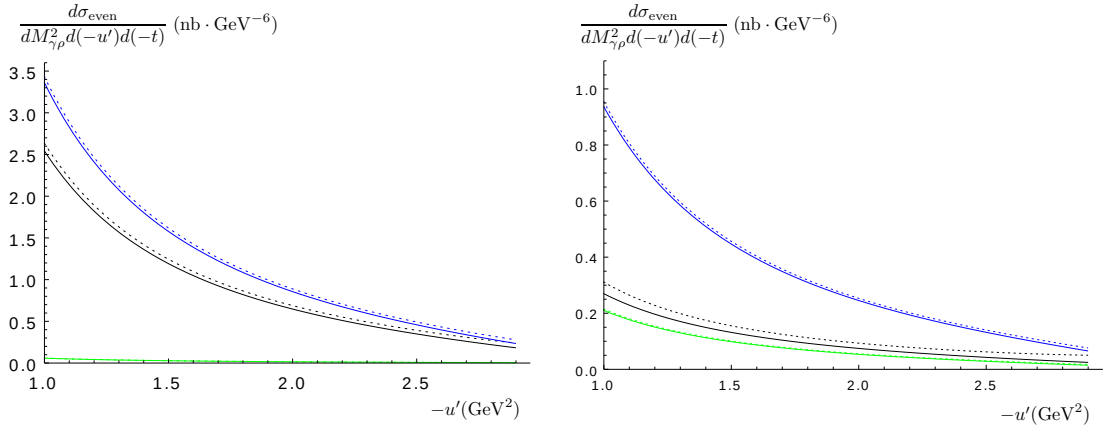

Figure 4.23: Differential cross section for a photon and a longitudinally polarized ρ meson production, for the proton (left) and the neutron (right), at $M^2_{\gamma\rho} = 4\ \text{GeV}^2$. Both vector and axial GPDs are included. In black the contributions of both u and d quarks, in blue the contribution of the u quark, and in green the contribution of the d quark. Solid: "valence" model, dotted: "standard" model. This figure shows the dominance of the u-quark contribution due to the charge effect. Note that the interference between $u-$quark and $d-$quark contributions is important and negative.

In Fig. 4.24, we show the relative contributions of the GPDs H and $\tilde{H}$ involving vector and axial correlators. The vector contribution dominates. The two parameterizations of the axial GPD $\tilde{H}^q(x,\xi,t)$ give quite different results, the one corresponding to the unbroken sea ("standard") scenario being less negligible than the other one ("valence"). As a simple calculation shows, there is no interference effect between H and $\tilde{H}$ contributions due to lack of a sufficient number of transverse momenta in the tensor structures.

Fig. 4.25 shows the dependence on $M^2_{\gamma\rho}$. The production of the $\gamma\rho$ pair with a large value of $M^2_{\gamma\rho}$ is severely suppressed as anticipated. However, the $-u'$ range allowed by our kinematical requirements

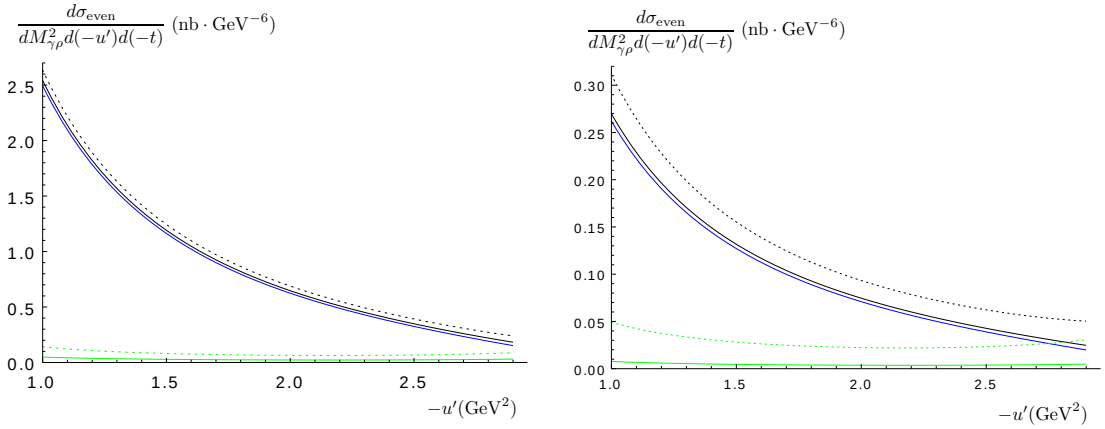

Figure 4.24: Differential cross section for a photon and a longitudinally polarized ρ meson production, for the proton (left) and the neutron (right), at $M^2_{\gamma\rho} = 4$ GeV^2. Both u and d quark contributions are included. In black the contributions of both vector and axial amplitudes, in blue the contribution of the vector amplitude, and in green the contribution of the axial amplitude. Solid: "valence" model, dotted: "standard" model. This figure shows the dominance of the vector GPD contributions. There is no interference between the vector and axial amplitudes.

is narrower for smaller values of $M^2_{\gamma\rho}$. The two curves for each value of $M^2_{\gamma\rho}$ correspond to the two parameterizations of $\tilde{H}(x,\xi,t)$, the lines corresponding to the unbroken sea scenario lying above the other one.

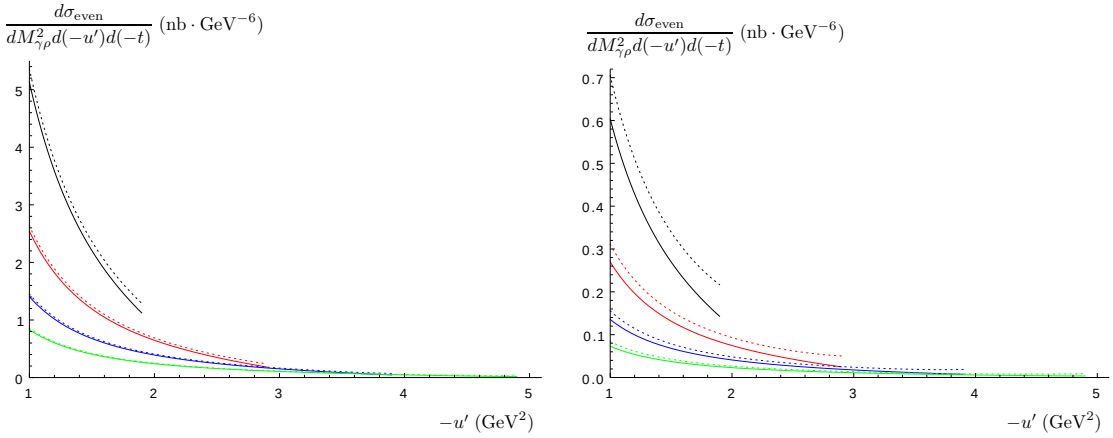

Figure 4.25: Differential cross section for a photon and a longitudinally polarized ρ meson production, for the proton (left) and the neutron (right), as a function of $-u'$, for $M^2_{\gamma\rho} = 3, 4, 5, 6$ GeV^2 (resp. in black, red, blue, green). Solid: "valence" model, dotted: "standard" model.

4.8.4 Single differential cross sections

To get an estimate of the total rate of events of interest for our analysis, we first get the $M^2_{\gamma\rho}$ dependence of the differential cross section integrated over u' and t,

$$\frac{d\sigma}{dM^2_{\gamma\rho}} = \int_{(-t)_{min}}^{(-t)_{max}} d(-t) \int_{(-u')_{min}}^{(-u')_{max}} d(-u')\, F_H^2(t) \times \frac{d\sigma}{dt\, du' dM^2_{\gamma\rho}}\bigg|_{-t=(-t)_{min}} . \tag{4.148}$$

Since this is mostly an order of magnitude estimate, we use a simple factorized universal dipole $t-$dependence of GPDs,

$$F_H(t) = \frac{C^2}{(t-C)^2}\,, \tag{4.149}$$

with $C = 0.71$ GeV^2. For a more precise study dedicated to an impact picture of the nucleon [170–175], a more sophisticated approach [176] should be used. The domain of integration over u' and t is discussed in detail in Appendix B.4.

The differential cross section we obtain $d\sigma/dM^2_{\gamma\rho}$ is shown in Fig. 4.26 for various values of $S_{\gamma N}$ covering the JLab-12 energy range. These cross sections show a maximum around $M^2_{\gamma\rho} \approx 3$ GeV^2, for most energy values.

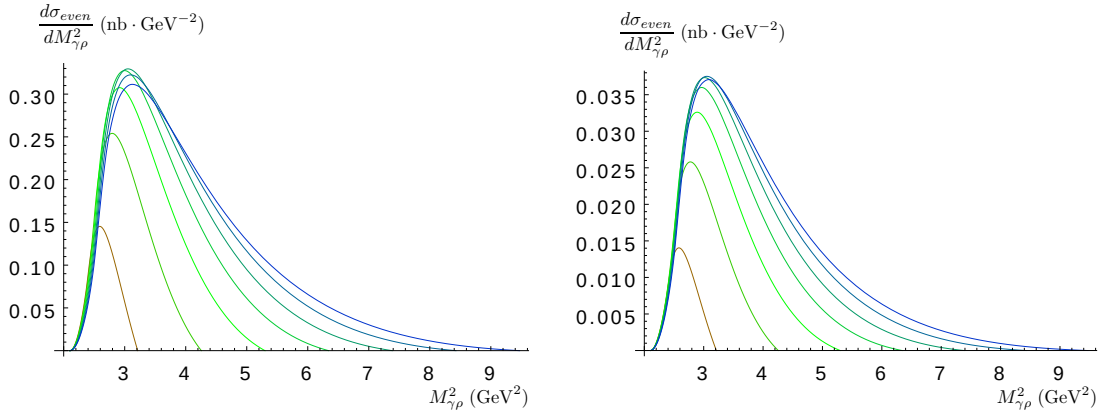

Figure 4.26: Differential cross section $d\sigma/dM^2_{\gamma\rho}$ for a photon and a longitudinally polarized ρ meson production, on a proton (left) or neutron (right) target. The values of $S_{\gamma N}$ vary in the set 8, 10, 12, 14, 16, 18, 20 GeV^2. (from 8: left, brown to 20: right, blue), covering the JLab energy range. Here, we use the "valence" scenario.

4.8.5 Integrated cross sections and variation with respect to $S_{\gamma N}$

For $S_{\gamma N} = 20$ GeV^2, the integration over $M^2_{\gamma\rho}$ of our above results within our allowed kinematical region, here 2.10 GeV^2 $< M^2_{\gamma\rho} <$ 9.47 GeV^2 (see Appendix B.4), allows to obtain the cross sections $\sigma^{\rm proton}_{\rm odd} \simeq 0.54$ pb and $\sigma^{\rm proton}_{\rm even} \simeq 0.76$ nb for the proton, and $\sigma^{\rm neutron}_{\rm odd} \simeq 0.42$ pb and $\sigma^{\rm neutron}_{\rm even} \simeq 0.084$ nb for the neutron.

The variation with respect to $S_{\gamma N}$ could be obtained by following the whole chain of steps described above. However, this can be obtained almost directly. Our aim is now to show that the only knowledge of the set of numerical results computed for a given value of $S_{\gamma N}$, which we take in practice as $S_{\gamma N} = 20$ GeV^2, is sufficient to deduce a whole set of results for any arbitrary smaller values of $\tilde{S}_{\gamma N}$. The key points are the following.

First, the amplitudes only depend on α, ξ and on the GPDs (which are computed as grids indexed by ξ). Since $\alpha = -u'/M^2_{\gamma\rho}$, it is thus possible to use exactly the set of already computed amplitudes if one selects the same set of (α, ξ)

Second, one should note that to a given value of

$$\xi = \frac{M^2_{\gamma\rho}}{2(S_{\gamma N} - M^2) - M^2_{\gamma\rho}} \tag{4.150}$$

corresponds an infinite set of couples of values $(M^2_{\gamma\rho}, S_{\gamma N})$.

In practice, we use our set of results obtained for $S_{\gamma N} = 20$ GeV^2, indexed by $M^2_{\gamma\rho}$ and $-u'$.

Then, choosing a new value of $\tilde{S}_{\gamma N}$, we obtain a set of values of $\tilde{M}^2_{\gamma\rho}$ indexed by the set of values of $M^2_{\gamma\rho}$ (which vary from 2.2 up to 10 GeV^2, with a 0.1 GeV^2 step), through the relation

$$\tilde{M}^2_{\gamma\rho} = M^2_{\gamma\rho} \frac{\tilde{S}_{\gamma N} - M^2}{S_{\gamma N} - M^2}, \tag{4.151}$$

which is deduced from Eq. (4.150), and for each of these $\tilde{M}^2_{\gamma\rho}$ a set of values of $-\tilde{u}'$, using the relation

$$-\tilde{u}' = \frac{\tilde{M}^2_{\gamma\rho}}{M^2_{\gamma\rho}}(-u'). \tag{4.152}$$

which gives the indexation of allowed values of $-\tilde{u}'$ as function of known values of $(-u')$.

It is now easy to check that this mapping from a given $S_{\gamma N}$ to a lower $\tilde{S}_{\gamma N}$ provides a set of $(\tilde{M}^2_{\gamma\rho}, -\tilde{u}')$ which exhaust the required domain.

Consider first the range in $\tilde{M}^2_{\gamma\rho}$. From Eq. (B.109), which defines the minimal value of $M^2_{\gamma\rho}$, independent of $S_{\gamma N}$, this value is mapped to a smaller value than required, when passing from $S_{\gamma N}$ to $\tilde{S}_{\gamma N}$. From Eq. (B.115), it is possible to show that $M^2_{\gamma\rho\,\mathrm{Max}}$ is mapped to a value $\tilde{M}^2_{\gamma\rho\,\mathrm{Max}}$ slightly larger than the new required value $M'^2_{\gamma\rho\,\mathrm{Max}}$ (this comes from the little dependency of $\bar{M}$ with respect to $S_{\gamma N}$). Thus, the mapping covers the whole required domain in $\tilde{M}^2_{\gamma\rho}$ (with a negligible loss of precision since a few points are mapped outside the domain and thus cut).

Now, let us consider the range in $-u'$. Again, since the minimal value $(-u')_{\min}$ is fixed, this value is mapped to a smaller value than required, when passing from $S_{\gamma N}$ to $\tilde{S}_{\gamma N}$. Concerning the maximal value $(-u')_{\mathrm{maxMax}}$, from Eq. (B.111) it is a linear function of $M^2_{\gamma\rho}$ of the form

$$(-u')_{\mathrm{maxMax}} = -A + M^2_{\gamma\rho}\,, \tag{4.153}$$

with $A > 0$. The mapping of $M^2_{\gamma\rho}$ leads to the maximal required value

$$(-u')'_{\mathrm{maxMax}} = -A + \tilde{M}^2_{\gamma\rho}\,. \tag{4.154}$$

But the mapping in $-u'$ will transform $(-u')_{\mathrm{maxMax}}$ to

$$(-\tilde{u}')_{\mathrm{maxMax}} = \frac{\tilde{M}^2_{\gamma\rho}}{M^2_{\gamma\rho}}(-A + M^2_{\gamma\rho}) = -A\frac{\tilde{M}^2_{\gamma\rho}}{M^2_{\gamma\rho}} + \tilde{M}^2_{\gamma\rho}\,, \tag{4.155}$$

which shows that the maximal value $(-\tilde{u}')_{\mathrm{maxMax}}$ of $(-\tilde{u}')$ obtained from the mapping is larger than the needed $(-u')'_{\mathrm{maxMax}}$, since $-A < -A\frac{\tilde{M}^2_{\gamma\rho}}{M^2_{\gamma\rho}} < 0$.

We have thus shown that one can obtain the dependency of amplitudes and thus of cross sections for the whole range in $S_{\gamma N}$ from a single set of computation (at $S_{\gamma N} = 20$ GeV^2), thus avoiding the use of a very large amount of CPU time.

Then, for the obtained cross section which was obtained at a given value of $\tilde{S}_{\gamma N}$, the integration over the $(-t, -u')$ phase-space and then over $M^2_{\gamma\rho}$ is performed similarly to $S_{\gamma N} = 20$ GeV^2 case. One finally gets the integrated cross section shown in Fig. 4.27 for the proton and neutron targets, and for both parameterizations of the axial GPDs[12]. These cross sections prove that our process is measurable in the typical kinematical conditions and integrated luminosity of a JLab@12GeV experiment. Counting rates on a proton target are predicted to be one order of magnitude larger than on a neutron target.

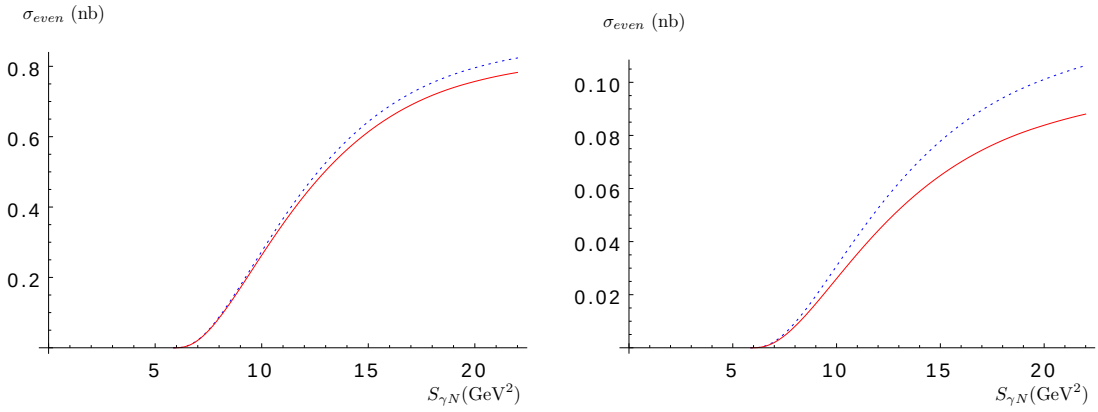

Figure 4.27: Integrated cross section for a photon and a longitudinally polarized ρ meson production, on a proton (left) or neutron (right) target. The solid red curves correspond to the "valence" scenario while the dashed blue curves correspond to the "standard" one.

[12] A quadratic extrapolation is performed for the small domain above $S_{\gamma N} = 20$ GeV^2.

4.8.6 Results for the chiral-odd case

Let us now pass to the chiral-odd case, where a transversely polarized ρ meson is produced together with the photon. This process now probes the chiral-odd transversity quark distributions which are connected to the transversity PDFs.

In order to evaluate the theoretical uncertainty in the chiral-odd sector, for each of the two parameterizations of the transversity PDFs, we use a set of 1500 trials with their value of the χ^2 test, as provided by the authors of Ref. [169], between -2σ and $+2\sigma$. Their 9-parameters χ^2 distribution (see the appendix of Ref. [177] for details) is given by

$$P_{\chi^2}(x) = \frac{e^{-x/2}x^{7/2}}{105\sqrt{2\pi}} \tag{4.156}$$

We further renormalize this distribution in order to include on one hand the fact that the 1500 trials only cover the $[-2\sigma, +2\sigma]$ interval, and on the other hand discretization corrections. We then create a histogram of these configurations, with a distribution weighted by the above described renormalized χ^2 distribution. This weighted histogram allows us to finally compute the -2σ and $+2\sigma$ values of the cross-section. We perform this analysis at $-u' = 1$ GeV^2 and for three typical values of $M^2_{\gamma\rho}$ (2.2, 4, 6 GeV^2), for the "standard" scenario. We then extract the two typical configurations which gives cross-section close to the -2σ and $+2\sigma$ values, which we now use both for the "standard" and "valence" scenarios in order to evaluate the typical theoretical uncertainty.

Fig. 4.28 shows the $M^2_{\gamma\rho}$ dependence of this cross section, both for the proton and the neutron. Similarly to the chiral-even case, the production of the $\gamma\rho$ pair with a large value of $M^2_{\gamma\rho}$ is severely suppressed. Similarly, the $-u'$ range allowed by our kinematical requirements is narrower for smaller values of $M^2_{\gamma\rho}$. Comparing the chiral-even case, see Figs. 4.23, 4.24, 4.25 and the chiral-odd case, see Fig. 4.28, one should note the very different behaviors of the differential cross section when varying $-u'$. In the case of a proton probe, we show in Fig. 4.28 (left) as error bands the maximal and minimal values of the cross-section (the maximal values are obtained with the "standard" trial at $+2\sigma$ and the minimal values with the "valence" trial at -2σ).

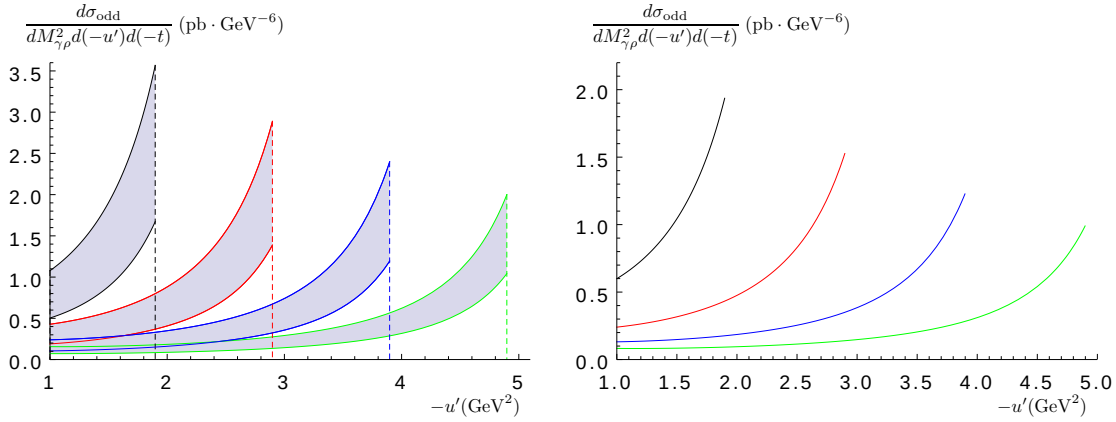

Figure 4.28: Differential cross section for the production of a photon and a transversally polarized ρ meson, for a proton target (left) and a neutron target (right), as a function of $-u'$, for $M^2_{\gamma\rho} = 3, 4, 5, 6$ GeV^2 (resp. in black, red, blue, green). The error bands on the l.h.s. panel (proton) correspond to the procedure discussed in the text. For the neutron, we only show the results for the "valence" case.

Similarly to the chiral-even case, we perform the integration in the $(-t, -u')$ phase-space. The differential cross section $d\sigma_{\rm odd}/dM^2_{\gamma\rho}$ we obtain is shown in Fig. 4.29 for $S_{\gamma N} = 20$ GeV^2, with the different sets of results depending on the sets of transversity PDFs which we use, as explained above.

In Fig. 4.30, we show the differential cross section $d\sigma_{\rm odd}/dM^2_{\gamma\rho}$ for various values of $S_{\gamma N}$ covering the JLab-12 energy range. These cross sections show a maximum around a similar range of $M^2_{\gamma\rho} \approx 3$ GeV^2, for most energy values.

Finally, the dependency of the integrated cross section with respect to $S_{\gamma N}$ is shown in Fig. 4.31, both for proton and neutron, for the two "valence" and "standard" scenarios.

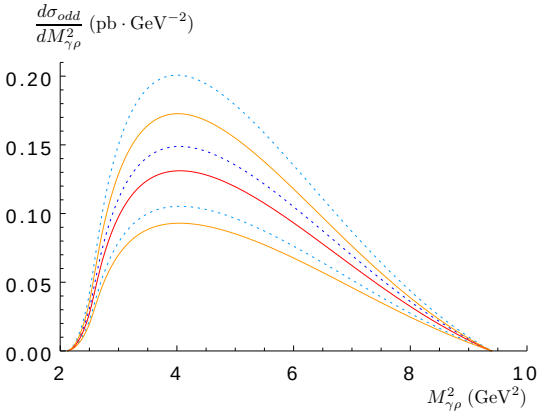

Figure 4.29: Differential cross section $d\sigma/dM^2_{\gamma\rho}$ for a photon and a transversally polarized ρ meson production on a proton target for $S_{\gamma N} = 20$ GeV^2. The various curves differ with respect to the ansatz for the PDFs δq used to build the GPD H_T. The dotted curves correspond to the "standard" polarized PDFs while the solid curves use the "valence" polarized PDFs. The deep-blue and red curves are central values while the light-blue and orange ones are the results obtained at $\pm 2\sigma$.

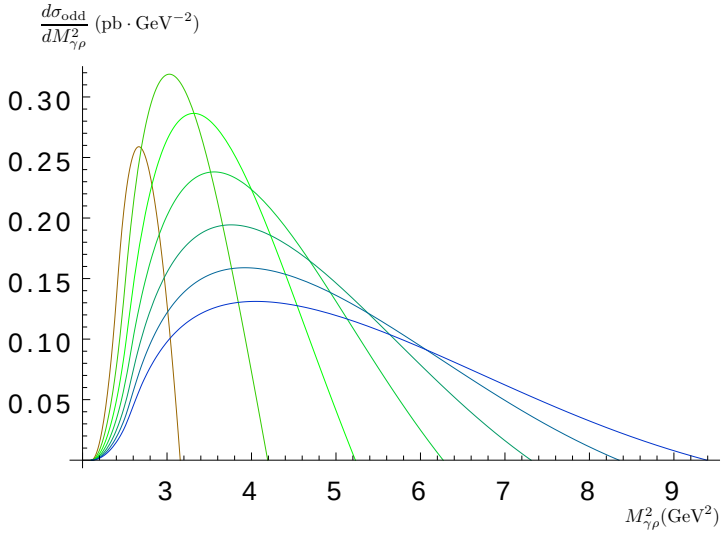

Figure 4.30: Differential cross section $d\sigma/dM^2_{\gamma\rho}$ for a photon and a transversally polarized ρ meson production on a proton target. The values of $S_{\gamma N}$ vary in the set 8, 10, 12, 14, 16, 18, 20 GeV^2. (from 8: left, brown to 20: right, blue), covering the JLab energy range. We use here the "valence" scenario.

4.9 Counting rates

Using the Weizsäcker-Williams distribution, one can obtain counting rates. This distribution is given by [178, 179]

$$f(x) = \frac{\alpha_{\rm em}}{2\pi}\left\{2m_e^2 x\left(\frac{1}{Q^2_{\rm max}} - \frac{1-x}{m_e^2 x^2}\right) + \frac{\left((1-x)^2+1\right)\ln\frac{Q^2_{\rm max}(1-x)}{m_e^2 x^2}}{x}\right\}, \tag{4.157}$$

where x is the fraction of energy lost by the incoming electron, m_e is the electron mass and $Q^2_{\rm max}$ is the typical maximal value of the virtuality of the echanged photon, which we take to be 0.1 GeV^2. Using the expression for x as a function of the incoming electron energy E_e

$$x[S_{\gamma N}] = \frac{S_{\gamma N} - M^2}{2E_e M}, \tag{4.158}$$

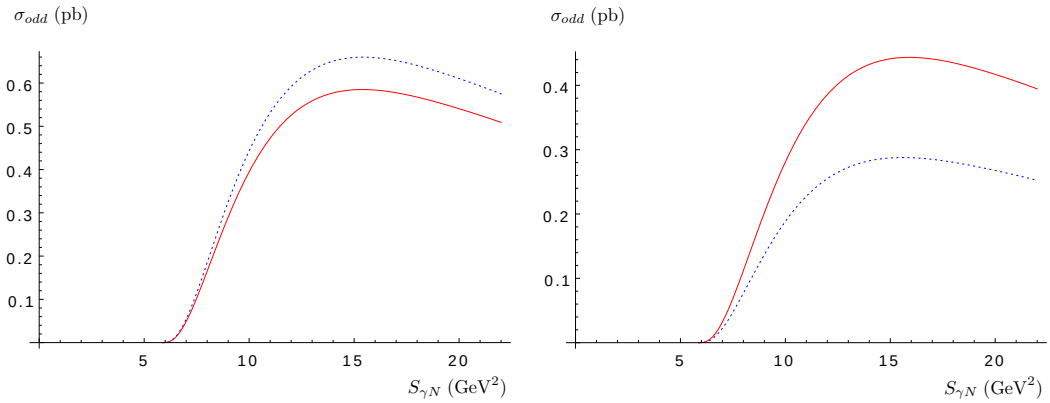

Figure 4.31: Integrated cross section for a photon and a transverse ρ meson production, on a proton (left) or neutron (right) target, as a function of $S_{\gamma N}$. The solid red curves correspond to the "valence" scenario while the dashed blue curves correspond to the "standard" one.

one can easily obtain integrated cross sections at the level of the eN process, using the relation

$$\sigma_{eN} = \int \sigma_{\gamma N}(x)\, f(x)\, dx = \int_{S_{\gamma N\,\mathrm{crit}}}^{S_{\gamma N\,\mathrm{max}}} \frac{1}{2E_e M}\, \sigma_{\gamma N}(x[S_{\gamma N}])\, f(x[S_{\gamma N}])\, dS_{\gamma N}\,. \tag{4.159}$$

The shape of the integrand

$$F(S_{\gamma N}) = \frac{1}{2E_e M}\, \sigma_{\gamma N}(x[S_{\gamma N}])\, f(x[S_{\gamma N}]) \tag{4.160}$$

of Eq. (4.159) is shown in Fig. 4.32.

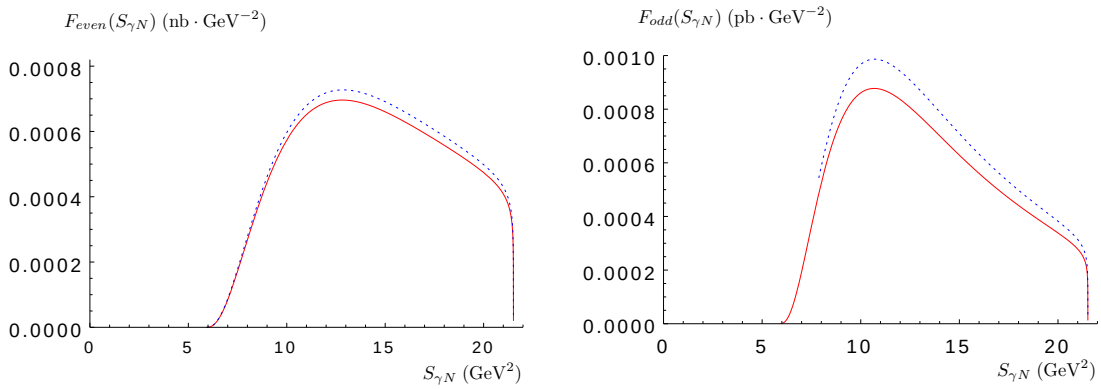

Figure 4.32: Shape of the integrand of σ_{eN}, as a function of the invariant mass of the hadronic produced state, on a proton target. Left: longitudinally polarized ρ meson production. Right: transverse ρ meson production. In solid-red: "valence". In dashed-blue: "standard".

Up to now we discussed the photoproduction of a $\gamma\rho$ pair without paying attention to the origin of the initial quasi-real photon. If it is emitted by a lepton beam, like in electroproductive DVCS, one should also consider Bethe-Heitler-type processes, in which the final real photon is emitted by the lepton beam. Let us however note that this mechanism involves an off-shell photon of momentum q, since in this case $q^2 = (p_\rho + \Delta)^2 \approx -2\xi s\alpha_\rho$ is large. Thus the Bethe-Heitler mechanism involves scattering amplitudes with four hard propagators, whereas the photoproduction mechanism considered so far involves only three hard propagators. We therefore expect the Bethe-Heitler contribution to be suppressed. A more precise discussion is left for the future.

At this point, we did not include any experimental constraint on the angular coverage of the final state particles. We discuss this issue in Appendix B.5, taking the constraints of JLab Hall B into account, and showing that this does not affect our predictions. We also show that a binning in the outgoing photon angle could help to enhance the chiral-odd versus chiral-even ratio, in particular for observables which are sensitive to the interference of the two amplitudes, beyond the scope of the present study.

We can now give our predictions for the counting rates. With an expected luminosity $\mathcal{L} = 100\,\mathrm{nb}^{-1}s^{-1}$ we obtain for 100 days of run: $7.5\ 10^3\ \rho_T$ and $3.4\ 10^6\ \rho_L$.

4.10 Conclusion

The analysis of the $\gamma N \to \gamma\rho^0 N'$ process in the generalized Bjorken kinematics where GPD factorization is expected to hold in a collinear QCD approach has shown interesting features.

Firstly, although any helicity state of the vector meson is populated at the same level in the twist expansion of the amplitude, the production of longitudinally polarized vector mesons turns out to be numerically dominant. This mostly comes from the difference in the normalization of chiral odd versus chiral even GPDs, as shown in our modelization (see Figs. 4.19-4.21). If our model underestimates the chiral odd GPDs (which might well be the case, since the constraints on the transversity distributions are still quite indirect), the data rates for ρ_T production will be higher.

Secondly, the magnitude of the cross section is large enough for the process to be analyzed in a quite detailed way by near-future experiments at JLab with photon beams originating from the 12 GeV electron beam. Detectors in Hall B, C and D seem to be perfectly suited for this study. A more detailed study is needed to decide on the feasibility of the experiment when taking into account of all detection efficiencies.

We restricted our analysis to unpolarized cross sections; this may be complemented by a computation of various polarization observables.

A NLO calculation should first confirm the validity of the factorization hypothesis for this process, and estimate the effects on the amplitude. Let us stress that, contrary to the DVCS (and TCS) case where gluon contributions turn out to be important at this level [161, 180], the charge conjugation property of the process studied here protects us from these contributions. We may thus expect that NLO corrections will be under control, without the necessity of a resummation procedure.

To conclude, the cross section of our process is a factor 400 more than the $\gamma P \to Pe^+e^-$ process, for similar values of the hard scale, for which experimental proposals have been approved at JLab, Thus, the study of our process appears feasible experimentally and promises to bring new important constraints on GPD physics.

We would like to mention that a similar study could be performed in principle in the Compass experiment at CERN where $S_{\gamma N} \sim 200$ GeV^2 and at LHC in ultraperipheral collisions [121], as well as in future electron proton collider projects like EIC [109] and LHeC [110].

Chapter 5

Conclusion

In this work we studied several exclusive processes as a way to get a better insight on some of the fundamental questions of QCD : resummation effects, saturation effects and non-perturbative physics.

The study which was performed in the first part of this thesis constitutes the first computation of the NLO impact factor for an exclusive process using the shockwave formalism.
Due to the fact that it was obtained with completely general kinematics, it is a strong basis for a lot of precision phenomenology at asymptotic energies. Very few processes have been described with such accuracy in the k_t-factorization formalism, hence we expect our result to improve greatly our understanding of QCD in its Regge limit. The use of the shockwave approach rather than the BFKL formalism allows our results to hold when considering processes in eA collisions. Thus it is a step towards precision physics in the saturation regime, where non-linear effects become important.
Our computation opened a way for similar NLO computations in the shockwave approach. In this thesis we presented how to adapt our results for the computation of the $\gamma^* \to \gamma^*$ impact factor and we showed how to obtain the impact factor for the production of an open $c\bar{c}$ pair and for the production of a charmonium in some cases. Moreover, we showed how to adapt the present computation to the production of a light vector meson and how such a result would allow one to verify previous results for the correspondence between the linearized BK equation and the BFKL equation.

In the second part of this thesis, we performed the full feasibility study for the photoproduction of a ρ meson and a photon, giving numerical predictions for JLab@12GeV. We expect the proposed process to be a probe of GPDs, the non-forward extension of the non-perturbative building blocks in collinear factorization. The original idea behind our study was to probe transversity GPDs which are chiral-odd, hence elusive, quantities. Our results hint that the chiral-odd contribution to this process is highly suppressed, thus hard to probe experimentally, however a more involved study which would include the density matrix of the final state may lead to more optimistic predictions in the future. In any case, our process constitutes a very good way of probing the usual GPDs, for universality checks and for new constraints on these quantities. Our results can be extended in the future to the electroproduction case by adding Bethe-Heitler contributions in which the photon in the final state is emitted by the electron, and a NLO computation could be performed in order to check the validity of the factorization hypothesis for this process.

Part IV

Appendices

Appendix A

Finite part of the $\gamma^* \to q\bar{q}$ and $\gamma^* \to q\bar{q}g$ impact factors

A.1 Finite part of the $\gamma^* \to q\bar{q}$ impact factor

A.1.1 Building-block integrals

Throughout this section, we will need the following integrals

$$I_1^k(\vec{q}_1,\,\vec{q}_2,\,\Delta_1,\,\Delta_2) \equiv \frac{1}{\pi}\int \frac{d^d\vec{l}\,(l_\perp^k)}{\left[(\vec{l}-\vec{q}_1)^2+\Delta_1\right]\left[(\vec{l}-\vec{q}_2)^2+\Delta_2\right]\vec{l}^{\,2}}, \tag{A.1}$$

$$I_2(\vec{q}_1,\,\vec{q}_2,\,\Delta_1,\,\Delta_2) \equiv \frac{1}{\pi}\int \frac{d^d\vec{l}}{\left[(\vec{l}-\vec{q}_1)^2+\Delta_1\right]\left[(\vec{l}-\vec{q}_2)^2+\Delta_2\right]}, \tag{A.2}$$

$$I_3^k(\vec{q}_1,\,\vec{q}_2,\,\Delta_1,\,\Delta_2) \equiv \frac{1}{\pi}\int \frac{d^d\vec{l}\,(l_\perp^k)}{\left[(\vec{l}-\vec{q}_1)^2+\Delta_1\right]\left[(\vec{l}-\vec{q}_2)^2+\Delta_2\right]}, \tag{A.3}$$

$$I^{jk}(\vec{q}_1,\,\vec{q}_2,\,\Delta_1,\,\Delta_2) \equiv \frac{1}{\pi}\int \frac{d^d\vec{l}\left(l_\perp^j l_\perp^k\right)}{\left[(\vec{l}-\vec{q}_1)^2+\Delta_1\right]\left[(\vec{l}-\vec{q}_2)^2+\Delta_2\right]\vec{l}^{\,2}}\,. \tag{A.4}$$

The arguments of these integrals will be different for each diagram so we will write them explicitly before giving the expression of each diagram, but we will ommit them in the equations for reader's convenience. Explicit results for the first 3 integrals in Eqs. (A.1-A.4) are obtained by a straightforward Feynman parameter integration. Let us compute explicitely I_1^k as an example : Let us first use Feyman's trick and shift $l_\perp$ to get textbook integrals :

$$\begin{aligned}
I_1^k &\equiv \frac{1}{\pi}\int d^d\vec{l}\frac{l_\perp^k}{\left[\left(\vec{l}-\vec{q}_1\right)^2+\Delta_1\right]\left[\left(\vec{l}-\vec{q}_2\right)^2+\Delta_2\right]\left[\vec{l}^{\,2}-i0\right]} \qquad (A.5)\\
&= \frac{2}{\pi}\int_0^1 d\alpha_1 d\alpha_2 \int \frac{d^d\vec{l}\,(l_\perp^k)}{\left[\left(\vec{l}-\alpha_1\vec{q}_1-\alpha_2\vec{q}_2\right)^2+\alpha_1\vec{q}_1^{\,2}+\alpha_2\vec{q}_2^{\,2}-(\alpha_1\vec{q}_1+\alpha_2\vec{q}_2)^2+\alpha_1\Delta_1+\alpha_2\Delta_2\right]^3}\\
&= \frac{2}{\pi}\int_0^1 d\alpha_1 d\alpha_2 \int d^d\vec{l}\frac{\alpha_1 q_{1\perp}^k+\alpha_2 q_{2\perp}^k}{\left[\vec{l}^{\,2}+\alpha_1\vec{q}_1^{\,2}+\alpha_2\vec{q}_2^{\,2}-(\alpha_1\vec{q}_1+\alpha_2\vec{q}_2)^2+\alpha_1\Delta_1+\alpha_2\Delta_2\right]^3}\\
&= \frac{\Gamma\left(3-\frac{d}{2}\right)\pi^{\frac{d}{2}}}{\pi}\int_0^1 d\alpha_1 d\alpha_2 \frac{\alpha_1 q_{1\perp}^k+\alpha_2 q_{2\perp}^k}{\left[\alpha_1\vec{q}_1^{\,2}+\alpha_2\vec{q}_2^{\,2}-(\alpha_1\vec{q}_1+\alpha_2\vec{q}_2)^2+\alpha_1\Delta_1+\alpha_2\Delta_2\right]^{3-\frac{d}{2}}}\,. \qquad (A.6)
\end{aligned}$$

Now let us make the following change of variables :

$$(\alpha_1,\, \alpha_2) \;\; \to \;\; (\rho,\, \eta)\;, \tag{A.7}$$

$$\alpha_1 \;\; \equiv \;\; r\rho\,, \tag{A.8}$$

$$\alpha_2 \;\; \equiv \;\; r\,(1-\rho)\;. \tag{A.9}$$

Then :

$$I_1^k \;\; = \;\; \frac{\Gamma\left(3-\frac{d}{2}\right)\pi^{\frac{d}{2}}}{\pi}\int_0^1 dr d\rho \frac{\rho q_{1\perp}^k + (1-\rho)\, q_{2\perp}^k}{\left[\rho\vec{q}_1^{\,2} + (1-\rho)\,\vec{q}_2^{\,2} + \rho\Delta_{12} + \Delta_2 - r\left(\vec{q}_2 + \rho\vec{q}_{12}\right)^2\right]^{3-\frac{d}{2}}\left(r^{1-\frac{d}{2}}\right)}\,, \tag{A.10}$$

where $\Delta_{ij} = \Delta_i - \Delta_j$. Let us note that this integral is actually a convergent integral, so one can set $d = 2$ in the right hand side. Then one can perform the ρ integration :

$$I_1^k \;\; = \;\; \frac{\Gamma\left(3-\frac{d}{2}\right)\pi^{\frac{d}{2}}}{\pi}\int_0^1 dr d\rho \frac{\rho q_{1\perp}^k + (1-\rho)\, q_{2\perp}^k}{\left[r - \frac{\rho\vec{q}_1^{\,2} + (1-\rho)\vec{q}_2^{\,2} + \rho\Delta_{12} + \Delta_2}{\left(\vec{q}_2 + \rho\vec{q}_{12}\right)^2}\right]^2\left(\vec{q}_2 + \rho\vec{q}_{12}\right)^4} \tag{A.11}$$

$$\;\; = \;\; \frac{\Gamma\left(3-\frac{d}{2}\right)\pi^{\frac{d}{2}}}{\pi}\int_0^1 d\rho \frac{\rho q_{12\perp}^k + q_{2\perp}^k}{\left[\rho\left(\vec{q}_1^{\,2} - \vec{q}_2^{\,2} + \Delta_{12}\right) + \left(\vec{q}_2^{\,2} + \Delta_2\right)\right]\left[-\vec{q}_{12}^{\,2}\rho^2 + \rho\left(\vec{q}_{12}^{\,2} + \Delta_{12}\right) + \Delta_2\right]}\,. \tag{A.12}$$

Let us define the two roots of the second denominator :

$$\rho_1 \;\; = \;\; \frac{\left(\vec{q}_{12}^{\,2} + \Delta_{12}\right) - \sqrt{\left(\vec{q}_{12}^{\,2} + \Delta_{12}\right)^2 + 4\vec{q}_{12}^{\,2}\Delta_2}}{2\vec{q}_{12}^{\,2}} \tag{A.13}$$

$$\rho_2 \;\; = \;\; \frac{\left(\vec{q}_{12}^{\,2} + \Delta_{12}\right) + \sqrt{\left(\vec{q}_{12}^{\,2} + \Delta_{12}\right)^2 + 4\vec{q}_{12}^{\,2}\Delta_2}}{2\vec{q}_{12}^{\,2}}\,. \tag{A.14}$$

Then :

$$I_1^k \;\; = \;\; -\frac{1}{\vec{q}_{12}^{\,2}\left(\vec{q}_1^{\,2} - \vec{q}_2^{\,2} + \Delta_{12}\right)}\int_0^1 d\rho \frac{\rho q_{12\perp}^k + q_{2\perp}^k}{\left[\rho + \frac{\left(\vec{q}_2^{\,2} + \Delta_2\right)}{\left(\vec{q}_1^{\,2} - \vec{q}_2^{\,2} + \Delta_{12}\right)}\right]\left(\rho - \rho_1\right)\left(\rho - \rho_2\right)} \tag{A.15}$$

$$\;\; = \;\; -\frac{1}{\vec{q}_{12}^{\,2}\left(\vec{q}_1^{\,2} - \vec{q}_2^{\,2} + \Delta_{12}\right)\left(\rho_1 - \rho_2\right)} \tag{A.16}$$

$$\times\left[\frac{1}{\rho_1 + \frac{\left(\vec{q}_2^{\,2} + \Delta_2\right)}{\left(\vec{q}_1^{\,2} - \vec{q}_2^{\,2} + \Delta_{12}\right)}}\left(\int_0^1 d\rho \frac{\left(\rho_1 q_{12\perp}^k + q_{2\perp}^k\right)}{\left(\rho - \rho_1\right)} + \int_0^1 d\rho \frac{\frac{\left(\vec{q}_2^{\,2} + \Delta_2\right)}{\left(\vec{q}_1^{\,2} - \vec{q}_2^{\,2} + \Delta_{12}\right)}q_{12\perp}^k - q_{2\perp}^k}{\left[\rho + \frac{\left(\vec{q}_2^{\,2} + \Delta_2\right)}{\left(\vec{q}_1^{\,2} - \vec{q}_2^{\,2} + \Delta_{12}\right)}\right]}\right)\right.$$

$$\left. -\frac{1}{\rho_2 + \frac{\left(\vec{q}_2^{\,2} + \Delta_2\right)}{\left(\vec{q}_1^{\,2} - \vec{q}_2^{\,2} + \Delta_{12}\right)}}\left(\int_0^1 d\rho \frac{\left(\rho_2 q_{12\perp}^k + q_{2\perp}^k\right)}{\left(\rho - \rho_2\right)} + \int_0^1 d\rho \frac{\frac{\left(\vec{q}_2^{\,2} + \Delta_2\right)}{\left(\vec{q}_1^{\,2} - \vec{q}_2^{\,2} + \Delta_{12}\right)}q_{12\perp}^k - q_{2\perp}^k}{\left[\rho + \frac{\left(\vec{q}_2^{\,2} + \Delta_2\right)}{\left(\vec{q}_1^{\,2} - \vec{q}_2^{\,2} + \Delta_{12}\right)}\right]}\right)\right]$$

$$\;\; = \;\; -\frac{1}{\vec{q}_{12}^{\,2}\left(\vec{q}_1^{\,2} - \vec{q}_2^{\,2} + \Delta_{12}\right)}\left[\frac{\rho_1 q_{12\perp}^k + q_{2\perp}^k}{\left(\rho_1 + \frac{\left(\vec{q}_2^{\,2} + \Delta_2\right)}{\left(\vec{q}_1^{\,2} - \vec{q}_2^{\,2} + \Delta_{12}\right)}\right)\left(\rho_1 - \rho_2\right)}\ln\left(\frac{1-\rho_1}{-\rho_1}\right)\right. \tag{A.17}$$

$$\left. -\frac{\left(\vec{q}_2^{\,2} + \Delta_2\right)q_{1\perp}^k - \left(\vec{q}_1^{\,2} + \Delta_1\right)q_{2\perp}^k}{\left(\vec{q}_1^{\,2} - \vec{q}_2^{\,2} + \Delta_{12}\right)\left(\rho_1 + \frac{\left(\vec{q}_2^{\,2} + \Delta_2\right)}{\left(\vec{q}_1^{\,2} - \vec{q}_2^{\,2} + \Delta_{12}\right)}\right)\left(\rho_2 + \frac{\left(\vec{q}_2^{\,2} + \Delta_2\right)}{\left(\vec{q}_1^{\,2} - \vec{q}_2^{\,2} + \Delta_{12}\right)}\right)}\ln\left(\frac{\vec{q}_1^{\,2} + \Delta_1}{\vec{q}_2^{\,2} + \Delta_2}\right)\right]$$

$$-\frac{\rho_2 q_{12\perp}^k + q_{2\perp}^k}{\left(\rho_2 + \frac{(\vec{q}_2^{\,2}+\Delta_2)}{(\vec{q}_1^{\,2}-\vec{q}_2^{\,2}+\Delta_{12})}\right)(\rho_1-\rho_2)} \ln\left(\frac{1-\rho_2}{-\rho_2}\right)\Bigg] .$$

One can simplify this expression by using the following properties of the two roots :

$$\rho_1\rho_2 = -\frac{\Delta_2}{\vec{q}_{12}^{\,2}}, \tag{A.18}$$

$$\rho_1+\rho_2 = \left(\frac{\vec{q}_{12}^{\,2}+\Delta_{12}}{\vec{q}_{12}^{\,2}}\right), \tag{A.19}$$

$$\rho_1 = \frac{1}{2}\left(\frac{\vec{q}_{12}^{\,2}+\Delta_{12}}{\vec{q}_{12}^{\,2}}\right) + \frac{1}{2}(\rho_1-\rho_2), \tag{A.20}$$

$$\rho_2 = \frac{1}{2}\left(\frac{\vec{q}_{12}^{\,2}+\Delta_{12}}{\vec{q}_{12}^{\,2}}\right) - \frac{1}{2}(\rho_1-\rho_2).$$

One finally gets :

$$\begin{aligned} I_1^k &= \frac{q_{1\perp}^k}{2\left[\vec{q}_{12}^{\,2}\left(\vec{q}_1^{\,2}+\Delta_1\right)\left(\vec{q}_2^{\,2}+\Delta_2\right)-\left(\vec{q}_1^{\,2}-\vec{q}_2^{\,2}+\Delta_{12}\right)\left(\vec{q}_1^{\,2}\Delta_2-\vec{q}_2^{\,2}\Delta_1\right)\right]} \\ &\times \left\{\frac{\left(\vec{q}_2^{\,2}+\Delta_2\right)\vec{q}_{12}^{\,2}+\vec{q}_2^{\,2}\left(\Delta_1+\Delta_2\right)+\Delta_2\left(\Delta_{21}-2\vec{q}_1^{\,2}\right)}{(\rho_1-\rho_2)\,\vec{q}_{12}^{\,2}}\ln\left[\left(\frac{-\rho_1}{1-\rho_1}\right)\left(\frac{1-\rho_2}{-\rho_2}\right)\right]\right. \\ &\left.+\left(\vec{q}_2^{\,2}+\Delta_2\right)\ln\left[\frac{\Delta_2\left(\vec{q}_1^{\,2}+\Delta_1\right)^2}{\Delta_1\left(\vec{q}_2^{\,2}+\Delta_2\right)^2}\right]+(1\leftrightarrow 2)\right\}. \end{aligned} \tag{A.21}$$

I_2 and I_3^k only require textbook integrals. They read :

$$I_2 = \frac{1}{\vec{q}_{12}^{\,2}(\rho_1-\rho_2)}\ln\left[\left(\frac{-\rho_1}{1-\rho_1}\right)\left(\frac{1-\rho_2}{-\rho_2}\right)\right], \tag{A.22}$$

and

$$I_3^k = \frac{\left(\vec{q}_{12}^{\,2}+\Delta_{12}\right)q_1^k+\left(\vec{q}_{21}^{\,2}+\Delta_{21}\right)q_2^k}{2(\rho_1-\rho_2)(\vec{q}_{12}^{\,2})^2}\ln\left[\left(\frac{-\rho_1}{1-\rho_1}\right)\left(\frac{1-\rho_2}{-\rho_2}\right)\right]-\frac{q_{12}^k}{2\vec{q}_{12}^{\,2}}\ln\left(\frac{\Delta_1}{\Delta_2}\right). \tag{A.23}$$

Please note that in some cases the real part of Δ_1 or Δ_2 will be negative so the previous results can acquire an imaginary part from the imaginary part $\pm i0$ of the arguments.
The last integral in Eq. (A.4) can be expressed in terms of the other ones by writing

$$I^{jk} = I_{11}\left(q_{1\perp}^j q_{1\perp}^k\right) + I_{12}\left(q_{1\perp}^j q_{2\perp}^k + q_{2\perp}^j q_{1\perp}^k\right) + I_{22}\left(q_{2\perp}^j q_{2\perp}^k\right), \tag{A.24}$$

Then by projecting the previous relation on the (jk)-tensors formed by $q_{1\perp}^j$ and $q_{2\perp}^k$and solving for $(I_{11},\, I_{12},\, I_{22})$ gives :

$$I_{11} = \frac{\left(\vec{q}_2^{\,2}\right)^2\left(q_{1\perp j}q_{1\perp k}I^{jk}\right)-2\vec{q}_2^{\,2}\left(\vec{q}_1\cdot\vec{q}_2\right)\left(q_{1\perp j}q_{2\perp k}I^{jk}\right)+\left(\vec{q}_1\cdot\vec{q}_2\right)\left(q_{2\perp j}q_{2\perp k}I^{jk}\right)}{\left[\vec{q}_1^{\,2}\vec{q}_2^{\,2}-\left(\vec{q}_1\cdot\vec{q}_2\right)^2\right]^2}, \tag{A.25}$$

$$I_{12} = \frac{-\vec{q}_2^{\,2}\left(\vec{q}_1\cdot\vec{q}_2\right)\left(q_{1\perp j}q_{1\perp k}I^{jk}\right)+\left(\vec{q}_1^{\,2}\vec{q}_2^{\,2}+\left(\vec{q}_1\cdot\vec{q}_2\right)^2\right)\left(q_{1\perp j}q_{2\perp k}I^{jk}\right)-\vec{q}_1^{\,2}\left(\vec{q}_1\cdot\vec{q}_2\right)\left(q_{2\perp j}q_{2\perp k}I^{jk}\right)}{\left[\vec{q}_1^{\,2}\vec{q}_2^{\,2}-\left(\vec{q}_1\cdot\vec{q}_2\right)^2\right]^2}, \tag{A.26}$$

$$I_{22} = \frac{\left(\vec{q}_1\cdot\vec{q}_2\right)^2\left(q_{1\perp j}q_{1\perp k}I^{jk}\right)-2\vec{q}_1^{\,2}\left(\vec{q}_1\cdot\vec{q}_2\right)\left(q_{1\perp j}q_{2\perp k}I^{jk}\right)+\left(\vec{q}_1^{\,2}\right)^2\left(q_{2\perp j}q_{2\perp k}I^{jk}\right)}{\left[\vec{q}_1^{\,2}\vec{q}_2^{\,2}-\left(\vec{q}_1\cdot\vec{q}_2\right)^2\right]^2}. \tag{A.27}$$

Let us make the following remark :

$$\left(r_{1k}I^{jk}\right) = -\frac{1}{\pi}\int \frac{d^d\vec{l}\left(\vec{q}_1\cdot\vec{l}\right)\left(l_\perp^j\right)}{\left[(\vec{l}-\vec{q}_1)^2+\Delta_1\right]\left[(\vec{l}-\vec{q}_2)^2+\Delta_2\right]\vec{l}^{\,2}} \tag{A.28}$$

$$= \left(\frac{1}{2\pi}\int d^d\vec{l}\frac{l_\perp^j}{\left[(\vec{l}-\vec{q}_2)^2+\Delta_2\right]\vec{l}^{\,2}}\right) - \frac{1}{2}I_3^j - \frac{1}{2}\left(\vec{q}_1^{\,2}+\Delta_1\right)I_1^j \tag{A.29}$$

$$= -\frac{1}{2}\left[\frac{q_{2\perp}^j}{\vec{q}_2^{\,2}}\ln\left(\frac{\Delta_2}{\vec{q}_2^{\,2}+\Delta_2}\right) + I_3^j + \left(\vec{q}_1^{\,2}+\Delta_1\right)I_1^j\right], \tag{A.30}$$

and similarly

$$\left(r_{2k}I^{jk}\right) = -\frac{1}{2}\left[\frac{q_{1\perp}^j}{\vec{q}_1^{\,2}}\ln\left(\frac{\Delta_1}{\vec{q}_1^{\,2}+\Delta_1}\right) + I_3^j + \left(\vec{q}_2^{\,2}+\Delta_2\right)I_1^j\right]. \tag{A.31}$$

Applying these in Eqs. (A.25-A.27) allows one to conclude :

$$I_{11} = -\frac{1}{2}\frac{\left[\vec{q}_2^{\,2}q_{1\perp k} - \left(\vec{q}_1\cdot\vec{q}_2\right)q_{2\perp k}\right]}{\left[\vec{q}_1^{\,2}\vec{q}_2^{\,2} - \left(\vec{q}_1\cdot\vec{q}_2\right)^2\right]^2} \tag{A.32}$$
$$\times\left[\left(\frac{\vec{q}_1\cdot\vec{q}_2}{\vec{q}_1^{\,2}}\right)\ln\left(\frac{\vec{q}_1^{\,2}+\Delta_1}{\Delta_1}\right)q_{1\perp}^k + \left(\vec{q}_2\cdot\vec{q}_{21}\right)I_3^k + \left\{\vec{q}_2^{\,2}\left(\vec{q}_1\cdot\vec{q}_{12}\right) + \Delta_1\vec{q}_2^{\,2} - \Delta_2\left(\vec{q}_1\cdot\vec{q}_2\right)\right\}I_1^k\right],$$

$$I_{12} = \frac{-1}{4\left[\vec{q}_1^{\,2}\vec{q}_2^{\,2} - \left(\vec{q}_1\cdot\vec{q}_2\right)^2\right]}\ln\left(\frac{\vec{q}_1^{\,2}+\Delta_1}{\Delta_1}\right) \tag{A.33}$$
$$+\frac{\vec{q}_2^{\,2}\left(\vec{q}_1\cdot\vec{q}_2\right)}{2\left[\vec{q}_1^{\,2}\vec{q}_2^{\,2} - \left(\vec{q}_1\cdot\vec{q}_2\right)^2\right]^2}\left[\left(\vec{q}_1^{\,2}+\Delta_1\right)\left(q_{1\perp k}I_1^k\right) + \left(q_{1\perp k}I_3^k\right)\right]$$
$$-\frac{\left(\vec{q}_1^{\,2}\vec{q}_2^{\,2}\right) + \left(\vec{q}_1\cdot\vec{q}_2\right)^2}{4\left[\vec{q}_1^{\,2}\vec{q}_2^{\,2} - \left(\vec{q}_1\cdot\vec{q}_2\right)^2\right]^2}\left[\left(\vec{q}_2^{\,2}+\Delta_2\right)\left(q_{1\perp k}I_1^k\right) + \left(q_{1\perp k}I_3^k\right)\right] + (1\leftrightarrow 2),$$

$$I_{22} = I_{11}|_{(1\leftrightarrow 2)}. \tag{A.34}$$

This last expression makes it seem that there is a singularity when $\vec{q}_1$ and $\vec{q}_2$ are collinear or anticollinear. However, this singularity is non-physical and only appears when projecting on the particular basis of 2-dimensional symmetric tensors $(q_1^jq_1^k,\ q_1^jq_2^k+q_2^jq_1^k,\ q_2^jq_2^k)$. One can show that it disappears when projecting on the non-minimal basis $(q_1^jq_1^k,\ q_1^jq_2^k+q_2^jq_1^k,\ q_2^jq_2^k,\ g_\perp^{jk})$. For a further study, the reader is referred to the appendix in [181].

A.1.2 Diagram 4

Here the integrals from section (A.1) will have the following arguments :

$$\vec{q}_1 = \vec{p}_1 - \left(\frac{x-z}{x}\right)\vec{p}_q, \qquad \vec{q}_2 = \left(\frac{x-z}{x}\right)\left(x\vec{p}_{\bar{q}} - \bar{x}\vec{p}_q\right),$$
$$\Delta_1 = (x-z)\left(\bar{x}+z\right)Q^2, \quad \Delta_2 = -\frac{x\left(\bar{x}+z\right)}{\bar{x}\left(x-z\right)}\vec{q}_2^{\,2} - i0. \tag{A.35}$$

Let us write the impact factors in terms of these variables. They read :
(longitudinal NLO) $\times$ (longitudinal LO) contribution :

$$\left(\phi_4\right)_{LL} = -\frac{4(x-z)(\bar{x}+z)}{z}[-\bar{x}(x-z)(z+1)I_2 + q_{2\perp k}(2x^2-(2x-z)(z+1))I_1^k], \tag{A.36}$$

(longitudinal NLO) $\times$ (transverse LO) contribution :

$$(\phi_4)^j_{LT} = (1-2x)p_{q1'}{}^j_\perp\,(\phi_4)_{LL} - 4(x-z)(\bar{x}+z)(1-2x+z)[(\vec{q}_2\cdot\vec{p}_{q1'})g^j_{\perp k} + q^j_{2\perp}p_{q1'\perp k}]I^k_1\,, \tag{A.37}$$

(transverse NLO) $\times$ (longitudinal LO) contribution :

$$\begin{aligned}(\phi_4)^i_{TL} = 2\{&[(x-\bar{x}-z)q^i_{2\perp}q_{1\perp k} + (-8x\bar{x}-6xz+2z^2+3z+1)q^j_{1\perp}q_{2\perp k}]I^k_1\\ &- 2[4x^2 - x(3z+5) + (z+1)^2]q_{2\perp k}I^{ik} + (x-\bar{x}-z)\,(\vec{q}_2\cdot\vec{q}_1)\,I^i\\ &+ I_2[(x-\bar{x}-z)q^i_{2\perp} + \bar{x}(2(x-z)^2 - 5x + 3z + 1)q^i_{1\perp}]\\ &- \bar{x}[2(x-z)^2 - 5x + 3z + 1]I^i_3\\ &+ \frac{x\bar{x}(1-2x)}{z}[2q_{2\perp k}I^{ik} + I^i_3 - q^i_{1\perp}(2q_{2\perp k}I^k_1 + I_2)]\}\,,\end{aligned} \tag{A.38}$$

(transverse NLO) $\times$ (transverse LO) contribution :

$$\begin{aligned}(\phi_4)^{ij}_{TT} &= \left[(x-\bar{x}-2z)(x-\bar{x}-z)(\vec{q}_2\cdot\vec{p}_{q1'})q^i_{1\perp} + (z+1)((\vec{q}_1\cdot\vec{q}_2)\,p^i_{q1'\perp} - (\vec{q}_1\cdot\vec{p}_{q1'})q^i_{2\perp})\right]I^j_1\\ &+ 2\bar{x}[q_{2\perp k} - (x-z)q_{1\perp k}](p^i_{q1'\perp}I^{jk} - g^{ij}_\perp p_{q1'\perp l}I^{kl})\\ &+ 2(x-z)[(2\bar{x}+z)(\vec{q}_2\cdot\vec{p}_{q1'}) - \bar{x}(\vec{q}_1\cdot\vec{p}_{q1'})]I^{ij}\\ &+ [(1-z)((\vec{q}_1\cdot\vec{p}_{q1'})q^j_{2\perp} - (\vec{q}_2\cdot\vec{p}_{q1'})q^j_{1\perp}) - (1-2x)(\bar{x}-x+z)\,(\vec{q}_1\cdot\vec{q}_2)\,p^j_{q1'\perp}]I^i_1\\ &- 2\Big[(x-z)(\bar{x}q^j_{1\perp} - (2\bar{x}+z)q^j_{2\perp})p_{q1'\perp k}\\ &+ (1-2x)\left(4x^2 - (3z+5)x + (z+1)^2\right)q_{2\perp k}p_{q1'}{}^j_\perp\Big]\,I^{ik}\\ &- \bar{x}\,(\bar{x}-x)\left(2(x-z)^2 - 5x + 3z + 1\right)p^j_{q1'\perp}I^i_3\\ &+ \bar{x}\,(\bar{x}+z)\,(p^i_{q1'\perp}I^j_3 - g^{ij}_\perp p_{q1'\perp k}I^k_3)\end{aligned}$$

$$\begin{aligned}&+ I_2\Big[g^{ij}_\perp\,((1-z)(\vec{q}_2\cdot\vec{p}_{q1'}) - \bar{x}(1+x-z)(\vec{q}_1\cdot\vec{p}_{q1'}))\\ &+ ((1-z)q^j_{2\perp} - \bar{x}(1+x-z)q^j_{1\perp})p_{q1'}{}^i_\perp\\ &- (\bar{x}-x)\left((\bar{x}-x+z)q^i_{2\perp} - \bar{x}\left(2(x-z)^2 - 5x + 3z + 1\right)q^i_{1\perp}\right)p_{q1'}{}^j_\perp\Big]\\ &+ I^k_1\Big[g^{ij}_\perp\,((x-\bar{x}+z)(\vec{q}_1\cdot\vec{p}_{q1'})q_{2\perp k} + (1-z)(\vec{q}_2\cdot\vec{p}_{q1'})q_{1\perp k} - (z+1)\,(\vec{q}_1\cdot\vec{q}_2)\,p_{q1'\perp k})\\ &+ q^j_{1\perp}((x-\bar{x}+z)q_{2\perp k}p^i_{q1'\perp} - (z+1)q^i_{2\perp}p_{q1'\perp k})\\ &+ q^j_{2\perp}((x-\bar{x}-2z)(x-\bar{x}-z)q^i_{1\perp}p_{q1'\perp k} + (1-z)q_{1\perp k}p_{q1'}{}^i_\perp)\\ &- (1-2x)((1-2x+z)q^i_{2\perp}q_{1\perp k} - (2z^2+3z-x(8\bar{x}+6z)+1)q^i_{1\perp}q_{2\perp k})p_{q1'}{}^j_\perp\Big]\\ &+ \frac{x\bar{x}}{z}\Big[(x-\bar{x})^2p^j_{q1'\perp}(2q_{2\perp k}I^{ik} + I^i_3 - q^i_{1\perp}(I_2 + 2q_{2\perp k}I^k_1))\\ &+ p^i_{q1'\perp}(q^j_{1\perp}(I_2 + 2q_{2\perp k}I^k_1) - 2q_{2\perp k}I^{jk} - I^j_3)\\ &+ g^{ij}_\perp((\vec{q}_1\cdot\vec{p}_{q1'})(I_2 + 2q_{2\perp k}I^k_1) + p_{q1'\perp k}(2q_{2\perp l}I^{kl} + I^k_3))\Big]\,.\end{aligned} \tag{A.39}$$

A.1.3 Diagram 5

Here the integrals from section (A.2) will have the following arguments :

$$\vec{q}_1 = \vec{p}_{q1} - \frac{z}{x}\vec{p}_q, \quad \vec{q}_2 = \left(\frac{x-z}{x}\right)\vec{p}_3 - \frac{z}{x}\vec{p}_1\,, \tag{A.40}$$

$$\Delta_1 = \frac{z(x-z)}{x^2\bar{x}}(\vec{p}^{\,2}_{\vec{q}2} + x\bar{x}Q^2), \quad \Delta_2 = (x-z)(\bar{x}+z)Q^2\,, \tag{A.41}$$

With such variables, it is easy to see that the argument in the square roots in Eq. (A.14) is a full square, so that

$$\rho_1 = -\frac{x\bar{x}Q^2}{\vec{p}^{\,2}_{\vec{q}2}}\,, \quad \rho_2 = \frac{x(\bar{x}+z)}{\bar{x}(x-z)}\,. \tag{A.42}$$

In terms of the variables in Eq. (A.40), the impact factors read :
(longitudinal NLO) $\times$ (longitudinal LO) :

$$(\phi_5)_{LL} = \frac{4(x-z)(-2x(\bar{x}+z)+z^2+z)}{xz}\left[\bar{x}(x-z)I_2 - (zq_{1\perp k} - x\,(\bar{x}+z)\,q_{2\perp k})\,I_1^k\right], \tag{A.43}$$

(longitudinal NLO) $\times$ (transverse LO) :

$$\begin{aligned}(\phi_5)^j_{LT} &= (\bar{x}-x)p^j_{q1'\perp}\,(\phi_5)_{LL} \\ &+ \frac{4(x-z)(x-\bar{x}-z)}{x}\left(zq^k_{1\perp} - x(\bar{x}+z)q^k_{2\perp}\right)p_{q1'\perp l}\left(g^j_{\perp k}I^l_1 - g^l_{\perp k}I^j_1\right),\end{aligned} \tag{A.44}$$

(transverse NLO) $\times$ (longitudinal LO) :

$$\begin{aligned}(\phi_5)^i_{TL} &= 2\left[(x-\bar{x}-z)\,(\vec{q}_1\cdot\vec{q}_2) - \bar{x}(x-z)^2Q^2 + (\frac{z}{x}-x)\vec{q}_1^{\,2}\right]I^i_1 \\ &+ \frac{2}{x}\left[xq_{2\perp k}(-8x\bar{x}-6xz+2z^2+3z+1) + 2q_{1\perp k}(2xz-2x^2+x-z^2)\right]q^i_{1\perp}I^k_1 \\ &+ 2q^i_{2\perp}q_{1\perp k}(x-\bar{x}-z)I^k_1 + 2\frac{\bar{x}}{x}(x(8x-3)-6xz+2z^2+z)I^i_1 \\ &+ \frac{2}{x}\left[xq^i_{2\perp}(x-\bar{x}-z) + q^i_{1\perp}(8x^3-6x^2(z+2)+x(z+3)(2z+1)-2z^2)\right]I_2 \\ &- \frac{4}{x}\left[(x-z)(\bar{x}+z)q_{1\perp k} + x(4x^2-x(3z+5)+(z+1)^2)q_{2\perp k}\right]I^{ik} \\ &- \frac{4}{z}x\bar{x}(x-\bar{x})\left[q_{2\perp k}I^{ik} + I^i_3 - q^i_{1\perp}\left(q_{2\perp k}I^k_1 + I_2\right)\right],\end{aligned} \tag{A.45}$$

(transverse NLO) $\times$ (transverse LO) :

$$\begin{aligned}&(\phi_5)^{ij}_{TT} = -2(x-z)\left[\frac{z}{x}(\vec{q}_1\cdot\vec{p}_{q1'}) - (2\bar{x}+z)(\vec{q}_2\cdot\vec{p}_{q1'})\right]I^{ij} \\ +\;&\left[-\bar{x}(x-z)^2Q^2p^i_{q1'\perp} + (\bar{x}-x+2z)(\bar{x}-x+z)(\vec{q}_2\cdot\vec{p}_{q1'})q^i_{1\perp}\right. \\ -\;&(\vec{q}_1\cdot\vec{p}_{q1'})((z+1)q^i_{2\perp} - 2\frac{z}{x}(2x-z)q^i_{1\perp}) \\ +\;&\left.((z+1)\,(\vec{q}_1\cdot\vec{q}_2) - \left(x+\frac{z}{x}\right)\vec{q}_1^{\,2})p^i_{q1'\perp}\right]I^j_1 \\ -\;&2\frac{\bar{x}}{x}(xq_{2\perp k} + (x-z)q_{1\perp k})\left(g^{ij}_\perp p_{q1'\perp l}I^{kl} - p_{q1'}{}^i_\perp I^{jk}\right) \\ +\;&\left[\bar{x}\,(x-\bar{x})\,(x-z)^2Q^2p^j_{q1'\perp} - (z-1)(\vec{q}_1\cdot\vec{p}_{q1'})q^j_{2\perp}\right. \\ +\;&\left.(z-1)(\vec{q}_2\cdot\vec{p}_{q1'})q^j_{1\perp} + \frac{x-\bar{x}}{x}\left((x^2-z)\vec{q}_1^{\,2} + x(\bar{x}-x+z)(\vec{q}_1\cdot\vec{q}_2)\right)p^k_{q1'\perp}\right]I^i_1 \\ +\;&2\left[\frac{x-\bar{x}}{x}\left(x(4x^2-(3z+5)x+(z+1)^2)q_{2\perp k} + (x-z)(\bar{x}+z)q_{1\perp k}\right)p^j_{q1'\perp}\right. \\ -\;&\left.\frac{x-z}{x}\left(x(2x-z-2)q^j_{2\perp} + zq^j_{1\perp}\right)p_{q1'\perp k}\right]I^{ik} \\ +\;&\frac{\bar{x}\,(\bar{x}-x)}{x}\left(2z^2-6xz+z+x(8x-3)\right)p^j_{q1'\perp}I^i_3 \\ +\;&\left[(x-\bar{x})\left((\bar{x}-x+z)q^i_{2\perp} + \left(6(z+2)x-8x^2-(z+3)(2z+1)+2\frac{z^2}{x}\right)q^i_{1\perp}\right)p^j_{q1'\perp}\right. \\ +\;&\left.(1-z)(g^{ij}_\perp(\vec{q}_2\cdot\vec{p}_{q1'}) + q^k_{2\perp}p^i_{q1'\perp}) + (2x+z-3)(g^{ik}_\perp(\vec{q}_1\cdot\vec{p}_{q1'}) + q^k_{1\perp}p^i_{q1'\perp})\right]I_2 \\ +\;&\left(3\bar{x}+z-\frac{z}{x}\right)p^i_{q1'\perp}I^k_3 - \frac{\bar{x}}{x}(3x-z)g^{ij}_\perp p_{q1'\perp k}I^k_3 \\ +\;&\left[(x-\bar{x})p^j_{q1'\perp}\left\{(\bar{x}-x+z)q^i_{2\perp}q_{1\perp k} - (2z^2-6xz+3z-8x\bar{x}+1)q_{2\perp k}q^i_{1\perp}\right.\right. \\ -\;&\left.\left.2(\bar{x}-x+2z-\frac{z^2}{x})q_{1\perp k}q^i_{1\perp}\right\} + \bar{x}(x-z)^2Q^2g^{ij}_\perp p_{q1'\perp k}\right.\end{aligned}$$

$$
\begin{aligned}
&+ \quad (1-z)q_{1\perp k}(g_\perp^{ij}(\vec{q}_2\cdot\vec{p}_{q1'}) + q_{2\perp}^j p_{q1'\perp}^i) \\
&+ \quad ((x-\bar{x}+z)q_{2\perp k} - 2q_{1\perp k})\,(g_\perp^{ij}(\vec{q}_1\cdot\vec{p}_{q1'}) + q_{1\perp}^j p_{q1'\perp}^i) \\
&+ \quad g_\perp^{ij}\left(\left(x+\frac{z}{x}\right)\vec{q}_1^{\,2} - (z+1)(\vec{q}_1\cdot\vec{q}_2)\right)p_{q1'\perp k}
\end{aligned}
$$

$$
\begin{aligned}
&+ \quad \left((x-\bar{x}-2z)(x-\bar{x}-z)q_{1\perp}^i q_{2\perp}^j - (z+1)q_{2\perp}^i q_{1\perp}^j + 2(2x-z)\frac{z}{x}q_{1\perp}^i q_{1\perp}^j\right)p_{q1'\perp k}\Big]\, I_1^k \\
&+ \quad \frac{2x\bar{x}}{z}\Big[(x-\bar{x})^2 p_{q1'\perp}^j(q_{2\perp k}I^{ik} + I_3^i) - p_{q1'\perp}^i(q_{2\perp k}I^{jk} + I_3^k) + g_\perp^{ij}p_{q1'\perp k}(q_{2\perp l}I^{kl} + I_3^k) \\
&+ \quad (I_2 + q_{2\perp k}I_1^k)\left(g_\perp^{ij}(\vec{q}_1\cdot\vec{p}_{q1'}) + q_{1\perp}^j p_{q1'\perp}^i - (1-2x)^2 q_{1\perp}^i p_{q1'\perp}^j\right)\Big]\,. \qquad \text{(A.46)}
\end{aligned}
$$

A.1.4 Diagram 6

For this diagram we will introduce the variable

$$\vec{q} = \left(\frac{x-z}{x}\right)\vec{p}_3 - \frac{z}{x}\vec{p}_1\,. \qquad \text{(A.47)}$$

Then the impact factors read :
(longitudinal NLO) $\times$ (longitudinal LO) :

$$(\phi_6)_{LL} = -4x\bar{x}^2 J_0\,, \qquad \text{(A.48)}$$

(longitudinal NLO) $\times$ (transverse LO) :

$$(\phi_6)_{LT}^j = (1-2x)p_{q1'\perp}^j(\phi_6)_{LL}\,, \qquad \text{(A.49)}$$

(transverse NLO) $\times$ (longitudinal LO) :

$$(\phi_6)_{TL}^i = 2\bar{x}\left[(1-2x)p_{\bar{q}2\perp}^i J_0 - J_{1\perp}^i\right]\,, \qquad \text{(A.50)}$$

(transverse NLO) $\times$ (transverse LO) :

$$
\begin{aligned}
(\phi_6)_{TT}^{ij} = {}& \bar{x}\left[(x-\bar{x})^2 p_{\bar{q}2\perp}^i p_{q1'\perp}^j - g_\perp^{ij}(\vec{p}_{\bar{q}2}\cdot\vec{p}_{q1'}) - p_{q1'\perp}^i p_{\bar{q}2\perp}^j\right]J_0 \\
&+ \bar{x}\left[(x-\bar{x})p_{q1'\perp}^j g_{\perp k}^i - p_{q1'\perp k}g_\perp^{ij} + p_{q1'\perp}^i g_{\perp k}^j\right]J_{1\perp}^k\,. \qquad \text{(A.51)}
\end{aligned}
$$

We introduced

$$J_{1\perp}^k = \frac{(x-z)^2}{x^2}\frac{q_\perp^k}{\vec{q}^{\,2}}\ln\left(\frac{\vec{p}_{\bar{q}2}^{\,2} + x\bar{x}Q^2}{\vec{p}_{\bar{q}2}^{\,2} + x\bar{x}Q^2 + \frac{x^2\bar{x}}{z(x-z)}\vec{q}^{\,2}}\right), \qquad \text{(A.52)}$$

and

$$J_0 = \frac{z}{x(\vec{p}_{\bar{q}2}^{\,2} + x\bar{x}Q^2)} - \frac{2x(x-z)+z^2}{xz(\vec{p}_{\bar{q}2}^{\,2} + x\bar{x}Q^2)}\ln\left(\frac{x^2\bar{x}\mu^2}{z(x-z)(\vec{p}_{\bar{q}2}^{\,2} + x\bar{x}Q^2) + x^2\bar{x}\vec{q}^{\,2}}\right). \qquad \text{(A.53)}$$

A.2 Finite part of the $\gamma^* \to q\bar{q}g$ impact factor

Here we present the convoluted impact factors from section 5.

A.2.1 LL photon transition

$$\Phi_4^+(\vec{p}_1,\,\vec{p}_2,\,\vec{p}_3)\,\Phi_4^{+*}(\vec{p}_{1'},\,\vec{p}_{2'},\,\vec{p}_3) = \frac{8\left(p_\gamma^+\right)^4}{x_g^2\left(\frac{\vec{p}^{\,2}_{\bar{q}2'}}{x_{\bar{q}}(1-x_{\bar{q}})}+Q^2\right)\left(Q^2+\frac{\vec{p}^{\,2}_{q1'}}{x_q}+\frac{\vec{p}^{\,2}_{\bar{q}2'}}{x_{\bar{q}}}+\frac{\vec{p}^{\,2}_{g3'}}{x_g}\right)}$$
$$\times\left[\frac{x_{\bar{q}}\left(x_g^2 d+4x_q\left(x_q+x_g\right)\right)\left(x_q\vec{p}_{g3}-x_g\vec{p}_{q1}\right)\cdot\left(x_q\vec{p}_{g3'}-x_g\vec{p}_{q1'}\right)}{x_q\left(x_q+x_g\right)^2\left(\frac{\vec{p}^{\,2}_{\bar{q}2}}{x_{\bar{q}}(1-x_{\bar{q}})}+Q^2\right)\left(Q^2+\frac{\vec{p}^{\,2}_{q1}}{x_q}\frac{\vec{p}^{\,2}_{\bar{q}2}}{x_{\bar{q}}}+\frac{\vec{p}^{\,2}_{g3}}{x_g}\right)}\right.$$
$$\left.-\frac{(4x_qx_{\bar{q}}+2x_g-x_g^2 d)(x_{\bar{q}}\vec{p}_{g3}-x_g\vec{p}_{\bar{q}2})\cdot(x_q\vec{p}_{g3'}-x_g\vec{p}_{q1'})}{(x_{\bar{q}}+x_g)\left(x_q+x_g\right)\left(\frac{\vec{p}^{\,2}_{q1}}{x_q(1-x_q)}+Q^2\right)\left(Q^2+\frac{\vec{p}^{\,2}_{q1}}{x_q}\frac{\vec{p}^{\,2}_{\bar{q}2}}{x_{\bar{q}}}+\frac{\vec{p}^{\,2}_{g3}}{x_g}\right)}\right]+(q\leftrightarrow\bar{q}). \tag{A.54}$$

Now $(q\leftrightarrow\bar{q})$ stands for $p_q\leftrightarrow p_{\bar{q}}$, $p_1^{(\prime)}\leftrightarrow p_2^{(\prime)}$, $x_q\leftrightarrow x_{\bar{q}}$.

$$\Phi_3^+(\vec{p}_1,\,\vec{p}_2)\,\Phi_3^{+*}(\vec{p}_{1'},\,\vec{p}_{2'}) = \Phi_4^+(\vec{p}_1,\,\vec{p}_2,\,\vec{0})\,\Phi_4^{+*}(\vec{p}_{1'},\,\vec{p}_{2'},\,\vec{0})+A^{++}+B^{++}. \tag{A.55}$$

Here the first term in the r.h.s. is responsible for the emission of the gluon before crossing the shockwave, A describes the emission after the shockwave and B is the interference term. A and B are given by :

$$A^{++} = \frac{8x_{\bar{q}}\left(p_\gamma^+\right)^4\left(x_g^2 d+4x_q\left(x_q+x_g\right)\right)}{x_q(\vec{p}_g-\frac{x_g}{x_q}\vec{p}_q)^2\left(\frac{\vec{p}^{\,2}_{\bar{q}2}}{x_{\bar{q}}(1-x_{\bar{q}})}+Q^2\right)\left(\frac{\vec{p}^{\,2}_{\bar{q}2'}}{x_{\bar{q}}(1-x_{\bar{q}})}+Q^2\right)}$$
$$-\frac{8\left(p_\gamma^+\right)^4\left(2x_g-x_g^2 d+4x_qx_{\bar{q}}\right)(\vec{p}_g-\frac{x_g}{x_q}\vec{p}_q)\cdot(\vec{p}_g-\frac{x_g}{x_{\bar{q}}}\vec{p}_{\bar{q}})}{(\vec{p}_g-\frac{x_g}{x_q}\vec{p}_q)^2(\vec{p}_g-\frac{x_g}{x_{\bar{q}}}\vec{p}_{\bar{q}})^2\left(\frac{\vec{p}^{\,2}_{q1}}{x_q(1-x_q)}+Q^2\right)\left(\frac{\vec{p}^{\,2}_{\bar{q}2'}}{x_{\bar{q}}(1-x_{\bar{q}})}+Q^2\right)}+(q\leftrightarrow\bar{q}), \tag{A.56}$$

and

$$B^{++} = \left[\frac{8\left(p_\gamma^+\right)^4}{x_g\left(x_q+x_g\right)\left(\frac{\vec{p}^{\,2}_{\bar{q}2'}}{x_{\bar{q}}(1-x_{\bar{x}})}+Q^2\right)\left(Q^2+\frac{\vec{p}^{\,2}_{q1'}}{x_q}+\frac{\vec{p}^{\,2}_{\bar{q}2'}}{x_{\bar{q}}}+\frac{\vec{p}^{\,2}_{g}}{x_g}\right)}\right.$$
$$\times\left\{\frac{x_q\left(4x_qx_{\bar{q}}+x_g(2-x_g d)\right)(\vec{p}_g-\frac{x_g}{x_{\bar{q}}}\vec{p}_{\bar{q}})\cdot(\vec{p}_g-\frac{x_g}{x_q}\vec{p}_{q1'})}{(\vec{p}_g-\frac{x_g}{x_{\bar{q}}}\vec{p}_{\bar{q}})^2\left(\frac{\vec{p}^{\,2}_{q1}}{x_q(1-x_q)}+Q^2\right)}\right.$$
$$\left.\left.-\frac{x_{\bar{q}}\left(x_g^2 d+4x_q\left(x_q+x_g\right)\right)(\vec{p}_g-\frac{x_g}{x_q}\vec{p}_q)\cdot(\vec{p}_g-\frac{x_g}{x_q}\vec{p}_{q1'})}{(\vec{p}_g-\frac{x_g}{x_q}\vec{p}_q)^2\left(\frac{\vec{p}^{\,2}_{\bar{q}2}}{x_{\bar{q}}(1-x_{\bar{q}})}+Q^2\right)}\right\}+(q\leftrightarrow\bar{q})\right]$$
$$+(1\leftrightarrow1',2\leftrightarrow2'). \tag{A.57}$$

A.2.2 TL photon transition

$$\Phi_4^i(\vec{p}_1,\,\vec{p}_2,\,\vec{p}_3)\,\Phi_4^{+*}(\vec{p}_1,\,\vec{p}_2,\,\vec{p}_3) = \frac{-4\left(p_\gamma^+\right)^3}{\left(Q^2+\frac{\vec{p}^{\,2}_{q1}}{x_q}+\frac{\vec{p}^{\,2}_{\bar{q}2}}{x_{\bar{q}}}+\frac{\vec{p}^{\,2}_{g3}}{x_g}\right)\left(Q^2+\frac{\vec{p}^{\,2}_{q1'}}{x_q}+\frac{\vec{p}^{\,2}_{\bar{q}2'}}{x_{\bar{q}}}+\frac{\vec{p}^{\,2}_{g3'}}{x_g}\right)}$$
$$\times\left(\frac{x_g\left((\vec{P}\cdot\vec{p}_{q1})G_\perp^i-(\vec{G}\cdot\vec{p}_{q1})P_\perp^i\right)(x_g d+4x_q-4)-(\vec{G}\cdot\vec{P})p_{q1\perp}^i\,(2x_q-1)\left(4\left(x_q-1\right)x_{\bar{q}}-x_g^2 d\right)}{x_{\bar{q}}x_g^2\left(x_{\bar{q}}+x_g\right)^3\left(Q^2+\frac{\vec{p}^{\,2}_{q1}}{x_q(1-x_q)}\right)\left(Q^2+\frac{\vec{p}^{\,2}_{q1'}}{x_q(1-x_q)}\right)}\right.$$
$$\left.+\frac{x_g\left((\vec{P}\cdot\vec{p}_{q1})H_\perp^i-(\vec{H}\cdot\vec{p}_{q1})P_\perp^i\right)(x_g d+4x_q-2)-(\vec{H}\cdot\vec{P})p_{q1\perp}^i\,(2x_q-1)\left(x_g(2-x_g d)+4x_qx_{\bar{q}}\right)}{x_qx_g^2\left(x_q+x_g\right)\left(x_{\bar{q}}+x_g\right)^2\left(Q^2+\frac{\vec{p}^{\,2}_{\bar{q}2'}}{x_{\bar{q}}(1-x_{\bar{q}})}\right)\left(Q^2+\frac{\vec{p}^{\,2}_{q1}}{x_q(z+x_{\bar{q}})}\right)}\right)$$

$$+\frac{H_\perp^i\left(x_g(x_g d+d-2)+x_q\left(2-4x_{\bar q}\right)\right)x_{\bar q}}{x_g\left(x_q+x_g\right)^2\left(x_{\bar q}+x_g\right)\left(Q^2+\frac{\vec p_{\bar q 2'}^{\,2}}{x_{\bar q}(1-x_{\bar q})}\right)}\Bigg)+(q\leftrightarrow\bar q). \tag{A.58}$$

Here

$$G_\perp^i=x_{\bar q}p_{g3'\perp}^i-x_g p_{\bar q 2'\perp}^i,\quad H_\perp^i=x_q p_{g3'\perp}^i-x_g p_{q1'\perp}^i,\quad P_\perp^i=x_{\bar q}p_{g3\perp}^i-x_g p_{\bar q 2\perp}^i. \tag{A.59}$$

Similarly to the longitudinal to longitudinal photon transition, we write

$$\Phi_3^i(\vec p_1,\vec p_2)\,\Phi_3^{+*}(\vec p_{1'},\vec p_{2'})=\Phi_4^i(\vec p_1,\vec p_2,\vec 0)\,\Phi_4^{+*}(\vec p_{1'},\vec p_{2'},\vec 0)+A^{i+}+B^{i+}\,, \tag{A.60}$$

where A and B are now given by

$$\begin{aligned}A^{i+}=&\frac{4x_q\left(p_\gamma^+\right)^3}{\vec\Delta_{qg}^2\vec\Delta_{\bar q g}^2\left(x_q+x_g\right)^2\left(x_{\bar q}+x_g\right)\left(\frac{\vec p_{\bar q 2}^{\,2}}{x_{\bar q}(1-x_{\bar q})}+Q^2\right)\left(\frac{\vec p_{q1'}^{\,2}}{x_q(1-x_q)}+Q^2\right)}\\&\times\Big[x_g\left(4x_{\bar q}+x_g d-2\right)\left(\Delta_{qg\perp}^i(\vec p_{\bar q 2}\cdot\vec\Delta_{\bar q g})-\Delta_{\bar q g\perp}^i(\vec p_{\bar q 2}\cdot\vec\Delta_{qg})\right)\\&+\left(2x_{\bar q}-1\right)(\vec\Delta_{qg}\cdot\vec\Delta_{\bar q g})p_{\bar q 2\perp}^i\left(4x_q x_{\bar q}+x_g(2-x_g d)\right)\Big]\\&-\frac{4x_q\left(p_\gamma^+\right)^3\left(2x_{\bar q}-1\right)\left(x_g^2 d+4x_q\left(x_q+x_g\right)\right)p_{\bar q 2\perp}^i}{\vec\Delta_{qg}^2\left(x_q+x_g\right)^3\left(\frac{\vec p_{\bar q 2}^{\,2}}{x_{\bar q}(1-x_{\bar q})}+Q^2\right)\left(\frac{\vec p_{\bar q 2'}^{\,2}}{x_{\bar q}(1-x_{\bar q})}+Q^2\right)}+(q\leftrightarrow\bar q)\end{aligned} \tag{A.61}$$

and

$$\begin{aligned}B^{i+}=&4\left(p_\gamma^+\right)^3\Bigg(\frac{\Delta_{qg\perp}^i x_q x_{\bar q}\left(x_g^2 d+x_g d-2x_g+2x_q-4x_q x_{\bar q}\right)}{\vec\Delta_{qg}^2\left(x_q+x_g\right)^2\left(x_{\bar q}+x_g\right)\left(Q^2+\frac{\vec p_{q1}^{\,2}}{x_q}+\frac{\vec p_{\bar q 2}^{\,2}}{x_{\bar q}}+\frac{\vec p_g^{\,2}}{x_g}\right)\left(Q^2+\frac{\vec p_{\bar q 2'}^{\,2}}{x_{\bar q}(1-x_{\bar q})}\right)}\\&-\frac{(\vec J\cdot\vec\Delta_{qg})p_{\bar q 2\perp}^i\left(x_g^2 d+4x_q\left(x_q+x_g\right)\right)\left(1-2x_{\bar q}\right)+x_g\left((\vec J\cdot\vec p_{\bar q 2})\Delta_{qg\perp}^i-(\vec p_{\bar q 2}\cdot\vec\Delta_{qg})J_\perp^i\right)\left(x_g d+4x_{\bar q}-4\right)}{x_g\left(x_q+x_g\right)^3\vec\Delta_{qg}^2\left(Q^2+\frac{\vec p_{q1'}^{\,2}}{x_q}+\frac{\vec p_{\bar q 2'}^{\,2}}{x_{\bar q}}+\frac{\vec p_g^{\,2}}{x_g}\right)\left(Q^2+\frac{\vec p_{\bar q 2}^{\,2}}{x_{\bar q}(1-x_{\bar q})}\right)\left(Q^2+\frac{\vec p_{\bar q 2'}^{\,2}}{x_{\bar q}(1-x_{\bar q})}\right)}\\&-\frac{x_q\Big(x_g\Big((\vec K\cdot\vec p_{\bar q 2})\Delta_{qg\perp}^i-(\vec p_{\bar q 2}\cdot\vec\Delta_{qg})K_\perp^i\Big)(x_g d+4x_{\bar q}-2)+(\vec K\cdot\vec\Delta_{qg})p_{\bar q 2\perp}^i(1-2x_{\bar q})\left(x_g(x_g d-2)-4x_q x_{\bar q}\right)\Big)}{x_{\bar q}x_g\left(x_q+x_g\right)^2\left(x_{\bar q}+x_g\right)\vec\Delta_{qg}^2\left(Q^2+\frac{\vec p_{q1'}^{\,2}}{x_q}+\frac{\vec p_{\bar q 2'}^{\,2}}{x_{\bar q}}+\frac{\vec p_g^{\,2}}{x_g}\right)\left(Q^2+\frac{\vec p_{\bar q 2}^{\,2}}{x_{\bar q}(1-x_{\bar q})}\right)\left(Q^2+\frac{\vec p_{q1'}^{\,2}}{x_q(1-x_q)}\right)}\\&-\frac{x_g\Big((\vec p_{q1}\cdot\vec\Delta_{qg})X_\perp^i-(\vec X\cdot\vec p_{q1})\Delta_{q\perp}^i\Big)(x_g d+4x_q-2)+(\vec X\cdot\vec\Delta_{qg})p_{q1\perp}^i\left(1-2x_q\right)\left(x_g(x_g d-2)-4x_q x_{\bar q}\right)}{x_g\vec\Delta_{qg}^2\left(x_q+x_g\right)\left(x_{\bar q}+x_g\right)^2\left(Q^2+\frac{\vec p_{q1}^{\,2}}{x_q}+\frac{\vec p_{\bar q 2}^{\,2}}{x_{\bar q}}+\frac{\vec p_g^{\,2}}{x_g}\right)\left(Q^2+\frac{\vec p_{\bar q 2'}^{\,2}}{x_{\bar q}(1-x_{\bar q})}\right)\left(Q^2+\frac{\vec p_{q1}^{\,2}}{x_q(1-x_q)}\right)}\\&+\frac{x_g\Big((\vec X\cdot\vec p_{q1})\Delta_{\bar q g\perp}^i-(\vec p_{q1}\cdot\vec\Delta_{\bar q g})X_\perp^i\Big)(x_g d+4x_q-4)-(\vec X\cdot\vec\Delta_{\bar q g})p_{q1\perp}^i\left(2x_q-1\right)\left(4\left(x_q-1\right)x_{\bar q}-x_g^2 d\right)}{x_g\left(x_{\bar q}+x_g\right)^3\vec\Delta_{\bar q g}^2\left(Q^2+\frac{\vec p_{q1}^{\,2}}{x_q}+\frac{\vec p_{\bar q 2}^{\,2}}{x_{\bar q}}+\frac{\vec p_g^{\,2}}{x_g}\right)\left(Q^2+\frac{\vec p_{q1}^{\,2}}{x_q(1-x_q)}\right)\left(Q^2+\frac{\vec p_{q1'}^{\,2}}{x_q(1-x_q)}\right)}\Bigg)\\&+(q\leftrightarrow\bar q)\,.\end{aligned} \tag{A.62}$$

Here we used the following variables :

$$\begin{aligned}&X_\perp^i=x_{\bar q}p_{g\perp}^i-x_g p_{\bar q 2\perp}^i=P_\perp^i|_{p_3=0},\quad J_\perp^i=x_q p_{g\perp}^i-x_g p_{q1'\perp}^i=H_\perp^i|_{p_3'=0},\\&K_\perp^i=x_{\bar q}p_{g\perp}^i-x_g p_{\bar q 2'\perp}^i=G_\perp^i|_{p_3'=0}\,.\end{aligned} \tag{A.63}$$

A.2.3 TT photon transition

$$
\begin{aligned}
\Phi_4^i(\vec{p}_1,\,\vec{p}_2,\,\vec{p}_3)\Phi_4^k(\vec{p}_{1'},\,\vec{p}_{2'},\,\vec{p}_{3'})^* = &\left(\frac{\left(p_\gamma^+\right)^2}{\left(Q^2+\frac{\vec{p}_{q1}^{\,2}}{x_q}+\frac{\vec{p}_{\bar{q}2}^{\,2}}{x_{\bar{q}}}+\frac{\vec{p}_{g3}^{\,2}}{x_g}\right)\left(Q^2+\frac{\vec{p}_{q1'}^{\,2}}{x_q}+\frac{\vec{p}_{\bar{q}2'}^{\,2}}{x_{\bar{q}}}+\frac{\vec{p}_{g3'}^{\,2}}{x_g}\right)}\right.\\
\times\Bigg[&-\frac{g_\perp^{ik}x_qx_{\bar{q}}\left(dx_g+d-2+2x_{\bar{q}}\right)}{\left(x_q+x_g\right)^2\left(x_{\bar{q}}+x_g\right)}-\frac{2P_\perp^kp_{q1\perp}^i\left(1-2x_q\right)}{x_g\left(x_{\bar{q}}+x_g\right)^2\left(Q^2+\frac{\vec{p}_{q1}^{\,2}}{x_q(1-x_q)}\right)}\left(\frac{(d-2)x_g-2x_{\bar{q}}}{x_{\bar{q}}+x_g}+\frac{x_gd+2x_{\bar{q}}}{x_q+x_g}\right)\\
&-\frac{2\left(g_\perp^{ik}(\vec{P}\cdot\vec{p}_{q1})+P_\perp^ip_{q1\perp}^k\right)}{x_g\left(x_{\bar{q}}+x_g\right)^2\left(Q^2+\frac{\vec{p}_{q1}^{\,2}}{x_q(1-x_q)}\right)}\left(\frac{(d-4)x_g-2x_{\bar{q}}}{x_q+x_g}+\frac{(d-2)x_g-2x_{\bar{q}}}{x_{\bar{q}}+x_g}\right)\\
&-\frac{1}{x_qx_{\bar{q}}x_g^2\left(x_q+x_g\right)^2\left(x_{\bar{q}}+x_g\right)^2\left(Q^2+\frac{\vec{p}_{\bar{q}2'}^{\,2}}{x_{\bar{q}}(1-x_{\bar{q}})}\right)\left(Q^2+\frac{\vec{p}_{q1}^{\,2}}{x_q(1-x_q)}\right)}\Big\{(\vec{H}\cdot\vec{P})\left[p_{q1\perp}^ip_{\bar{q}2'\perp}^k\left(1-2x_q\right)\right.\\
&\times\left(1-2x_{\bar{q}}\right)\left(x_g(2-x_gd)+4x_qx_{\bar{q}}\right)+\left(g_\perp^{ik}(\vec{p}_{q1}\cdot\vec{p}_{\bar{q}2'})+p_{q1\perp}^kp_{\bar{q}2'\perp}^i\right)\left(x_g(2-(d-4)x_g)+4x_qx_{\bar{q}}\right)\Big]\\
&+\left((d-4)x_g-2\right)\Big[x_g(\vec{H}\cdot\vec{p}_{\bar{q}2'})(g_\perp^{ik}(\vec{P}\cdot\vec{p}_{q1})+P_\perp^ip_{q1\perp}^k)+x_gH_\perp^k\left((\vec{P}\cdot\vec{p}_{q1})p_{\bar{q}2'\perp}^i-(\vec{p}_{q1}\cdot\vec{p}_{\bar{q}2'})P_\perp^i\right)\Big]\\
&+\left((d-4)x_g+2\right)\Big[x_gH^i\left((\vec{P}\cdot\vec{p}_{\bar{q}2'})p_{q1\perp}^k-(\vec{p}_{q1}\cdot\vec{p}_{\bar{q}2'})P_\perp^k\right)+x_g(\vec{H}\cdot\vec{p}_{q1})(g_\perp^{ik}(\vec{P}\cdot\vec{p}_{\bar{q}2'})+P_\perp^kp_{\bar{q}2'\perp}^i)\Big]\\
&+2x_g\left((\vec{H}\cdot\vec{p}_{\bar{q}2'})P_\perp^k-(\vec{P}\cdot\vec{p}_{\bar{q}2'})H_\perp^k\right)p_{q1\perp}^i\left(1-2x_q\right)\left(x_gd+4x_{\bar{q}}-2\right)\Big\}\\
&-\frac{1}{x_qx_{\bar{q}}x_g^2\left(x_{\bar{q}}+x_g\right)^4\left(Q^2+\frac{\vec{p}_{q1}^{\,2}}{x_q(1-x_q)}\right)\left(Q^2+\frac{\vec{p}_{q1'}^{\,2}}{x_q(1-x_q)}\right)}\Big\{x_g\left((d-4)x_g-4x_{\bar{q}}\right)\\
&\times\Big[g_\perp^{ik}\left((\vec{G}\cdot\vec{p}_{q1'})(\vec{P}\cdot\vec{p}_{q1})-(\vec{G}\cdot\vec{p}_{q1})(\vec{P}\cdot\vec{p}_{q1'})\right)+(\vec{p}_{q1}\cdot\vec{p}_{q1'})\left(G_\perp^iP_\perp^k-G_\perp^kP_\perp^i\right)\\
&+2(\vec{G}\cdot\vec{p}_{q1'})\left(P_\perp^ip_{q1\perp}^k+P_\perp^kp_{q1\perp}^i\left(1-2x_q\right)\right)-2(\vec{G}\cdot\vec{p}_{q1})\left(P_\perp^kp_{q1'\perp}^i+P_\perp^ip_{q1'\perp}^k\left(1-2x_q\right)\right)\Big]\\
&+\left(\vec{G}\cdot\vec{P}\right)\Big[p_{q1\perp}^kp_{q1'\perp}^i-p_{q1\perp}^ip_{q1'\perp}^k\left(1-2x_q\right)^2+g_\perp^{ik}\left(\vec{p}_{q1}\cdot\vec{p}_{q1'}\right)\Big]\left(x_g^2d+4x_{\bar{q}}\left(x_{\bar{q}}+x_g\right)\right)\Big\}\Big]\\
&+\left(1\leftrightarrow1',2\leftrightarrow2',3\leftrightarrow3',i\leftrightarrow k\right))+(q\leftrightarrow\bar{q}).
\end{aligned}
\tag{A.64}
$$

Once more we write

$$
\Phi_3^i(\vec{p}_1,\,\vec{p}_2)\Phi_3^{k*}(\vec{p}_{1'},\,\vec{p}_{2'})=\Phi_4^i(\vec{p}_1,\,\vec{p}_2,\,\vec{0})\Phi_4^{k*}(\vec{p}_{1'},\,\vec{p}_{2'},\,\vec{0})+A^{ik}+B^{ik}. \tag{A.65}
$$

Then

$$
\begin{aligned}
A^{ik}=&\frac{-2\left(p_\gamma^+\right)^2}{\vec{\Delta}_{qg}^2\vec{\Delta}_{\bar{q}g}^2\left(x_q+x_g\right)^2\left(x_{\bar{q}}+x_g\right)^2\left(\frac{\vec{p}_{\bar{q}2}^{\,2}}{x_{\bar{q}}(1-x_{\bar{q}})}+Q^2\right)\left(\frac{\vec{p}_{q1'}^{\,2}}{x_q(1-x_q)}+Q^2\right)}\Big\{x_g((d-4)x_g-2)\\
&\times\Big[(\vec{p}_{q1'}\cdot\vec{\Delta}_{\bar{q}g})\left((\vec{p}_{\bar{q}2}\cdot\vec{\Delta}_{qg})g_\perp^{ik}+\Delta_{qg\perp}^ip_{\bar{q}2\perp}^k\right)-(\vec{\Delta}_{qg}\cdot\vec{\Delta}_{\bar{q}g})\left((\vec{p}_{q1'}\cdot\vec{p}_{\bar{q}2})g_\perp^{ik}+p_{q1'\perp}^ip_{\bar{q}2\perp}^k\right)\\
&+\Delta_{\bar{q}g\perp}^kp_{q1'\perp}^i(\vec{p}_{\bar{q}2}\cdot\vec{\Delta}_{qg})-\Delta_{qg\perp}^i\Delta_{\bar{q}g\perp}^k(\vec{p}_{q1'}\cdot\vec{p}_{\bar{q}2})\Big]+(\vec{\Delta}_{qg}\cdot\vec{\Delta}_{\bar{q}g})\\
&\times\left[(2x_q-1)\left(2x_{\bar{q}}-1\right)p_{q1'\perp}^kp_{\bar{q}2\perp}^i\left(4x_qx_{\bar{q}}+x_g(2-x_gd)\right)+4x_qx_{\bar{q}}\left((\vec{p}_{q1'}\cdot\vec{p}_{\bar{q}2})g_\perp^{ik}+p_{q1'\perp}^ip_{\bar{q}2\perp}^k\right)\right]\\
&+\left((\vec{p}_{q1'}\cdot\vec{\Delta}_{qg})\left((\vec{p}_{\bar{q}2}\cdot\vec{\Delta}_{\bar{q}g})g_\perp^{ik}+\Delta_{\bar{q}g\perp}^ip_{\bar{q}2\perp}^k\right)+\Delta_{qg\perp}^kp_{q1'\perp}^i(\vec{p}_{\bar{q}2}\cdot\vec{\Delta}_{\bar{q}g})-\Delta_{qg\perp}^k\Delta_{\bar{q}g\perp}^i(\vec{p}_{q1'}\cdot\vec{p}_{\bar{q}2})\right)\\
&\times x_g((d-4)x_g+2)+x_g\left(2x_{\bar{q}}-1\right)\left(x_gd+4x_q-2\right)p_{\bar{q}2\perp}^i\left(\Delta_{\bar{q}g\perp}^k(\vec{p}_{q1'}\cdot\vec{\Delta}_{qg})-\Delta_{qg\perp}^k(\vec{p}_{q1'}\cdot\vec{\Delta}_{\bar{q}g})\right)\\
&+x_g\left(2x_q-1\right)p_{q1'\perp}^k\left(4x_{\bar{q}}+x_gd-2\right)\left(\Delta_{qg\perp}^i(\vec{p}_{\bar{q}2}\cdot\vec{\Delta}_{\bar{q}g})-\Delta_{\bar{q}g\perp}^i(\vec{p}_{\bar{q}2}\cdot\vec{\Delta}_{qg})\right)\Big\}\\
&-\frac{2x_q\left(p_\gamma^+\right)^2\left(x_g^2d+4x_q\left(x_q+x_g\right)\right)\left((\vec{p}_{\bar{q}2}\cdot\vec{p}_{\bar{q}2'})g_\perp^{ik}-\left(1-2x_{\bar{q}}\right)^2p_{\bar{q}2\perp}^ip_{\bar{q}2'\perp}^k+p_{\bar{q}2'\perp}^ip_{\bar{q}2\perp}^k\right)}{x_{\bar{q}}\vec{\Delta}_{qg}^2\left(x_q+x_g\right)^4\left(\frac{\vec{p}_{\bar{q}2}^{\,2}}{x_{\bar{q}}(1-x_{\bar{q}})}+Q^2\right)\left(\frac{\vec{p}_{\bar{q}2'}^{\,2}}{x_{\bar{q}}(1-x_{\bar{q}})}+Q^2\right)}
\end{aligned}
$$

$$+ (q \leftrightarrow \bar{q}) \,, \tag{A.66}$$

and

$$\begin{aligned}
B^{ik} = & \left(\frac{2\left(p_\gamma^+\right)^2}{\vec{\Delta}_{qg}^2 \left(Q^2 + \frac{\vec{p}_{q1}^{\,2}}{x_q} + \frac{\vec{p}_{\bar{q}2}^{\,2}}{x_{\bar{q}}} + \frac{\vec{p}_g^{\,2}}{x_g}\right)\left(Q^2 + \frac{\vec{p}_{\bar{q}2'}^{\,2}}{x_{\bar{q}}(1-x_{\bar{q}})}\right)} \right. \\
& \times \left[\frac{((d-2)x_g - 2x_q)\, x_q}{(x_q+x_g)^3} \left(g_\perp^{ik} (\vec{p}_{\bar{q}2'} \cdot \vec{\Delta}_{qg}) + p^i_{\bar{q}2'\perp} \Delta^k_{qg\perp} + p^k_{\bar{q}2'\perp} \Delta^i_{qg\perp} (1-2x_{\bar{q}}) \right) \right. \\
& + \frac{x_q \left(((d-4)x_g - 2x_q) \left(g_\perp^{ik} (\vec{p}_{\bar{q}2'} \cdot \vec{\Delta}_{qg}) + p^i_{\bar{q}2'\perp} \Delta^k_{qg\perp} \right) + p^k_{\bar{q}2'\perp} \Delta^i_{qg\perp} (x_g d + 2x_q)(1-2x_{\bar{q}}) \right)}{(x_q+x_g)^2 (x_{\bar{q}}+x_g)} \\
& - \frac{1}{x_{\bar{q}} x_g (x_q+x_g)^2 (x_{\bar{q}}+x_g)^2 \left(Q^2 + \frac{\vec{p}_{q1}^{\,2}}{x_q(1-x_q)}\right)} \{ x_g((d-4)x_g + 2) \\
& \times \left[p^i_{q1\perp} \left((\vec{p}_{\bar{q}2'} \cdot \vec{\Delta}_{qg}) X^k_\perp - (\vec{X} \cdot \vec{p}_{\bar{q}2'}) \Delta^k_{qg\perp} \right) (2x_q - 1) - (\vec{X} \cdot \vec{p}_{\bar{q}2'}) \left(g_\perp^{ik} (\vec{p}_{q1} \cdot \vec{\Delta}_{qg}) + p^k_{q1\perp} \Delta^i_{qg\perp} \right) \right. \\
& \left. - X^k_\perp \left((\vec{p}_{q1} \cdot \vec{\Delta}_{qg}) p^i_{\bar{q}2'\perp} - (\vec{p}_{q1} \cdot \vec{p}_{\bar{q}2'}) \Delta^i_{qg\perp} \right) \right] + 4x_q x_g (1-2x_q)\, p^i_{q1\perp} \left((\vec{p}_{\bar{q}2'} \cdot \vec{\Delta}_{qg}) X^k_\perp - (\vec{X} \cdot \vec{p}_{\bar{q}2'}) \Delta^k_{qg\perp} \right) \\
& + x_g (1-2x_{\bar{q}}) (x_g d + 4x_q - 2)\, p^k_{\bar{q}2'\perp} \left((\vec{p}_{q1} \cdot \vec{\Delta}_{qg}) X^i_\perp - (\vec{X} \cdot \vec{p}_{q1}) \Delta^i_{qg\perp} \right) - x_g((d-4)x_g - 2) \\
& \times \left[\left(g_\perp^{ik} (\vec{X} \cdot \vec{p}_{q1}) + X^i_\perp p^k_{q1\perp} \right) (\vec{p}_{\bar{q}2'} \cdot \vec{\Delta}_{qg}) + \left((\vec{X} \cdot \vec{p}_{q1}) p^i_{\bar{q}2'\perp} - (\vec{p}_{q1} \cdot \vec{p}_{\bar{q}2'}) X^i_\perp \right) \Delta^k_{qg\perp} \right] \\
& + (\vec{X} \cdot \vec{\Delta}_{qg}) p^i_{q1\perp} p^k_{\bar{q}2'\perp} (1-2x_q)(1-2x_{\bar{q}}) (x_g(x_g d - 2) - 4x_q x_{\bar{q}}) \\
& \left. - (\vec{X} \cdot \vec{\Delta}_{qg}) \left(g_\perp^{ik} (\vec{p}_{q1} \cdot \vec{p}_{\bar{q}2'}) + p^k_{q1\perp} p^i_{\bar{q}2'\perp} \right) (x_g(2 - (d-4)x_g) + 4x_q x_{\bar{q}}) \right\} \\
& - \frac{1}{x_{\bar{q}} x_g (x_q+x_g)^4 \left(Q^2 + \frac{\vec{p}_{\bar{q}2}^{\,2}}{x_{\bar{q}}(1-x_{\bar{q}})}\right)} \{ x_g \left(x_g d + 4x_{\bar{q}} - 4 \right) [(1-2x_{\bar{q}}) \\
& \times \left(p^k_{\bar{q}2'\perp} \left((\vec{p}_{\bar{q}2} \cdot \vec{\Delta}_{qg}) V^i_\perp - (\vec{V} \cdot \vec{p}_{\bar{q}2}) \Delta^i_{qg\perp} \right) + p^i_{\bar{q}2\perp} \left((\vec{V} \cdot \vec{p}_{\bar{q}2'}) \Delta^k_{qg\perp} - (\vec{p}_{\bar{q}2'} \cdot \vec{\Delta}_{qg}) V^k_\perp \right) \right) \\
& + V^k_\perp \left((\vec{p}_{\bar{q}2} \cdot \vec{\Delta}_{qg}) p^i_{\bar{q}2'\perp} - (\vec{p}_{\bar{q}2} \cdot \vec{p}_{\bar{q}2'}) \Delta^i_{qg\perp} \right) + \left((\vec{p}_{\bar{q}2} \cdot \vec{p}_{\bar{q}2'}) V^i_\perp - (\vec{V} \cdot \vec{p}_{\bar{q}2}) p^i_{\bar{q}2'\perp} \right) \Delta^k_{qg\perp} \\
& + g_\perp^{ik} \left((\vec{V} \cdot \vec{p}_{\bar{q}2'}) (\vec{p}_{\bar{q}2} \cdot \vec{\Delta}_{qg}) - (\vec{V} \cdot \vec{p}_{\bar{q}2}) (\vec{p}_{\bar{q}2'} \cdot \vec{\Delta}_{qg}) \right) + p^k_{\bar{q}2\perp} \left((\vec{V} \cdot \vec{p}_{\bar{q}2'}) \Delta^i_{qg\perp} - (\vec{p}_{\bar{q}2'} \cdot \vec{\Delta}_{qg}) V^i_\perp \right)] \\
& + (\vec{V} \cdot \vec{\Delta}_{qg}) \left(p^i_{\bar{q}2\perp} p^k_{\bar{q}2'\perp} (1-2x_{\bar{q}})^2 - g_\perp^{ik} (\vec{p}_{\bar{q}2} \cdot \vec{p}_{\bar{q}2'}) - p^k_{\bar{q}2\perp} p^i_{\bar{q}2'\perp} \right) \left(x_g^2 d - 4x_q (x_{\bar{q}} - 1) \right) \}] \\
& + (1 \leftrightarrow 1', 2 \leftrightarrow 2', i \leftrightarrow k)) + (q \leftrightarrow \bar{q}).
\end{aligned} \tag{A.67}$$

Here we introduced

$$V^i_\perp = x_q p^i_{g\perp} - x_g p^i_{q1\perp}. \tag{A.68}$$

A.3 Integral $I(R,E)$

Here we will consider the integral (3.216)

$$I(R,E) \equiv - \int_0^{\frac{2E}{p_\gamma^+}} \frac{dz}{z} \int_{\left\{ \vec{u}^{\,2} > (p_\gamma^+)^2 \left(\frac{2E}{z p_\gamma^+} - 1 \right) \right\} \cap \Omega_{nc}} \frac{d\vec{u}}{\pi} \frac{(\frac{\vec{p}_j}{x_j} - \frac{\vec{p}_{\bar{j}}}{x_{\bar{j}}})^2}{(\vec{u} - \frac{\vec{p}_{\bar{j}}}{x_{\bar{j}}})^2 (\vec{u} - \frac{\vec{p}_j}{x_j})^2} \,, \tag{A.69}$$

where

$$\Omega_{nc} = \left\{ \left(\vec{u} - \frac{\vec{p}_j}{x_j} \right)^2 > \frac{R^2 \vec{p}_j^{\,2}}{x_j^2} \right\} \cap \left\{ \left(\vec{u} - \frac{\vec{p}_{\bar{j}}}{x_{\bar{j}}} \right)^2 > \frac{R^2 \vec{p}_{\bar{j}}^{\,2}}{x_{\bar{j}}^2} \right\} , \tag{A.70}$$

see Eq. (3.213). Introducing the variable $y = \frac{2E}{zp_\gamma^+} - 1$, one gets

$$I(R,E) = -\int_0^{+\infty} \frac{dy}{y+1} \int_{\{\vec{u}^{\,2} > y(p_\gamma^+)^2\} \cap \Omega_{nc}} \frac{d\vec{u}}{\pi} \frac{\left(\frac{\vec{p}_j}{x_j} - \frac{\vec{p}_{\bar{j}}}{x_{\bar{j}}}\right)^2}{\left(\vec{u} - \frac{\vec{p}_{\bar{j}}}{x_{\bar{j}}}\right)^2 \left(\vec{u} - \frac{\vec{p}_j}{x_j}\right)^2}\,. \tag{A.71}$$

The change of the integration order plus integration w.r.t. y yields

$$I(R,E) = -\int_{\Omega_{nc}} \frac{d\vec{u}}{\pi} \frac{\left(\frac{\vec{p}_j}{x_j} - \frac{\vec{p}_{\bar{j}}}{x_{\bar{j}}}\right)^2}{\left(\vec{u} - \frac{\vec{p}_{\bar{j}}}{x_{\bar{j}}}\right)^2 \left(\vec{u} - \frac{\vec{p}_j}{x_j}\right)^2} \ln\left(1 + \frac{\vec{u}^{\,2}}{(p_\gamma^+)^2}\right). \tag{A.72}$$

Next, introducing

$$v = \max\left(\left|\frac{\vec{p}_j}{x_j}\right|, \left|\frac{\vec{p}_{\bar{j}}}{x_{\bar{j}}}\right|\right), \tag{A.73}$$

one can split the integration area into 2 parts

$$\Omega_{nc} = \Omega_{nc_1} \cup \Omega_{nc_2}, \quad \Omega_{nc_1} = \{\vec{u}^{\,2} < (2v)^2\} \cap \Omega_{nc}, \quad \Omega_{nc_2} = \{\vec{u}^{\,2} > (2v)^2\}. \tag{A.74}$$

In the first domain $\frac{\vec{u}^{\,2}}{(p_\gamma^+)^2} < \frac{(2v)^2}{(p_\gamma^+)^2} = O\left(\frac{1}{s}\right)$. Hence one can estimate this integral by putting this maximal value into the logarithm and expanding it

$$\int_{\Omega_{nc_1}} \frac{d\vec{u}}{\pi} \frac{\left(\frac{\vec{p}_j}{x_j} - \frac{\vec{p}_{\bar{j}}}{x_{\bar{j}}}\right)^2}{\left(\vec{u} - \frac{\vec{p}_{\bar{j}}}{x_{\bar{j}}}\right)^2 \left(\vec{u} - \frac{\vec{p}_j}{x_j}\right)^2} \ln\left(1 + \frac{\vec{u}^{\,2}}{(p_\gamma^+)^2}\right) < O\left(\frac{1}{s}\right) \int_{\Omega_{nc_1}} \frac{d\vec{u}}{\pi} \frac{\left(\frac{\vec{p}_j}{x_j} - \frac{\vec{p}_{\bar{j}}}{x_{\bar{j}}}\right)^2}{\left(\vec{u} - \frac{\vec{p}_{\bar{j}}}{x_{\bar{j}}}\right)^2 \left(\vec{u} - \frac{\vec{p}_j}{x_j}\right)^2}. \tag{A.75}$$

Although the integral in the r.h.s. of this inequality contains $\ln R$, we neglect terms $\sim O\left(\frac{\ln R}{s}\right)$ in the Regge limit. In the second domain one can write

$$\begin{aligned}
&\int_{\Omega_{nc_2}} \frac{d\vec{u}}{\pi} \frac{\left(\frac{\vec{p}_j}{x_j} - \frac{\vec{p}_{\bar{j}}}{x_{\bar{j}}}\right)^2}{\left(\vec{u} - \frac{\vec{p}_{\bar{j}}}{x_{\bar{j}}}\right)^2 \left(\vec{u} - \frac{\vec{p}_j}{x_j}\right)^2} \ln\left(1 + \frac{\vec{u}^{\,2}}{(p_\gamma^+)^2}\right) \\
&< \int_{\Omega_{nc_2}} \frac{d\vec{u}}{\pi} \frac{\left(\frac{\vec{p}_j}{x_j} - \frac{\vec{p}_{\bar{j}}}{x_{\bar{j}}}\right)^2}{(u-v)^4} \ln\left(1 + \frac{\vec{u}^{\,2}}{(p_\gamma^+)^2}\right) \sim O\left(\frac{v^{\,2}}{(p_\gamma^+)^2}\right) = O\left(\frac{1}{s}\right),
\end{aligned} \tag{A.76}$$

where the latter integral is easy to take. Finally,

$$I(R,E) = O\left(\frac{\ln R}{s}\right). \tag{A.77}$$

Therefore we neglect this contribution.

Appendix B

Computation details for part 2

B.1 Contributions of the various diagrams

For completeness, we present here the formulae for the contributions of the various diagrams of Fig. 4.22.

B.1.1 Chiral-even sector

Vector case

$$\begin{aligned} tr_D^V[A_1] &= tr_D\left[\hat{p}_\rho\hat{\varepsilon}_k^*\frac{z\hat{p}_\rho+\hat{k}}{(zp_\rho+k)^2+i\epsilon}\hat{\varepsilon}_q\frac{z\hat{p}_\rho+\hat{k}-\hat{q}}{(zp_\rho+k-q)^2+i\epsilon}\,\gamma^\mu\,\hat{p}\,\gamma_\mu\,\frac{1}{(-\bar{z}p_\rho-(x-\xi)p)^2+i\epsilon}\right] \\ &= \frac{8\bar{z}s\bar{\alpha}\left[\frac{2z-1}{\alpha}(\varepsilon_{q\perp}\cdot p_{\rho\perp})(\varepsilon_{k\perp}^*\cdot p_{\rho\perp})-s\xi(\varepsilon_{q\perp}\cdot\varepsilon_{k\perp}^*)\right]}{((zp_\rho+k)^2+i\epsilon)((zp_\rho+k-q)^2+i\epsilon)((-\bar{z}p_\rho-(x-\xi)p)^2+i\epsilon)} \\ &= \frac{2\left[\alpha\xi sT_A-(z-\bar{z})\,T_B\right]}{\alpha\bar{\alpha}\xi^2s^2z\bar{z}\,(x-\xi+i\epsilon)}, \end{aligned} \tag{B.1}$$

$$\begin{aligned} tr_D^V[A_2] &= tr_D\left[\hat{p}_\rho\hat{\varepsilon}_q\frac{z\hat{p}_\rho-\hat{q}}{(zp_\rho-q)^2+i\epsilon}\hat{\varepsilon}_k^*\frac{z\hat{p}_\rho+\hat{k}-\hat{q}}{(zp_\rho+k-q)^2+i\epsilon}\,\gamma^\mu\,\hat{p}\,\gamma_\mu\,\frac{1}{(-\bar{z}p_\rho-(x-\xi)p)^2+i\epsilon}\right] \\ &= \frac{8\bar{z}s\bar{\alpha}\left[\frac{2z-1}{\alpha}(\varepsilon_{q\perp}\cdot p_{\rho\perp})(\varepsilon_{k\perp}^*\cdot p_{\rho\perp})+s\xi\alpha(\varepsilon_{q\perp}\cdot\varepsilon_{k\perp}^*)\right]}{((zp_\rho-q)^2+i\epsilon)((zp_\rho+k-q)^2+i\epsilon)((-\bar{z}p_\rho-(x-\xi)p)^2+i\epsilon)} \\ &= \frac{2\left[\alpha^2\xi sT_A+(z-\bar{z})\,T_B\right]}{\alpha^2\bar{\alpha}\xi^2s^2z\bar{z}\,(x-\xi+i\epsilon)}, \end{aligned} \tag{B.2}$$

$$\begin{aligned} tr_D^V[A_3] &= tr_D\left[\hat{p}_\rho\hat{\varepsilon}_q\frac{z\hat{p}_\rho-\hat{q}}{(zp_\rho-q)^2+i\epsilon}\gamma^\mu\frac{(x+\xi)\hat{p}-\hat{k}}{((x+\xi)p-k)^2+i\epsilon}\,\hat{\varepsilon}_k^*\,\hat{p}\,\gamma_\mu\,\frac{1}{(\bar{z}p_\rho+(x-\xi)p)^2+i\epsilon}\right] \\ &= \frac{8s\alpha\,\left[-\frac{z}{\alpha}(\varepsilon_{q\perp}\cdot p_{\rho\perp})\,(\varepsilon_{k\perp}^*\cdot p_{\rho\perp})-s\xi(\varepsilon_{q\perp}\cdot\varepsilon_{k\perp}^*)\right]}{((zp_\rho-q)^2+i\epsilon)(((x+\xi)p-k)^2+i\epsilon)((\bar{z}p_\rho+(x-\xi)p)^2+i\epsilon)} \\ &= \frac{-4\left[\alpha\xi sT_A+zT_B\right]}{\alpha^2\bar{\alpha}\xi s^2z\bar{z}\,(x+\xi-i\epsilon)\,(x-\xi+i\epsilon)}, \end{aligned} \tag{B.3}$$

$$\begin{aligned} tr_D^V[A_4] &= tr_D\left[\hat{p}_\rho\hat{\varepsilon}_q\frac{z\hat{p}_\rho-\hat{q}}{(zp_\rho-q)^2+i\epsilon}\gamma^\mu\hat{p}\hat{\varepsilon}_k^*\frac{\hat{k}+(x-\xi)\hat{p}}{(k+(x-\xi)p)^2+i\epsilon}\gamma_\mu\frac{1}{(zp_\rho-q-(x+\xi)p)^2+i\epsilon}\right] \\ &= \frac{8s\left[-\bar{z}\,(\varepsilon_{q\perp}\cdot p_{\rho\perp})\,(\varepsilon_{k\perp}^*\cdot p_{\rho\perp})-s\xi\,\alpha\alpha_\rho\,(\varepsilon_{q\perp}\cdot\varepsilon_{k\perp}^*)\right]}{((zp_\rho-q)^2+i\epsilon)((k+(x-\xi)p)^2+i\epsilon)((zp_\rho-q-(x+\xi)p)^2+i\epsilon)} \\ &= \frac{4\left[\alpha\bar{\alpha}\xi sT_A+\bar{z}T_B\right]}{\alpha^2\xi s^2z\,(x-\xi+i\epsilon)\left[(x+\xi+i\epsilon)-z\,(2\alpha\xi+\bar{\alpha}\,(x+\xi+i\epsilon))\right]}, \end{aligned} \tag{B.4}$$

$$
\begin{aligned}
tr_D^V[A_5] &= tr_D\left[\hat{p}_\rho\hat{\varepsilon}_q\frac{z\hat{p}_\rho-\hat{q}}{(zp_\rho-q)^2+i\epsilon}\gamma^\mu\hat{p}\gamma_\mu\frac{-\bar{z}\hat{p}_\rho-\hat{k}}{(-\bar{z}p_\rho-k)^2+i\epsilon}\,\varepsilon_k^*\,\frac{1}{(zp_\rho-q-(x+\xi)p)^2+i\epsilon}\right]\\
&= \frac{8s\left[\frac{(\bar{z}-z)(z\bar{\alpha}-1)}{\alpha}\,(\varepsilon_{q\perp}\cdot p_{\rho\perp})\,(\varepsilon_{k\perp}^*\cdot p_{\rho\perp})+s\xi\,\alpha\,(\varepsilon_{q\perp}\cdot\varepsilon_{k\perp}^*)\right]}{((zp_\rho-q)^2+i\epsilon)((-\bar{z}p_\rho-k)^2+i\epsilon)((zp_\rho-q-(x+\xi)p)^2+i\epsilon)} \qquad \text{(B.5)}\\
&= \frac{2\left[-\alpha^2\xi sT_A+(1-2z)\,(1-\bar{\alpha}z)\,T_B\right]}{\alpha^2\xi^2s^2z\bar{z}\left[(x+\xi+i\epsilon)-z\,(2\alpha\xi+\bar{\alpha}\,(x+\xi+i\epsilon))\right]},
\end{aligned}
$$

$$
\begin{aligned}
&tr_D^V[B_2]\\
&= tr_D\left[\hat{p}_\rho\gamma^\mu\frac{\hat{q}+(x+\xi)\hat{p}-\hat{k}}{(q+(x+\xi)p-k)^2+i\epsilon}\hat{\varepsilon}_k^*\,\frac{\hat{q}+(x+\xi)\hat{p}}{(q+(x+\xi)p)^2+i\epsilon}\,\hat{\varepsilon}_q\,\hat{p}\,\gamma_\mu\frac{1}{(-\bar{z}p_\rho-(x-\xi)p)^2+i\epsilon}\right]\\
&= \frac{4s^2(x-\xi)\bar{\alpha}(\varepsilon_{q\perp}\cdot\varepsilon_{k\perp}^*)}{(q+(x+\xi)p-k)^2+i\epsilon)((q+(x+\xi)p)^2+i\epsilon)((-\bar{z}p_\rho-(x-\xi)p)^2+i\epsilon)} \qquad \text{(B.6)}\\
&= \frac{4\,T_A}{\bar{\alpha}\bar{z}s\,(x+\xi+i\epsilon)\,(x-\xi+i\epsilon)},
\end{aligned}
$$

$$
\begin{aligned}
&tr_D^V[B_3]\\
&= tr_D\left[\hat{p}_\rho\gamma^\mu\frac{\hat{q}+(x+\xi)\hat{p}-\hat{k}}{(q+(x+\xi)p-k)^2+i\epsilon}\hat{\varepsilon}_q\,\frac{(x+\xi)\hat{p}-\hat{k}}{((x+\xi)p-k)^2+i\epsilon}\,\hat{\varepsilon}_k^*\,\hat{p}\,\gamma_\mu\frac{1}{(-\bar{z}p_\rho-(x-\xi)p)^2+i\epsilon}\right]\\
&= -\frac{4s^2\bar{\alpha}\alpha(x-\xi)(\varepsilon_{q\perp}\cdot\varepsilon_{k\perp}^*)}{((q+(x+\xi)p-k)^2+i\epsilon)(((x+\xi)p-k)^2+i\epsilon)((-\bar{z}p_\rho-(x-\xi)p)^2+i\epsilon)} \qquad \text{(B.7)}\\
&= \frac{4T_A}{\bar{\alpha}\bar{z}s\,(x+\xi-i\epsilon)\,(x-\xi+i\epsilon)},
\end{aligned}
$$

$$
\begin{aligned}
&tr_D^V[B_4]\\
&= tr_D\left[\hat{p}_\rho\gamma^\mu\frac{\hat{q}+(x+\xi)\hat{p}}{(q+(x+\xi)p)^2+i\epsilon}\hat{\varepsilon}_q\hat{p}\hat{\varepsilon}_k^*\frac{(x-\xi)\hat{p}+\hat{k}}{((x-\xi)p+k)^2+i\epsilon}\,\gamma_\mu\,\frac{1}{(\bar{z}p_\rho+k+(x-\xi)p)^2+i\epsilon}\right]\\
&= \frac{8s^2\xi\alpha(\varepsilon_{q\perp}\cdot\varepsilon_{k\perp}^*)}{((q+(x+\xi)p)^2+i\epsilon)(((x-\xi)p+k)^2+i\epsilon)((\bar{z}p_\rho+k+(x-\xi)p)^2+i\epsilon)} \qquad \text{(B.8)}\\
&= \frac{8\xi T_A}{(x-\xi+i\epsilon)\,(x+\xi+i\epsilon)\,s\left[(x+\xi+i\epsilon)-z\,(2\alpha\xi+\bar{\alpha}\,(x+\xi+i\epsilon))\right]},
\end{aligned}
$$

$$
\begin{aligned}
&tr_D^V[B_5]\\
&= tr_D\left[\hat{p}_\rho\gamma^\mu\frac{\hat{q}+(x+\xi)\hat{p}}{(q+(x+\xi)p)^2+i\epsilon}\hat{\varepsilon}_q\hat{p}\gamma_\mu\frac{-\bar{z}\hat{p}_\rho-\hat{k}}{(-\bar{z}p_\rho-k)^2+i\epsilon}\,\hat{\varepsilon}_k^*\,\frac{1}{(\bar{z}p_\rho+k+(x-\xi)p)^2+i\epsilon}\right]\\
&= \frac{8s\left[\frac{\bar{z}}{\alpha}\,(\varepsilon_{q\perp}\cdot p_{\rho\perp})\,(\varepsilon_{k\perp}^*\cdot p_{\rho\perp})+\,s\xi\alpha_\rho\,(\varepsilon_{q\perp}\cdot\varepsilon_{k\perp}^*)\right]}{((q+(x+\xi)p)^2+i\epsilon)((-\bar{z}p_\rho-k)^2+i\epsilon)((\bar{z}p_\rho+k+(x-\xi)p)^2+i\epsilon)}\,, \qquad \text{(B.9)}\\
&= \frac{4\left[\alpha\bar{\alpha}\xi sT_A+zT_B\right]}{\alpha\xi s^2\bar{z}\,(x+\xi+i\epsilon)\left[(x+\xi+i\epsilon)-z\,(2\alpha\xi+\bar{\alpha}\,(x+\xi+i\epsilon))\right]}.
\end{aligned}
$$

Axial case

$$
\begin{aligned}
&tr_D^A[A_1]\\
&= tr_D\left[\hat{p}_\rho\hat{\varepsilon}_k^*\frac{z\hat{p}_\rho+\hat{k}}{(zp_\rho+k)^2+i\epsilon}\hat{\varepsilon}_q\frac{z\hat{p}_\rho+\hat{k}-\hat{q}}{(zp_\rho+k-q)^2+i\epsilon}\,\gamma^\mu\,\hat{p}\,\gamma^5\,\gamma_\mu\,\frac{1}{(-\bar{z}p_\rho-(x-\xi)p)^2+i\epsilon}\right]
\end{aligned}
$$

$$= \frac{8i\frac{\bar{z}}{\alpha}\left[(1-2\alpha)(\varepsilon_{q\perp}\cdot p_{\rho\perp})\,\epsilon^{p\,n\,p_{\rho\perp}\,\varepsilon^*_{k\perp}} + (\varepsilon^*_{k\perp}\cdot p_{\rho\perp})\,\epsilon^{p\,n\,p_{\rho\perp}\,\varepsilon_{q\perp}}\right]}{((zp_\rho+k)^2+i\epsilon)((zp_\rho+k-q)^2+i\epsilon)((-\bar{z}p_\rho-(x-\xi)p)^2+i\epsilon)}$$

$$= \frac{2i\left[T_{A_5}-(\alpha-\bar{\alpha})\,T_{B_5}\right]}{\alpha\bar{\alpha}^2\xi^2 s^3 z\bar{z}\,(x-\xi+i\epsilon)}, \tag{B.10}$$

$$tr_D^A\,[A_2]$$

$$= tr_D\left[\hat{p}_\rho\hat{\varepsilon}_q\frac{z\hat{p}_\rho-\hat{q}}{(zp_\rho-q)^2+i\epsilon}\hat{\varepsilon}^*_k\frac{z\hat{p}_\rho+\hat{k}-\hat{q}}{(zp_\rho+k-q)^2+i\epsilon}\,\gamma^\mu\,\hat{p}\,\gamma^5\,\gamma_\mu\,\frac{1}{(-\bar{z}p_\rho-(x-\xi)p)^2+i\epsilon}\right]$$

$$= -\frac{8i\bar{z}\,\left[(\varepsilon_{q\perp}\cdot p_{\rho\perp})\,\epsilon^{p\,n\,p_{\rho\perp}\,\varepsilon^*_{k\perp}} - \frac{2-\alpha}{\alpha}(\varepsilon^*_{k\perp}\cdot p_{\rho\perp})\,\epsilon^{p\,n\,p_{\rho\perp}\,\varepsilon_{q\perp}}\right]}{((zp_\rho-q)^2+i\epsilon)((zp_\rho+k-q)^2+i\epsilon)((-\bar{z}p_\rho-(x-\xi)p)^2+i\epsilon)}$$

$$= \frac{2i\left[(\alpha-2)\,T_{A_5}+\alpha T_{B_5}\right]}{\alpha^2\bar{\alpha}^2\xi^2 s^3 z\bar{z}\,(x-\xi+i\epsilon)}, \tag{B.11}$$

$$tr_D^A\,[A_3]$$

$$= tr_D\left[\hat{p}_\rho\hat{\varepsilon}_q\frac{z\hat{p}_\rho-\hat{q}}{(zp_\rho-q)^2+i\epsilon}\gamma^\mu\frac{(x+\xi)\hat{p}-\hat{k}}{((x+\xi)p-k)^2+i\epsilon}\,\hat{\varepsilon}^*_k\,\hat{p}\,\gamma^5\,\gamma_\mu\,\frac{1}{(\bar{z}p_\rho+(x-\xi)p)^2+i\epsilon}\right]$$

$$= \frac{8i\,\left[\left(-2z+\frac{1}{\alpha_\rho}\right)\,(\varepsilon_{q\perp}\cdot p_{\rho\perp})\,\epsilon^{p\,n\,p_{\rho\perp}\,\varepsilon^*_{k\perp}} - \frac{1}{\alpha_\rho}\,(\varepsilon^*_{k\perp}\cdot p_{\rho\perp})\,\epsilon^{p\,n\,p_{\rho\perp}\,\varepsilon_{q\perp}}\right]}{((zp_\rho-q)^2+i\epsilon)(((x+\xi)p-k)^2+i\epsilon)((\bar{z}p_\rho+(x-\xi)p)^2+i\epsilon)}$$

$$= \frac{4i\left[T_{A_5}-(1-2\bar{\alpha}z)\,T_{B_5}\right]}{\alpha^2\bar{\alpha}^2\xi s^3 z\bar{z}\,(x-\xi+i\epsilon)\,(x+\xi-i\epsilon)}, \tag{B.12}$$

$$tr_D^A\,[A_4]$$

$$= tr_D\left[\hat{p}_\rho\hat{\varepsilon}_q\frac{z\hat{p}_\rho-\hat{q}}{(zp_\rho-q)^2+i\epsilon}\gamma^\mu\hat{p}\gamma^5\hat{\varepsilon}^*_k\frac{\hat{k}+(x-\xi)\hat{p}}{(k+(x-\xi)p)^2+i\epsilon}\,\gamma_\mu\,\frac{1}{(zp_\rho-q-(x+\xi)p)^2+i\epsilon}\right]$$

$$= \frac{8i\,\left[(1-2z)\,(\varepsilon_{q\perp}\cdot p_{\rho\perp})\,\epsilon^{p\,n\,p_{\rho\perp}\,\varepsilon^*_{k\perp}} + (\varepsilon^*_{k\perp}\cdot p_{\rho\perp})\,\epsilon^{p\,n\,p_{\rho\perp}\,\varepsilon_{q\perp}}\right]}{((zp_\rho-q)^2+i\epsilon)((k+(x-\xi)p)^2+i\epsilon)((zp_\rho-q-(x+\xi)p)^2+i\epsilon)}$$

$$= \frac{4i\left[T_{A_5}+(1-2z)\,T_{B_5}\right]}{\alpha^2\xi s^3 z\,(x-\xi+i\epsilon)\left[(x+\xi+i\epsilon)-z\,(2\alpha\xi+\bar{\alpha}\,(x+\xi+i\epsilon))\right]}, \tag{B.13}$$

$$tr_D^A\,[A_5]$$

$$= tr_D\left[\hat{p}_\rho\hat{\varepsilon}_q\frac{z\hat{p}_\rho-\hat{q}}{(zp_\rho-q)^2+i\epsilon}\gamma^\mu\hat{p}\,\gamma^5\,\gamma_\mu\frac{-\bar{z}\hat{p}_\rho-\hat{k}}{(-\bar{z}p_\rho-k)^2+i\epsilon}\,\varepsilon^*_k\,\frac{1}{(zp_\rho-q-(x+\xi)p)^2+i\epsilon}\right]$$

$$= \frac{8i\,\left[\frac{2z(1-\alpha)-1}{1-\alpha}\,(\varepsilon_{q\perp}\cdot p_{\rho\perp})\,\epsilon^{p\,n\,p_{\rho\perp}\,\varepsilon^*_{k\perp}} + \frac{1+(1-\alpha)(1-2z)}{\alpha(1-\alpha)}(\varepsilon^*_{k\perp}\cdot p_{\rho\perp})\,\epsilon^{p\,n\,p_{\rho\perp}\,\varepsilon_{q\perp}}\right]}{((zp_\rho-q)^2+i\epsilon)((-\bar{z}p_\rho-k)^2+i\epsilon)((zp_\rho-q-(x+\xi)p)^2+i\epsilon)}$$

$$= \frac{2i\left[(2-\alpha-2\bar{\alpha}z)\,T_{A_5}-\alpha\,(1-2\bar{\alpha}z)\,T_{B_5}\right]}{\alpha^2\bar{\alpha}\xi^2 s^3 z\bar{z}\left[(x+\xi+i\epsilon)-z\,(2\alpha\xi+\bar{\alpha}\,(x+\xi+i\epsilon))\right]}, \tag{B.14}$$

$$tr_D^A\,[B_2] = tr_D\left[\hat{p}_\rho\,\gamma^\mu\frac{\hat{q}+(x+\xi)\hat{p}-\hat{k}}{(q+(x+\xi)p-k)^2+i\epsilon}\hat{\varepsilon}^*_k\,\frac{\hat{q}+(x+\xi)\hat{p}}{(q+(x+\xi)p)^2+i\epsilon}\,\hat{\varepsilon}_q\,\hat{p}\,\gamma^5\,\gamma_\mu\right.$$
$$\left.\times\frac{1}{(-\bar{z}p_\rho-(x-\xi)p)^2+i\epsilon}\right]$$

$$= \frac{4i\,\frac{x-\xi}{\xi\alpha}\left[(\varepsilon_{q\perp}\cdot p_{\rho\perp})\,\epsilon^{p\,n\,p_{\rho\perp}\,\varepsilon^*_{k\perp}} - (\varepsilon^*_{k\perp}\cdot p_{\rho\perp})\,\epsilon^{p\,n\,p_{\rho\perp}\,\varepsilon_{q\perp}}\right]}{((q+(x+\xi)p-k)^2+i\epsilon)((q+(x+\xi)p)^2+i\epsilon)((-\bar{z}p_\rho-(x-\xi)p)^2+i\epsilon)}$$

$$= \frac{4i\left[T_{A_5}-T_{B_5}\right]}{\alpha\bar{\alpha}^2\xi s^3\bar{z}\,(x-\xi+i\epsilon)\,(x+\xi+i\epsilon)}, \tag{B.15}$$

$$
\begin{aligned}
tr_D^A\left[B_3\right] &= tr_D\left[\hat{p}_\rho\,\gamma^\mu\frac{\hat{q}+(x+\xi)\hat{p}-\hat{k}}{(q+(x+\xi)p-k)^2+i\epsilon}\hat{\varepsilon}_q\,\frac{(x+\xi)\hat{p}-\hat{k}}{((x+\xi)p-k)^2+i\epsilon}\,\hat{\varepsilon}_k^*\,\hat{p}\,\gamma^5\,\gamma_\mu\right.\\
&\left.\times\frac{1}{(-\bar{z}p_\rho-(x-\xi)p)^2+i\epsilon}\right]\\
&=\frac{4i\,\frac{x-\xi}{\xi}\left[\left(\varepsilon_{q\perp}\cdot p_{\rho\perp}\right)\epsilon^{p\,n\,p_{\rho\perp}\,\varepsilon^*_{k\perp}}-\left(\varepsilon^*_{k\perp}\cdot p_{\rho\perp}\right)\epsilon^{p\,n\,p_{\rho\perp}\,\varepsilon_{q\perp}}\right]}{((q+(x+\xi)p-k)^2+i\epsilon)(((x+\xi)p-k)^2+i\epsilon)((-\bar{z}p_\rho-(x-\xi)p)^2+i\epsilon)}\\
&=\frac{-4i\left[T_{A_5}-T_{B_5}\right]}{\alpha\bar{\alpha}^2\xi s^3\bar{z}\left(x-\xi+i\epsilon\right)\left(x+\xi-i\epsilon\right)},
\end{aligned}
\tag{B.16}
$$

$$
\begin{aligned}
tr_D^A\left[B_4\right] &= tr_D\left[\hat{p}_\rho\gamma^\mu\frac{\hat{q}+(x+\xi)\hat{p}}{(q+(x+\xi)p)^2+i\epsilon}\hat{\varepsilon}_q\hat{p}\,\gamma^5\,\hat{\varepsilon}_k^*\frac{(x-\xi)\hat{p}+\hat{k}}{((x-\xi)p+k)^2+i\epsilon}\,\gamma_\mu\right.\\
&\left.\times\frac{1}{(\bar{z}p_\rho+k+(x-\xi)p)^2+i\epsilon}\right]\\
&=\frac{\frac{8i}{1-\alpha}\left[\left(\varepsilon_{q\perp}\cdot p_{\rho\perp}\right)\epsilon^{p\,n\,p_{\rho\perp}\,\varepsilon^*_{k\perp}}-\left(\varepsilon^*_{k\perp}\cdot p_{\rho\perp}\right)\epsilon^{p\,n\,p_{\rho\perp}\,\varepsilon_{q\perp}}\right]}{((q+(x+\xi)p)^2+i\epsilon)(((x-\xi)p+k)^2+i\epsilon)((\bar{z}p_\rho+k+(x-\xi)p)^2+i\epsilon)}\\
&=\frac{8i\left[T_{A_5}-T_{B_5}\right]}{\alpha\bar{\alpha}s^3\left(x-\xi+i\epsilon\right)\left(x+\xi+i\epsilon\right)\left[\left(x+\xi+i\epsilon\right)-z\left(2\alpha\xi+\bar{\alpha}\left(x+\xi+i\epsilon\right)\right)\right]},
\end{aligned}
\tag{B.17}
$$

$$
\begin{aligned}
tr_D^A\left[B_5\right] &= tr_D\left[\hat{p}_\rho\gamma^\mu\frac{\hat{q}+(x+\xi)\hat{p}}{(q+(x+\xi)p)^2+i\epsilon}\hat{\varepsilon}_q\hat{p}\gamma^5\gamma_\mu\frac{-\bar{z}\hat{p}_\rho-\hat{k}}{(-\bar{z}p_\rho-k)^2+i\epsilon}\,\hat{\varepsilon}_k^*\right.\\
&\left.\times\frac{1}{(\bar{z}p_\rho+k+(x-\xi)p)^2+i\epsilon}\right]\\
&=-\frac{8i}{\alpha}\frac{\left[(2\bar{z}-1)\,\left(\varepsilon^*_{k\perp}\cdot p_{\rho\perp}\right)\epsilon^{p\,n\,p_{\rho\perp}\,\varepsilon_{q\perp}}-\left(\varepsilon_{q\perp}\cdot p_{\rho\perp}\right)\epsilon^{p\,n\,p_{\rho\perp}\,\varepsilon^*_{k\perp}}\right]}{((q+(x+\xi)p)^2+i\epsilon)((-\bar{z}p_\rho-k)^2+i\epsilon)((\bar{z}p_\rho+k+(x-\xi)p)^2+i\epsilon)}\\
&=\frac{4i\left[(1-2z)\,T_{A_5}-T_{B_5}\right]}{\alpha\xi s^3\bar{z}\left(x+\xi+i\epsilon\right)\left[\left(x+\xi+i\epsilon\right)-z\left(2\alpha\xi+\bar{\alpha}\left(x+\xi+i\epsilon\right)\right)\right]}.
\end{aligned}
\tag{B.18}
$$

B.1.2 Chiral-odd sector

$$
\begin{aligned}
&tr_D^{CO}\left[A_3\right]_j\\
&=tr_D\left[\hat{p}_\rho\hat{\varepsilon}^*_\rho\hat{\varepsilon}_q\frac{z\hat{p}_\rho-\hat{q}}{(zp_\rho-q)^2+i\epsilon}\gamma^\mu\frac{(x+\xi)\hat{p}-\hat{k}}{((x+\xi)p-k)^2+i\epsilon}\,\hat{\varepsilon}_k^*\,\hat{p}\,\gamma_{\perp\,j}\,\gamma_\mu\,\frac{1}{(\bar{z}p_\rho+(x-\xi)p)^2+i\epsilon}\right]\\
&=\frac{16\left[(p\cdot k)\,\varepsilon^*_{k\perp j}\left(\left(\varepsilon_q\cdot p_\rho\right)\left(q\cdot\varepsilon^*_\rho\right)-\left(q\cdot p_\rho\right)\left(\varepsilon_q\cdot\varepsilon^*_\rho\right)\right)-\epsilon^{p_\rho\,\varepsilon^*_\rho\,q\,\varepsilon_q}\,\epsilon^{p\,\nu\,k\,\varepsilon^*_k}g_{\perp\nu j}\right]}{(((x+\xi)p-k)^2+i\epsilon)^2\left((zp_\rho-q)^2+i\epsilon\right)^2\left((\bar{z}\,p_\rho+(x-\xi)p)^2+i\epsilon\right)^2}\\
&=\frac{T_{A\perp j}}{2\alpha^2\bar{\alpha}s^3\xi z\bar{z}\left(x-\xi+i\epsilon\right)\left(x+\xi-i\epsilon\right)}
\end{aligned}
\tag{B.19}
$$

$$
\begin{aligned}
&tr_D^{CO}\left[A_4\right]_j\\
&=tr_D\left[\hat{p}_\rho\hat{\varepsilon}^*_\rho\hat{\varepsilon}_q\frac{z\hat{p}_\rho-\hat{q}}{(zp_\rho-q)^2+i\epsilon}\gamma^\mu\hat{p}\gamma_{\perp\,j}\hat{\varepsilon}^*_k\frac{\hat{k}+(x-\xi)\hat{p}}{(k+(x-\xi)p)^2+i\epsilon}\,\gamma_\mu\,\frac{1}{(zp_\rho-q-(x+\xi)p)^2+i\epsilon}\right]\\
&=\frac{16\left[(p\cdot k)\,\varepsilon^*_{k\perp j}\left(\left(\varepsilon_q\cdot p_\rho\right)\left(q\cdot\varepsilon^*_\rho\right)-\left(q\cdot p_\rho\right)\left(\varepsilon_q\cdot\varepsilon^*_\rho\right)\right)-\epsilon^{p_\rho\,\varepsilon^*_\rho\,q\,\varepsilon_q}\,\epsilon^{p\,\nu\,k\,\varepsilon^*_k}g_{\perp\nu j}\right]}{((k+(x-\xi)p)^2+i\epsilon)^2\left((zp_\rho-q)^2+i\epsilon\right)^2\left(((x+\xi)p-zp_\rho+q)^2+i\epsilon\right)^2}\\
&=-\frac{T_{A\perp j}}{2\alpha^2\xi s^3 z\left(x-\xi+i\epsilon\right)\left[\left(x+\xi+i\epsilon\right)-z\left(2\alpha\xi+\bar{\alpha}\left(x+\xi+i\epsilon\right)\right)\right]}
\end{aligned}
\tag{B.20}
$$

$$
\begin{aligned}
&tr_D^{CO}\left[B_5\right]_j = \\
&tr_D\left[\hat{p}_\rho \hat{\varepsilon}_\rho^* \gamma^\mu \frac{\hat{q}+(x+\xi)\hat{p}}{(q+(x+\xi)p)^2+i\epsilon} \hat{\varepsilon}_q \hat{p} \gamma_{\perp\, j} \gamma_\mu \frac{-\bar{z}\hat{p}_\rho - \hat{k}}{(-\bar{z}p_\rho - k)^2+i\epsilon} \hat{\varepsilon}_k^* \frac{1}{(\bar{z}p_\rho + k + (x-\xi)p)^2+i\epsilon}\right] \\
&= 2\frac{4s\, \varepsilon_{q\perp\, j}\left((p_\rho\cdot\varepsilon_k^*)(\varepsilon_\rho^*\cdot k) - s\xi\,(\varepsilon_k^*\cdot\varepsilon_\rho^*)\right) - \epsilon^{k\,\varepsilon_k^*\,p_\rho\,\varepsilon_\rho^*}\,\epsilon^{q\,\varepsilon_q\,p\,\nu} g_{\perp\nu j}}{((-\bar{z}p_\rho - k)^2+i\epsilon)\,((zp_\rho - q - (x-\xi)p)^2+i\epsilon)((q+(x+\xi)p)^2+i\epsilon)} \qquad \text{(B.21)} \\
&= \frac{T_{B\perp j}}{2\xi s^3 \bar{z}\,(x+\xi+i\epsilon)\,[(x+\xi+i\epsilon) - z\,(2\alpha\xi + \bar{\alpha}\,(x+\xi+i\epsilon))]}.
\end{aligned}
$$

B.2 Integration over z and x

B.2.1 Building block integrals for the numerical integration over x

Here, we list the building block integrals which are involved in the numerical evaluation of the scattering amplitudes. Consider a generic GPD f. We define

$$
\begin{aligned}
I_a[f] &= \int_{-1}^{1} \frac{1}{(-\xi+x+i\epsilon)(2\xi+\bar{\alpha}(-\xi+x+i\epsilon))} f(x,\xi)\,dx\,, && \text{(B.22)}\\
I_b[f] &= \int_{-1}^{1} \frac{1}{(2\xi+(1-\alpha)(-\xi+x+i\epsilon))^2} f(x,\xi)\,dx\,, && \text{(B.23)}\\
I_c[f] &= \int_{-1}^{1} \frac{\ln\left(\frac{\xi+x+i\epsilon}{\alpha(-\xi+x+i\epsilon)}\right)}{(2\xi+\bar{\alpha}(-\xi+x+i\epsilon))^3} f(x,\xi)\,dx\,, && \text{(B.24)}\\
I_d[f] &= \int_{-1}^{1} \frac{\ln\left(\frac{\xi+x+i\epsilon}{\alpha(-\xi+x+i\epsilon)}\right)}{(2\xi+\bar{\alpha}(-\xi+x+i\epsilon))^2} f(x,\xi)\,dx\,, && \text{(B.25)}\\
I_e[f] &= \int_{-1}^{1} \frac{1}{-\xi+x+i\epsilon} f(x,\xi)\,dx\,, && \text{(B.26)}\\
I_f[f] &= \int_{-1}^{1} \frac{1}{\xi+x+i\epsilon} f(x,\xi)\,dx\,, && \text{(B.27)}\\
I_g[f] &= \int_{-1}^{1} \frac{1}{\xi+x-i\epsilon} f(x,\xi)\,dx\,, && \text{(B.28)}\\
I_h[f] &= \int_{-1}^{1} \frac{\ln\left(\frac{\xi+x+i\epsilon}{\alpha(-\xi+x+i\epsilon)}\right)}{2\xi+\bar{\alpha}(-\xi+x+i\epsilon)} f(x,\xi)\,dx\,, && \text{(B.29)}\\
I_i[f] &= \int_{-1}^{1} \frac{1}{2\xi+\bar{\alpha}(-\xi+x+i\epsilon)} f(x,\xi)\,dx\,, && \text{(B.30)}\\
I_j[f] &= \int_{-1}^{1} \frac{1}{(-\xi+x+i\epsilon)(\xi+x+i\epsilon)\,(2\xi+\bar{\alpha}(-\xi+x+i\epsilon))} f(x,\xi)\,dx\,, && \text{(B.31)}\\
I_l[f] &= \int_{-1}^{1} \frac{1}{(\xi+x+i\epsilon)\,(2\xi+\bar{\alpha}(-\xi+x+i\epsilon))} f(x,\xi)\,dx\,, && \text{(B.32)}\\
I_k[f] &= \int_{-1}^{1} \frac{1}{(\xi+x+i\epsilon)\,(2\xi+\bar{\alpha}(-\xi+x+i\epsilon))^2} f(x,\xi)\,dx\,. && \text{(B.33)}
\end{aligned}
$$

Each of these integrals are finite and are evaluated numerically, using our models for the various involved GPDs. After computing this set of integrals, the evaluation of the scattering amplitude is straightforward using the decomposition given in the two next subsections. Below, we will not indicate the function f, since it is obvious from the context.

B.2.2 Chiral-odd case

For the chiral-odd case, diagrams A_3 and A_4 contribute to the structure $T^i_{A\perp}$ while diagrams B_1 and B_5 contribute to the structure $T^i_{B\perp}$. Thus, writing

$$tr_D^{CO}[A_3]^i + tr_D^{CO}[A_4]^i = T_A^{CO}\, T^i_{A\perp} \tag{B.34}$$

and

$$tr_D^{CO}[B_1]^i + tr_D^{CO}[B_5]^i = T_B^{CO}\, T^i_{B\perp}\,, \tag{B.35}$$

we get

$$\begin{aligned} T_A^{CO}\phi(z) &= \frac{1}{s^3}\left[\frac{3(1-z)}{\alpha^2\xi(\xi-x-i\epsilon)(\alpha(-\xi+x+i\epsilon)+(1-z)(2\xi+(1-\alpha)(-\xi+x+i\epsilon)))}\right. \\ &\left. -\frac{3}{\alpha\bar\alpha^2\xi(\xi-x-i\epsilon)(\xi+x-i\epsilon)}\right] \end{aligned} \tag{B.36}$$

and

$$\begin{aligned} T_B^{CO}\phi(z) &= \frac{1}{s^3}\left[-\frac{3}{(1-\alpha)\xi(\xi-x-i\epsilon)(\xi+x+i\epsilon)}\right. \\ &\left. +\frac{3z}{\xi(\xi+x+i\epsilon)(\alpha(-\xi+x+i\epsilon)+(1-z)(2\xi+(1-\alpha)(-\xi+x+i\epsilon)))}\right]. \end{aligned} \tag{B.37}$$

The integral with respect to z is trivially performed in the case of a DA expanded in the basis of Gegenbauer polynomials. We restrict ourselves to the case of an asymptotic DA $\phi(z) = 6z\bar z$ for which one gets

$$\begin{aligned} \int_0^1 T_A^{CO}\phi(z)\,dz = \frac{1}{s^3}\Bigg[&-\frac{3}{\alpha\bar\alpha^2\xi(\xi-x-i\epsilon)(\xi+x-i\epsilon)} \\ &+\frac{3}{\alpha^2\xi(\xi-x-i\epsilon)(2\xi+(1-\alpha)(-\xi+x+i\epsilon))}+\frac{3\ln\left(\frac{\xi+x+i\epsilon}{\alpha(-\xi+x+i\epsilon)}\right)}{\alpha\xi(2\xi+(1-\alpha)(-\xi+x+i\epsilon))^2}\Bigg]\,, \end{aligned} \tag{B.38}$$

and

$$\begin{aligned} \int_0^1 T_B^{CO}\phi(z)\,dz = \frac{1}{s^3}\Bigg[&-\frac{3}{(1-\alpha)\xi(\xi-x-i\epsilon)(\xi+x+i\epsilon)} \\ &-\frac{3}{\xi(\xi+x+i\epsilon)(2\xi+(1-\alpha)(-\xi+x+i\epsilon))}+\frac{3\ln\left(\frac{\xi+x+i\epsilon}{\alpha(-\xi+x+i\epsilon)}\right)}{\xi(2\xi+(1-\alpha)(-\xi+x+i\epsilon))^2}\Bigg]. \end{aligned} \tag{B.39}$$

Let us note that the last term in the previous expressions (B.38) and (B.39) might seem to have a double pole when $x = -\frac{1+\alpha}{\bar\alpha}\xi - i\epsilon$. However the logarithm cancels under such conditions, so this pole is actually a simple pole.

Writing the integrals with respect to x of the product of (B.38) and (B.39) with the GPD $H_T^q(x\xi)$ in terms of building block integrals, we have the dimensionless coefficients

$$N^q_{T\,A} \equiv s^3\int_{-1}^1\int_0^1 T_A^{CO}\phi(z)\,dz\,H_T(x,\xi)\,dx = -\frac{3}{\alpha^2\xi}I_a + \frac{3}{\alpha\xi}I_d + \frac{3}{2\alpha^2\bar\alpha\xi^2}(I_e - I_g)\,, \tag{B.40}$$

and

$$N^q_{T\,B} \equiv s^3\int_{-1}^1\int_0^1 T_B^{CO}\phi(z)\,dz\,H_T(x,\xi)\,dx = -\frac{3}{\xi}I_l + \frac{3}{\xi}I_d + \frac{3}{2\bar\alpha\xi^2}(I_e - I_f)\,. \tag{B.41}$$

B.2.3 Chiral-even case

For the chiral-even case, we only present the result in terms of building block integrals after integration over z and integration over x when multiplied by GPDs.

Vector part

From the symmetry of $\phi(z)$, the integration over z of the product of diagrams A_1 and A_2 with $\phi(z)$ leads to vanishing T_B parts (their T_B components are antisymmetric) and to identical T_A parts.

We decompose the trace involved in a diagram $diag$ as

$$tr_D^V[diag] = T_A^V[diag]\, T_A + T_B^V[diag]\, T_B\,, \tag{B.42}$$

and we denote the dimensionless coefficients

$$N_A^q[diag] \equiv s \int_{-1}^{1}\int_0^1 T_A^V[diag]\, \phi(z)\, dz\, H(x,\xi)\, dx\,, \tag{B.43}$$

$$N_B^q[diag] \equiv s^2 \int_{-1}^{1}\int_0^1 T_B^V[diag]\, \phi(z)\, dz\, H(x,\xi)\, dx\,. \tag{B.44}$$

For further use, we define the coefficient obtained when summing over the set of diagrams A_k and B_k

$$N_A^q \equiv \sum_{diag} N_A^q[diag] \tag{B.45}$$

and

$$N_B^q \equiv \sum_{diag} N_B^q[diag]\,. \tag{B.46}$$

We get for diagrams A_k

$$\begin{aligned}
N_A^q[A_1] &= N_A^q[A_2] = \frac{2}{\bar\alpha\xi} I_e\,, && \text{(B.47)}\\
N_A^q[A_3] &= -\frac{2}{\alpha\bar\alpha\xi}(I_e - I_g)\,, && \text{(B.48)}\\
N_A^q[A_4] &= \frac{4\bar\alpha}{\alpha}\left(I_a - \alpha I_d\right)\,, && \text{(B.49)}\\
N_A^q[A_5] &= -\frac{2}{\xi} I_h && \text{(B.50)}
\end{aligned}$$

and

$$\begin{aligned}
N_B^q[A_3] &= -\frac{1}{\alpha^2\bar\alpha\xi^2}(I_e - I_g)\,, && \text{(B.51)}\\
N_B^q[A_4] &= \frac{2}{\alpha^2\xi} I_a - \frac{4}{\alpha\xi} I_b - \frac{8}{\bar\alpha} I_c + \frac{4}{\bar\alpha\xi} I_d\,, && \text{(B.52)}\\
N_B^q[A_5] &= \frac{8}{\alpha\xi} I_b + \frac{16}{\bar\alpha} I_c - \frac{4(1+\alpha)}{\alpha\bar\alpha\xi} I_d\,. && \text{(B.53)}
\end{aligned}$$

For diagrams B_k we obtain for the T_A part

$$\begin{aligned}
N_A^q[B_1] &= -\frac{2\alpha}{\bar\alpha\xi}(I_e - I_f)\,, && \text{(B.54)}\\
N_A^q[B_2] &= \frac{1}{\bar\alpha\xi}(I_e - I_f)\,, && \text{(B.55)}\\
N_A^q[B_3] &= \frac{1}{\bar\alpha\xi}(I_e - I_g)\,, && \text{(B.56)}\\
N_A^q[B_4] &= 4\xi(I_j + 2\alpha I_k - 2\alpha I_c)\,, && \text{(B.57)}\\
N_A^q[B_5] &= 4\bar\alpha(I_d - I_l)\,, && \text{(B.58)}
\end{aligned}$$

and for the non-vanishing T_B part

$$\begin{aligned}
N_B^q[B_1] &= \frac{1}{\bar\alpha\alpha\xi^2}(I_e - I_f)\,, && \text{(B.59)}\\
N_B^q[B_5] &= -\frac{6}{\alpha\xi} I_l + 8 I_k - \frac{4}{\xi} I_b - \frac{8}{\bar\alpha} I_c + \frac{4}{\alpha\bar\alpha\xi} I_d\,. && \text{(B.60)}
\end{aligned}$$

Axial part

We decompose the trace involved in a diagram $diag$ as

$$tr_D^A[diag] = T_{A_5}^A[diag]\, T_{A_5} + T_{B_5}^A[diag]\, T_{B_5}\,, \tag{B.61}$$

and we denote the dimensionless coefficients

$$\tilde{N}_{A_5}^q[diag] \equiv s^3 \int_{-1}^{1}\int_{0}^{1} T_{A_5}^A[diag]\,\phi(z)\,dz\,\tilde{H}^q(x,\xi)\,dx\,, \tag{B.62}$$

$$\tilde{N}_{B_5}^q[diag] \equiv s^3 \int_{-1}^{1}\int_{0}^{1} T_{B_5}^A[diag]\,\phi(z)\,dz\,\tilde{H}^q(x,\xi)\,dx\,. \tag{B.63}$$

Similarly to the vector case, we define the coefficient obtained when summing over the set of diagrams A_k and B_k

$$\tilde{N}_{A_5}^q \equiv \sum_{diag} \tilde{N}_{A_5}^q[diag] \tag{B.64}$$

and

$$\tilde{N}_{B_5}^q \equiv \sum_{diag} \tilde{N}_{B_5}^q[diag]\,. \tag{B.65}$$

We get for diagrams A_k

$$\tilde{N}_{A_5}^q[A_1] = -\frac{2i}{\alpha\bar{\alpha}^2\xi^2} I_e\,, \tag{B.66}$$

$$\tilde{N}_{A_5}^q[A_2] = \frac{2i(2-\alpha)}{\alpha^2\bar{\alpha}^2\xi^2} I_e\,, \tag{B.67}$$

$$\tilde{N}_{A_5}^q[A_3] = -\frac{2i}{\alpha^2\bar{\alpha}^2\xi^2}(I_e - I_g)\,, \tag{B.68}$$

$$\tilde{N}_{A_5}^q[A_4] = -\frac{4i}{\alpha^2\xi}(I_a - \alpha I_d)\,, \tag{B.69}$$

$$\tilde{N}_{A_5}^q[A_5] = -\frac{8i}{\alpha\bar{\alpha}\xi} I_d + \frac{2i}{\alpha\bar{\alpha}\xi^2} I_h - \frac{4i}{\alpha^2\xi^2} I_i \tag{B.70}$$

and

$$\tilde{N}_{B_5}^q[A_1] = \frac{2i(1-2\alpha)}{\alpha\bar{\alpha}^2\xi^2} I_e\,, \tag{B.71}$$

$$\tilde{N}_{B_5}^q[A_2] = \frac{2i(1-2\alpha)}{\alpha\bar{\alpha}^2\xi^2} I_e\,, \tag{B.72}$$

$$\tilde{N}_{B_5}^q[A_3] = -\frac{2i}{\alpha\bar{\alpha}^2\xi^2}(I_e - I_g)\,, \tag{B.73}$$

$$\tilde{N}_{B_5}^q[A_4] = -\frac{8i}{\alpha\xi} I_b - \frac{16i}{\bar{\alpha}} I_c + \frac{4i(1+\alpha)}{\alpha\bar{\alpha}\xi} I_d\,, \tag{B.74}$$

$$\tilde{N}_{B_5}^q[A_5] = -\frac{8i}{\bar{\alpha}\xi} I_d + \frac{2i}{\alpha\bar{\alpha}\xi^2} I_h - \frac{4i}{\alpha\xi^2} I_i\,. \tag{B.75}$$

For diagrams B_k we obtain for the T_{A_5} part

$$\tilde{N}_{A_5}^q[B_1] = \frac{2i}{\alpha\bar{\alpha}^2\xi^2}(I_e - I_f)\,, \tag{B.76}$$

$$\tilde{N}_{A_5}^q[B_2] = -\frac{i}{\alpha\bar{\alpha}^2\xi^2}(I_e - I_f)\,, \tag{B.77}$$

$$\tilde{N}_{A_5}^q[B_3] = \frac{1}{2\xi}(I_e - I_g)\,, \tag{B.78}$$

$$\tilde{N}_{A_5}^q[B_4] = -\frac{4i}{\alpha\bar{\alpha}} I_j - \frac{8i}{\bar{\alpha}} I_k + \frac{8i}{\bar{\alpha}} I_c\,, \tag{B.79}$$

$$\tilde{N}_{A_5}^q[B_5] = -\frac{8i}{\alpha\xi} I_b - \frac{16i}{\bar{\alpha}} I_c + \frac{4i}{\bar{\alpha}\xi} I_d + \frac{4i}{\alpha\bar{\alpha}\xi} I_d\,, \tag{B.80}$$

and for the T_{B_5} part

$$\tilde{N}^q_{B_5}[B_1] = \frac{2i}{\bar{\alpha}^2\xi^2}(I_e - I_f)\,, \tag{B.81}$$

$$\tilde{N}^q_{B_5}[B_2] = -\frac{i}{\alpha\bar{\alpha}^2\xi^2}(I_e - I_f)\,, \tag{B.82}$$

$$\tilde{N}^q_{B_5}[B_3] = \frac{i}{\alpha\bar{\alpha}^2\xi^2}(I_e - I_g)\,, \tag{B.83}$$

$$\tilde{N}^q_{B_5}[B_4] = \tilde{N}^q_{A_5}[B_4]\,, \tag{B.84}$$

$$\tilde{N}^q_{B_5}[B_5] = -\frac{4i}{\alpha\xi}(I_d - I_l)\,. \tag{B.85}$$

B.3 Some details on kinematics

In this section we give further useful expressions for kinematics.

B.3.1 Exact kinematics

Combining Eqs. (4.68) and (4.69) one gets

$$M^2_{\gamma\rho} - t = 2\xi s\left(1 - \frac{2\xi M^2}{s(1-\xi^2)}\right) + \frac{4\xi^2 M^2}{1-\xi^2} = 2\xi s\,. \tag{B.86}$$

From Eq. (4.67), one gets

$$s = \frac{S_{\gamma N} - M^2}{1+\xi}\,, \tag{B.87}$$

so that we finally obtain

$$\tau \equiv \frac{M^2_{\gamma\rho} - t}{S_{\gamma N} - M^2} = \frac{2\xi}{1+\xi}\,, \tag{B.88}$$

and thus

$$\xi = \frac{\tau}{2-\tau}\,. \tag{B.89}$$

B.3.2 Exact kinematics for $\Delta_\perp = 0$

In the case $\Delta_\perp = 0$, we now provide the exact formulas in order to get the set of parameters $s, \xi, \alpha, \alpha_\rho, \vec{p}^{\,2}, (-t)_{\min}$ as functions of $M_{\gamma\rho}, S_{\gamma N}, -u'$.

In the limit $\Delta_\perp = 0$, Eq. (4.69) reads, using Eq. (B.87),

$$\bar{M}^2_{\gamma\rho} = \frac{2\xi}{1+\xi}\left(1 - \frac{2\xi}{1-\xi}\bar{M}^2\right) \tag{B.90}$$

with $\bar{M}^2 = M^2/(S_{\gamma N} - M^2)$ and $\bar{M}^2_{\gamma\rho} = M^2_{\gamma\rho}/(S_{\gamma N} - M^2)$. Thus, ξ is solution of the quadratic equation

$$\xi^2(\bar{M}^2_{\gamma\rho} - 2 - 4\bar{M}^2) + 2\xi - \bar{M}^2_{\gamma\rho} = 0 \tag{B.91}$$

the solution to be kept being

$$\xi = \frac{-1 + \sqrt{1 + \bar{M}^2_{\gamma\rho}(\bar{M}^2_{\gamma\rho} - 2 - 4\bar{M}^2)}}{\bar{M}^2_{\gamma\rho} - 2 - 4\bar{M}^2}\,. \tag{B.92}$$

The value of $(-t)_{\min}$ is obtained by setting $\vec{\Delta}_t = 0$ in Eq. (4.68), i.e.

$$(-t)_{\min} = \frac{4\xi^2 M^2}{1-\xi^2}\,. \tag{B.93}$$

Combined with Eqs. (B.89) and (B.88) one easily see that $(-t)_{\min}$ is obtained from the solution of

$$\bar{T}^2(1+\bar{M}^2)+\bar{T}(2\bar{M}^2\,\bar{M}_{\gamma\rho}^2+\bar{M}_{\gamma\rho}^2-1)+\bar{M}^2\,\bar{M}_{\gamma\rho}^4=0 \tag{B.94}$$

with $\bar{T}=(-t)_{\min}/(S_{\gamma N}-M^2)$, the solution to be kept being

$$(-t)_{\min}=\frac{1-\bar{M}_{\gamma\rho}^2(1+2\bar{M}^2)-\sqrt{1+\bar{M}_{\gamma\rho}^2(\bar{M}_{\gamma\rho}^2-2-4\bar{M}^2)}}{2(1+\bar{M}^2)}(S_{\gamma N}-M^2)\,. \tag{B.95}$$

From Eq. (4.71) we have

$$\vec{p}_t^{\,2}=-m_\rho^2+\alpha_\rho(m_\rho^2-u') \tag{B.96}$$

so that using Eq. (4.65) which now reads

$$2\,\xi=\frac{\vec{p}_t^{\,2}}{s\,\alpha}+\frac{\vec{p}_t^{\,2}+m_\rho^2}{s\,\alpha_\rho}\,, \tag{B.97}$$

we obtain

$$2\,\xi=-\frac{\alpha_\rho}{\alpha}\frac{u'}{s}-\frac{1-\alpha_\rho}{\alpha s}m_\rho^2-\frac{u'}{s}+\frac{m_\rho}{s}\,. \tag{B.98}$$

Eq. (4.66) reads

$$\alpha_\rho=1-\alpha-\frac{2\,\xi\,M^2}{s\,(1-\xi^2)}\,. \tag{B.99}$$

so that

$$\alpha=\frac{1}{2\xi s}\left(-u'-\frac{2\,\xi\,M^2}{s\,(1-\xi^2)}(-u'+m_\rho^2)\right)\,. \tag{B.100}$$

Thus, computing ξ through Eq. (B.92) and then s through Eq. (B.87), Eq. (B.100) allows to compute the value of α. The value of α_ρ is then obtained using Eq. (B.99). Finally, $\vec{p}_t^{\,2}$ is computed using Eq. (B.96).

B.3.3 Approximated kinematics in the Bjorken limit

In this limit, $\bar{M}_{\gamma\rho}$ and $S_{\gamma N}$ are parametrically large, and s is of the order of $S_{\gamma N}$. Neglecting $\vec{\Delta}_t^{\,2}$, m_ρ^2, t and M^2 in front of s, (except in the definition of τ where we keep as usual M^2 in the denominator of Eq. (B.88)), we thus have

$$M_{\gamma\rho}^2 \;\approx\; 2\xi s\approx\frac{\vec{p}_t^{\,2}}{\alpha\bar{\alpha}}\,, \tag{B.101}$$

$$\alpha_\rho \;\approx\; 1-\alpha\equiv\bar{\alpha}\,, \tag{B.102}$$

$$\xi \;=\; \frac{\tau}{2-\tau}\quad,\quad \tau\approx\frac{M_{\gamma\rho}^2}{S_{\gamma N}-M^2}\,, \tag{B.103}$$

$$-t' \;\approx\; \bar{\alpha}\,M_{\gamma\rho}^2\quad,\quad -u'\approx\alpha\,M_{\gamma\rho}^2\,. \tag{B.104}$$

The skewedness ξ thus reads

$$\xi=\frac{M_{\gamma\rho}^2}{2S_{\gamma N}-2M^2-M_{\gamma\rho}^2} \tag{B.105}$$

and the parameter s is given, using Eq. (B.87), by

$$s=S_{\gamma N}-M^2-\frac{M_{\gamma\rho}^2}{2}\,. \tag{B.106}$$

B.4 Phase space integration

B.4.1 Phase space evolution

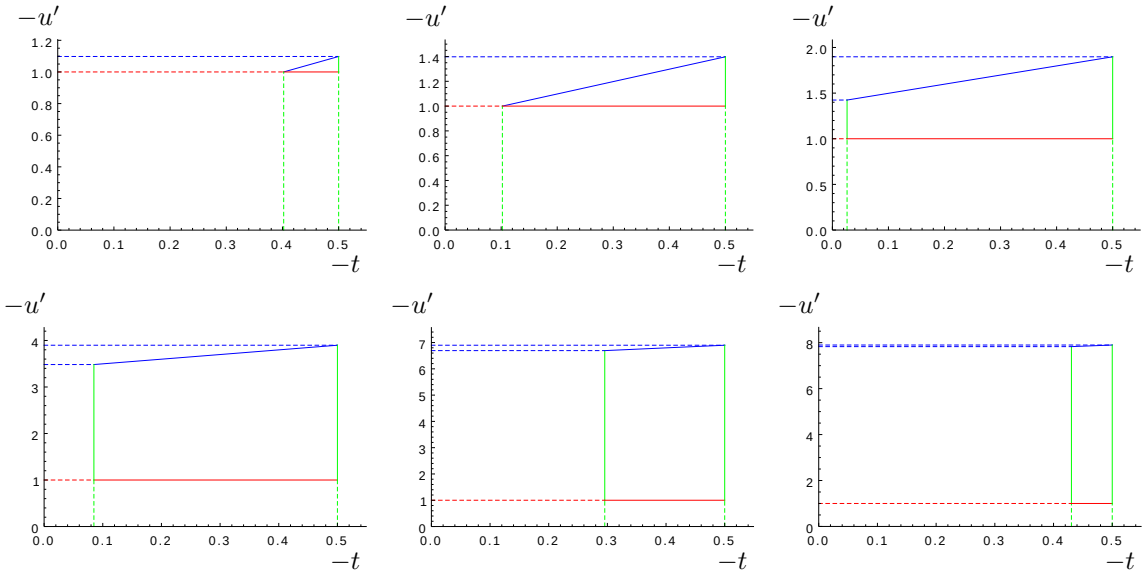

Figure B.1: Evolution of the phase space for $M_{\gamma\rho} = 2.2$ GeV^2 (up left), $M^2_{\gamma\rho} = 2.5$ GeV^2 (up center), $M_{\gamma\rho} = 3$ GeV^2 (up right), $M_{\gamma\rho} = 5$ GeV^2 (down left), $M_{\gamma\rho} = 8$ GeV^2 (down center), $M_{\gamma\rho} = 9$ GeV^2 (down right).

The phase space integration in the $(-t, -u')$ plane should take care of several cuts. This phase space evolves with increasing $M^2_{\gamma\rho}$ from a triangle to a trapezoid, as shown in Fig. B.1. These two cases and the corresponding parameters are displayed in Figs. B.2 and B.3.

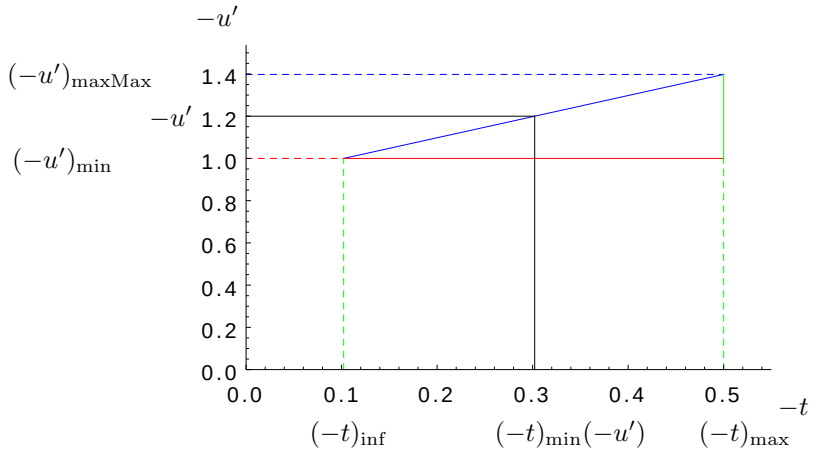

Figure B.2: Triangle-like phase space, illustrated for the case of $M_{\gamma\rho} = 2.5$ GeV^2.

Let us discuss these various cuts with some details. First, since we rely on factorization at large angle, we enforce the two constraints $-u' > (-u')_{\rm min}$, and $-t' > (-t')_{\rm min}$, and take $(-u')_{\rm min} = (-t')_{\rm min} = 1$ GeV^2 . The first constraint is the red line in Figs. B.2 and B.3, while the second, using the relation $M^2_{\gamma\rho} + t' + u' = t + m^2_\rho$, is given by

$$-u'(-t) = -t - m^2_\rho + M^2_{\gamma\rho} - (-t')_{\rm min} \,, \tag{B.107}$$

and shown as a blue line.

The variable $(-t)$ varies from $(-t)_{\rm min}$, determined by kinematics, up to a maximal value $(-t)_{\rm max}$ which we fix to be $(-t)_{\rm max} = 0.5\ {\rm GeV}^2$, these two boundaries being shown in green in Fig. B.3.

The value of $(-t)_{\rm min}$ is given by Eq. (B.95). In the domain of $M^2_{\gamma\rho}$ for which the phase-space is a triangle, as illustrated in Fig. B.2, the minimal value of $-t$ is actually above $(-t)_{\rm min}$. For a given value of $M^2_{\gamma\rho}$, this minimal value of $-t$ is given, using Eq. (B.107), by

$$(-t)_{\rm inf} = m_\rho^2 - M^2_{\gamma\rho} + (-t')_{\rm min} + (-u')_{\rm min}\,, \tag{B.108}$$

with $(-t)_{\rm min} \leqslant (-t)_{\rm inf}$.

This constraint on $-t$ leads to a minimal value of $M^2_{\gamma\rho}$, denoted as $M^2_{\gamma\rho\,{\rm crit}}$, when $(-t)_{\rm inf} = (-t)_{\rm max}$, which thus reads

$$M^2_{\gamma\rho\,{\rm crit}} = (-u')_{\rm min} + (-t')_{\rm min} + m_\rho^2 - (-t)_{\rm max}\,. \tag{B.109}$$

With our chosen values of $(-u')_{\rm min}$, $(-t')_{\rm min}$ and $(-t')_{\rm max}$ we have $M^2_{\gamma\rho\,{\rm crit}} \simeq 2.10\ {\rm GeV}^2$, below which the phase-space is empty. We note that this value, independent of $S_{\gamma N}$, ensures that the $s-$channel Mandelstam variable $M^2_{\gamma\rho} \geqslant M^2_{\gamma\rho\,{\rm crit}}$ is indeed large enough as it should be for large angle scattering.

For the purpose of integration, we define, for $-(u')_{\rm min} \leqslant -u'$,

$$(-t)_{\rm min}(-u') = m_\rho^2 - M^2_{\gamma\rho} + (-t')_{\rm min} - u'\,. \tag{B.110}$$

We denote the maximal value of $-u'$ as $(-u')_{\rm maxMax}$, attained when $-t = (-t)_{\rm max}$, and given by

$$(-u')_{\rm maxMax} = (-t)_{\rm max} - m_\rho^2 + M^2_{\gamma\rho} - (-t')_{\rm min}\,, \tag{B.111}$$

see Fig. B.2.

The phase-space becomes a trapezoid when $(-t)_{\rm inf} = (-t)_{\rm min}$, *i.e.* according to Eq. (B.108) when

$$M^2_{\gamma\rho} = -(-t)_{\rm min} + (-t')_{\rm min} + (-u')_{\rm min} + m_\rho^2\,. \tag{B.112}$$

Combined with Eq. (B.94), this leads to

$$M^2_{\gamma\rho\,{\rm trans}} = (S_{\gamma N} - M^2)\,\bar m^2\,\frac{1-\bar m^2(1+\bar M^2)}{1-\bar m^2}\,, \tag{B.113}$$

where

$$\bar m^2 = \frac{(-u')_{\rm min} + (-t')_{\rm min} + m_\rho^2}{S_{\gamma N} - M^2}\,. \tag{B.114}$$

With our choice of parameters, we get $M^2_{\gamma\rho\,{\rm trans}} \simeq 2.58\ {\rm GeV}^2$ in the case of $S_{\gamma N} = 20\ {\rm GeV}^2$.

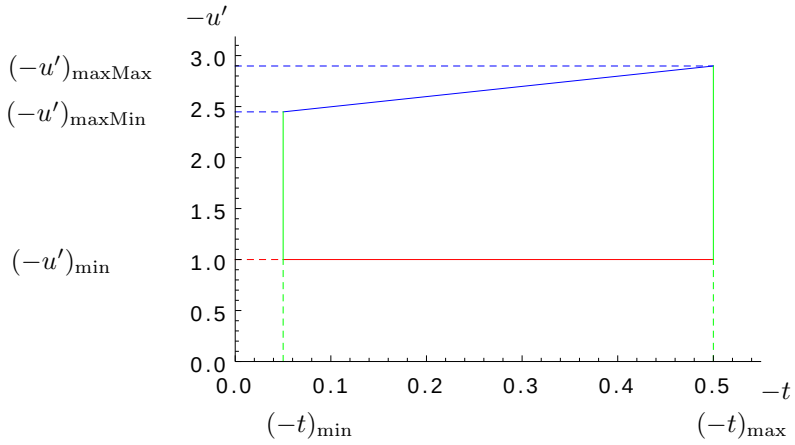

Figure B.3: Trapezoid-like phase space, illustrated for the case $M^2_{\gamma\rho} = 4\ {\rm GeV}^2$ and $S_{\gamma N} = 20\ {\rm GeV}^2$.

Above this value, the phase-space is a trapezoid, illustrated in Fig. B.3. This trapezoid reduces to an empty domain when $(-t)_{\min} = (-t)_{\max}$. From the solution of Eq. (B.94), this occurs for

$$M^2_{\gamma\rho\,\mathrm{Max}} = (S_{\gamma N} - M^2)\frac{-(1+2\bar{M}^2)(-\bar{t})_{\max} + \sqrt{(-\bar{t})_{\max}((-\bar{t})_{\max} + 4\bar{M}^2)}}{2\bar{M}^2}\,, \tag{B.115}$$

with $\bar{M}^2 = M^2/(S_{\gamma N} - M^2)$ and $(-\bar{t})_{\max} = (-t)_{\max}/(S_{\gamma N} - M^2)$. With our choice of parameters, we get $M^2_{\gamma\rho\,\mathrm{Max}} \simeq 9.47\ \mathrm{GeV}^2$ in the case of $S_{\gamma N} = 20\ \mathrm{GeV}^2$. This value decreases with decreasing values of $S_{\gamma N}$.

The minimal value of $S_{\gamma N}$ is obtained from the constraint $M^2_{\gamma\rho\,\mathrm{crit}} = M^2_{\gamma\rho\,\mathrm{Max}}$ and equals $S_{\gamma N\mathrm{crit}} \simeq 5.87\ \mathrm{GeV}^2$.

Finally, let us briefly discuss the invariant mass $M^2_{\rho N'}$, which should be restricted to be far above any possible resonance. Using Eq. (4.72), for a given value of $S_{\gamma N}$, a careful study of the allowed phase space shows that $M^2_{\rho N'}$ is minimal when $-u' = (-u')_{\mathrm{maxMax}}$ and $M^2_{\gamma\rho} = M^2_{\gamma\rho\,\mathrm{Max}}$, and for $\vec{\Delta}_t$ and $\vec{p}_t$ anti collinear, with $|\vec{\Delta}_t|$ being the value corresponding to $-t = (-t)_{\max}$. This minimal value increases with $S_{\gamma N}$. Its minimal value is thus obtained when $S_{\gamma N} = S_{\gamma N\mathrm{crit}}$, this value being $M^2_{\rho N'\mathrm{Min}} \simeq 3.4\ \mathrm{GeV}^2$ which is far above the resonance region.

B.4.2 Method for the phase space integration

Using the above described phase-space, the integrated cross section reads

$$\begin{aligned}
&\frac{d\sigma}{dM^2_{\gamma\rho}} = \theta(M^2_{\gamma\rho\,\mathrm{crit}} < M^2_{\gamma\rho} < M^2_{\gamma\rho\,\mathrm{trans}}) \\
&\times \int_{(-u')_{\min}}^{(-u')_{\mathrm{maxMax}}} d(-u') \int_{(-t)_{\min}(-u')}^{(-t)_{\max}} d(-t)\, F(t)^2\, \frac{d\sigma}{dM^2_{\gamma\rho} d(-u') d(-t)}\bigg|_{(-t)_{\min}} \\
&+ \theta(M^2_{\gamma\rho\,\mathrm{trans}} < M^2_{\gamma\rho} < M^2_{\gamma\rho\,\mathrm{Max}}) \\
&\times \left\{ \int_{(-u')_{\min}}^{(-u')_{\mathrm{maxMin}}} d(-u') \int_{(-t)_{\min}}^{(-t)_{\max}} d(-t)\, F(t)^2\, \frac{d\sigma}{dM^2_{\gamma\rho} d(-u') d(-t)}\bigg|_{(-t)_{\min}} \right. \\
&\left. + \int_{(-u')_{\mathrm{maxMin}}}^{(-u')_{\mathrm{maxMax}}} d(-u') \int_{(-t)_{\min}(-u')}^{(-t)_{\max}} d(-t)\, F(t)^2\, \frac{d\sigma}{dM^2_{\gamma\rho} d(-u') d(-t)}\bigg|_{(-t)_{\min}} \right\}.
\end{aligned} \tag{B.116}$$

Using our explicit dipole ansatz for $F(t)$, see Eq. (4.149), we obtain

$$\begin{aligned}
&\frac{d\sigma}{dM^2_{\gamma\rho}} = \frac{C^4}{3}\left[\theta(M^2_{\gamma\rho\,\mathrm{crit}} < M^2_{\gamma\rho} < M^2_{\gamma\rho\,\mathrm{trans}}) \right. \\
&\times \int_{(-u')_{\min}}^{(-u')_{\mathrm{maxMax}}} d(-u') \left[\frac{1}{((-t)_{\max} - C)^3} - \frac{1}{((-t)_{\min}(-u') - C)^3}\right] \frac{d\sigma}{dM^2_{\gamma\rho} d(-u') d(-t)}\bigg|_{(-t)_{\min}} \\
&+ \theta(M^2_{\gamma\rho\,\mathrm{trans}} < M^2_{\gamma\rho} < M^2_{\gamma\rho\,\mathrm{Max}}) \\
&\times \left\{ \left[\frac{1}{((-t)_{\max} - C)^3} - \frac{1}{((-t)_{\min} - C)^3}\right] \int_{(-u')_{\min}}^{(-u')_{\mathrm{maxMin}}} d(-u')\, \frac{d\sigma}{dM^2_{\gamma\rho} d(-u') d(-t)}\bigg|_{(-t)_{\min}} \right. \\
&\left. \left. + \int_{(-u')_{\mathrm{maxMin}}}^{(-u')_{\mathrm{maxMax}}} d(-u') \left[\frac{1}{((-t)_{\max} - C)^3} - \frac{1}{((-t)_{\min}(-u') - C)^3}\right] \frac{d\sigma}{dM^2_{\gamma\rho} d(-u') d(-t)}\bigg|_{(-t)_{\min}} \right\} \right],
\end{aligned} \tag{B.117}$$

which is our building formula for the numerical evaluation of integrated cross sections.

B.5 Angular cut over the outgoing photon

In order to take into account limitations of detection of the produced photon, it is necessary to know the photon scattering angle in the rest frame of the nucleon target. The incoming nucleon momentum p_1^μ in

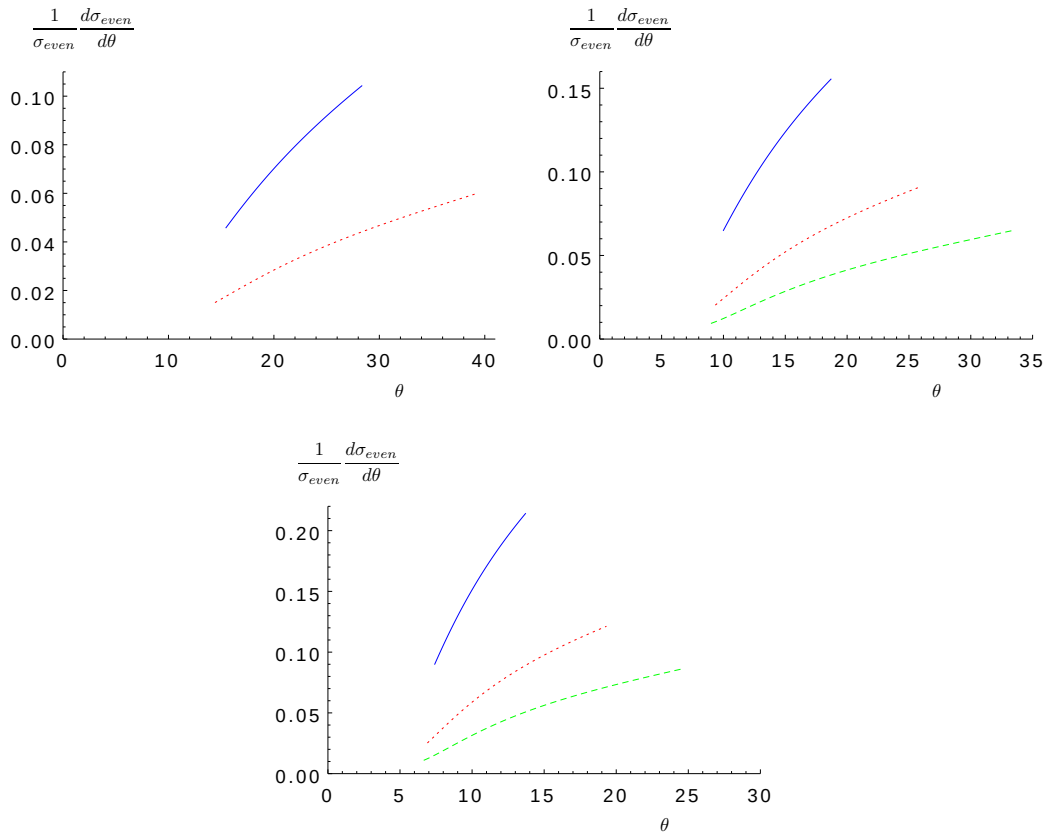

Figure B.4: Angular distribution in the chiral-even case. Up, left: $S_{\gamma N} = 10$ GeV^2, for $M^2_{\gamma\rho} = 3$ GeV^2 (solid blue) and $M^2_{\gamma\rho} = 4$ GeV^2 (dotted red). Up, right: $S_{\gamma N} = 15$ GeV^2, for $M^2_{\gamma\rho} = 3$ GeV^2 (solid blue), $M^2_{\gamma\rho} = 4$ GeV^2 (dotted red) and $M^2_{\gamma\rho} = 5$ GeV^2 (dashed green). Down: $S_{\gamma N} = 20$ GeV^2, for $M^2_{\gamma\rho} = 3$ GeV^2 (solid blue), $M^2_{\gamma\rho} = 4$ GeV^2 (dotted red) and $M^2_{\gamma\rho} = 5$ GeV^2 (dashed green).

Eq. (4.63) and the one in its rest frame $p^\mu_{1rf} = (M, 0, 0, 0)$ are related by the longitudinal boost along z axis characterized by the rapidity ζ such that, in the Bjorken limit,

$$\cosh\zeta = \frac{1}{2}\left[\frac{M}{\sqrt{s}(1+\xi)} + \frac{\sqrt{s}(1+\xi)}{M}\right] . \tag{B.118}$$

The incoming photon flies almost towards the $-z$ axis, in the light-cone and in the rest frame, so that the scattering angle θ of the produced photon in the nucleon rest frame with respect to this direction satisfies

$$\tan\theta = -\frac{2Ms(1+\xi)\parallel \vec{p}_t - \frac{\vec{\Delta}_t}{2} \parallel}{-\alpha(1+\xi)^2 s^2 + (\vec{p}_t - \frac{\vec{\Delta}_t}{2})^2 M^2} . \tag{B.119}$$

Using the relation $\alpha = M^2_{\gamma\rho}/(-u')$, see Eq. (B.104), one gets from this expression $\tan\theta$ as a function of $-u'$, which we formally write

$$\tan\theta = f(-u') . \tag{B.120}$$

From this relation, θ being positive, one should take

$$\text{for } \tan\theta > 0, \quad \theta = \arctan(\tan\theta), \tag{B.121}$$

$$\text{for } \tan\theta < 0, \quad \theta = \pi + \arctan(\tan\theta) , \tag{B.122}$$

where $\tan\theta$ is given by Eq. (B.119).

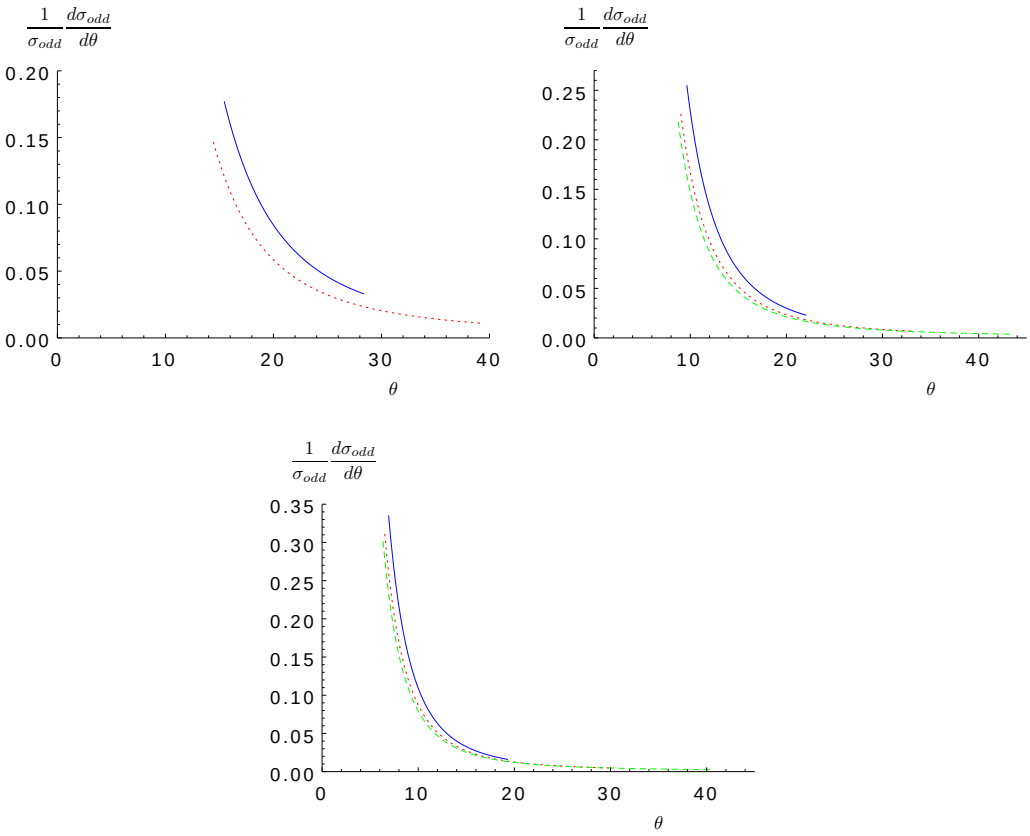

Figure B.5: Angular distribution in the chiral-odd case. Up, left: $S_{\gamma N} = 10$ GeV^2, for $M^2_{\gamma\rho} = 3$ GeV^2 (solid blue) and $M^2_{\gamma\rho} = 4$ GeV^2 (dotted red). Up, right: $S_{\gamma N} = 15$ GeV^2, for $M^2_{\gamma\rho} = 3.5$ GeV^2 (solid blue), $M^2_{\gamma\rho} = 5$ GeV^2 (dotted red) and $M^2_{\gamma\rho} = 6.5$ GeV^2 (dashed green). Down: $S_{\gamma N} = 20$ GeV^2, for $M^2_{\gamma\rho} = 4$ GeV^2 (solid blue), $M^2_{\gamma\rho} = 6$ GeV^2 (dotted red) and $M^2_{\gamma\rho} = 8$ GeV^2 (dashed green).

For simplicity, we now perform our analysis in the case $\vec{\Delta}_t = 0$, and thus write

$$\tan\theta = -\frac{2Ms(1+\xi)\,p_t}{-\alpha(1+\xi)^2 s^2 + \vec{p}_t^{\,2} M^2}, \tag{B.123}$$

where $p_t = \|\,\vec{p}_t\,\|$.

Using the formulas given in Sec. B.3.3, one can compute α as a function of θ . One gets

$$\text{for } \tan\theta > 0, \quad \alpha = \frac{(1+\xi+\tilde{\tau})\,\tilde{\tau}\,\tan^2\theta + a\left(1+\sqrt{1+\tan^2\theta}\right)}{(1+\xi+\tilde{\tau})^2\tan^2\theta + 2a}, \tag{B.124}$$

$$\text{for } \tan\theta < 0, \quad \alpha = \frac{(1+\xi+\tilde{\tau})\,\tilde{\tau}\,\tan^2\theta + a\left(1-\sqrt{1+\tan^2\theta}\right)}{(1+\xi+\tilde{\tau})^2\tan^2\theta + 2a}, \tag{B.125}$$

where

$$a = \frac{4M^2_{\gamma\rho}}{s}, \tag{B.126}$$

$$\tilde{\tau} = \frac{2\xi}{1+\xi}\frac{M^2_{\gamma\rho}}{s} = \tau\frac{M^2_{\gamma\rho}}{s}, \tag{B.127}$$

thus providing $-u'$ as a function of θ using $-u' = \alpha M^2_{\gamma\rho}$, see Eq. (B.104).

The angular distribution of the produced photon can easily be obtained from the differential cross-section by using the relation

$$\frac{d\theta}{d(-u')} = \frac{f'(-u')}{1+f^2(-u')} \tag{B.128}$$

so that we get

$$\frac{1}{\sigma}\frac{d\sigma}{d\theta} = \frac{1}{\sigma}\frac{d\sigma}{d(-u')}\frac{d(-u')}{d\theta} = \frac{1}{\sigma}\frac{d\sigma}{d(-u')}\frac{1+f^2(-u'[\theta])}{f'(-u'[\theta])}\,. \tag{B.129}$$

The obtained angular distribution is shown in Fig. B.4 for the chiral-even case, and in Fig. B.5 for the chiral-odd case. In the chiral-even case, the obtained angular distribution is an increasing function of θ, while in the chiral-odd case, it decreases with increasing θ. In both cases, the distributions are dominated by moderate values of θ.

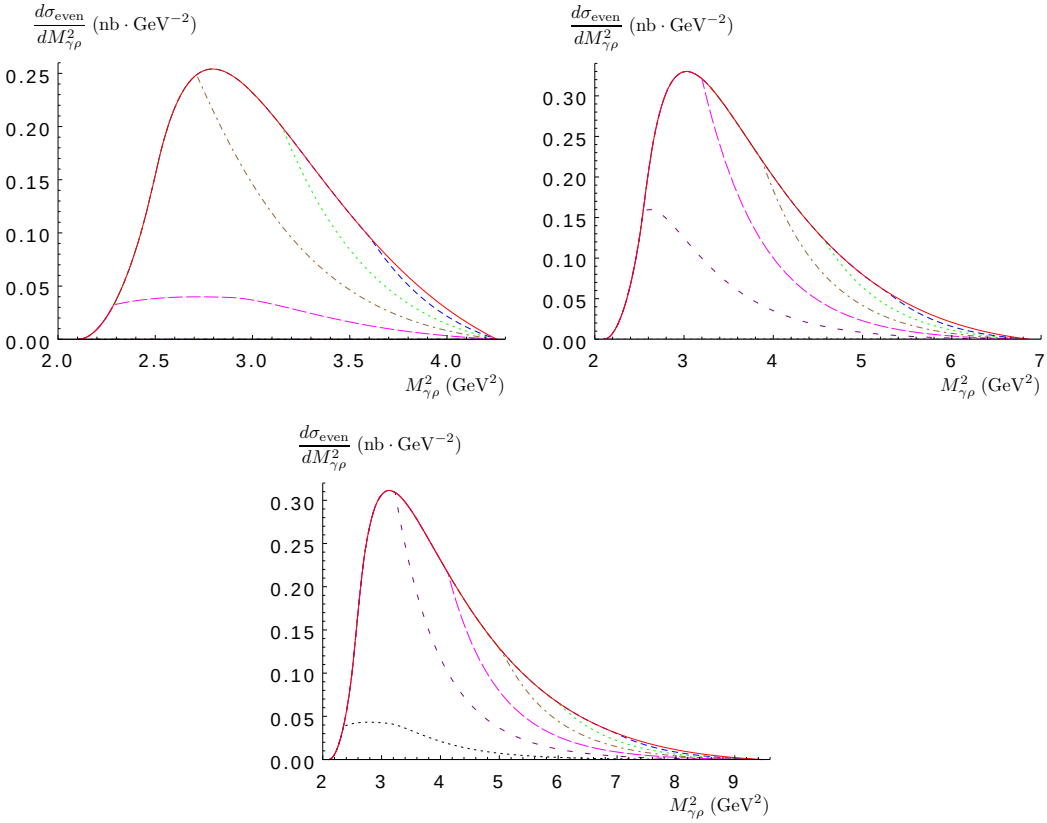

Figure B.6: The differential cross section $\frac{d\sigma_{\rm even}}{dM^2_{\gamma\rho}}$. Solid red: no angular cut. Other curves show the effect of an upper angular cut θ for the out-going γ: $35°$ (dashed blue), $30°$ (dotted green), $25°$ (dashed-dotted brown), $20°$ (long-dashed magenta), $15°$ (short-dashed purple) and $10°$ (dotted black). Up, left: $S_{\gamma N} = 10$ GeV^2. Up, right: $S_{\gamma N} = 15$ GeV^2. Down: $S_{\gamma N} = 20$ GeV^2.

In practice, at JLab, in Hall B, the outgoing photon could be detected with an angle between $5°$ and $35°$ from the incoming beam.

The effect of an upper angular cut can be seen in Fig. B.6 for the chiral-even case, and in Fig. B.7 for the chiral-odd case. As seen from Figs. B.4 and B.5, it mainly affects the low $S_{\gamma N}$ domain. In particular, the effect of the JLab $35°$ upper cut remains negligible as shown in Figs. B.6 and B.7, both for the chiral-even and chiral-odd cases.

One should note that using cuts on θ, it is possible to reduce dramatically the contribution of the chiral-even contribution, in particular in the region of $S_{\gamma N}$ around 20 GeV^2, while moderately reducing the chiral-odd contribution. Putting additional cuts on $M^2_{\gamma\rho}$, like $M^2_{\gamma\rho} > 6$ GeV^2, allows to increase the

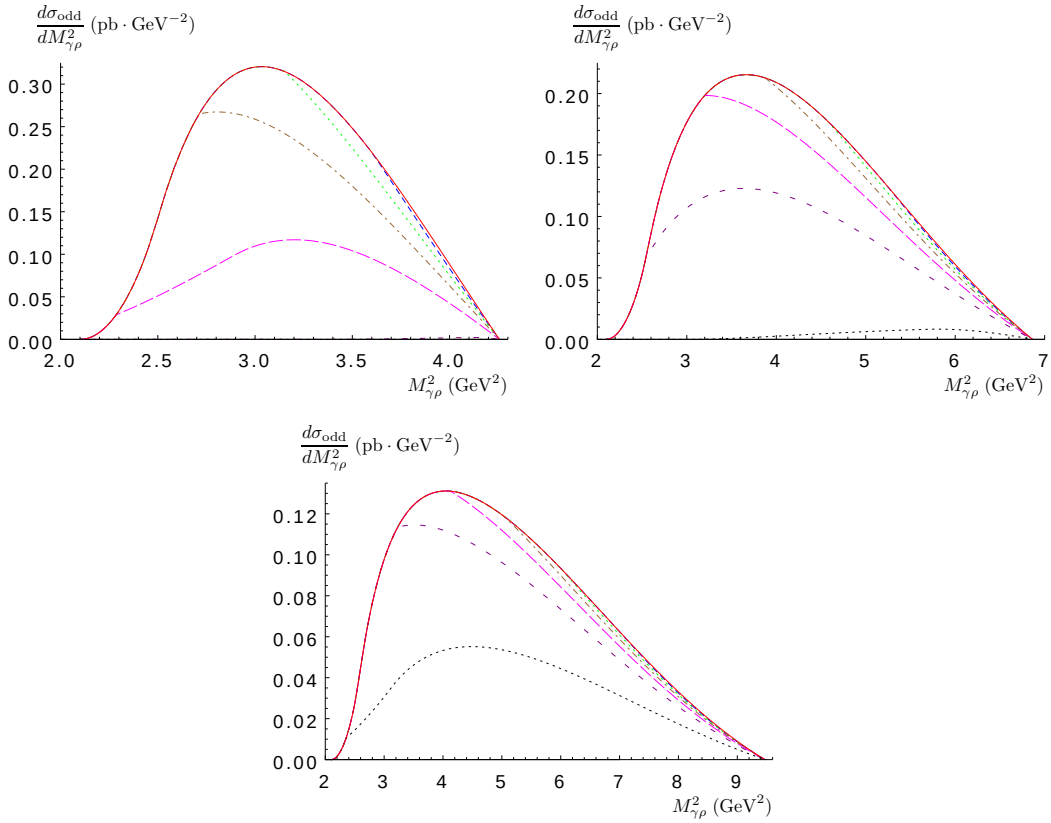

Figure B.7: The differential cross section $\frac{d\sigma_{\rm odd}}{dM^2_{\gamma\rho}}$. Solid red: no angular cut. Other curves show the effect of an upper angular cut θ for the out-going γ: $35°$ (dashed blue), $30°$ (dotted green), $25°$ (dashed-dotted brown), $20°$ (long-dashed magenta), $15°$ (short-dashed purple) and $10°$ (dotted black). Up, left: $S_{\gamma N} = 10$ GeV^2. Up, right: $S_{\gamma N} = 15$ GeV^2. Down: $S_{\gamma N} = 20$ GeV^2.

ratio odd versus even from $\sim$ 1/900 to $\sim$ 1/40, keeping about 3% of the chiral-odd contribution, for typically $S_{\gamma N}$ between 18 GeV^2 and the maximal value 21.5 GeV^2. This in principle would lead, dealing with observables sensitive to the interference between the chiral-odd and the chiral-even contributions, to a relative signal of the order of 15%.

Bibliography

[1] R. P. Feynman, *Very high-energy collisions of hadrons*, *Phys. Rev. Lett.* **23** (1969) 1415–1417.

[2] J. D. Bjorken, *Asymptotic Sum Rules at Infinite Momentum*, *Phys. Rev.* **179** (1969) 1547–1553.

[3] D. J. Gross and F. Wilczek, *ULTRAVIOLET BEHAVIOR OF NON-ABELIAN GAUGE THEORIES*, *Phys. Rev. Lett.* **30** (1973) 1343–1346.

[4] D. J. Gross and F. Wilczek, *Asymptotically Free Gauge Theories. 1*, *Phys. Rev.* **D8** (1973) 3633–3652.

[5] H. D. Politzer, *RELIABLE PERTURBATIVE RESULTS FOR STRONG INTERACTIONS?*, *Phys. Rev. Lett.* **30** (1973) 1346–1349.

[6] V. N. Gribov and L. N. Lipatov, *Deep inelastic e p scattering in perturbation theory*, *Sov. J. Nucl. Phys.* **15** (1972) 438–450.

[7] L. N. Lipatov, *The parton model and perturbation theory*, *Sov. J. Nucl. Phys.* **20** (1975) 94–102.

[8] G. Altarelli and G. Parisi, *Asymptotic freedom in parton language*, *Nucl. Phys.* **B126** (1977) 298.

[9] Y. L. Dokshitzer, *Calculation of the Structure Functions for Deep Inelastic Scattering and e^+e^- Annihilation by Perturbation Theory in Quantum Chromodynamics*, *Sov. Phys. JETP* **46** (1977) 641–653.

[10] A. V. Efremov and A. V. Radyushkin, *Factorization and Asymptotical Behavior of Pion Form-Factor in QCD*, *Phys. Lett.* **B94** (1980) 245–250.

[11] G. R. Farrar and D. R. Jackson, *The Pion Form-Factor*, *Phys. Rev. Lett.* **43** (1979) 246.

[12] G. P. Lepage and S. J. Brodsky, *Exclusive Processes in Quantum Chromodynamics: Evolution Equations for Hadronic Wave Functions and the Form-Factors of Mesons*, *Phys. Lett.* **B87** (1979) 359–365.

[13] X.-D. Ji and J. Osborne, *One-loop corrections and all order factorization in deeply virtual Compton scattering*, *Phys. Rev.* **D58** (1998) 094018, [hep-ph/9801260].

[14] J. C. Collins and A. Freund, *Proof of factorization for deeply virtual Compton scattering in QCD*, *Phys. Rev.* **D59** (1999) 074009, [hep-ph/9801262].

[15] J. C. Collins, L. Frankfurt, and M. Strikman, *Factorization for hard exclusive electroproduction of mesons in QCD*, *Phys. Rev.* **D56** (1997) 2982–3006, [hep-ph/9611433].

[16] V. S. Fadin, E. A. Kuraev, and L. N. Lipatov, *On the Pomeranchuk Singularity in Asymptotically Free Theories*, *Phys. Lett.* **B60** (1975) 50–52.

[17] E. A. Kuraev, L. N. Lipatov, and V. S. Fadin, *Multi - Reggeon Processes in the Yang-Mills Theory*, *Sov. Phys. JETP* **44** (1976) 443–450.

[18] E. A. Kuraev, L. N. Lipatov, and V. S. Fadin, *The Pomeranchuk Singularity in Nonabelian Gauge Theories*, *Sov. Phys. JETP* **45** (1977) 199–204.

[19] I. I. Balitsky and L. N. Lipatov, *The Pomeranchuk Singularity in Quantum Chromodynamics*, *Sov. J. Nucl. Phys.* **28** (1978) 822–829.

[20] M. Froissart, *Asymptotic behavior and subtractions in the Mandelstam representation*, *Phys. Rev.* **123** (1961) 1053–1057.

[21] L. V. Gribov, E. M. Levin, and M. G. Ryskin, *Semihard Processes in QCD*, *Phys. Rept.* **100** (1983) 1–150.

[22] I. Balitsky, *Operator expansion for high-energy scattering*, *Nucl. Phys.* **B463** (1996) 99–160, [hep-ph/9509348].

[23] I. Balitsky, *Factorization for high-energy scattering*, *Phys. Rev. Lett.* **81** (1998) 2024–2027, [hep-ph/9807434].

[24] I. Balitsky, *Factorization and high-energy effective action*, *Phys. Rev.* **D60** (1999) 014020, [hep-ph/9812311].

[25] I. Balitsky, *Effective field theory for the small-x evolution*, *Phys. Lett.* **B518** (2001) 235–242, [hep-ph/0105334].

[26] J. Jalilian-Marian, A. Kovner, A. Leonidov, and H. Weigert, *The BFKL equation from the Wilson renormalization group*, *Nucl. Phys.* **B504** (1997) 415–431, [hep-ph/9701284].

[27] J. Jalilian-Marian, A. Kovner, A. Leonidov, and H. Weigert, *The Wilson renormalization group for low x physics: Towards the high density regime*, *Phys. Rev.* **D59** (1999) 014014, [hep-ph/9706377].

[28] J. Jalilian-Marian, A. Kovner, and H. Weigert, *The Wilson renormalization group for low x physics: Gluon evolution at finite parton density*, *Phys. Rev.* **D59** (1999) 014015, [hep-ph/9709432].

[29] J. Jalilian-Marian, A. Kovner, A. Leonidov, and H. Weigert, *Unitarization of gluon distribution in the doubly logarithmic regime at high density*, *Phys. Rev.* **D59** (1999) 034007, [hep-ph/9807462].

[30] A. Kovner, J. G. Milhano, and H. Weigert, *Relating different approaches to nonlinear QCD evolution at finite gluon density*, *Phys. Rev.* **D62** (2000) 114005, [hep-ph/0004014].

[31] H. Weigert, *Unitarity at small Bjorken x*, *Nucl. Phys.* **A703** (2002) 823–860, [hep-ph/0004044].

[32] E. Iancu, A. Leonidov, and L. D. McLerran, *Nonlinear gluon evolution in the color glass condensate. I*, *Nucl. Phys.* **A692** (2001) 583–645, [hep-ph/0011241].

[33] E. Iancu, A. Leonidov, and L. D. McLerran, *The renormalization group equation for the color glass condensate*, *Phys. Lett.* **B510** (2001) 133–144, [hep-ph/0102009].

[34] E. Ferreiro, E. Iancu, A. Leonidov, and L. McLerran, *Nonlinear gluon evolution in the color glass condensate. II*, *Nucl. Phys.* **A703** (2002) 489–538, [hep-ph/0109115].

[35] Y. V. Kovchegov, *Small-x F_2 structure function of a nucleus including multiple pomeron exchanges*, *Phys. Rev.* **D60** (1999) 034008, [hep-ph/9901281].

[36] Y. V. Kovchegov, *Unitarization of the BFKL pomeron on a nucleus*, *Phys. Rev.* **D61** (2000) 074018, [hep-ph/9905214].

[37] E. Iancu, K. Itakura, and L. McLerran, *Geometric scaling above the saturation scale*, *Nucl. Phys.* **A708** (2002) 327–352, [hep-ph/0203137].

[38] F. Gelis, T. Lappi, and R. Venugopalan, *High energy factorization in nucleus-nucleus collisions*, *Phys. Rev.* **D78** (2008) 054019, [arXiv:0804.2630].

[39] I. Balitsky and G. A. Chirilli, *Rapidity evolution of Wilson lines at the next-to-leading order*, *Phys. Rev.* **D88** (2013) 111501, [arXiv:1309.7644].

[40] A. Kovner, M. Lublinsky, and Y. Mulian, *Jalilian-Marian, Iancu, McLerran, Weigert, Leonidov, Kovner evolution at next to leading order*, *Phys. Rev.* **D89** (2014), no. 6 061704, [arXiv:1310.0378].

[41] I. Balitsky, *Quark contribution to the small-x evolution of color dipole*, *Phys. Rev.* **D75** (2007) 014001, [hep-ph/0609105].

[42] Y. V. Kovchegov and H. Weigert, *Triumvirate of Running Couplings in Small-x Evolution*, *Nucl. Phys.* **A784** (2007) 188–226, [hep-ph/0609090].

[43] I. Balitsky and G. A. Chirilli, *Next-to-leading order evolution of color dipoles*, *Phys. Rev.* **D77** (2008) 014019, [arXiv:0710.4330].

[44] I. Balitsky and G. A. Chirilli, *NLO evolution of color dipoles in N=4 SYM*, *Nucl. Phys.* **B822** (2009) 45–87, [arXiv:0903.5326].

[45] R. E. Gerasimov and A. V. Grabovsky, *Evolution equation for 3-quark Wilson loop operator*, *JHEP* **04** (2013) 102, [arXiv:1212.1681].

[46] I. Balitsky and A. V. Grabovsky, *NLO evolution of 3-quark Wilson loop operator*, *JHEP* **01** (2015) 009, [arXiv:1405.0443].

[47] F. Dominguez, A. H. Mueller, S. Munier, and B.-W. Xiao, *On the small-x evolution of the color quadrupole and the WeizsÃď ckerâĂŞWilliams gluon distribution*, *Phys. Lett.* **B705** (2011) 106–111, [arXiv:1108.1752].

[48] J. Jalilian-Marian and Y. V. Kovchegov, *Inclusive two-gluon and valence quark-gluon production in DIS and pA*, *Phys. Rev.* **D70** (2004) 114017, [hep-ph/0405266]. [Erratum: Phys. Rev.D71,079901(2005)].

[49] A. Dumitru and J. Jalilian-Marian, *Two-particle correlations in high energy collisions and the gluon four-point function*, *Phys. Rev.* **D81** (2010) 094015, [arXiv:1001.4820].

[50] A. Dumitru and J. Jalilian-Marian, *Forward dijets in high-energy collisions: Evolution of QCD n-point functions beyond the dipole approximation*, *Phys. Rev.* **D82** (2010) 074023, [arXiv:1008.0480].

[51] A. V. Grabovsky, *On the low-x NLO evolution of 4 point colorless operators*, *JHEP* **09** (2015) 194, [arXiv:1507.0862].

[52] I. Balitsky and A. Tarasov, *Rapidity evolution of gluon TMD from low to moderate x*, *JHEP* **10** (2015) 017, [arXiv:1505.0215].

[53] I. Balitsky and A. Tarasov, *Gluon TMD in particle production from low to moderate x*, arXiv:1603.0654.

[54] T. Altinoluk, N. Armesto, G. Beuf, M. MartÃ■nez, and C. A. Salgado, *Next-to-Eikonal corrections in the CGC*, *PoS* **DIS2014** (2014) 089.

[55] T. Altinoluk, N. Armesto, G. Beuf, and A. Moscoso, *Next-to-next-to-eikonal corrections in the CGC*, *JHEP* **01** (2016) 114, [arXiv:1505.0140].

[56] M. Wusthoff and A. D. Martin, *The QCD description of diffractive processes*, *J. Phys.* **G25** (1999) R309–R344, [hep-ph/9909362].

[57] G. Wolf, *Review of High Energy Diffraction in Real and Virtual Photon Proton scattering at HERA*, *Rept. Prog. Phys.* **73** (2010) 116202, [arXiv:0907.1217].

[58] **H1** Collaboration, A. Aktas *et. al.*, *Diffractive deep-inelastic scattering with a leading proton at HERA*, *Eur. Phys. J.* **C48** (2006) 749–766, [hep-ex/0606003].

[59] **H1** Collaboration, A. Aktas *et. al.*, *Measurement and QCD analysis of the diffractive deep- inelastic scattering cross-section at HERA*, *Eur. Phys. J.* **C48** (2006) 715–748, [hep-ex/0606004].

[60] **ZEUS Collaboration** Collaboration, S. Chekanov *et. al.*, *Dissociation of virtual photons in events with a leading proton at HERA*, *Eur. Phys. J.* **C38** (2004) 43–67, [hep-ex/0408009].

[61] **ZEUS** Collaboration, S. Chekanov *et. al.*, *Study of deep inelastic inclusive and diffractive scattering with the ZEUS forward plug calorimeter*, *Nucl. Phys.* **B713** (2005) 3–80, [hep-ex/0501060].

[62] F. Aaron, C. Alexa, V. Andreev, S. Backovic, A. Baghdasaryan, *et. al.*, *Measurement of the cross section for diffractive deep-inelastic scattering with a leading proton at HERA*, *Eur. Phys. J.* **C71** (2011) 1578, [arXiv:1010.1476].

[63] **H1 Collaboration** Collaboration, F. Aaron *et. al.*, *Inclusive Measurement of Diffractive Deep-Inelastic Scattering at HERA*, *Eur. Phys. J.* **C72** (2012) 2074, [arXiv:1203.4495].

[64] **ZEUS Collaboration** Collaboration, S. Chekanov *et. al.*, *Deep inelastic scattering with leading protons or large rapidity gaps at HERA*, *Nucl. Phys.* **B816** (2009) 1–61, [arXiv:0812.2003].

[65] **H1 Collaboration, ZEUS Collaboration** Collaboration, F. Aaron *et. al.*, *Combined inclusive diffractive cross sections measured with forward proton spectrometers in deep inelastic ep scattering at HERA*, *Eur. Phys. J.* **C72** (2012) 2175, [arXiv:1207.4864].

[66] J. C. Collins, *Proof of factorization for diffractive hard scattering*, *Phys. Rev.* **D57** (1998) 3051–3056, [hep-ph/9709499].

[67] J. Bartels, J. R. Ellis, H. Kowalski, and M. Wusthoff, *An analysis of diffraction in deep-inelastic scattering*, *Eur. Phys. J.* **C7** (1999) 443–458, [hep-ph/9803497].

[68] M. Wusthoff, *Photon diffractive dissociation in deep inelastic scattering*, *PhD* (1995).

[69] E. Gotsman, E. Levin, and U. Maor, *Diffractive leptoproduction of small masses in QCD*, *Nucl. Phys.* **B493** (1997) 354–396, [hep-ph/9606280].

[70] M. Wusthoff, *Large rapidity gap events in deep inelastic scattering*, *Phys. Rev.* **D56** (1997) 4311–4321, [hep-ph/9702201].

[71] J. Bartels, H. Jung, and M. Wusthoff, *Quark - anti-quark gluon jets in DIS diffractive dissociation*, *Eur. Phys. J.* **C11** (1999) 111–125, [hep-ph/9903265].

[72] J. Bartels, H. Jung, and A. Kyrieleis, *Massive c anti-c g: Calculation in diffractive DIS and diffractive D* production at HERA*, *Eur. Phys. J.* **C24** (2002) 555–560, [hep-ph/0204269].

[73] C. Marquet, *A Unified description of diffractive deep inelastic scattering with saturation*, *Phys. Rev.* **D76** (2007) 094017, [arXiv:0706.2682].

[74] R. Boussarie, A. V. Grabovsky, L. Szymanowski, and S. Wallon, *Impact factor for high-energy two and three jets diffractive production*, *JHEP* **09** (2014) 026, [arXiv:1405.7676].

[75] R. Boussarie, A. V. Grabovsky, L. Szymanowski, and S. Wallon, *On the one loop $\gamma^{(*)} \to q\bar{q}$ impact factor and the exclusive diffractive cross sections for the production of two or three jets*, arXiv:1606.0041.

[76] R. Boussarie, A. V. Grabovsky, L. Szymanowski, and S. Wallon, *Diffractive production of jets at high-energy in the QCD shock-wave approach*, in *Photon 2015: International Conference on the Structure and Interactions of the Photon and the 21th International Workshop on Photon-Photon Collisions and International Workshop on High Energy Photon Linear Colliders Novosibirsk, Russia, June 15-19, 2015*, 2015. arXiv:1511.0278.

[77] R. Boussarie, A. Grabovsky, L. Szymanowski, and S. Wallon, *Photon dissociation into two and three jets: initial and final state corrections*, *Acta Phys. Polon. Supp.* **8** (2015) 897, [arXiv:1512.0077].

[78] V. S. Fadin and L. N. Lipatov, *BFKL pomeron in the next-to-leading approximation*, *Phys. Lett.* **B429** (1998) 127–134, [hep-ph/9802290].

[79] M. Ciafaloni and G. Camici, *Energy scale(s) and next-to-leading BFKL equation*, *Phys. Lett.* **B430** (1998) 349–354, [hep-ph/9803389].

[80] V. Fadin and R. Fiore, *Non-forward BFKL pomeron at next-to-leading order*, *Phys. Lett.* **B610** (2005) 61–66, [hep-ph/0412386].

[81] V. S. Fadin and R. Fiore, *Non-forward NLO BFKL kernel*, *Phys. Rev.* **D72** (2005) 014018, [hep-ph/0502045].

[82] K. J. Golec-Biernat and M. Wusthoff, *Saturation effects in deep inelastic scattering at low Q^2 and its implications on diffraction*, *Phys. Rev.* **D59** (1999) 014017, [hep-ph/9807513].

[83] K. Golec-Biernat and M. Wusthoff, *Saturation in diffractive deep inelastic scattering*, *Phys. Rev.* **D60** (1999) 114023, [hep-ph/9903358].

[84] G. A. Chirilli and Y. V. Kovchegov, *Solution of the NLO BFKL Equation and a Strategy for Solving the All-Order BFKL Equation*, *JHEP* **06** (2013) 055, [arXiv:1305.1924].

[85] A. V. Grabovsky, *On the solution to the NLO forward BFKL equation*, *JHEP* **09** (2013) 098, [arXiv:1307.3152].

[86] **ZEUS** Collaboration, H. Abramowicz *et. al.*, *Production of exclusive dijets in diffractive deep inelastic scattering at HERA*, *Eur. Phys. J.* **C76** (2016), no. 1 16, [arXiv:1505.0578].

[87] V. Fadin, R. Fiore, A. Grabovsky, and A. Papa, *Connection between complete and Moebius forms of gauge invariant operators*, *Nucl. Phys.* **B856** (2012) 111–124, [arXiv:1109.6634].

[88] C. Marquet and H. Weigert, *New observables to test the Color Glass Condensate beyond the large-N_c limit*, *Nucl. Phys.* **A843** (2010) 68–97, [arXiv:1003.0813].

[89] D. Y. Ivanov and A. Papa, *The next-to-leading order forward jet vertex in the small-cone approximation*, *JHEP* **1205** (2012) 086, [arXiv:1202.1082].

[90] I. Balitsky and G. A. Chirilli, *Photon impact factor in the next-to-leading order*, *Phys. Rev.* **D83** (2011) 031502, [arXiv:1009.4729].

[91] I. Balitsky and G. A. Chirilli, *Photon impact factor and k_T-factorization for DIS in the next-to-leading order*, *Phys. Rev.* **D87** (2013) 014013, [arXiv:1207.3844].

[92] G. Beuf, *Dipole factorization for DIS at NLO I: Loop correction to the photon to quark-antiquark light-front wave-functions*, arXiv:1606.0077.

[93] R. Boussarie, B. DuclouÃľ, L. Szymanowski, and S. Wallon, *Production of a forward J/psi and a backward jet at the LHC*, in *Photon 2015: International Conference on the Structure and Interactions of the Photon and the 21th International Workshop on Photon-Photon Collisions and International Workshop on High Energy Photon Linear Colliders Novosibirsk, Russia, June 15-19, 2015*, 2015. arXiv:1511.0218.

[94] D. Colferai, F. Schwennsen, L. Szymanowski, and S. Wallon, *Mueller Navelet jets at LHC - complete NLL BFKL calculation*, *JHEP* **12** (2010) 026, [arXiv:1002.1365].

[95] B. Ducloué, L. Szymanowski, and S. Wallon, *Confronting Mueller-Navelet jets in NLL BFKL with LHC experiments at 7 TeV*, *JHEP* **1305** (2013) 096, [arXiv:1302.7012].

[96] F. Caporale, D. Y. Ivanov, B. Murdaca, and A. Papa, *Mueller-Navelet small-cone jets at LHC in next-to-leading BFKL*, *Nucl. Phys.* **B877** (2013) 73–94, [arXiv:1211.7225].

[97] F. Caporale, B. Murdaca, A. Sabio Vera, and C. Salas, *Scale choice and collinear contributions to Mueller-Navelet jets at LHC energies*, *Nucl. Phys.* **B875** (2013) 134–151, [arXiv:1305.4620].

[98] F. Caporale, D. Yu. Ivanov, B. Murdaca, and A. Papa, *Brodsky-Lepage-Mackenzie optimal renormalization scale setting for semihard processes*, *Phys. Rev.* **D91** (2015), no. 11 114009, [arXiv:1504.0647].

[99] F. G. Celiberto, D. Yu. Ivanov, B. Murdaca, and A. Papa, *Mueller-Navelet jets at LHC: BFKL versus high-energy DGLAP*, *Eur. Phys. J.* **C75** (2015), no. 6 292, [arXiv:1504.0823].

[100] A. H. Mueller and H. Navelet, *An Inclusive Minijet Cross-Section and the Bare Pomeron in QCD*, *Nucl. Phys.* **B282** (1987) 727.

[101] **CMS** Collaboration, V. Khachatryan *et. al.*, *Azimuthal decorrelation of jets widely separated in rapidity in pp collisions at $\sqrt{s} = 7$ TeV*, *Submitted to: JHEP* (2016) [arXiv:1601.0671].

[102] B. DuclouÃľ, L. Szymanowski, and S. Wallon, *Evidence for high-energy resummation effects in Mueller-Navelet jets at the LHC*, *Phys. Rev. Lett.* **112** (2014) 082003, [arXiv:1309.3229].

[103] F. Caporale, D. Yu. Ivanov, B. Murdaca, and A. Papa, *MuellerâĂŞNavelet jets in next-to-leading order BFKL: theory versus experiment*, *Eur. Phys. J.* **C74** (2014), no. 10 3084, [arXiv:1407.8431]. [Erratum: Eur. Phys. J.C75,no.11,535(2015)].

[104] **H1 Collaboration** Collaboration, F. Aaron *et. al.*, *Measurement of Dijet Production in Diffractive Deep-Inelastic Scattering with a Leading Proton at HERA*, *Eur. Phys. J.* **C72** (2012) 1970, [arXiv:1111.0584].

[105] **ZEUS Collaboration** Collaboration, S. Chekanov *et. al.*, *Diffractive photoproduction of dijets in ep collisions at HERA*, *Eur. Phys. J.* **C55** (2008) 177–191, [arXiv:0710.1498].

[106] **H1 Collaboration** Collaboration, F. Aaron *et. al.*, *Diffractive Dijet Photoproduction in ep Collisions at HERA*, *Eur. Phys. J.* **C70** (2010) 15–37, [arXiv:1006.0946].

[107] M. Klasen and G. Kramer, *Factorization breaking in diffractive dijet photoproduction*, *Eur. Phys. J.* **C38** (2004) 93–104, [hep-ph/0408203].

[108] M. Klasen and G. Kramer, *Review of factorization breaking in diffractive photoproduction of dijets*, *Mod. Phys. Lett.* **A23** (2008) 1885–1907, [arXiv:0806.2269].

[109] D. Boer *et. al.*, *Gluons and the quark sea at high energies: Distributions, polarization, tomography*, arXiv:1108.1713.

[110] **LHeC Study Group** Collaboration, J. L. Abelleira Fernandez *et. al.*, *A Large Hadron Electron Collider at CERN: Report on the Physics and Design Concepts for Machine and Detector*, *J. Phys.* **G39** (2012) 075001, [arXiv:1206.2913].

[111] T. Altinoluk, N. Armesto, G. Beuf, and A. H. Rezaeian, *Diffractive Dijet Production in Deep Inelastic Scattering and Photon-Hadron Collisions in the Color Glass Condensate*, *Phys. Lett.* **B758** (2016) 373–383, [arXiv:1511.0745].

[112] Y. Hatta, B.-W. Xiao, and F. Yuan, *Probing the Small-x Gluon Tomography in Correlated Hard Diffractive Dijet Production in DIS*, *Phys. Rev. Lett.* **116** (2016), no. 20 202301, [arXiv:1601.0158].

[113] **LHCb** Collaboration, R. Aaij *et. al.*, *Exclusive J/ψ and ψ(2S) production in pp collisions at $\sqrt{s} = 7$ TeV*, *J. Phys.* **G40** (2013) 045001, [arXiv:1301.7084].

[114] **LHCb** Collaboration, R. Aaij *et. al.*, *Updated measurements of exclusive J/ψ and ψ(2S) production cross-sections in pp collisions at $\sqrt{s} = 7$ TeV*, *J. Phys.* **G41** (2014) 055002, [arXiv:1401.3288].

[115] **LHCb** Collaboration, R. Aaij *et. al.*, *Measurement of the exclusive Îě production cross-section in pp collisions at $\sqrt{s} = 7$ TeV and 8 TeV*, *JHEP* **09** (2015) 084, [arXiv:1505.0813].

[116] **ALICE** Collaboration, B. B. Abelev *et. al.*, *Exclusive J/ψ photoproduction off protons in ultra-peripheral p-Pb collisions at $\sqrt{s_{\mathrm{NN}}} = 5.02$ TeV*, *Phys. Rev. Lett.* **113** (2014), no. 23 232504, [arXiv:1406.7819].

[117] **ALICE** Collaboration, E. Abbas *et. al.*, *Charmonium and e^+e^- pair photoproduction at mid-rapidity in ultra-peripheral Pb-Pb collisions at $\sqrt{s_{\mathrm{NN}}}$=2.76 TeV*, *Eur. Phys. J.* **C73** (2013), no. 11 2617, [arXiv:1305.1467].

[118] **ALICE** Collaboration, B. Abelev *et. al.*, *Coherent J/ψ photoproduction in ultra-peripheral Pb-Pb collisions at $\sqrt{s_{NN}} = 2.76$ TeV*, *Phys. Lett.* **B718** (2013) 1273–1283, [arXiv:1209.3715].

[119] **ALICE** Collaboration, J. Adam *et. al.*, *Coherent ψ(2S) photo-production in ultra-peripheral Pb Pb collisions at $\sqrt{s}_{\mathrm{NN}}$ = 2.76 TeV*, *Phys. Lett.* **B751** (2015) 358–370, [arXiv:1508.0507].

[120] **CMS** Collaboration, V. Khachatryan *et. al.*, *Coherent J/Psi photoproduction in ultra-peripheral PbPb collisions at sqrt(s[NN]) = 2.76 TeV with the CMS experiment*, arXiv:1605.0696.

[121] **LHC Forward Physics Working Group** Collaboration, e. Royon, C. *et. al.*, *LHC Forward Physics*, .

[122] V. Guzey and M. Klasen, *Diffractive dijet photoproduction in ultraperipheral collisions at the LHC in next-to-leading order QCD*, *JHEP* **04** (2016) 158, [arXiv:1603.0605].

[123] D. Y. Ivanov, M. I. Kotsky, and A. Papa, *The impact factor for the virtual photon to light vector meson transition*, *Eur. Phys. J.* **C38** (2004) 195–213, [hep-ph/0405297].

[124] I. V. Anikin, D. Yu. Ivanov, B. Pire, L. Szymanowski, and S. Wallon, *On the description of exclusive processes beyond the leading twist approximation*, *Phys. Lett.* **B682** (2010) 413–418, [arXiv:0903.4797].

[125] I. V. Anikin, D. Yu. Ivanov, B. Pire, L. Szymanowski, and S. Wallon, *QCD factorization of exclusive processes beyond leading twist: gamma*T —> rho(T) impact factor with twist three accuracy*, *Nucl. Phys.* **B828** (2010) 1–68, [arXiv:0909.4090].

[126] S. Wandzura and F. Wilczek, *Sum Rules for Spin Dependent Electroproduction: Test of Relativistic Constituent Quarks*, *Phys. Lett.* **B72** (1977) 195–198.

[127] P. Ball and V. M. Braun, *The ρ Meson Light-Cone Distribution Amplitudes of Leading Twist Revisited*, *Phys. Rev.* **D54** (1996) 2182–2193, [hep-ph/9602323].

[128] P. Ball, V. M. Braun, Y. Koike, and K. Tanaka, *Higher twist distribution amplitudes of vector mesons in QCD: Formalism and twist three distributions*, *Nucl. Phys.* **B529** (1998) 323–382, [hep-ph/9802299].

[129] V. S. Fadin, R. Fiore, and A. V. Grabovsky, *On the discrepancy of the low-x evolution kernels*, *Nucl. Phys.* **B820** (2009) 334–363, [arXiv:0904.0702].

[130] V. Fadin, R. Fiore, and A. Grabovsky, *Matching of the low-x evolution kernels*, *Nucl. Phys.* **B831** (2010) 248–261, [arXiv:0911.5617].

[131] E. Iancu, J. D. Madrigal, A. H. Mueller, G. Soyez, and D. N. Triantafyllopoulos, *Collinearly-improved BK evolution meets the HERA data*, *Phys. Lett.* **B750** (2015) 643–652, [arXiv:1507.0365].

[132] J. L. Albacete, *Resummation of double collinear logs in BK evolution versus HERA data*, arXiv:1507.0712.

[133] G. A. Chirilli and Y. V. Kovchegov, *$\gamma^*\gamma^*$ Cross Section at NLO and Properties of the BFKL Evolution at Higher Orders*, *JHEP* **05** (2014) 099, [arXiv:1403.3384]. [Erratum: JHEP08,075(2015)].

[134] D. Yu. Ivanov, B. Murdaca, and A. Papa, *The $\gamma^*\gamma^*$ total cross section in next-to-leading order BFKL and LEP2 data*, *JHEP* **10** (2014) 058, [arXiv:1407.8447].

[135] A. Ayala, M. Hentschinski, J. Jalilian-Marian, and M. E. Tejeda-Yeomans, *Polarized 3 parton production in inclusive DIS at small x*, arXiv:1604.0852.

[136] G. Beuf, *NLO corrections for the dipole factorization of DIS structure functions at low x*, *Phys. Rev.* **D85** (2012) 034039, [arXiv:1112.4501].

[137] G. T. Bodwin, E. Braaten, E. Eichten, S. L. Olsen, T. K. Pedlar, and J. Russ, *Quarkonium at the Frontiers of High Energy Physics: A Snowmass White Paper*, in *Community Summer Study 2013: Snowmass on the Mississippi (CSS2013) Minneapolis, MN, USA, July 29-August 6, 2013*, 2013. arXiv:1307.7425.

[138] N. Brambilla *et. al.*, *Heavy quarkonium: progress, puzzles, and opportunities*, *Eur. Phys. J.* **C71** (2011) 1534, [arXiv:1010.5827].

[139] M. Bedjidian *et. al.*, *Hard probes in heavy ion collisions at the LHC: Heavy flavor physics*, 2004. hep-ph/0311048.

[140] K. Goeke, M. V. Polyakov, and M. Vanderhaeghen, *Hard Exclusive Reactions and the Structure of Hadrons*, *Prog. Part. Nucl. Phys.* **47** (2001) 401–515, [hep-ph/0106012].

[141] M. Diehl, *Generalized parton distributions*, *Phys. Rept.* **388** (2003) 41–277, [hep-ph/0307382].

[142] A. V. Belitsky and A. V. Radyushkin, *Unraveling hadron structure with generalized parton distributions*, *Phys. Rept.* **418** (2005) 1–387, [hep-ph/0504030].

[143] S. Boffi and B. Pasquini, *Generalized parton distributions and the structure of the nucleon*, *Riv. Nuovo Cim.* **30** (2007) 387, [arXiv:0711.2625].

[144] V. D. Burkert and M. Diehl, *Generalized parton distributions*, . In *Close, Frank (ed.) et al.: Electromagnetic interactions and hadronic structure* 359-423.

[145] M. Guidal, *Generalized Parton Distributions and deep virtual Compton scattering*, *Prog. Part. Nucl. Phys.* **61** (2008) 89–105.

[146] D. Y. Ivanov, B. Pire, L. Szymanowski, and O. V. Teryaev, *Probing chiral-odd GPD's in diffractive electroproduction of two vector mesons*, *Phys. Lett.* **B550** (2002) 65–76, [hep-ph/0209300].

[147] R. Enberg, B. Pire, and L. Szymanowski, *Transversity GPD in photo- and electroproduction of two vector mesons*, *Eur. Phys. J.* **C47** (2006) 87–94, [hep-ph/0601138].

[148] M. El Beiyad, B. Pire, M. Segond, L. Szymanowski, and S. Wallon, *Photoproduction of a pi rhoT pair with a large invariant mass and transversity generalized parton distribution*, *Phys. Lett.* **B688** (2010) 154–167, [arXiv:1001.4491].

[149] S. Kumano, M. Strikman, and K. Sudoh, *Novel two-to-three hard hadronic processes and possible studies of generalized parton distributions at hadron facilities*, *Phys. Rev.* **D80** (2009) 074003, [/05.1453].

[150] A. B. Larionov and M. Strikman, *Exploring QCD dynamics in medium energy γA semiexclusive collisions*, arXiv:1606.0076.

[151] R. Boussarie, B. Pire, L. Szymanowski, and S. Wallon, *On $\gamma N \to \gamma \rho N'$ at large $\gamma\rho$ invariant mass*, in *Photon 2015: International Conference on the Structure and Interactions of the Photon and the 21th International Workshop on Photon-Photon Collisions and International Workshop on High Energy Photon Linear Colliders Novosibirsk, Russia, June 15-19, 2015*, 2015. arXiv:1511.0437.

[152] R. Boussarie, B. Pire, L. Szymanowski, and S. Wallon, *Revealing transversity GPDs through the photoproduction of a photon and a ρ meson*, *EPJ Web Conf.* **112** (2016) 01006, [arXiv:1602.0177].

[153] **LHPC, SESAM** Collaboration, P. Hagler, J. W. Negele, D. B. Renner, W. Schroers, T. Lippert, and K. Schilling, *Moments of nucleon generalized parton distributions in lattice QCD*, *Phys. Rev.* **D68** (2003) 034505, [hep-lat/0304018].

[154] **QCDSF** Collaboration, M. Gockeler, R. Horsley, D. Pleiter, P. E. L. Rakow, A. Schafer, G. Schierholz, and W. Schroers, *Generalized parton distributions from lattice QCD*, *Phys. Rev. Lett.* **92** (2004) 042002, [hep-ph/0304249].

[155] **QCDSF** Collaboration, M. Gockeler *et. al.*, *Quark helicity flip generalized parton distributions from two-flavor lattice QCD*, *Phys. Lett.* **B627** (2005) 113–123, [hep-lat/0507001].

[156] **QCDSF** Collaboration, M. Gockeler *et. al.*, *Transverse spin structure of the nucleon from lattice QCD simulations*, *Phys. Rev. Lett.* **98** (2007) 222001, [hep-lat/0612032].

[157] G. P. Lepage and S. J. Brodsky, *Exclusive Processes in Perturbative Quantum Chromodynamics*, *Phys. Rev.* **D22** (1980) 2157.

[158] G. R. Farrar, G. Sterman, and H. yi Zhang, *Absence of Sudakov factors in large angle photoproduction and Compton scattering*, *Phys. Rev. Lett.* **62** (1989) 2229.

[159] D. Mueller, D. Robaschik, B. Geyer, F. M. Dittes, and J. Horejsi, *Wave functions, evolution equations and evolution kernels from light-ray operators of QCD*, *Fortschr. Phys.* **42** (1994) 101, [hep-ph/9812448].

[160] E. R. Berger, M. Diehl, and B. Pire, *Timelike Compton scattering: Exclusive photoproduction of lepton pairs*, *Eur. Phys. J.* **C23** (2002) 675–689, [hep-ph/0110062].

[161] B. Pire, L. Szymanowski, and J. Wagner, *NLO corrections to timelike, spacelike and double deeply virtual Compton scattering*, *Phys. Rev.* **D83** (2011) 034009, [arXiv:1101.0555].

[162] I. V. Anikin, B. Pire, and O. V. Teryaev, *On the gauge invariance of the DVCS amplitude*, *Phys. Rev.* **D62** (2000) 071501, [hep-ph/0003203].

[163] V. Braun, A. Manashov, and B. Pirnay, *Finite-t and target mass corrections to deeply virtual Compton scattering*, *Phys. Rev. Lett.* **109** (2012) 242001, [arXiv:1209.2559].

[164] M. Diehl, *Generalized parton distributions with helicity flip*, *Eur. Phys. J.* **C19** (2001) 485–492, [hep-ph/0101335].

[165] A. V. Radyushkin, *Double distributions and evolution equations*, *Phys. Rev.* **D59** (1999) 014030, [hep-ph/9805342].

[166] S. Goloskokov and P. Kroll, *Transversity in hard exclusive electroproduction of pseudoscalar mesons*, *Eur. Phys. J.* **A47** (2011) 112, [arXiv:1106.4897].

[167] M. Gluck, E. Reya, and A. Vogt, *Dynamical parton distributions revisited*, *Eur. Phys. J.* **C5** (1998) 461–470, [hep-ph/9806404].

[168] M. Gluck, E. Reya, M. Stratmann, and W. Vogelsang, *Models for the polarized parton distributions of the nucleon*, *Phys. Rev.* **D63** (2001) 094005, [hep-ph/0011215].

[169] M. Anselmino, M. Boglione, U. D'Alesio, S. Melis, F. Murgia, and A. Prokudin, *Simultaneous extraction of transversity and Collins functions from new SIDIS and e+e- data*, *Phys. Rev.* **D87** (2013) 094019, [arXiv:1303.3822].

[170] M. Burkardt, *Impact parameter dependent parton distributions and off- forward parton distributions for zeta $\to$ 0*, *Phys. Rev.* **D62** (2000) 071503, [hep-ph/0005108].

[171] J. P. Ralston and B. Pire, *Femto-photography of protons to nuclei with deeply virtual Compton scattering*, *Phys. Rev.* **D66** (2002) 111501, [hep-ph/0110075].

[172] M. Diehl, *Generalized parton distributions in impact parameter space*, *Eur. Phys. J.* **C25** (2002) 223–232, [hep-ph/0205208].

[173] M. Burkardt, *Transverse deformation of parton distributions and transversity decomposition of angular momentum*, *Phys. Rev.* **D72** (2005) 094020, [hep-ph/0505189].

[174] M. Diehl and P. Hagler, *Spin densities in the transverse plane and generalized transversity distributions*, *Eur. Phys. J.* **C44** (2005) 87–101, [hep-ph/0504175].

[175] A. Mukherjee, D. Chakrabarti, and R. Manohar, *Chiral Odd Generalized Parton Distributions in Position Space*, *AIP Conf. Proc.* **1149** (2009) 533–538, [arXiv:0902.1461].

[176] M. Diehl and P. Kroll, *Nucleon form factors, generalized parton distributions and quark angular momentum*, *Eur. Phys. J.* **C73** (2013), no. 4 2397, [arXiv:1302.4604].

[177] M. Anselmino, M. Boglione, U. D'Alesio, A. Kotzinian, S. Melis, F. Murgia, A. Prokudin, and C. Turk, *Sivers Effect for Pion and Kaon Production in Semi-Inclusive Deep Inelastic Scattering*, *Eur. Phys. J.* **A39** (2009) 89–100, [arXiv:0805.2677].

[178] P. Kessler, *The Weizsacker-Williams Method and Similar Approximation Methods in Quantum Electrodynamics*, *Acta Phys. Austriaca* **41** (1975) 141–188.

[179] S. Frixione, M. L. Mangano, P. Nason, and G. Ridolfi, *Improving the Weizsacker-Williams approximation in electron - proton collisions*, *Phys. Lett.* **B319** (1993) 339–345, [hep-ph/9310350].

[180] H. Moutarde, B. Pire, F. Sabatie, L. Szymanowski, and J. Wagner, *On timelike and spacelike deeply virtual Compton scattering at next to leading order*, arXiv:1301.3819.

[181] A. V. Bogdan and A. V. Grabovsky, *Radiative corrections to the Reggeized quark - Reggeized quark - gluon effective vertex*, *Nucl. Phys.* **B773** (2007) 65–83, [hep-ph/0701144].

Titre : Étude perturbative de différents processus exclusifs en QCD aux énergies hautes et modérées

Mots clés : Processus exclusifs, Chromodynamique quantique perturbative, kt-factorisation, B-JIMWLK, Factorisation colinéaire, Jets vers l'avant

Résumé : Aux énergies assez hautes, les processus de Chromodynamique Quantique (QCD) peuvent être factorisés en une partie dite *dure*, calculable via la méthode perturbative des diagrammes de Feynman grâce à la petitesse de la constante de couplage, et une partie *non-perturbative* qui doit être obtenue expérimentalement, modelée ou calculée à partir d'autres méthodes comme par exemple la QCD sur réseau. Cependant, la petitesse de la constante de couplage de QCD dans la partie perturbative peut être compensée par de grands logarithmes
émergeant de la compensation de divergences *molles* ou *colinéaires*, ou de la présence de plusieurs échelles cinématiques. De telles contributions logarithmiquement compensées doivent être resommées, afin d'obtenir l'équation d'évolution DGLAP aux énergies modérées et l'équation BFKL ou B-JIMWLK dans la limite des très hautes énergies. Aux énergies les plus hautes, des effets de recombinaison gluonique mènent à la saturation, qui peut être décrite avec le formalisme des *ondes de choc de QCD*, ou *CGC*. Dans cette thèse, l'étude de certains processus exclusifs décrits via la QCD perturbative est proposée, afin d'améliorer la compréhension de la factorisation en QCD, et des effets de resommation et de saturation.
Dans la première partie de ce manuscrit, le premier calcul d'une quantité exclusive au premier ordre sous-dominant (NLO) effectué à l'aide du formalisme des ondes de choc de QCD est détaillé. L'amplitude pour la production ouverte d'une paire quark-antiquark y est dérivée, puis la manière de construire une section efficace finie pour la production exclusive d'un double jet vers l'avant dans un processus diffractif à partir de cette amplitude est décrite. Une étude précise phénoménologique et expérimentale de ce processus devrait permettre une grande avancée dans la compréhension des effets de resommation, via ici l'échange d'un Pomeron en diffraction, objet naturellement décrit par la resommation de logarithmes provenant de la compensation de divergences molles aux hautes énergies. Le résultat présenté ici est valable lorsque l'énergie dans le centre de masse du processus hadronique approche la limite de saturation ou pour des collisions impliquant des ions lourds. En conséquence, une telle étude serait une bonne méthode d'analyse des effets de saturation.
Dans la deuxième partie, il est montré que l'étude expérimentale de la photoproduction d'un méson léger et d'un photon aux énergies modérées constitue un bon moyen d'accéder aux Distributions de Partons Généralisées (GPDs), l'une des généralisations des quantitées non-perturbatives apparaissant en factorisation colinéaire. En principe, une telle étude devrait donner accès aux GPDs conservant l'hélicité, mais aussi aux GPDs renversant l'hélicité, encore jamais observées expérimentalement. Une étude de faisabilité complète pour ce processus à JLab@12GeV est détaillée.

Title: Perturbative study of selected exclusive QCD processes at high and moderate energies

Keywords: Exclusive processes, Perturbative Quantum Chromodynamics, kt-factorization, B-JIMWLK, Collinear factorization, Forward jets

Abstract: At high enough energies, QCD processes can be factorized into a hard part, which can be computed by using the smallness of the strong coupling to apply the perturbative Feynman diagram method, and a non-perturbative part which has to be fitted to experimental data, modeled or computed using other tools like for example lattice QCD. However the smallness of the strong coupling in the perturbative part can be compensated by large logarithms which arise from the cancellation of soft or collinear divergences, or by the presence of multiple kinematic scales. Such logarithmically-enhanced contributions must be resummed, leading to the DGLAP evolution at moderate energies and to the BFKL or B-JIMWLK equation in the high energy limit. For the largest energies gluon recombination effects lead to saturation, which can be described in the color glass condensate (CGC) or shockwave formalism. In this thesis, we propose to study several exclusive perturbative QCD processes in order to get a better understanding of factorization, resummation and saturation effects.
In the first part we perform the first computation of an exclusive quantity at Next-to-Leading-Order (NLO) accuracy using the QCD shockwave formalism. We calculate the NLO amplitude for the diffractive production of an open quark-antiquark pair, then we manage to construct a finite cross section using this amplitude by studying the exclusive diffractive production of a dijet. Precise phenomenological and experimental analysis of this process should give a great insight on high energy resummation due to the exchange of a Pomeron in diffraction, which is naturally described by the resummation of logarithms emerging from the soft divergences of high energy QCD. Our result holds as the center of mass energy grows towards the saturation scale or for diffraction off a dense target so one could use it to study saturation effects.
In the second part we show how the experimental study of the photoproduction of a light meson and a photon at moderate energy should be a good probe for Generalized Parton Distributions (GPDs), one of the generalizations of the non-perturbative building blocks in collinear factorization. In principle such a study would give access to both helicity-conserving and helicity-flip GPDs. We give numerical predictions for this process at JLAB@12GeV.